Biochemical basis of pancreatic islet β-cell adaptation and failure in high fat fed diet-induced obese mice

Anfal Al-Mass

Division of Experimental Medicine

Faculty of Medicine

McGill University, Montreal

September 2016

A thesis submitted to McGill University in partial fulfillment of the requirements of the degree of Master of Science.

Table of contents.

Abstract

Diet induced obese (DIO) mice can be stratified according to their weight gain in response to high fat diet as low responders (LDR) and high responders (HDR). This provides an animal model to study β-cell failure and the transition to prediabetes (LDR) and early diabetes (HDR). C57BL/6N mice were fed for 8 weeks with a normal chow diet (ND) or a high fat diet and stratified as LDR and HDR. Freshly isolated islets from ND, LDR and HDR mice were studied *ex-vivo* for mitochondrial metabolism, AMPK activity and signalling, the expression and activity of key enzymes of energy metabolism, cholesterol synthesis, and mRNA profiling. Severely compromised glucose-induced insulin secretion in HDR islets, as compared to ND and LDR islets, was associated with suppressed AMP-kinase activity. HDR islets also showed reduced acetyl-CoA carboxylase activity and enhanced activity of 3-hydroxy-3-methylglutaryl-CoA reductase, which led respectively to elevated fatty acid oxidation and increased cholesterol biosynthesis. HDR islets also displayed mitochondrial membrane hyperpolarization and reduced ATP turnover in the presence of elevated glucose. Expression of protein kinase Cε, which reduces both lipolysis and production of signals for insulin secretion, was elevated in DIO islets. Genes whose expression increased or decreased by more than 1.2-fold were minor between LDR and ND islets (17 differentially expressed), but were prominent between HDR and ND islets (1508 differentially expressed). In HDR islets, the affected genes are implicated in the regulation of the cell cycle and cell proliferation, AMPK signaling, mitochondrial metabolism and cholesterol metabolism. In conclusion, chronically reduced AMPK activity, mitochondrial dysfunction, elevated cholesterol biosynthesis in islets, and substantial alterations in gene expression accompany β-cell failure in HDR islets. The β-cell compensation process in the pre-diabetic state (LDR) is largely independent of transcriptional adaptive changes, whereas the transition to early diabetes (HDR) is associated with major alterations in gene expression.

Résumé

Les souris DIO (obèses induite par une diète) peuvent être stratifiées selon leur gain de poids en réponse à une diète riche en graisses, soit les faibles répondeurs (LDR) et les forts répondeurs (HDR). Ce dernier permet l'étude du l'insensibilité des cellules β au glucose et les transitions vers le prédiabète (LDR) et le diabète précoce (HDR). Les souris C57BL / 6N ont été nourries pendant 8 semaines avec un régime alimentaire normal (ND) ou un régime riche en graisses et stratifiées en LDR et HDR. Les îlots des souris ND, LDR et HDR ont été isolés fraîchement afin d'étudier en ex vivo le métabolisme mitochondrial, l'activité de l'AMPK et sa signalisation, l'expression et l'activité des enzymes clés du métabolisme énergétique, la synthèse du cholestérol et le profilage de l'ARNm. En comparant les différents îlots HDR, ND et LDR, la sécrétion d'insuline sévèrement compromise et induite par le glucose dans les îlots HDR est expliquée par une suppression de l'activité de l'AMPK. Les îlots HDR ont également mis en évidence une activité réduite de l'enzyme acétyl-CoA carboxylase et une augmentation de l'activité du 3-hydroxy-3-méthylglutaryl-CoA réductase, ce qui a conduit respectivement à une oxydation élevée des acides gras et une augmentation de la biosynthèse du cholestérol. Ainsi, ces îlots HDR ont démontré une hyperpolarisation de la membrane mitochondriale et une baisse du taux d'ATP en présence d'une quantité élevée de glucose. L'expression de la protéine kinase Cε, capable de réduire à la fois la lipolyse et la production de signaux pour la sécrétion d'insuline, a été élevée dans les îlots DIO. Le nombre de gènes dont l'expression a augmenté ou diminué de plus de 1,2 fois était mineur entre LDR et îlots ND (17 différentiellement exprimés), mais était important entre HDR et îlots ND (1508 différentiellement exprimés). Dans les îlots HDR, en particulier les gènes affectés, ces derniers étaient impliqués dans le cycle cellulaire, la prolifération cellulaire, la signalisation AMPK, le métabolisme mitochondrial et le métabolisme du cholestérol. En conclusion, l'activité de l'AMPK chroniquement réduite, le dysfonctionnement mitochondrial, l'augmentation de la biosynthèse du cholestérol dans les îlots ainsi que les modifications considérables dans l'expression génique sont associés à l'insensibilité des cellules β des îlots de Langerhans HDR au glucose. Le processus de compensation dans les cellules β à l'état prédiabétique (LDR) est en grande partie indépendant aux changements adaptatifs transcriptionnels, alors que la transition vers le diabète précoce (HDR) est associée à des modifications importantes dans l'expression des gènes.

Acknowledgements

First and foremost I would like to thank my supervisors Dr. Marc Prentki and Dr. Rob Sladek for their outstanding support, guidance and patient throughout my MSc. degree. I had the great pleasure of working closely with both of them where I gained a great and rich insight to two different school of thinking that opens your mind not only in science but in life in general. In the lab I was always surrounded by a rich and supportive learning environment and working on motivating projects that brought lots of challenges and exciting finding that changes our filed.

I would like also to thank the senior scientists in the lab: Dr. Marie-Line Peyot, Dr. Julien Lamontagne, Dr. Erik Joly and Dr. Murthy Madiraju; each in your own way guided me and taught me a lot. Specially, Marie-Line and Julien, with whom I worked very closely, they was always there for me when I needed help and I learned many things from them.

Thanks to everyone in the Prentki laboratory, past and present, it was a pleasure working with every day. A special thank you to the technicians who make our work so much easier, and whose value is not always well recognized, thank you for being there for us. Many thanks also to Alix, for her emotional support; she was always there to listen when we needed someone and she always kipping us humble and appreciative.

I would like also to thank the students and post doctoral fellows in the lab, it was a true pleasure sharing the good and the bad with you guys and I wouldn`t choose a better people to share this with. Thank you for the support and time. Steven, thank you for your knowledge, time and help with the analysis I could have not done it without you.

Finally, I must express my very profound gratitude to my family and friends, especially to my parents for providing me with unfailing support and continuous encouragement throughout my years of study and through the process of researching and writing this thesis. This accomplishment would not have been possible without them. Thank you.

List of Abbreviations

ABCA1: ATP-binding cassette transporter

ABHD6: alpha/beta-Hydrolase domain containing 6

ACC: acetyl-CoA carboxylase

ADP: adenosine diphosphate

AMP: adenosine monophosphate

AMPK: AMP-activated protein kinase

ATGL: adipose triglyceride lipase

ATP: adenosine tri-phosphate

BMI: body mass index

cAMP: cyclic adenosine monophosphate

DAG: diacylglycerol

DIO: diet-induced obesity

ETC: electron transport chain

FA-CoA: fatty acyl-CoA

$FADH_2$: flavin adenine dinucleotide

FAS: fatty acid synthase

FBS: fetal bovine serum

FBS: fetal bovine serum

FCCP: carbonilcyanide p-triflouromethoxyphenylhydrazone

FFA: free fatty acid

GDH: glutamate dehydrogenase

GL/FFA cycle: glycerolipid/free fatty acid cycle

GLP-1: glucagon-like peptide-1

GLUT1: glucose transporter 1

GLUT2: glucose transporter 2

GLUT4: glucose transporter 4

GPR40: G-protein-coupled receptor 40

GSIS: glucose-stimulated insulin secretion

GTP: guanosine-5'-triphosphate

H_2O_2: hydrogen peroxide

HDR: high diet responder

HFD: high-fat diet
HMGCR: 3-Hydroxy- 3-Methyl Glutaryl-CoA reductase
HRP: horseradish peroxidase
HSL: hormone-sensitive lipase
IGT: impaired glucose tolerance
IL-6: interleukin 6
IRS-1: insulin-receptor substrate 1
KCl: potassium chloride
LC-CoA: long-chain acyl-CoA
LDR: low diet responder
LKB1: liver kinase B1
MAG: monoacylglycerol
MAGL: monoacylglycerol lipase
Mal-CoA: malonyl-CoA
MCD: malonyl-CoA decarboxylase
MCF: metabolic coupling factors
MCP-1: monocyte chemotactic protein-1
NAD: nicotinamide adenine dinucleotide
NADH: nicotinamide adenine dinucleotide (reduced)
NADPH: nicotinamide adenine dinucleotide phosphate hydrogen
ND: normal diet
NGT: normal glucose tolerance
OCR: oxygen consumption rate
OGTT: oral glucose tolerance test
PCR: polymerase chain reaction
PDH: pyruvate dehydrogenase
PKCε: protein kinase Cε
ROS: reactive oxygen species
SDS-PAGE: sodium dodecyl sulfatepolyacrylamide gel electrophoresis
SIRT1: sirtuin (silent mating type information regulation 2 homolog) 1
T2D: Type 2 diabetes
TCA: tricarboxylic acid
TCF7L2: transcription factor 7- like 2

TG: triacylglycerol

TNF- α: tumor necrosis factor-α

UCP2: uncoupling protein 2

α-KG: α-ketoglutarate

$\Delta\psi_{mito}$: mitochondrial membrane potential

Contribution of Authors

Anfal Al-Mass and Émilie Pepin took care of the mice, there diet, weight and health. Anfal Al-Mass, Émilie Pepin, Camille Attané, Roxane Lussier and Marie-Line Peyot were reponsible for grouping and sacrificing the mice, islet isolation and measurement of blood metabolic parameters. Anfal Al-Mass, Émilie Pepin and Marie-Line Peyot performed and analyzed immunoblotting, mitochondrial membrane potential and insulin secretion. Anfal Al-Mass and Marie-Line Peyot performed and analyzed the transcriptomic profiling and Kezhuo Zhang and Robert Sladek helped with the analysis. Anfal Al-Mass and Marie-Line Peyot performed islet oxygen consumption with the help of Julien Lamontagne and total cholesterol content. Anfal Al-Mass and Marie-Line Peyot did the functional classification of differentially expressed genes for all the comparison groups. Anfal Al-Mass designed primers and performed quantitative Real time-PCR on all the primers. S.R.Murthy Madiraju, Erik Joly, Neil B. Ruderman and Marc Prentki conceived and designed the experiments. Roxane Lussier contributed reagents, materials and analysis tools. Analysis of the data was performed by Anfal Al-Mass, Émilie Pepin and Marie-Line Peyot with the help of S.R.Murthy Madiraju, Erik Joly, Robert Sladek and Marc Prentki. Anfal Al-Mass, Émilie Pepin, Marie-Line Peyot, S.R.Murthy Madiraju and Marc Prentki wrote the paper.

List of Figures and Tables.

Chapter 1 – Introduction

1.1 Diabetes Mellitus.

Diabetes Mellitus is a metabolic disorder characterized by hyperglycemia resulting from defects in insulin secretion by the pancreatic β-cells (β-cell dysfunction) and/or insulin action (insulin resistance) (Stein, Maloney, & Pollin, 2014). Pathogenic processes that are involved in the development of diabetes can range from autoimmune destruction of the pancreatic β-cells resulting in insulin deficiency; to abnormalities in carbohydrate, fat, and protein metabolism that result in resistance to insulin action on target tissues. Impairment in insulin secretion and defects in insulin action often coexist; and it is mostly unclear which abnormality is the primary cause of the hyperglycemia (American Diabetes, 2014). In nearly the entire world, diabetes is one of the most common chronic diseases, and because of changes in lifestyle that lead to reduced physical activities and increased obesity, diabetes continue to increase in numbers and significance overall. The estimated worldwide prevalence of diabetes among adults was 285 million in 2010, and this value is predicted to rise to around 439 million by 2030 (Nolan, Damm, & Prentki, 2011).

1.2 Pathogenesis of type 2 diabetes.

Type 2 diabetes (T2D), one of many types of diabetes, is defined as a metabolic disorder of fuel homoeostasis characterized by hyperglycemia and altered lipid metabolism caused by islet β-cell dysfunction and insulin resistance due to genetic and environmental factors (Nolan et al., 2011). The symptoms of T2D develop gradually with time and start to show when the blood glucose levels become very high. Chronic hyperglycemia, if not controlled through drugs, nutritional or physical intervention, can affect the function of tissues and organs, such as the kidneys, nerves and eyes (Amos, McCarty, & Zimmet, 1997). Thus, untreated or poorly treated T2D can become a serious health and social problem as a result of secondary complications, and greatly reduces both the quality of life and the life span. Most individuals with T2D are obese, with obesity itself causing some degree of insulin resistance. The risk of T2D increases with increasing age, obesity, and lack of physical activity (Stumvoll, Goldstein, & van Haeften, 2005). It occurs more

often in individuals with hypertension or dyslipidemia, and its occurrence varies in different racial and ethnic subgroups. It is often associated with a strong genetic predisposition (American Diabetes, 2014). Nevertheless, T2D genetics are complex and not clearly understood.

T2D can be classified into two major groups based on body mass index (BMI) (Perry et al., 2012). Obese T2D is a major contributor to the pandemic of T2D, where environmental factors such as increased availability of food and decreased opportunity and motivation for physical activity play a major role in increasing T2D risk. Lean T2D is usually found in elderly individuals and in poor and developing countries.

The global obesity epidemic significantly contributes to the rapid increase in T2D prevalence. Insulin resistance directly links obesity with T2D; however, obesity induced insulin resistance is not the only cause for T2D and may even be protective for tissues such as the heart and skeletal muscle where it prevents excess nutrient entry in an overnutrition state to reduce damage to these tissues (Nolan, Ruderman, Kahn, Pedersen, & Prentki, 2015). Hyperglycemia appears only when β-cells are unable to secrete sufficient insulin to compensate for the insulin resistance. Early on there was a misconception regarding the primary cause of hyperglycemia in T2D. It was suggested that insulin resistance in the liver, skeletal muscles and adipose tissue precedes the increase in blood glucose and it is the primary cause of T2D (Martin et al., 1992); however, later studies have suggested that this is not entirely true (Gerich, 1998; Leahy, 2005). In older studies, the oral glucose tolerance test (OGTT) was used to diagnose T2D: in this test, patients are given a specific amount of glucose and the observed relationship between the 2h plasma glucose level and the 2h plasma insulin level shows an inverted U relationship, with plasma insulin levels increasing to a peak around 200 mg/dl followed by a progressive decrease. For individuals that show impaired glucose tolerance (IGT) during the OGTT, the increase in insulin secretion was always observed despite the decrease in glucose tolerance. This was interpreted to indicate that insulin resistance, rather than insulin deficiency (or β-cell dysfunction), is responsible for the development of IGT; and that the development of diabetes will follow when the β-cell can no longer compensate for this insulin resistance (DeFronzo, Bonadonna, & Ferrannini, 1992; Lillioja et al., 1988). In contrast, more recent studies showed that individuals with IGT already have impaired insulin secretion (Larsson & Ahren, 1996; Polonsky, Sturis, & Bell, 1996). These studies took into consideration the fact that insulin response to a meal normally occurs in a biphasic pattern, and that the amount of insulin released

is highly responsive to the prevailing glucose value (Leahy, 2005). These studies measured the 30 min insulin values after a meal (first phase of insulin secretion) (Fig. 1.1), and showed that defective first phase of insulin secretion occurred long before the onset of T2D (Gerich, 1998; Leahy, 2005) (Fig. 1.1). These observations showed that there is impaired β-cell function before the onset of IGT and that this may actually cause hyperglycemia before insulin resistance is present.

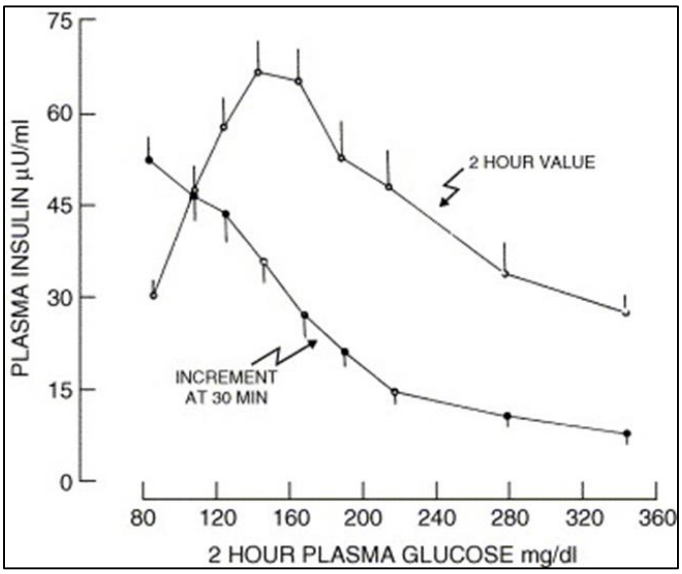

Figure 1.1. Relationship between 2 h plasma glucose with 30 min and 2 h plasma insulin values during oral glucose tolerance tests. (It shows the dichotomy between 30min and 2h insulin values across a wide range of glucose values) (Leahy, 2005)

Many subsequent studies have highlighted the fact that T2D appears in insulin resistant patients only when β-cells are not physiologically functional (Leahy, 2005; Poitout & Robertson, 2002; Prentki, Joly, El-Assaad, & Roduit, 2002). This explains why a high proportion of obese people do not develop T2D; since functional β-cells can compensate for insulin resistance of the peripheral tissues by increasing the amount of insulin secreted into the blood. Through a mechanism called compensation, β-cells increase in mass and physiological function, leading to elevated levels of insulin secretion in response to glucose and other secretagogues (Fig. 1.2) (Prentki & Nolan, 2006). When β-cells can no longer compensate for the insulin resistance, the progression toward T2D increases (Butler et al., 2003; Leahy, 2005). Therefore, obesity induced

insulin resistance and β-cell dysfunction are the two major risk factors for T2D (Prentki & Nolan, 2006; Reaven, 1997).

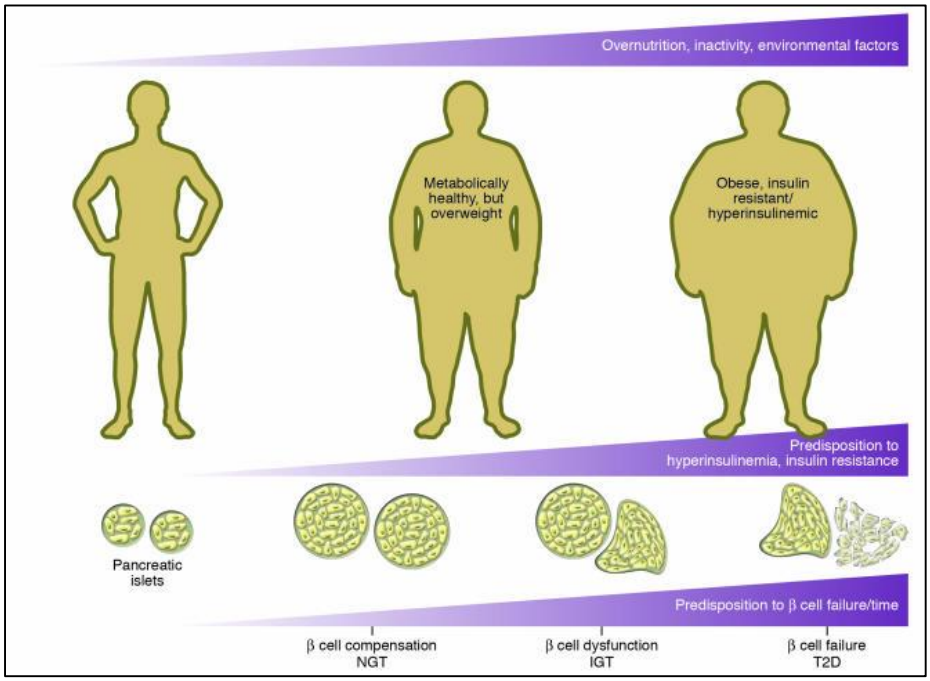

Figure 1.2. Pathogenesis of type 2 diabetes (Prentki & Nolan, 2006)

1.3 Obesity and type 2 diabetes.

Energy homeostasis plays a large role in the survivor of human species, which is a precise balance between energy intake and energy expenditure (Woods, Seeley, Porte, & Schwartz, 1998). Normal body weight is maintained when the energy intake (macronutrient intake) is equal to the energy expenditure (macronutrient oxidation) (Imbeault, Saint-Pierre, Almeras, & Tremblay, 1997). The life style of humans has changed through time. In the past, most people did more physical and hard work to obtain a sufficient life style and earn their living, and energy homeostasis is well balanced. In recent years this balance has changed, due to increasing technology and increasing wealth (leading to many people having lower levels of occupational physical activity). In parallel, the development of the fast food industry has led to food choices shifting to highly caloric meals rich in saturated fatty acids and starch but low in fiber, together with sugar-sweetened beverages at relatively low cost (Mela, 2001). In the presence of an inactive lifestyle, energy intake has often exceeded the daily energy expenditure. This excess

energy is mostly stored in the form of triacylglycerol (TG) in different tissues in the body, contributing to increase body weight and eventually obesity (Alappat & Awad, 2010). As a result, the prevalence of obesity around the world has increased over the last years; and obesity has become a major social and economic burden, especially in developed countries. A report from the National Diabetes Surveillance System indicated that approximately 25% of all Canadian adults are obese as are 10% of children (Anis et al., 2010).

1.3.1 Insulin resistance.

The association of obesity with systemic insulin resistance is thought to be a primary cause for cardiovascular disease, hypertension, T2D and other diseases (Guo, 2014). Insulin resistance is a condition characterized by the inability of target tissues, such as skeletal muscle, liver or adipose tissue, to respond to insulin. As a result insulin can't function properly and higher levels of insulin are needed to achieve the same metabolic effects. Insulin resistance develops mostly in people who are overweight, obese and in people who live an inactive lifestyle. Both obesity and T2D are associated with insulin resistance; however, most obese insulin-resistant individuals do not develop hyperglycemia, which occurs in those with co-existing β-cell dysfunction. The degree of insulin resistance is determined in part by the level of FFA in the plasma and impaired β-cell function (Kahn, Hull, & Utzschneider, 2006). There are many mechanisms that have been proposed to link obesity with insulin resistance and T2D, including (i) increased production of adipokines and cytokines, that contribute to insulin resistance [such as tumor necrosis factor-α (TNF- α) and resistin (Deng & Scherer, 2010)]; (ii) increased abdominal fat deposition, especially in the liver and skeletal muscle (Larson-Meyer et al., 2011); and (iii) mitochondrial dysfunction and the activation of protein kinase C isoforms by diacylglycerol (Erion & Shulman, 2010; Morino, Petersen, & Shulman, 2006), which could be an important defect linking obesity to diabetes, both by decreasing insulin sensitivity and by compromising β-cell function (Bournat & Brown, 2010) (Fig. 1.2).

In obese individuals, free fatty acid (FFA) levels in the plasma are increased and correlate positively with the degree of insulin resistance (Capurso & Capurso, 2012). Lipolysis in adipocytes is responsible for the increase in FFA. In the fasting state of healthy individuals, insulin levels are decreased and glucagon levels are elevated, which will lead to the increased activity of the lipase enzymes, and lipolysis in the adipocytes. Tissues such as the liver and

skeletal muscle use dispose of the generated FFA through fatty acid oxidation to provide energy. In obese subjects, the regulation of lipolytic enzymes in adipose tissues is disrupted, as insulin can't suppress lipolysis, resulting in elevated lipolysis generated FFA in the plasma (Arner & Langin, 2014). The role of FFA in inducing insulin resistance in skeletal muscle and liver is well known as shown in (Fig. 1.3) (Morino et al., 2006).

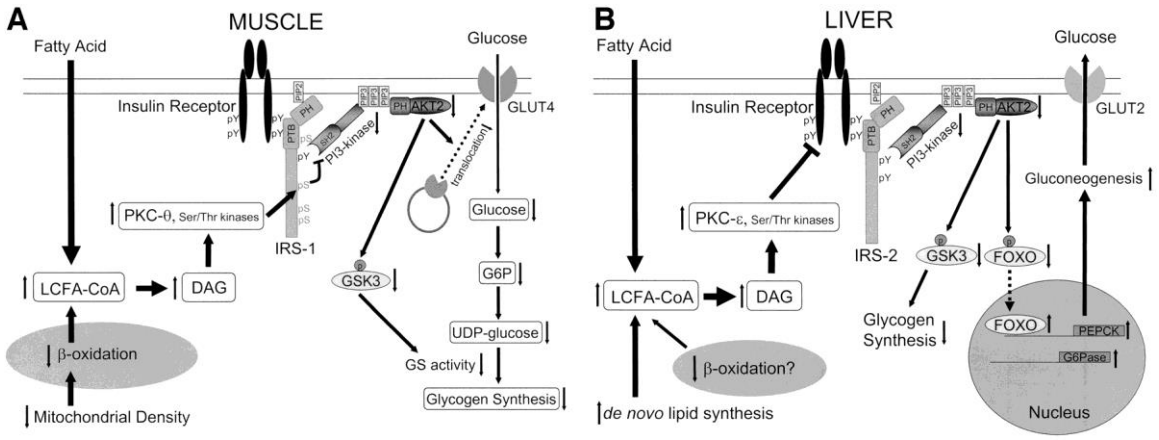

Figure 1.3. The molecular mechanism of fat-induced insulin resistance in skeletal muscle (A) and liver (B). A: Increases in intramyocellular fatty acyl CoAs and diacylglycerol due to increased delivery from plasma and/or reduced β-oxidation due to mitochondrial dysfunction activate serine/threonine kinases such as protein kinase C (PKC-θ rodents, PKC-β and -δ humans) in skeletal muscle. The activated kinases phosphorylate serine residues on IRS-1 and inhibit insulin-induced PI 3-kinase activity, resulting in reduced insulin-stimulated AKT2 activity. Lowered AKT2 activity fails to activate GLUT4 translocation, and other downstream AKT2-dependent events, and consequently insulin-induced glucose uptake is reduced. B: Increases in hepatic diacylglycerol content due to increased delivery of fatty acids from the plasma and/or increased de novo lipid synthesis and/or reduced β-oxidation activate protein kinase C-ε (and potentially other serine kinases), leading to reduced insulin receptor kinase activity and reduced IRS-2 tyrosine phosphorylation, resulting in reduced insulin stimulation of glycogen synthase activation and decreased phosphorylation of forkhead box protein O (FOXO), leading to increased hepatic gluconeogenesis. DAG, diacylglycerol; PTB, phosphotyrosine binding domain; PH, pleckstrin homology domain; SH2, src homology domain; GSK3, glycogen synthase kinase-3 (Morino et al., 2006).

1.3.1.1 Insulin resistance in skeletal muscles.

Skeletal muscles account for about 75% of the glucose clearance (Klip & Paquet, 1990). Insulin, once secreted into the bloodstream, binds to its receptor on the surface of the myocytes and activates insulin-receptor substrate 1 (IRS-1). Activation of IRS-1 triggers a signaling cascade which results in the translocation of glucose transporter 4 (GLUT4) at the plasma membrane, the entry of glucose and lowering glycaemia. Glucose is then metabolized for energy or stored by the muscle as glycogen. Studies in insulin resistant, obese with normal glucose tolerance (NGT) or with T2D individuals, have shown that insulin resistance is partly caused by decreased activation of IRS-1 by the insulin receptor (Cusi et al., 2000). This decrease is caused by phosphorylation of Ser residues of the IRS-1. It results in a reduction of GLUT4 translocation to the membrane and glucose uptake, which contributes to increase blood glucose levels and reduce the capacity of myocytes to store energy as glycogen. The presence of GLUT4 in the plasma membrane of muscle cells is essential for proper insulin sensitivity because the mutation of this transporter gene in the muscle results in severe glucose intolerance (Zisman et al., 2000).

1.3.1.2 Insulin resistance in adipose tissue.

Adipose tissue has the role of storing excess nutrients in the form of triacylglycerol (TG) in lipid droplets (Guilherme, Virbasius, Puri, & Czech, 2008). These lipids can then be hydrolyzed in the fasting state to provide energy. Adipocytes have the same glucose transporter as muscles, GLUT4, and its translocation to the membrane by the action of insulin and have the same regulation mechanism. In hyperglycemia, insulin stimulates lipogenesis in adipocytes and activation of key enzymes in this pathway (such as pyruvate dehydrogenase (PDH), acetyl-CoA carboxylase (ACC) and fatty acid synthase (FAS)). Insulin also inhibits lipolysis and decreases the activity of some lipases like hormone-sensitive lipase (HSL) (Meijssen et al., 2001). Overall, insulin induces the storage of glucose as fat.

Another function of the adipose tissue is to secrete various adipokines (hormones), such as leptin, resistin, and adiponectin, as well as pro-inflammatory molecules including monocyte chemotactic protein-1 (MCP-1) and interleukin 6 (IL-6) to regulate appetite, energy expenditure and insulin resistance (Kershaw & Flier, 2004). In obesity with insulin resistance, there is a decrease in the expression of adiponectin (a hormone associated with an increase of insulin

sensitivity) and an increase in the secretion of the molecule chemoattractant MCP-1 (Sartipy & Loskutoff, 2003). This induces components of the immune system, like macrophages, which secrete the pro-inflammatory molecule TNF- α in adipose tissue (Hotamisligil, Arner, Caro, Atkinson, & Spiegelman, 1995). This molecule increases lipolysis and decreases lipogenesis, causing an increase in the concentration of fatty acids in the circulation. The rise in fatty acids has a direct impact on other tissues by stimulating gluconeogenesis in the liver and by inhibiting glucose uptake in the liver and muscles, thus contributing to the increase in glycaemia (Bajaj & Defronzo, 2003). In addition, the TNF- α is an inhibitor of the insulin signaling pathway that contributes to insulin resistance in adipose tissue and muscle.

1.3.1.3 Insulin resistance in the liver.

The liver is another important organ for glucose and fat metabolism and systemic energy homeostasis that plays a role in insulin resistance. During fasting, the needs of glucose in the brain are mostly fulfilled by the liver gluconeogenesis. In contrast, in the fed state, the liver can store the glucose as glycogen or lipids. In rodents, the liver and β-cell expresses the glucose transporter 2 (GLUT2) having a great ability to transport glucose (due to its small affinity for this substrate and high Vmax) and the expression of GLUT2 is not regulated by insulin (Thorens, 2015).

Insulin controls several hepatic functions. First, it inhibits the production of glucose by the liver in two ways: by reducing glycogenolysis (glycogen breakdown to glucose) via the modulation of gene expression of glycogen metabolism (Leclercq, Da Silva Morais, Schroyen, Van Hul, & Geerts, 2007) and decreasing gluconeogenesis by inhibiting the rate limiting enzyme, phosphoenolpyruvate carboxykinase (PEPCK) (Sutherland, O'Brien, & Granner, 1996). Furthermore, insulin regulates the metabolism of fatty acids by the liver by inhibiting the synthesis of the lipoprotein VLDL (very low-density lipoprotein) by increasing the degradation of the ApoB protein and increasing lipogenesis (Meshkani & Adeli, 2009).

The action of insulin on hepatocytes is both direct via its binding to its receptor on the surface of hepatocytes (Michael et al., 2000) and indirect by modulating the circulating concentrations of glucose and fatty acid by affecting other tissues (Bergman & Ader, 2000). Insulin resistance in the liver has severe consequences on glucose homeostasis by causing a

decrease in the capacity of the hormone to reduce gluconeogenesis, and by promoting glycogenolysis (Meshkani & Adeli, 2009). Thus, liver-specific insulin receptor knockout mice exhibit dramatic insulin resistance, severe glucose intolerance, and a failure of insulin to suppress hepatic glucose production and to regulate hepatic gene expression (Michael et al., 2000).

1.4 Genetics of type 2 diabetes.

The heritability of T2D is estimated to be higher than 50%, based on results from twin studies (Nolan et al., 2011). T2D is generally considered as a complex syndrome of a polygenic nature. With the introduction of high-throughput genotyping techniques, genome-wide association studies (GWAS) have identified over 70 loci associated with T2D, such as ACDC, CAPN10, ENPP1, HNF4A, TCF7L2, SLC308A, IDE-KIF11, EXT2-ALX4 (Sladek et al., 2007; Voight et al., 2010). A greater number of these loci are associated with impaired β-cell function than with impaired insulin sensitivity and this may reflect the technical complexity of identifying loci associated with insulin resistance (Nolan et al., 2011). Alternatively, if as discussed above insulin resistance is largely a protective process from fuel excess (Nolan et al., 2015) and a biomarker of defective energy homeostasis rather than directly implicated in impaired glucose homeostasis, then there is no reason to believe that insulin resistance genes should be found in T2D genetic studies. Thus, adipose tissue selective insulin receptor knockout protects against obesity and obesity-related glucose intolerance (Bluher et al., 2002) and a muscle-specific insulin receptor knockout exhibits features of the metabolic syndrome without altering glucose tolerance (Bruning et al., 1998).

One of the prominent T2D loci with a high odd ratio is transcription factor 7- like 2 (TCF7L2), which is involved in the Wnt signaling pathway. In response to activation of the wnt pathway, TCF7L2 mediates the activation of the pro-glucagon gene and the production of the insulin secreting promoting agent GLP-1 by intestinal L-cells (Jin & Liu, 2008). *In vitro* and clinical studies confirm that expression of variant TCF7L2 can lead to increased risk of developing T2D due to a defect in insulin secretion (da Silva Xavier et al., 2012; McCarthy, Rorsman, & Gloyn, 2013). Another susceptibility gene is the solute carrier family 30, member 8 (SLC30A8), encoding the zinc carrier ZnT8 (zinc transporter 8) (Sladek et al., 2007). This carrier is present on the surface of insulin granules secreted by β-cells and transports zinc molecules

important for the formation of the proinsulin hexamer. Also it was shown that increased expression of the ZnT8 is associated with increase in insulin secretion (Chimienti et al., 2006). Other T2D risk genes that are important for β-cell or islet function include the regulatory subunit Kir6.2 and the Insulin Degrading Enzyme (IDE); as well as the Hematopoietically Expressed Homeobox protein (HHEX), which is an important regulator of pancreas development and islet function (Sladek et al., 2007; Zhang, McKenna, Bogue, & Kaestner, 2014).

Other T2D risk genes are involved in insulin resistance, including genes encoding (i) the Peroxisome Proliferator-Activated Receptor Gamma (PPARG) transcription factor; (ii) the Ectonucleotide Pyrophosphatase/Phosphodiesterase protein (ENPP), a transmembrane glycoprotein inhibiting insulin receptor; and (iii) IRS-1, a protein associated with the insulin receptor (Bonnefond, Froguel, & Vaxillaire, 2010; Rung et al., 2009; Sladek et al., 2007; Voight et al., 2010).

Large-scale sequencing does not support the idea that lower-frequency variants have a major role in predisposition to T2D (Fuchsberger et al., 2016). Despite the numerous genes identified so far, their exact role in the pathogenesis of T2D is still unclear. Many efforts are currently made to unravel the mechanisms implicated and this may eventually lead to novel targets for T2D therapy.

1.5 Animal models of type 2 diabetes.

Due to the high prevalence of T2D worldwide, extensive research is being performed to develop new anti-diabetic drugs and determine their mechanism of action. Therefore, a number of T2D animal models have been developed and improved over the years, of which rodent models are the most prevalent. However, none of the models can represent the onset and development of human T2D in all its details. Nevertheless, the existing rodent models provide opportunities to study the complex pathogenesis and progression process of T2D (Kaplan & Wagner, 2006).

As mentioned above, T2D can be classified into two groups based on BMI and there are rodent models for each group. The typical examples of non-obese or lean T2D model are the Goto-Kakizaki rat (GK rat) and Spontaneously Diabetic Torii (SDT) rat (Table 1) (Goto, Kakizaki, & Masaki, 1976; King, 2012; Wang et al., 2013). In model systems, obesity can be induced by naturally occurring mutations, genetic manipulation or high fat feeding (Wang et al.,

2013). The genetically manipulated obese models also can be divided into two groups having either monogenic or polygenic backgrounds (Chatzigeorgiou, Halapas, Kalafatakis, & Kamper, 2009). These models are severely obese, hyperinsulinemic and insulin resistant, so drugs such as insulin sensitizers and anti-hyperglycemic agents are often tested in these models, in an attempt to determine their ability to decrease glycemia, reduce body weight, promote insulin secretion and improve peripheral insulin sensitivity (Hariri & Thibault, 2010; Oakes et al., 2005).

Monogenic models of obesity are commonly used in T2D research even though monogenic mutations rarely cause obesity in humans. A defect in leptin signaling is one of the most widely used monogenic models of obesity. Leptin has an important role in inducing satiety, so the lack of functional leptin can cause hyperphagia and eventually obesity (King, 2012). The $Lep^{ob/ob}$ mice, $Lepr^{db/db}$ mice and Zucker fatty diabetic rat (ZDF) are the most typical examples of T2D obese models with monogenic backgrounds (Table 1) (H. Chen et al., 1996; Lindstrom, 2007; Phillips et al., 1996; Srinivasan & Ramarao, 2007; Yang & Santamaria, 2006).

The polygenic models gives a variety of genotypes and conditions that may provide a more accurate model of human T2D (Wang et al., 2013). These models have been used in different studies designed to reverse the symptoms of T2D, understand more about the interplay of obesity and glucose homeostasis or study diabetic complications (Buck et al., 2011; Kluth et al., 2011; Yoshinari & Igarashi, 2011). KK and NZO mice and OLETF rats are examples of commonly used obese T2D models with polygenic backgrounds (Table 1) (Andrikopoulos et al., 1993; Clee & Attie, 2007; Kawano et al., 1992; King, 2012; Wang et al., 2013). The polygenic models of T2D include the well-characterized obese T2D model of high fat feeding used in this study, which involves inducing T2D by feeding a high fat diet to non-obese mice without any genetic modification (Peyot et al., 2010; Winzell & Ahren, 2004).

Table 1.1. Details of some animal models of type 2 diabetes:

Name	Characteristics	Possible uses	(ref.)
Non-obese models			
GK rat	Glucose intolerance Defective glucose-induced insulin secretion	Treatments to improve β-cell function and survival Studying the mechanisms of diabetes complications (renal, retinal and peripheral nerve lesions)	(Goto, Kakizaki et al. 1976) (King 2012)
SDT rat	Glucose intolerance, Hyperglycemia Hypoinsulinemia, Hypertriglyceridemia		(Wang, Sun et al. 2013)
Obese models (Monogenic)			
Lep$^{ob/ob}$ mice	Severely obese, Hyperinsulinaemia Hyperlipidaemia, Lack of complete β-cell failure		(Yang and Santamaria 2006) (Lindstrom 2007)
Lepr$^{db/db}$ mice	Obese, Hyperglycaemic, Hyperinsulinaemic, Hyperphagic	Treatments to improve insulin resistance Treatments to improve β-cell function	(Chen, Charlat et al. 1996) (Srinivasan and Ramarao 2007)
ZDF Rats	Obese, Hyperinsulinaemic, Hyperlipidaemic, Hyperphagic, Hypertensive, IGT		(Phillips, Liu et al. 1996) (Srinivasan and Ramarao 2007)
Obese models (polygenic)			
KK mice	Mildly obese, Severe hyperinsulinaemia Hyperleptinaemic, Insulin resistance(muscle and adipose tissue)		(Clee and Attie 2007) (King 2012)
OLETF rat	Mild obesity, Hyperinsulinemia, Hypertriglyceridemia, Insulin resistance, Hyperglycaemia	Treatments to improve insulin resistance Treatments to improve β-cell function	(Kawano, Hirashima et al. 1992) (Wang, Sun et al. 2013)
NZO mice	Obese, Hyperinsulinaemic, Hepatic insulin resistance, Leptin resistance (hyperleptinaemic), Hyperphagic		(Andrikopoulos, Rosella et al. 1993) (King 2012)
Induced obesity			
High fat feeding (mice or rats)	Obese, Hyperinsulinaemic, Altered glucose homeostasis	Treatments to prevent diet-induced obesity Treatments to improve β-cell function and insulin resistance	(Winzell and Ahren 2004) (Peyot, Pepin et al. 2010)

1.5.1 Diet induced obesity mouse model.

The high fat feeding model of C57BL/6 mice was first described in 1988 (Surwit, Kuhn, Cochrane, McCubbin, & Feinglos, 1988). In this diet induced obesity (DIO) model, in response to the hyperlipidemic diet (high fat diet, around 60% of energy derived from fat), the mice become obese, hyperinsulinemic and have altered glucose homeostasis (Winzell & Ahren, 2004). The DIO mice can show differences in body weight in comparison with control mice fed a normal diet within a week of starting the high fat diet (HFD) (Peyot et al., 2010; Winzell & Ahren, 2004). To have a larger and more consistent difference in weight gain compared to normal diet mice, the mice are fed the HFD for several weeks (typically 8-12 weeks). The weight gain is associated with insulin resistance and lack of β-cell compensation; and leads to impaired glucose tolerance and mild fed and fasted hyperglycemia (King, 2012).

Since obesity in this model is induced by an environmental factor (diet) rather than genetic factors, this model is thought to mimic the human situation more accurately than genetic models of obesity induced diabetes. It was recently found that C57BL/6 mice supplied by the Jackson Laboratory (C57BL/6J) carry a five-exon deletion in the nicotinamide nucleotide transhydrogenase gene (*Nnt*), which encodes a mitochondrial enzyme involved in NADPH production (Aston-Mourney et al., 2007; Toye et al., 2005). Importantly, C57BL/6 supplied by Taconic or Charles River (C57BL/6N) do not have the mutation (Simon et al., 2013). This *Nnt* mutation has been associated with impaired glucose-stimulated insulin secretion (GSIS) and glucose intolerance compared to mouse strains carrying the wild-type *Nnt* (Fergusson et al., 2014), and mice on a mixed NJ background also show reduced GSIS *in vivo* and *ex-vivo* in comparison to NN mice (Attane et al., 2016). In addition, transgenic expression of the wild-type *Nnt* gene in C57BL/6J rescues β-cell function and glucose tolerance (Freeman, Hugill, Dear, Ashcroft, & Cox, 2006). All this suggests that caution should be taken when studying β-cell function as well as glucose and energy homeostasis in C57BL/6J mice.

The C57BL/6N mouse model can be stratified according to their body weight at 8 weeks of HFD into low (LDR) and high responders (HDR) to the high fat diet , which allows the study of different phases of the development of T2D- and obesity-linked β-cell dysfunction (developed in the Prentki Lab, (Peyot et al., 2010)). HDR mice are more obese, insulin resistant, glucose intolerant, hyperglycemic and have a more defective β-cell function than LDR mice. HDR mice

partially compensate for insulin resistance by increasing β-cell mass and proliferation. LDR mice have an intermediate phenotype and are only slightly glucose intolerant and hyperglycemic. Compared to LDR islets, HDR islets show more defective GSIS along with additional alterations in islet lipid metabolism (i.e. increased free fatty acid oxidation and free cholesterol levels). Islet glycerolipid/free fatty acid (GL/FFA) cycling and lipolysis are defective in both DIO groups. Also, the glucose-stimulated ATP content was markedly decreased in DIO islets. The LDR and HDR groups allow for analysis of islet β-cell mass and function in response to different levels of insulin resistance with corresponding very mild perturbation of glucose homeostasis and overt but mild hyperglycemia, respectively. We propose, that when extended to obese humans, these two groups correspond to the pre-diabetes and early diabetes phases of T2D (Peyot et al., 2010).

1.6 The role of β-cells in diabetes.

The main role of β-cells is to secrete insulin in response to different signals in order to maintain glycemia in a specific range. The β-cells have to also maintain the synthesis of proinsulin with correct post-translational modification; ensure insulin secretory granules are ready for secretion; sense nutrient concentrations in blood; produce metabolic coupling factors (MCF) linking glucose and other fuels metabolism to insulin exocytosis; sense various neurohormonal signals; and appropriately release insulin granules by activation of a complex exocytosis machinery. Hence, any alteration in one of those mechanisms controlling insulin secretion may lead to hyperglycemia and the development of diabetes.

1.6.1 The endocrine pancreas.

β-cells are part of the islets of Langerhans of the pancreas. These islets correspond to the region that secretes endocrine hormones in the pancreas and comprise 1 to 2% of the total mass of the pancreas. The islets are composed of five cell types: α-cells produce glucagon; β-cells make up more than 90% of the islets and synthesize insulin; and δ-cells secrete somatostatin which account for about 5% of the total islet cell mass. The islet also includes a small number of PP and ε-cells, which produce pancreatic polypeptide and ghrelin, respectively (Elayat, el-Naggar, & Tahir, 1995).

1.6.2 Glycemic control by the β-cell

Glucose homeostasis in the blood is primarily regulated by two main hormones glucagon and insulin secreted by pancreatic α- and β-cells. When glucose levels in the blood are low, the α-cells secrete glucagon, which promotes production of glucose by the liver by activating the degradation of glycogen storage by glycogenolysis and inducing synthesis of glucose by gluconeogenesis. Both mechanisms lead to the release of glucose in the blood to restore normal glycemia. In contrast, insulin is secreted by β-cells in response to hyperglycemia. Insulin plays a key role in regulating blood sugar by acting on peripheral tissues such as liver, adipose tissue and skeletal muscle. The elevated insulin levels in the blood promote the glucose entry into skeletal muscle and adipose tissue to be stored as glycogen and triglycerides, respectively. In addition, insulin induces the inhibition of gluconeogenesis by the liver and the production of free fatty acids and glycerol from adipose tissue aiming to restore normal glycemia (DeFronzo, 2004). Thus, glycerol is used by gluconeogenesis in the liver to produce more glucose particularly in the fasted state.

The main function of β-cells is to maintain glucose homeostasis via the secretion of insulin in response to hyperglycemia. Other than glucose, there are fuel and non-fuel stimuli for insulin secretion by β-cells, including amino acids (leucine, glutamine and arginine); fatty acids; neurotransmitters (e.g. acetylcholine); and incretins (gut-derived hormones) such as gastric inhibitory polypeptide (GIP) and glucagon-like peptide-1 (GLP-1) (DeFronzo, 2004; Leclerc et al., 2004; Maechler & Wollheim, 2001).

1.6.3 Glucose-induced insulin secretion by β-cells.

Insulin secretion in response to glucose is biphasic with a rapid first phase and a long sustained second phase (Straub & Sharp, 2002). The first phase peaks within 5min and results primarily from the exocytosis of granules docked on the plasma membrane (Prentki, Matschinsky, & Madiraju, 2013). The first phase of GSIS involves the so-called classical K_{ATP}/Ca^{2+} signaling pathway of secretion (Prentki et al., 2013). In this pathway glucose rapidly enters the β-cells via GLUT2 in mice and GLUT1 in humans (Hiriart & Aguilar-Bryan, 2008). Then glucose is phosphorylated by the high Km enzyme glucokinase and is further metabolized in glycolysis and subsequently in the tricarboxylic acid (TCA) cycle and provides reducing equivalents (NADH)

for the respiratory chain within mitochondria to produce ATP (Herman & Kahn, 2006). Then ATP is transported into the cytoplasm, where it binds to the Kir6.2 subunit of the K_{ATP} channel leading to K_{ATP} channel closure and depolarisation of the plasma membrane (Ashcroft, 2005). The depolarisation triggers the opening of the L-type voltage-gated calcium channels, which leads to the influx of Ca^{2+} ions from the extracelluar space to the cytoplasm which triggers the exocytosis of insulin secretory vesicles (Straub & Sharp, 2002). This pathway is called the K_{ATP} -channel dependent insulin secretion pathway; since calcium uptake and insulin release both depend on potassium channel closure by ATP (Fig. 1.4).

In the second phase of GSIS, insulin is released in response to increased intracellular free calcium levels and additional coupling factors for secretion. The mechanism of the second phase it less well understood, but is known to be affected by changes in the concentration and activity of cAMP, phospholipase C, plasma membrane phosphoinositides (Straub & Sharp, 2002; Tengholm & Gylfe, 2009) and additional molecules, such as the generation of mitochondrial NADH, malonyl-CoA, long chain-CoA esters and their derivatives (Prentki, 1996; Prentki, Tornheim, & Corkey, 1997). Additional candidates MCF have more recently been identified and these will be discussed below. With respect to the mode of action of long chain free fatty acids on insulin secretion, it involves both their intracellular metabolism and the G-protein-coupled receptor GPR40/FFAR1 (Burant, 2013; Poitout & Lin, 2013). There are some differences in insulin secretion in different species especially in the second phase. In mouse islets *ex-vivo*, the second phase insulin secretion is small and even negligible, while in the islets from rats and humans, second phase insulin secretion contributes to more than 50% of total insulin released during the first hour of insulin secretion (Zawalich, Bonnet-Eymard, & Zawalich, 1997). However, in the presence of exogenous fatty acids GSIS is quite prominent even in mouse islets (Ferdaoussi et al., 2012).

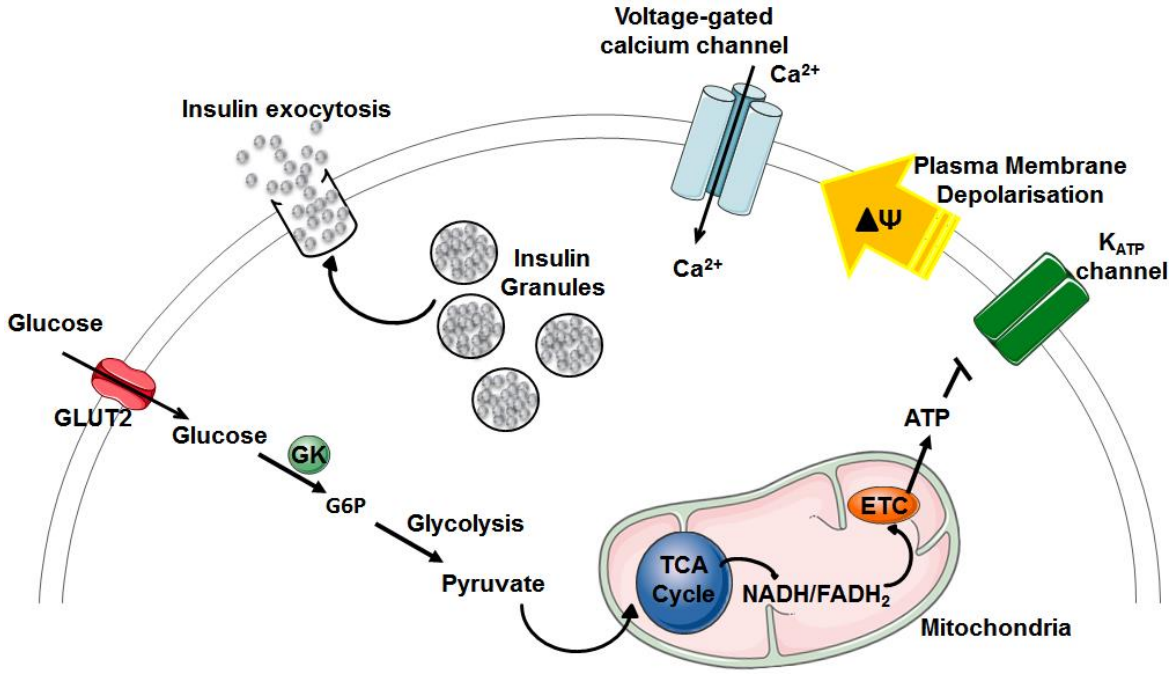

Figure 1.4. Classical pathway of insulin secretion in the β-cell. Glucose is transported into the cell via GLUT2 (mouse). Glucose is then metabolised in the cytosol and mitochondria to yield ATP. ATP closes the K_{ATP} -channels on the plasma membrane, which leads to membrane depolarisation. This triggers the opening of voltage-gated calcium channels and calcium influx into the cytosol will stimulates insulin granule exocytosis. G6P = glucose-6-phosphate, GK = glucokinase, ETC = electron transport chain.

1.6.3.1 Fatty acids and amino acids in insulin secretion.

Pancreatic β-cells have different mechanisms to sense fuels and non-fuels in the plasma to release insulin and avoid hypoglycemia. Glucose is the most potent nutrient regulating insulin secretion in the β-cell. This is supported by many studies in mouse, rat and human islets that show that elevated glucose induces a biphasic insulin release (Henquin, Nenquin, Stiernet, & Ahren, 2006; Prentki et al., 1997). However, various fatty acids and amino acids also act as insulin secretagogues.

FFA effects on insulin secretion can be beneficial or harmful depending on the duration of exposure and the glucose concentration. Short-term exposure of β-cells to FFA enhances

insulin secretion at high glucose concentrations; but at normal glucose concentration, short-term β-cell exposure to FFA has only a small effect (Carpentier et al., 1999). On the other hand, long-term exposure of β-cells to FFA can lead to β-cell dysfunction, particularly at high glucose concentrations (termed glucolipotoxicity). The potential mechanisms of the short term effect of FFA on insulin secretion can be explained by different pathways (Nolan, Madiraju, Delghingaro-Augusto, Peyot, & Prentki, 2006). One mechanism involves intracellular metabolism and the AMP-activated protein kinase (AMPK)/malonyl-CoA (Mal-CoA)/long-chain acyl-CoA (LC-CoA) signaling network (Prentki et al., 2002; Roduit et al., 2004). At high glucose, Mal-CoA is elevated in the β-cell and because it inhibits FA oxidation via its interaction with carnitine palmitoyltransferase 1, the rate limiting step of β-oxidation of FFA, FFA metabolism is directed to esterification, resulting in the increased availability of LC-CoA for the glycerolipid/ free fatty acid (GL/FFA) cycle which also produces MCF that enhance insulin secretion. At low glucose levels, Mal-CoA levels decrease and FA oxidation is enhanced, which lowers the availability of LC-CoA to enter GL/FFA cycle to produce MCF and leads to reduced insulin secretion (Prentki et al., 2002). In this metabolic lipid signal network AMPK phosphorylates acetyl-CoA carboxylase (ACC) and MCD, the enzymes that regulate Mal-CoA synthesis and degradation, respectively.

Another mechanism where FFA can affect insulin secretion is through the FFA receptor GPR40/FFAR1. This G-protein-coupled receptor is highly expressed in mouse, rat and human islets and various β-cell lines; and is activated by medium to long chain FFA. Overexpression of GPR40 in pancreatic β-cells enhances GSIS and improves glucose tolerance in normal and diabetic mice (Nagasumi et al., 2009). Conversely, GPR40 KO mice show reduced fatty acid amplification of GSIS *in vivo* and *ex vivo* (Kebede et al., 2008). It is estimated that 50% of FFA-amplified insulin secretion is contributed by GRP40, while the rest is contributed by other mechanism such as intracellular FFA metabolism (Kebede et al., 2008; Latour et al., 2007).

Amino acids, such as L-alanine and glutamine and leucine, can induce insulin secretion (Fajans, Floyd, Knopf, & Conn, 1967). L-alanine can be metabolized to produce ATP, a MCF for insulin secretion (P. Newsholme, Gaudel, & McClenaghan, 2010). Glutamine is converted to glutamate via glutaminase, which is used by glutamate dehydrogenase (GDH) in the mitochondrial to produce α-ketoglutarate (α-KG) that enters the TCA cycle and produces ATP and various anaplerosis-derived MCF (Prentki et al., 2013). Leucine is also known to activate

GDH and enhances the effect of glutamine in inducing insulin secretion via the TCA cycle (Malaisse et al., 1982).

1.6.3.2 Metabolic coupling factors (MCF) of insulin secretion.

As mentioned above there are many fuel and non-fuel stimuli, such as glucose and FFA, that can activate β-cell metabolism and regulate insulin secretion. Depending on the availability of these fuels, their metabolism leads to the production of various MCFs to promote insulin release (Prentki et al., 2013). These MCFs can come from different metabolic pathways like TCA cycle, GL/FFA cycling and electron transport chain (Fig. 1.5).

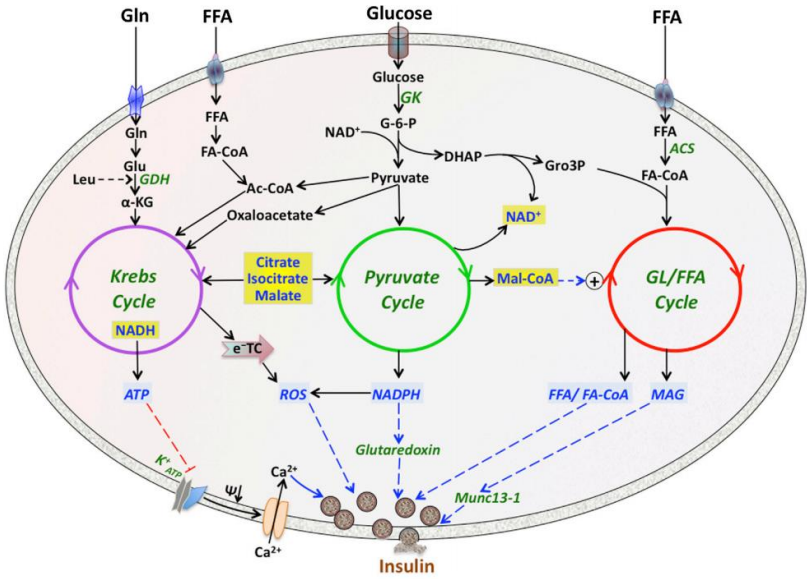

Figure 1.5. Relationship between three fuel-driven metabolic cycles that generate MCFs in the β-cell and insulin secretion. Glucose, FFAs, and glutamine (Gln) are metabolized in the β-cell to provide substrates that enter the Krebs cycle, pyruvate cycle, and glycerolipid/FFA (GL/FFA) cycle. Glutamate dehydrogenase (GDH), α-ketoglutarate (α-KG), GDH is allosterically by Leu, FFA-CoA esters (FA-CoA), acyl-CoA synthase (ACS), acetyl-CoA (Ac-CoA), glucokinase (GK), glucose-6-phosphate (G-6-P), dihydroxyacetone phosphate (DHAP), glycerol-3-phosphate (Gro3P), malonyl-CoA (MalCoA), mitochondrial electron transport chain (eTC). (Prentki et al., 2013).

1.6.3.2.1 Anaplerosis and cataplerosis-derived signals.

Cataplerosis and anaplerosis respectively represent the efflux of TCA cycle intermediates from mitochondria into the cytosol, and their replenishment. Both processes are quantitatively similar because the TCA cycle is not a sink for glucose carbons (Schuit et al., 1997). In β-cells, anaplerotic and cataplerotic pathways provide carbon precursors of MCF for insulin secretion. Pyruvate cycling is important in glucose-stimulated insulin secretion. Pyruvate carboxylase (PC) is well expressed in β-cells and its levels are reduced in islets isolated from T2D patients (Jensen et al., 2006). Decreasing PC activity either by a pharmacological inhibitor or by down-regulation decreases GSIS, while increasing its activity by overexpression increases insulin secretion (Farfari, Schulz, Corkey, & Prentki, 2000).

Pyruvate cycling allows high glycolytic flux via NADH re-oxidation and the production of different MCFs like Mal-CoA, glutamate, NADPH, and GTP (Guay, Madiraju, Aumais, Joly, & Prentki, 2007). Mal-CoA is formed by carboxylation of acetyl-CoA (catalyzed by ACC); and regulates fatty acid oxidation through the allosteric inhibition of carnitine palmitoyltransferase 1 (CPT1). The hypothesis that Mal-CoA acts as a MCF is supported by many studies and the level of Mal-CoA in response to glucose or Gln plus Leu is correlated with GSIS (Prentki et al., 2002; Roduit et al., 2004). Also, GSIS is reduced when ACC activity is decreased by specific inhibitors or downregulated, while overexpression of ACC leads to reducing the levels of Mal-CoA and consequently GSIS in the presence of FFA.

Glutamate directly enhances insulin granule exocytosis in β-cell lines, indicating that it could act as a MCF. It has been also shown that overexpression of glutamate decarboxylase in β cells reduces glutamate levels and GSIS (Vetterli et al., 2012). Also, humans and mice deficient in GDH develop hyperinsulinemia (Stanley et al., 1998). NADPH is also considered as a MCF for insulin secretion (MacDonald, Chaplen, Triplett, Gong, & Drought, 2006; Pongratz, Kibbey, Shulman, & Cline, 2007). The ratio of NADPH/$NADP^+$ correlates with GSIS in rodent islets as well as in different β-cell lines (Gray, Alavian, Jonas, & Heart, 2012). There are two suggested mechanisms of the action for NADPH: the redox protein glutaredoxin (GRX) and the voltage dependent K+ channels (Kv). The reduced and oxidized forms of GRX are controlled by NADPH and $NADP^+$ (Ivarsson et al., 2005). Overexpression of GRX increases GSIS and down regulation of GRX reduces GSIS in rat islets (Reinbothe et al., 2009). There is evidence that

NADPH can directly bind to the β subunit of the K_v channel to regulate its activity and its inhibition favors sustained plasma membrane depolarization and hence Ca^{2+} influx that promotes insulin secretion (Kilfoil, Tipparaju, Barski, & Bhatnagar, 2013).

GTP has been proposed to be a MCF as well and GTP levels increase in parallel with increasing glucose concentration (Kibbey et al., 2007). GTP is produced by the TCA cycle in the mitochondrion by a GTP-specific isoform of succinyl-CoA synthase (GTP-SCS) and reduced levels of this enzyme are associated with decreased insulin secretion (Kibbey et al., 2007). It has also been shown that GTP can directly promote insulin exocytosis permeabilized β-cells in a calcium-independent manner (Kowluru, 2003).

1.6.3.2.2 Electron transport-derived signals.

The mitochondrial electron transport chain (ETC) is linked to insulin secretion by affecting the energy state of the β-cell and the production of ATP (Maechler, 2013). The ETC transfers electrons from complex I (NADH) and complex II ($FADH_2$) along the complexes on the inner membrane to complex IV where they are used to reduce oxygen to H_2O. The transfer of electrons is coupled to pumping of protons through complex I, III and IV into the inner membrane space, creating a membrane potential (proton gradient) across the inner mitochondrial membrane. When protons move down the proton gradient back to the mitochondrial matrix through complex V (ATP synthase), it is able to use the proton motive force, created by the proton gradient, to phosphorylate ADP to produce ATP (Duchen, 2004). ATP is then transported back to the cytoplasm where it is used as an energy source, and importantly also used as a signaling molecule to stimulate insulin secretion from β-cells (Maechler & Wollheim, 2001).

The ETC plays an important role in generating various MCFs, including ATP, ADP, AMP, cAMP, ROS and reduced cytochrome c, to promote GSIS. Inhibition of different complexes of the ETC is associated with reduced GSIS (Prentki et al., 2013). The role of different adenine nucleotides, including ATP, ADP and AMP in regulating K_{ATP} channels specially ATP is well known (Ghosh, Ronner, Cheong, Khalid, & Matschinsky, 1991; Loubatieres-Mariani, Chapal, Lignon, & Valette, 1979). ATP is also proposed to be required for insulin granule processing, and may be directly implicated in exocytosis. A correlation between elevated ATP levels and second phase insulin secretion in mouse islets has been shown. AMPK,

a fuel sensor and a negative regulator of insulin secretion, is also regulated by the AMP/ATP ratio. At high glucose levels, the AMP/ATP ratio is lower, which may indicate that ATP can play an important role in reducing AMPK activity (Lamontagne et al., 2009). ADP works in an opposite way from ATP; it is responsible for opening the K_{ATP} channels. At high glucose, reduced ADP levels contribute to closure of K_{ATP} channels. Furthermore, cAMP is also proposed to be a MCF in insulin secretion: at high glucose levels, the level of cAMP is elevated possibly because its formation is limited by ATP acting as a substrate for some adenylate cyclase isoforms (Prentki & Matschinsky, 1987), and oscillations of cAMP content in β-cells is well correlated with insulin secretion (Yajima et al., 1999).

In the ETC, complex I and complex III are the major sites for ROS formation (Q. Chen, Vazquez, Moghaddas, Hoppel, & Lesnefsky, 2003) that are produced physiologically in cells during nutrient oxidation. ROS (superoxide, the hydroxyl radical, and hydrogen peroxide (H_2O_2) are highly reactive compounds that can damage cells when present at high levels. Nevertheless, at relatively low concentrations, ROS can be signals in various cellular processes (Maechler et al., 2010). The role of ROS in β-cell function depends on its concentration and time of elevation. Chronic ROS exposure results in β-cell dysfunction. In contrast, acute ROS exposure may function as a MCF to promote insulin secretion (Leloup et al., 2009). Many studies have focused on studying H_2O_2 to investigate the effect of ROS on GSIS in the β-cell (P. Newsholme et al., 2009; Pi et al., 2007). Thus, H_2O_2 it is more stable, uncharged, and is a diffusible molecule unlike superoxide for example. On the technical part, the current ROS measurement tools are not very reliable and additional work is needed to test this possibility. However, the precise ROS targets in the β-cell for insulin secretion have not been identified yet (Prentki et al., 2013).

Studies have shown that glucose increases ROS levels in rodent islets and β-cell lines; and decreasing ROS levels by ROS scavengers reduces GSIS (Leloup et al., 2009; Pi et al., 2007). However, some studies show opposite results, as mice lacking the NADPH oxidase NOX2 (reduced production of superoxide) show increased rather than reduced insulin secretion (Li et al., 2012). In addition, GSIS does not change in the islets with overexpression of H_2O_2–inactivating catalase (Gurgul, Lortz, Tiedge, Jorns, & Lenzen, 2004). In sum there is no consensus concerning the role of ROS in GSIS and this may result from the different experimental conditions of the various studies, in particular under basal fuel conditions. This will

be further discussed in the ROS experimental part section of this thesis. Further work is needed to evaluate the role of ROS acting as MCF for insulin secretion.

1.6.3.2.3 GL/FFA cycling and lipid signaling for insulin secretion.

The glycerolipid/free fatty acid (GL/FFA) cycle was first described in 1965 (E. A. Newsholme & Crabtree, 1976). Since then, this cycle has been shown to be located at the center of metabolic networks, tightly linking glucose and FFA metabolism, and to play important roles in regulating many signaling molecules controlling numerous biological processes (Prentki & Madiraju, 2008, 2012). The GL/FFA cycle involves the esterification of FFA onto a glycerol backbone to synthesize glycerolipids followed by their hydrolysis with the release of the FFA that can be re-esterified to re-enter the cycle (Prentki & Madiraju, 2008).

Glucose metabolism increases both arms of GL/FFA cycle (lipogenesis and lipolysis), which are well correlated with GSIS (Prentki & Madiraju, 2012). It has been shown that blocking lipolysis by the panlipase inhibitor orlistat inhibits GSIS. Similarly, decreasing various lipase (ATGL and HSL) activities by either specific inhibitors or down regulation or gene deletion reduces GSIS (Peyot et al., 2009; Peyot et al., 2004; T. Tang et al., 2013). All these reports strongly support the role of GL/FFA cycling in insulin secretion.

Different lipid species, including DAG, MAG, FFA and FA-CoA, generated via GL/FFA cycling may function as MCF to promote insulin secretion (Prentki et al., 2013). Recently it was shown that MAG, especially 1-MAG species with long-chain saturated fatty acids, is a lipid signal that contributes to GSIS as a MCF (Zhao et al., 2014). In the β-cells, ABHD6, rather than MAGL, is the main MAG hydrolase. It been shown that genetic or siRNA knockdown of ABHD6 enhances GSIS and overexpressing of ABHD6 reduces GSIS in the β-cell (Zhao et al., 2014). Additionally, 1-MAG appears to play a role in insulin secretion not only in response to glucose but other fuel stimuli, and its level regulates the secretory response to various neurohromonal agonists (Zhao et al., 2015).

1.6.3.3 Cholesterol and insulin secretion.

Cholesterol is an important component of the plasma membrane, where it plays an essential role in membrane organization, dynamics, and function. Cholesterol and products of cholesterol biosynthesis can influence insulin secretion in β-cells. Studies have shown a direct link between

elevated serum cholesterol and reduced GSIS (Hao, Head, Gunawardana, Hasty, & Piston, 2007; Zuniga-Hertz et al., 2015). Cholesterol accumulation in β-cells has been associated with the reduction of exocytosis that occurs in T2D (Brunham, Kruit, Hayden, & Verchere, 2010). It was also shown that β-cells lacking the ABCA1 cholesterol transporter show increased cholesterol contents associated with reduced GSIS (Kruit et al., 2011). In addition, islets form rat fed a high fat diet that are highly responsive to the diet in term of obesity and hyperglycemia show accumulation of free cholesterol (Peyot et al., 2010).

Hydroxymethylglutaryl-CoA reductase (HMGCR) is an enzyme that catalyzes the rate-limiting step in the cholesterol biosynthesis pathway. This enzyme is one of the downstream targets of AMPK, which has an important role in insulin secretion. Downstream of this step, isoprenoid intermediates are formed which are involved in post-translational modifications of several proteins that participate in secretory pathways and these intermediated may also play a role in insulin secretion (Zuniga-Hertz et al., 2015).

1.6.4 β-cell compensation mechanisms.

Initially, the resistance of peripheral tissues to insulin induced a compensatory phase where the mass of β-cells and their function are enhanced in order to produce and secrete more insulin to compensate for this resistance (Prentki & Nolan, 2006). Subsequently, hyperinsulinemia is observed but blood glucose levels remain normal. Glucose levels are not the only factor responsible for the adaptive increase in insulin secretion in response to increased insulin resistance (Kahn et al., 2006). The abundance of other circulating nutrients, which is a characteristic of obesity, also contributes to the compensatory increase in insulin secretion from the β-cell. In obese individuals, increased concentrations of circulating FFA and triglycerides enhance the GL/FFA cycling and the associated production of small lipid signaling molecules like MAG, DAG and FA-CoA that may function as MCFs to promote insulin secretion. Also the increased FFA and triglyceride levels increase GPR40 activation, which can also contribute to enhanced insulin secretion (Nolan et al., 2006; Roduit et al., 2004). Additional factors that contribute to β-cell compensation include GLP-1, an incretin secreted by intestinal L-cells, which is known to promote β-cell proliferation and inhibit β-cell apoptosis; and which also acts as a glucoincretin that amplifies GSIS (Baggio & Drucker, 2006). In parallel, autocrine actions of insulin and insulin-like growth factor 1 and 2 (IGF1 and IGF2) may contribute to the

proliferation and cell survival through insulin receptor substrate 2 (IRS2) (Modi et al., 2015) and the signaling cascade of protein kinase B (PKB) (Jetton et al., 2005). Finally, the increased central nervous system stimulation of the pancreas can contribute to the compensatory increase in insulin secretion and growth of β-cells.

1.6.5 β-cell dysfunction.

The β-cell dysfunction seen in T2D is characterized by a chronic and abnormal increase of nutrients, which leads to altered insulin secretion through mechanisms that include β-cell exhaustion with degranulation (decrease in the number and the content of insulin secretory granules), reduced insulin biosynthesis and impaired metabolic signaling (Leahy, 2005). Early stages of β-cell dysfunction are characterized by decreased first phase insulin secretion and decreased β-cell mass. Apoptosis may be one of the causes of the decrease in β-cell mass in T2D (Prentki & Nolan, 2006). There are many suggested mechanisms implicated in β-cell dysfunction, including, glucotoxicity, lipotoxicity, glucolipotoxicity, ER stress, oxidative stress and inflammation (Leahy, 2005; Prentki & Nolan, 2006). We discuss in more detail below the mechanism of glucolipotoxicity, glucotoxicity and lipotoxicity in inducing β-cell dysfunction.

1.6.5.1 Glucolipotoxicity.

Glucolipotoxicity is a term used to describe the toxic combined effect of glucose and fat when present in the β-cell simultaneously (Prentki et al., 2002). This concept was initially advanced by the labs of Dr. M Prentki and Dr. B Corkey and has been widely accepted. Glucolipotoxicity is defined as the synergistic chronic effect of elevated concentrations of glucose and fatty acids in inducing β-cell dysfunction, and therefore glucolipotoxicity shares features with glucotoxicity, such as decreased GSIS and decreased total insulin content of β-cells. Glucolipotoxicity also induces β-cell dysfunction in a unique fashion. Elevated glucose concentrations alone are not overly toxic to islet cells in the prediabetic stage, where β-cells adapt via changes in gene expression, such as induction of glycolytic and anaplerotic genes. These changes enhance GSIS and possibly glucose detoxification in the pancreatic β-cell via the release of cataplerosis derived molecules such as citrate (Farfari et al., 2000). Elevated fatty acids alone also are non-toxic for the β-cell since they can be oxidized in the β-cell at low glucose levels because levels of glucose-derived Mal-CoA (which inhibit β-oxidation of fatty acids) are low. However, prolonged

exposure to high glucose and FFAs results in the accumulation of FA-CoA and favours their esterification to promote the accumulation of potentially toxic complex lipids when found in excess, in particular lysophosphatidate, DAG and phosphatidate (El-Assaad et al., 2003; El-Assaad et al., 2010). These factors may cause impaired GSIS and biosynthesis and promote apoptotic cell death (Poitout et al., 2010; Prentki & Madiraju, 2012).

1.6.5.1.1 Glucotoxicity.

Glucotoxicity of β-cells is defined as dysfunction induced by the chronic exposure of these cells to high concentrations of glucose, resulting in impaired GSIS and insulin gene expression as well as apoptosis under certain conditions (Harmon et al., 1999). After chronic high glucose exposure, β-cell lines and rodent and human islets show reduced GSIS and insulin content (Boyd & Moss, 1993; Olson, Redmon, Towle, & Robertson, 1993). In cell lines, prolonged exposure to high glucose levels alters β-cell-specific genes such as the transcription factors Pdx-1, BETA2/NeuroD and MafA, and other genes related to the glycolytic pathway (Sharma, Olson, Robertson, & Stein, 1995; Ye, Tai, Linning, Szabo, & Olson, 2006). Similar results have been obtained in rat islets cultured *ex vivo* for up to six weeks (Jacqueminet, Briaud, Rouault, Reach, & Poitout, 2000). It is understandable that repeated and prolonged exposure to hyperglycemia will likely lead to β-cell degranulation and exhaustion, but the mechanisms underlying this process are believed to be complex.

The proposed mechanism for glucotoxicity is closely related to the remodeling of glucose metabolism in the β-cell (Robertson, Harmon, Tran, Tanaka, & Takahashi, 2003). Instead of glucose being metabolized by glycolysis and the TCA cycle, additional pathways are activated that include glyceraldehyde autoxidation, lipogenesis with DAG formation and PKC activation, and sorbitol metabolism leading to the accumulation of ROS (Poitout & Robertson, 2002). Due to the poor defense mechanisms against ROS available in β-cells (due to low superoxide dismutase, catalase and glutathione peroxidase levels), ROS production from the altered pathways for glucose metabolism eventually leads to β-cell dysfunction.

1.6.5.1.2 Lipotoxicity.

T2D is commonly associated with elevated levels of TG and FFA in the plasma. Whereas FFA amplifies GSIS acutely, chronic *in vitro* exposure to high concentrations of FFA impairs β-cell

function and viability (Gremlich, Bonny, Waeber, & Thorens, 1997). This long-term effect is associated with changes in gene expression, impaired GSIS and eventual β-cell apoptosis. The effect also depends on the type of fatty acid species (chain length and degree of saturation). Saturated fatty acids (e.g. palmitate and stearate) strongly induce ER stress and β-cell apoptosis; while unsaturated fatty acids (e.g. oleate and palmitoleate), elevate basal insulin release and impair GSIS without affecting cell viability (Cnop, Hannaert, Hoorens, Eizirik, & Pipeleers, 2001) (El-Assaad et al., 2003). Mitochondria isolated from oleate-treated β-cell lines display depolarization and elevated ROS production that suggests a link between lipid toxic effects and oxidative stress (Koshkin, Wang, Scherer, Chan, & Wheeler, 2003). However, *in vivo* experiments with rats chronically infused with lipids have shown alterations in GSIS but did not report apoptosis, indicating some β-cell dysfunction caused by elevated fatty acids *in vivo* but no true toxicity (Giacca, Xiao, Oprescu, Carpentier, & Lewis, 2011).

1.7 AMP-activated protein kinase (AMPK).

Energy metabolism, mitochondrial function and generation of ATP in the β-cell are essential for proper β-cell function and insulin secretion. Any dysfunction in these mechanisms can lead to impaired β-cell function and development of T2D. Thus, it is important to understand the pathways that regulate β-cell energy homeostasis. AMP-activated protein kinase (AMPK) is one of the main enzymes involved in the regulation of cellular energy homeostasis; it is activated by low energy levels associated with a rise in the cellular AMP/ATP ratio (Corton, Gillespie, & Hardie, 1994). AMPK is a serine/threonine protein kinase that phosphorylates proteins with a specific sequence motif (Corton, Gillespie, Hawley, & Hardie, 1995). Generally any stress condition that causes reduction of cellular ATP, such as hypoxia, starvation, heat shock or exercise leads to the activation of AMPK (Viollet et al., 2009).

Human tumour suppressor liver kinase B1 (LKB1) activates AMPK by phosphorylating threonine 172, located in the activation loop of the catalytic subunit (Shackelford & Shaw, 2009). Active AMPK enhances ATP-producing, catabolic processes that help to restore the depleted energy levels. These include glucose transport, glycolysis, mitochondrial biogenesis and fatty acid oxidation (Kurth-Kraczek, Hirshman, Goodyear, & Winder, 1999; Reznick et al., 2007). AMPK also reduces ATP consumption, anabolic processes such as protein translation, fatty acid and cholesterol synthesis. AMPK therefore acts as a fuel sensor and restores energy

balance in the short term by phosphorylation of key enzymes like 6-phosphofructo-2-kinase (PFK 2) (glucose metabolism) and ACC (fatty acid metabolism) and long term through regulation of gene expression (Heidrich et al., 2010; Kurth-Kraczek et al., 1999).

AMPK consists of a complex of three subunits, catalytic subunit α and two regulatory subunits β and γ. Each is encoded by a different gene, and each subunit is expressed as at least two different isoforms. For example the α catalytic subunits expresses AMPKα1 (Prkaa1) and AMPKα2 (Prkaa2) (Hawley et al., 1996). Also it is important to mention that AMPKα1 and α2 proteins are detected in the rodent insulinoma cell lines MIN6 and INS1and also in islets (da Silva Xavier et al., 2000). But for the β and γ subunits there are no studies that have been done for either their expression or subcellular localization in β-cells.

1.7.1 Role of AMPK role in β-cells

AMPK is an important regulator for β-cell metabolism and function (Fu, Eberhard, & Screaton, 2013). However, the roles of β-cell AMPK in insulin secretion, metabolism and the regulation of β-cell growth or apoptosis are uncertain with many contradictory results in the literature. Nevertheless there is some consensus that AMPK acts as a negative regulator of fuel induced insulin secretion (Prentki et al., 2013). The possible reasons for the debates in β-cell AMPK studies is that most of the studies have been done on immortalize insulinoma cell lines as β-cell models such as INS-1 and MIN6 (Hohmeier & Newgard, 2004). Also it may be because manipulation of AMPK involves the overexpression of constitutively active or dominant negative constructs of AMPK, or the use of pharmacological agents to activate (AICAR, metformin) or inhibit AMPK. The problem in using pharmacological agents in the activation and inhibition of AMPK is that the drugs are not very specific. For example AICAR (5-aminoimidazole-4-carboxamide ribonucleoside) has been long used as an activator of AMPK and many AMPK studies have been based on AICAR activated AMPK (Corton et al., 1995). AICAR is metabolised in the cell, which leads to accumulation of 5-aminoimidazole-4-carboxamide ribonucleoside (ZMP), a mimic of AMP, without changing the cellular ATP/ADP or ATP/AMP ratio. ZMP is then thought to act similarly to AMP in activating AMPK (Corton et al., 1995). However, ZMP can also activate other enzymes within the cell such as the glycolytic enzyme fructose-1,6-bisphosphatase, which is also regulated by AMP (Iancu, Mukund, Fromm, & Honzatko, 2005). With respect to the molecular approaches to change the expression level of

AMPK subunits, a problem is that this enzyme is involved in many biological functions and regulates the expression of numerous genes such that the resulting effects may be indirect. Hence the current approaches to determine the function of AMPK in β-cells all have limitiations and it is unclear whether the observed results are attributable to AMPK itself.

While gene-targetted mouse models have provided information regarding the role of the AMPK pathway in β-cells; even these studies have been inconclusive and controversial. For example, AMPKα2 global-null mice showed impaired glucose homeostasis and reduced GSIS *in vivo* (Beall et al., 2010). In contrast, deletion of the AMPK upstream kinase, LKB1, in β-cells leads to enhanced insulin secretion and improved glucose tolerance *in vivo* (Sun et al., 2010). *In vitro* GSIS was normal in the LKB1 KO islets but β-cell mass, islet size and β-cell size were increased (Sun et al., 2010). Overall, the β-cell AMPK studies indicate that AMPK has an essential role in regulating β-cell gene expression, growth, survival and insulin secretion, but how exactly it regulates these functions positively or negatively remains uncertain.

1.8 Rationale of the thesis.

Type 2 diabetes (T2D) is a metabolic disorder of fuel homoeostasis characterized by hyperglycemia and altered lipid metabolism caused by islet β-cell dysfunction and insulin resistance due to genetic and environmental factors (Nolan et al., 2011). Obesity is a major risk factor in the pathogenesis of T2D, especially when it is associated with dyslipidemia, hyperinsulinemia, and insulin resistance. β-cell dysfunction is a very important key element in the development of the obesity-associated T2D. In obese subjects, insulin resistance is a common feature and insulin secretion is increased by the β-cell to compensate for the reduction in insulin action and maintaining normoglycemia. Only when the β-cells fail to compensate for the increase in insulin resistance of peripheral tissues, obese individuals develop T2D.

Our lab is interested in studying the regulation mechanisms of insulin secretion in the β-cell in health and diabetes. While the knowledge of the mechanisms responsible for initiation of insulin secretion in the β-cell in response to glucose and fatty acids has made much progress in recent years, the mechanisms causing β-cell dysfunction in metabolic diseases are still poorly understood. Studying these mechanisms in animal models in the context of prediabetes with obesity, where hyperglycemia develops gradually leading to T2D as in human T2D is important

to better understand the etiology of this disease. Several models have helped in the understanding of some of the effects of obesity and T2D on β-cell function, in particular the obese Zucker Diabetic Fatty rats, *ob/ob* and *db/db* mice (Delghingaro-Augusto et al., 2009; King, 2012; Nolan et al., 2006). However, these models are of an extreme nature with rapid development of pronounced T2D and with genetic modifications in leptin signaling that are extremely rare in humans. The diet-induced obese (DIO) C57BL/6N mouse on the other hand is considered a polygenic model of mild T2D that more closely resembles human T2D. In this model, C57BL/6N mice a fed a high fat calorie diet initially display insulin resistance and β- cell failure with defective GSIS, then gradually develop hyperglycemia. Work done in our lab (Peyot et al., 2010) has recently extended the scope of this widely-used model to uncover differences between the prediabetes and early diabetes states with the goal of identifying causal factors in β-cell failure. Our lab has shown that the DIO mice can be stratified into two groups according to the effect of HFD on body weight gain. The low responders to HFD (LDR) have the characteristics of an obese pre-diabetes state in humans with overall β-cell compensation for insulin resistance and show only mild impairment in GSIS. The high responders to HFD (HDR) are more obese, insulin resistant, hyperinsulinemic and hyperglycemic than the LDR group and show more prominent signs of β-cell dysfunction that altogether mimics the obese early diabetic state in humans. Hence, this stratified DIO model gives the opportunity to study the mechanism of β-cell dysfunction in response to diet and different levels of obesity and insulin resistance.

The first paper describing the stratified DIO mice (Peyot et al., 2010) characterized the model in term of insulin resistance, insulin secretion *in vivo* and *ex vivo*, pancreatic β-cell growth apoptosis and mass, blood chemistry and identified some alterations in β- cell function in DIO mice versus controls and differences among the HDR and LDR groups. The DIO islets showed, in the absence of steatosis and reduced β- cell mass, altered GL/FFA cycling and the HDR group also exhibited enhanced fat oxidation and cholesterol accumulation that could contribute to their more pronounced secretory defect. The goal of the follow up study included in this thesis was to obtain deeper insight into the biochemical differences between the LDR and HDR DIO mice and to discover alterations in β- cell gene expression that may lead to the discovery of key causal factors of β- cell failure. Because the GL/FFA cycle is regulated by AMPK (Gauthier et al., 2008) and PKCε (Cantley et al., 2009); and because AMPK (Rutter & Leclerc, 2009) and

mitochondrial metabolism are central to β- cell metabolism, growth, GSIS and cholesterol metabolism, we chose to study these enzymes and processes in the stratified DIO model. A major thrust of this work was also to identify differences in islet gene expression between the two DIO groups and control mice and between LDR and HDR islets with the hope that a few prominent and relevant changes might reveal avenues to pursue in term of genes involved in β-cell compensation and failure.

1.8.1 Hypothesis.

The transition of the pancreatic β- cell from obesity associated prediabetes to early diabetes entails changes in AMPK and PKCε activity as well as mitochondrial metabolism and cholesterol accumulation that may affect β- cell function, and changes in the expression of key β-cell genes that may also be causally implicated in β- cell failure.

1.8.2 General objective.

To gain insight into the molecular basis of β-cell adaptation and failure in diabetes associated with excess food and fat intake.

1.8.2.1 Specific objectives and experiments.

- To measure AMPK and PKCε expression and activity in DIO LDR and HDR C56BL/6N mouse islets versus control islets, along with its upstream regulators and downstream targets, as candidates for the impaired β-cell function in this rodent model of T2D.
- To measure mitochondrial membrane potential, O2 consumption, ATP production, uncoupling and ROS production in control and DIO islets.
- To measure islet cholesterol biosynthesis and the expression of cholesterol metabolism genes in the various groups.
- To carry on a discovery approach using transcriptomics and microarray to identify changes in particular mRNA that may give hints as to key protein players and pathways involved in the transition from a normal to prediabetes state and from prediabetes to early diabetes.

Chapter 2 – β-cell dysfunction in the DIO mouse model

2.1 Pancreatic β-cell dysfunction in diet-induced obese mice: roles of AMP-kinase, protein kinase Cε, mitochondrial and cholesterol metabolism, and alterations in gene expression

Work in this chapter has been published as: Pepin, E., **A. Al-Mass**, C. Attane, K. Zhang, J. Lamontagne, R. Lussier, S. R. Madiraju, E. Joly, N. B. Ruderman, **R. Sladek, M. Prentki** and M. L. Peyot (2016). "Pancreatic beta-Cell Dysfunction in Diet-Induced Obese Mice: Roles of AMP-Kinase, Protein Kinase Cepsilon, Mitochondrial and Cholesterol Metabolism, and Alterations in Gene Expression." PLoS One 11(4): e0153017.

2.1.1 Abstract.

Diet induced obese (DIO) mice can be stratified according to their weight gain in response to high fat diet as low responders (LDR) and high responders (HDR). This allows the study of β-cell failure and the transitions to prediabetes (LDR) and early diabetes (HDR). C57BL/6N mice were fed for 8 weeks with a normal chow diet (ND) or a high fat diet and stratified as LDR and HDR. Freshly isolated islets from ND, LDR and HDR mice were studied *ex-vivo* for mitochondrial metabolism, AMPK activity and signalling, the expression and activity of key enzymes of energy metabolism, cholesterol synthesis, and mRNA profiling. Severely compromised glucose-induced insulin secretion in HDR islets, as compared to ND and LDR islets, was associated with suppressed AMP-kinase activity. HDR islets also showed reduced acetyl-CoA carboxylase activity and enhanced activity of 3-hydroxy-3-methylglutaryl-CoA reductase, which led respectively to elevated fatty acid oxidation and increased cholesterol biosynthesis. HDR islets also displayed mitochondrial membrane hyperpolarization and reduced ATP turnover in the presence of elevated glucose. Expression of protein kinase Cε, which reduces both lipolysis and production of signals for insulin secretion, was elevated in DIO islets. Genes whose expression increased or decreased by more than 1.2-fold were minor between LDR and ND islets (17 differentially expressed), but were prominent between HDR and ND islets (1508 differentially expressed). In HDR islets, particularly affected genes were related to cell cycle and proliferation, AMPK signaling, mitochondrial metabolism and cholesterol metabolism.

In conclusion, chronically reduced AMPK activity, mitochondrial dysfunction, elevated cholesterol biosynthesis in islets, and substantial alterations in gene expression accompany β-cell failure in HDR islets. The β-cell compensation process in the prediabetic state (LDR) is largely independent of transcriptional adaptive changes, whereas the transition to early diabetes (HDR) is associated with major alterations in gene expression.

2.1.2 Introduction.

Obesity when associated with dyslipidemia, hyperinsulinemia, and insulin resistance, increases the risk of developing type 2 diabetes (T2D), cardiovascular disease and certain cancers (Farooqi & O'Rahilly, 2006). Obesity-associated T2D is generally thought to result from the inability of pancreatic islets to secrete sufficient insulin to compensate for the increased insulin resistance of peripheral tissues (Nolan et al., 2011; Poitout & Robertson, 2008). Alternatively, the initial hyperinsulinemia may drive obesity, and insulin resistance and T2D follow as a result of β-cell failure via its exhaustion and other mechanisms (Andrikopoulos, 2010; Corkey, 2012; Prentki & Nolan, 2006).

Several studies have shown that β-cell mitochondrial and lipid metabolism (Fex et al., 2009; Maechler, 2013; Prentki et al., 2013) as well as AMP-activated protein kinase (AMPK) (Rutter & Leclerc, 2009); and protein kinase Cε (PKCε) (Cantley et al., 2009) signaling play major roles in the regulation of insulin secretion. Fatty acids augment glucose-stimulated insulin secretion (GSIS) by β-cells via the receptor FFAR1(Mancini & Poitout, 2013) and the generation of metabolic coupling factors (Nolan et al., 2006), in particular 1-monoacylglycerol (Zhao et al., 2014), generated by the lipolysis arm of the glycerolipid/free fatty acid (GL/FFA) cycle (Prentki & Madiraju, 2008). However, chronic exposure of the β-cell to elevated FFA causes metabolic stress and curtails the GSIS response via glucolipotoxicity (Giacca et al., 2011; Prentki & Nolan, 2006).

High fat diet-induced obese (DIO) mice gradually develop hyperglycemia (Surwit et al., 1988) and defective GSIS (Collins et al., 2010; Lee, Opara, Surwit, Feinglos, & Akwari, 1995; Wencel et al., 1995); they represent a model of mild diabetes resembling human T2D. We recently showed that C57BL/6N DIO mice, that do not harbor a mutation in the nicotinamide

nucleotide transhydrogenase gene (Fergusson et al., 2014), display heterogeneity in their weight gain response and can be stratified as low HFD responders (LDR) and high HFD responders (HDR) (Peyot et al., 2010). LDR mice have a moderate phenotype with obesity, β-cell compensation for insulin resistance and mild β-cell dysfunction. Essentially, they show characteristics of 'pre-diabetes' in humans. HDR mice in turn have the characteristics of 'early-diabetes' with more severe β-cell dysfunction. Both LDR and HDR DIO mice exhibit reduced GSIS and altered free fatty acid (FFA) metabolism with HDR mouse islets showing more defective secretion in association with elevated β-oxidation of FFA and free cholesterol accumulation in β-cells (Peyot et al., 2010). Thus, a comparison of the responses of these stratified DIO mice with the same genetic background offers a unique opportunity to enhance our understanding of the mechanisms involved in both the development of obesity-linked β-cell dysfunction, and the transition from pre-diabetes to early diabetes.

The present study provides evidence that altered β-cell AMPK and PKCε signaling, mitochondrial dysfunction, enhanced cholesterol synthesis and deposition, and major changes in gene expression contribute to β-cell failure in the most diet responsive HDR mice.

2.1.3 Materials and Methods.

2.1.3.1 Materials.

Glucose-free RPMI 1640 media was purchased from Gibco (Burlington, ON, Canada). Fatty-acid free BSA and all chemicals, unless otherwise specified, were purchased from Sigma-Aldrich (St-Louis, MO, USA). Rhodamine 123 was obtained from Molecular Probes (Burlington, ON, Canada). Cell culture supplies were purchased from Corning (New York, USA). Antibodies for Western blotting were purchased from Cell Signaling Technology (Beverly, MA, USA) except SIRT1, phosphor-Ser^{79} ACC and phospho-Ser^{872} HMG-CoA reductase (Millipore, Billerica, MA, USA), PKCε, phosphor-Ser^{729} PKCε and LKB1 (Santa Cruz Biotechnology, Santa Cruz, CA, USA) and tubulin (Abcam, Cambridge, MA, USA). Protein concentration was determined using a BCA kit (Pierce, Rockford, IL, USA).

2.1.3.2 Animals and diets.

Five-week old male C57BL/6N mice with a pure genetic background were purchased from Charles River Laboratories (Raleigh, NC, USA). They were housed two per cage, on a 12h light/dark cycle at 21°C with free access to water and a standard diet (Teklad Global 18% protein rodent diet, 15% fat by energy, Harland Teklad, Madison, WI, USA). After one week of acclimatization, the mice were fed either the standard normal diet (ND) or high fat diet (HFD) for 8 weeks (Bioserv F-3282, 60% energy from fat, Frenchtown, NJ, USA). Body weight was measured weekly and at 7.5 weeks, blood glucose was measured in fed mice with a portable glucometer (Contour, Bayer, Toronto, ON, Canada). After 8 weeks, HFD fed mice were stratified into LDR and HDR groups according to their body weight gain, and plasma parameters (insulin, cholesterol, non-esterified free fatty acid and triglycerides) were determined in fed mice as described previously (Peyot et al., 2010). None of the animals involved in this study showed sign of illness. At the end of the HFD protocol, all mice were anesthetized with intraperitoneal injection of ketamine/xylazine. Anesthesia was confirmed by lack of responsiveness to toe pinching and all efforts were made to minimize animal suffering. Animals were sacrificed by cervical dislocation and blood was collected by cardiac puncture followed by removal of pancreas. All procedures were approved by the Institutional Committee for the Protection of Animals at the Centre de Recherche du Centre Hospitalier de l'Université de Montréal and were done in accordance with the Canadian Council of Animal Care guidelines.

2.1.3.3 Islet isolation and culture.

Islets from ND, LDR and HDR mice were isolated as described before (Peyot et al., 2009) with the exception that Liberase TL (Roche Diagnostic, Laval, QC, Canada) was used instead of collagenase XI for pancreatic tissue digestion. After isolation, islets were allowed to recover for 2h at 37°C in RPMI complete medium containing 3 mM glucose and supplemented with 10% (w/v) fetal bovine serum (FBS) (Peyot et al., 2009).

2.1.3.4 Insulin secretion.

After recovery, islets were distributed in 12-well plates at a density of 10 islets per well and preincubated for 45 min at 37°C in Krebs-Ringer bicarbonate buffer containing 10 mM HEPES

(pH 7.4) (KRBH), 0.5% defatted bovine serum albumin (d-BSA), and 3 mM glucose. They were then incubated for 1 h in KRBH/0.5% d-BSA at 3, 8, and 16 mM glucose or 3 mM glucose with 35 mM KCl. After 1h, media were kept for insulin measurements by radioimmunoassay. Total islet insulin content was measured by radioimmunoassay (Peyot et al., 2009) following acid–ethanol (0.2 mM HCl in 75% ethanol) extraction.

2.1.3.5 Mitochondrial membrane potential.

Isolated islets were dispersed by trypsinization and cultured overnight on glass coverslips coated with poly-lysine (Sigma-Aldrich, Oakville, ON, Canada) in RPMI complete medium containing 5.5 mM glucose and supplemented with 10% FBS. Islet cells were starved for 2h in RPMI complete medium with 3 mM glucose and then loaded for 25 min with 10µg/mL Rhodamine-123 in KRBH supplemented with 2.8 mM glucose and 0.5% BSA. Fluorescence intensity was measured by confocal microscopy following incubations at 3 mM and 16 mM glucose, and at 3 mM glucose in the presence of 25 µM carbonyl cyanide 4-(trifluoromethoxy) phenylhydrazone (FCCP) (Diao et al., 2008).

2.1.3.6 Islet oxygen consumption.

Batches of 75 hand-picked islets were placed in to a 24-well Seahorse islet plate. Islets were preincubated for 40 min at 37°C without CO_2 in DMEM supplemented with 2 mM L-glutamine, 1 mM sodium pyruvate, 1% FBS and 3 mM glucose before loading in to the XF24 analyzer (Seahorse Bioscience, Billerica, MA, USA). Oxygen consumption rate (OCR) was measured for 20 min at 3 mM glucose to assess basal respiration, and after glucose levels were elevated to 16 mM for 50 min to determine glucose-induced O_2 consumption. Finally, different inhibitors of the respiratory chain or uncouplers were added by three successive injections to assess uncoupled respiration, maximal respiration and non-mitochondrial respiration, respectively: oligomycin (F1F0-ATP synthase inhibitor; 5 µM); FCCP (uncoupler; 1 µM) and rotenone plus antimycin A (complex I and III inhibitors, both at 5 µM). ATP turnover at 16 mM glucose (OCR 16 mM glucose – OCR oligomycin), uncoupled respiration (OCR FCCP – OCR oligomycin), and maximal respiration (OCR FCCP – OCR rotenone plus antimycin) were calculated (Wikstrom et al., 2012).

2.1.3.7 Immunoblotting.

To determine the expression of specific proteins, isolated islets were washed three times with PBS, resuspended in lysis buffer (50 mM HEPES pH 7.5, 1% NP40, 2 mM sodium orthovanadate, 4 mM EDTA, 10 μg/mL aprotinin, 1 μg/mL leupeptin, 100 mM sodium fluoride, 10 mM sodium pyrophosphate, 1 mM phenylmethanesulfonylfluoride) and snap-frozen in liquid nitrogen till use. For the determinations of various phosphoproteins, isolated islets were preincubated for 1h in KRBH containing 0.5% d-BSA and 3 mM glucose, and subsequently incubated for 30 min at 3 or 16 mM glucose. Islets were then washed three times with PBS, resuspended in lysis buffer and snap-frozen in liquid nitrogen. Total protein extracts (15 μg) from ND, LDR and HDR islets were separated on 4-15% gradient SDS-PAGE (Bio-Rad, Missisauga, ON, Canada) and transferred to PVDF-Immobilon membranes (Millipore, Billerica, MA, USA). Membranes were probed with antibodies against total-AMPKα (1/500 in 5% milk, #2532), phospho-Thr^{172} AMPKα (1/1000 in 5% BSA, #2535), total-acetyl-CoA carboxylase (ACC, 1/500 in 5% milk, #3662), phospho-Ser^{79} ACC (1/1000 in 5% milk, #07-303), SIRT1 (1/1000 in 5% milk, #09-844), phospho-Ser^{872} HMG-CoA reductase (1/400 in 5% milk, #09-356), total-PKCε (1/500 in 5% BSA, #sc-214), phospho-Ser^{729} PKCε (1/250 in 5% BSA, #sc-12355) and total-LKB1 (1/500 in 5% BSA, #sc32245). Alpha tubulin (1/10000 in 5% milk, #ab4074) was used as a loading control. Protein bands were detected using an HRP-labeled anti-rabbit IgG (Bio-Rad, Mississauga, ON, Canada) and a SuperSignal West Pico chemiluminescent kit (Thermo Scientific, Rockford, IL, USA). Protein bands were quantified using Scion Image (Frederick, MD, USA).

2.1.3.8 Total cholesterol content.

After 2h recovery in RPMI complete medium supplemented with 1% FBS at 3 mM glucose, batches of 100 islets from ND, LDR and HDR mice were distributed in 6-well plates and incubated for 3h at 37°C in RPMI 1% FBS and 3 mM or 16 mM glucose. At the end of the incubation, total islet cholesterol (free cholesterol plus cholesterol esters) was measured (Peyot et al., 2010).

2.1.3.9 Transcriptomic Profiling.

Total RNA was extracted from 300 islets for 8 separate mice from each group (ND, LDR, HDR: 8 islet isolations per group), using the RNeasy Mini kit (Qiagen, Valencia, CA, USA) following the manufacturer's protocol. The quality of the total RNA was evaluated on an Agilent 2100 Bioanalyzer system (Agilent, Palo Alto, CA, USA). Microarray analysis was performed on total RNA using the GeneChip Mouse Gene 1.0 ST microarrays (eight arrays per group; Affymetrix, Santa Clara, CA, USA). One hundred nanograms of total RNA were processed using the Ambion WT Expression Kit (Invitrogen). The resulting fragmented and labeled single-stranded cDNA was processed according to the Affymetrix protocol. The Partek (St. Louis, MO, USA) Genomics Suite was used for data analysis. The data were normalized by Robust Multichip Average (RMA) algorithm, which uses background adjustment, quantile normalization, and summarization. After correction of statistical significance for multiple comparisons using false discovery rate; the transcripts that showed significant differences in expression between the HDR, LDR and ND groups (i.e. whose expression increased or decreased by more than 1.2 fold change, p <0.05) were classified using pathway enrichment analysis using Ingenuity Pathways Analysis (IPA; Ingenuity Systems, Redwood City, CA, USA).

2.1.3.10 Quantitative Real time-PCR.

Total RNA was extracted from islets as described above. Gene expression was determined by a standard curve method and normalized to the expression of beta-actin. Real-time PCR analysis was performed on Rotor-Gene R3000 (Corbett Research, Mortlake, NSW, Australia) using Quantitech Sybrgreen (Qiagen, Mississauga, ON, Canada) according to the manufacturer's instructions. Primers, listed in supplementary Table 1 (S1 table), were designed using Primer3 software. Results are expressed as the ratio of target mRNA to beta-actin mRNA.

2.1.3.11 Statistical analysis.

Data are expressed as mean ± SEM. Statistical significance was calculated by ANOVA with Tukey or Bonferroni post-hoc testing, as indicated, using GraphPad Prism 6.0. A p value of <0.05 was considered significant.

2.1.4 Results.

2.1.4.1 Impaired insulin secretion and mitochondrial dysfunction in DIO islets.

Insulin secretion was measured in freshly isolated islets from ND, LDR and HDR mice. Increasing the ambient glucose concentration from 3 to 16 mM stimulated insulin secretion in control ND islets by 3 fold, a response that was reduced in LDR islets and almost completely abolished in HDR islets (Fig. 2.1A), as previously observed (Peyot et al., 2010). A very similar pattern of events was observed when KCl-induced insulin secretion was studied (Fig. 2.1A).

Mitochondria in the β-cell generate signals for insulin secretion and their dysfunction is associated with reduced GSIS and the development of T2D (Mulder & Ling, 2009; Stiles & Shirihai, 2012). We assessed whether mitochondrial function is defective in islets of mice with DIO. Mitochondrial membrane potential ($\Delta\psi_{mito}$) measurements in HDR islets showed hyperpolarization in response to 16 mM glucose while $\Delta\psi_{mito}$ was similar in LDR and ND islets (Fig. 2.1B). We also examined mitochondrial respiration (Fig. 2.1C). There was no change in basal (Fig. 2.1D), maximal (Fig. 2.1G), uncoupled (Fig. 2.1H) and non-mitochondrial respiration (Fig. 2.1I) in DIO islets compared to ND islets. Glucose-induced O_2 consumption was reduced in LDR and HDR islets without reaching statistical significance (Fig. 2.1E), and glucose-induced ATP turnover was decreased to the same extent in both LDR and HDR islets (Fig. 2.1F). Lack of change in the oxidation of ^{14}C-glucose to $^{14}CO_2$ in LDR and HDR islets was noticed in our earlier study (Peyot et al., 2010). Thus, some mitochondrial dysfunction is apparent in both LDR and HDR islets but the alteration is more prominent in the HDR group which exhibited mitochondrial hyperpolarization at high glucose.

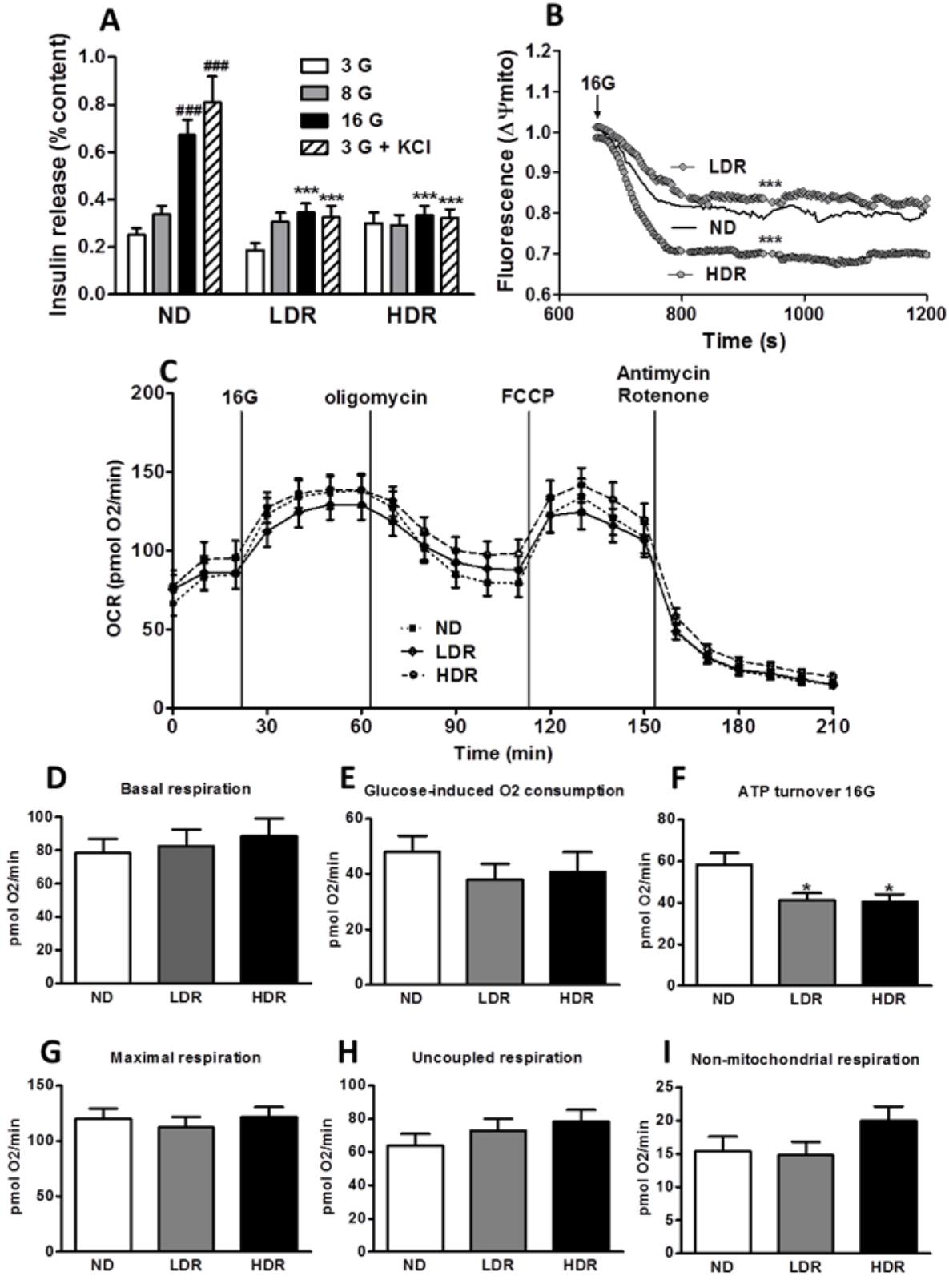
A
Insulin release (% content)
3 G
8 G
16 G
3 G + KCl
ND
LDR
HDR
B
Fluorescence (ΔΨmito)
16G
LDR
ND
HDR
Time (s)
C
OCR (pmol O2/min)
16G
oligomycin
FCCP
Antimycin
Rotenone
Time (min)
D
Basal respiration
E
Glucose-induced O2 consumption
F
ATP turnover 16G
G
Maximal respiration
H
Uncoupled respiration
I
Non-mitochondrial respiration
pmol O2/min

Figure 2.1. Defective insulin secretion and mitochondrial dysfunction in DIO islets. (A) Insulin secretion was measured in freshly isolated islets from normal diet (ND), and obese high fat diet fed low responders (LDR) and high responders (HDR) mice. Groups of 10 islets were incubated 1 h in KRBH at 3, 8, or 16 mM glucose (G) or 3 mM glucose ± 35 mM KCl. Means ± SEM of 10–12 determinations from islets of 6 animals per group in three separate experiments. ***p<0.001 versus ND for the same glucose concentration; ###p<0.001 versus 3 mM glucose; one-way ANOVA, Tukey post-hoc test. (B) Mitochondrial membrane potential (Δψmito) measured by Rhodamine123 fluorescence in dispersed islet cells from ND, LDR and HDR mice. Δψmito was initially measured at 3 mM glucose to set a baseline and then at 16 mM glucose. Data were normalized to baseline fluorescence. Means of 6 (ND) or 5 (LDR and HDR) mice. ***p<0.0001 vs ND; One-way ANOVA, repeated measures, Tukey post-hoc test. (C) Mitochondrial O_2 consumption rate (OCR) measured at 3 mM glucose and then at 16 mM glucose (16G). (D) Baseline respiration at 3 mM glucose, (E) glucose-induced respiration as the difference in OCR between 16 and 3 mM glucose, (F) ATP-turnover at 16G, (G) maximal respiration, (H) uncoupled respiration and (I) non-mitochondrial respiration were determined using mitochondrial inhibitors. Means ± SEM of 5 mice per group, each with quadruplicate observations. *p<0.05 versus ND; One-way ANOVA, Tukey post-hoc test.

2.1.4.2 Altered AMPK activity and enhanced cholesterol synthesis in HDR islets.

The fuel sensor AMPK plays a central role in energy homeostasis and chronic alterations in its activity have been implicated in diseases associated with the metabolic syndrome (N. B. Ruderman, Carling, Prentki, & Cacicedo, 2013). AMPK activation caused by increases in AMP and ADP and upstream kinases (N. Ruderman & Prentki, 2004), is associated with elevated fatty acid oxidation and decreased cholesterol biosynthesis due to the inactivation of acetyl CoA carboxylase (ACC) (Hardie, Ross, & Hawley, 2012) and HMG-CoA reductase (HMGCR) (Carling, Clarke, Zammit, & Hardie, 1989), respectively. Glucose acutely reduces AMPK activity in the β-cell and increased AMPK activity in isolated islets has been shown to decrease GSIS (da Silva Xavier et al., 2003). The chronic effects of AMPK alterations are less understood.

We noticed an increase in total AMPKα abundance in DIO islets, which was significant in the HDR group (Fig. 2.2A). Activation of AMPK, as indicated by phospho-AMPK levels, was as expected decreased in ND, LDR and HDR islets incubated with elevated glucose (Fig. 2.2B). Interestingly, phospho-AMPK levels, expressed as a function of either tubulin or total AMPK, greatly decreased in DIO islets particularly under basal conditions (3 mM glucose) in comparison to ND islets and this decrease was more pronounced in HDR islets (Fig. 2.2B and 2.2C). We then examined whether the altered phospho-AMPK levels in DIO islets impacted AMPK's downstream targets. There were no changes in total protein levels of the AMPK target ACC or of its phosphorylation in LDR islets, but a slight increase in phospho-ACC levels was noticed in HDR islets (Fig. 2.2D and 2.2E). Even though phospho-ACC levels in response to high glucose treatment islets decreased in ND and LDR islets, presumably due to changes in phospho-AMPK, such was not the case in HDR islets (Fig. 2.2E). Moreover, when expressed as the difference between 16 and 3 mM glucose, ACC phosphorylation was increased in HDR islets compared to both the ND and LDR groups (Fig. 2.2E, inset). There was no change in total levels of SIRT1 (Fig. 2.2F), a putative downstream target of AMPK or in its upstream kinase LKB1 (Fig. 2.2G). Phosphorylation of HMGCR, which inactivates this enzyme, was similar at both low and high glucose in LDR islets as compared to ND islets; however, this was decreased by nearly 50% in HDR islets (Fig. 2.2H), indicating that the activity of HMGCR which catalyzes the rate limiting step in the biogenesis of cholesterol was higher in HDR islets. This change in HMGCR phosphorylation status was reflected in total islet cholesterol levels, which were also not responsive to elevated glucose concentration in HDR vs ND islets, and showed an increase in HDR islets relative to ND and LDR islets (Fig 2.3).

Overall, in DIO conditions and particularly in the HDR group, glucose regulation of AMPK activity in the islets is completely obliterated and this impacts the AMPK targets ACC (reduced activity) with a resulting increase in fat oxidation (Peyot et al., 2010), and HMGCR (enhanced activity) in association which decreases cholesterol synthesis and deposition.

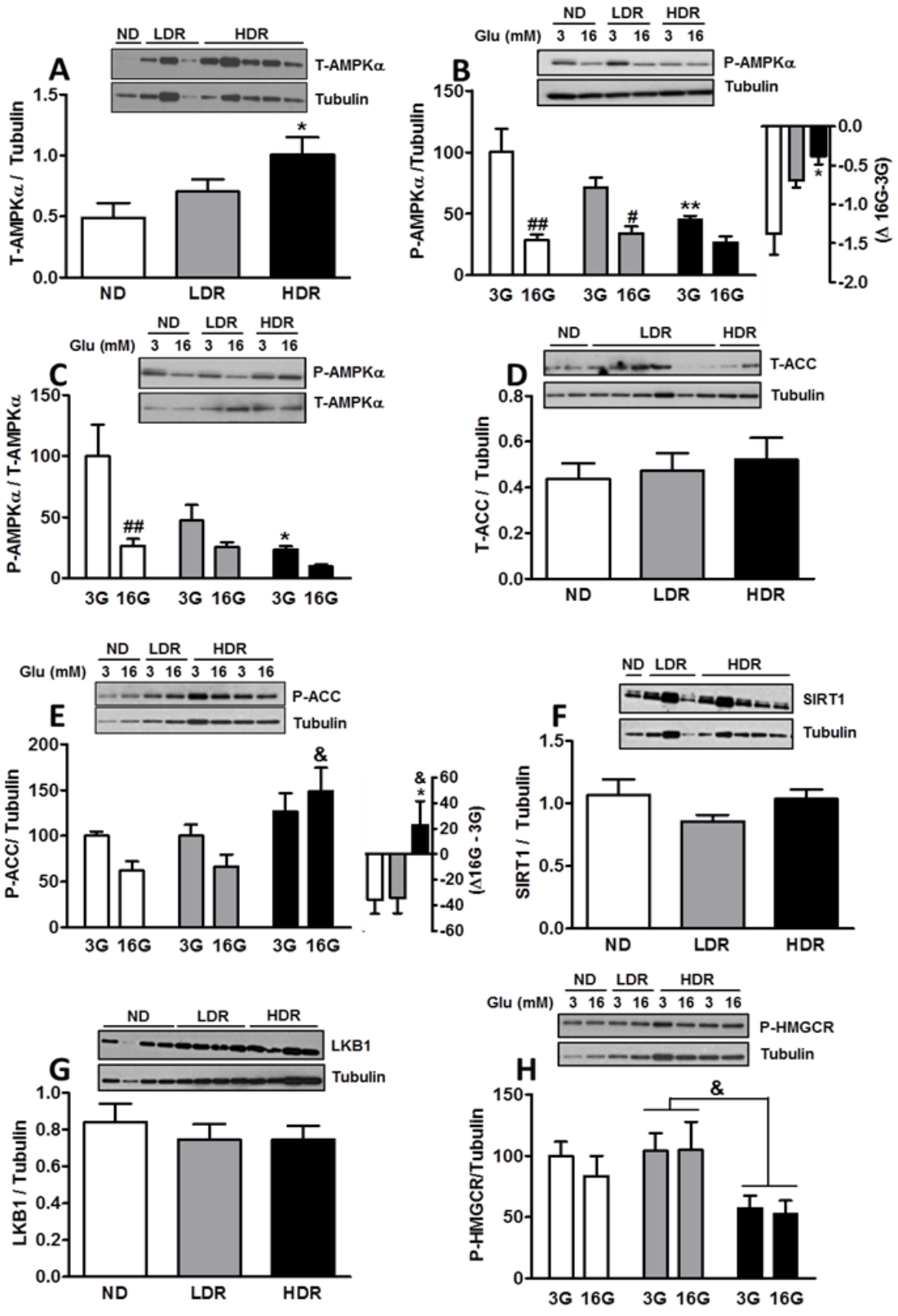
A
ND LDR HDR
T-AMPKα
Tubulin
T-AMPKα / Tubulin
ND LDR HDR
B
Glu (mM) 3 16 3 16 3 16
P-AMPKα
Tubulin
P-AMPKα /Tubulin
(Δ 16G-3G)
3G 16G 3G 16G 3G 16G
C
Glu (mM) 3 16 3 16 3 16
P-AMPKα
T-AMPKα
P-AMPKα / T-AMPKα
D
T-ACC
Tubulin
T-ACC / Tubulin
ND LDR HDR
E
Glu (mM) 3 16 3 16 3 16 3 16
P-ACC
Tubulin
P-ACC/ Tubulin
(Δ16G - 3G)
F
SIRT1
Tubulin
SIRT1 / Tubulin
G
LKB1
Tubulin
LKB1 / Tubulin
H
Glu (mM) 3 16 3 16 3 16 3 16
P-HMGCR
Tubulin
P-HMGCR/Tubulin

Figure 2.2. Altered activities of AMP-Kinase, acetyl-CoA carboxylase and HMG-CoA reductase in HDR islets. (A) Total AMPKα (n=16-23); (B,C) phospho-AMPKα (P-Thr172 n=6-14); (D) Total ACC (n=12-18); (E) phospho-ACC (P-Ser79) (n=7-9); (F) Total SIRT1 (n=19-22); (G) Total LKB1 (n=6-11); and (H) phospho-HMGCR (P-Ser872) (n=6-12). Tubulin or total AMPK (T-AMPK) were used for normalization. Graphs represent means ± SEM for the number of determinations per experimental conditions in parenthesis. (A,D,F,G) non-treated islets. (B,C,E,H) islets treated at 3 mM (3G) or 16 mM (16G) glucose for 30 min and data are expressed as % of ND islets at 3 mM glucose (3G). # $p<0.05$, ##$p<0.01$ vs 3G for the same islet group; * $p<0.05$, ** $p<0.01$ vs ND for the same glucose concentration; & $p<0.05$ for HDR vs LDR of the same glucose concentration, One-way Anova, Tukey post-hoc test. ND: white; LDR: gray; HDR: black.

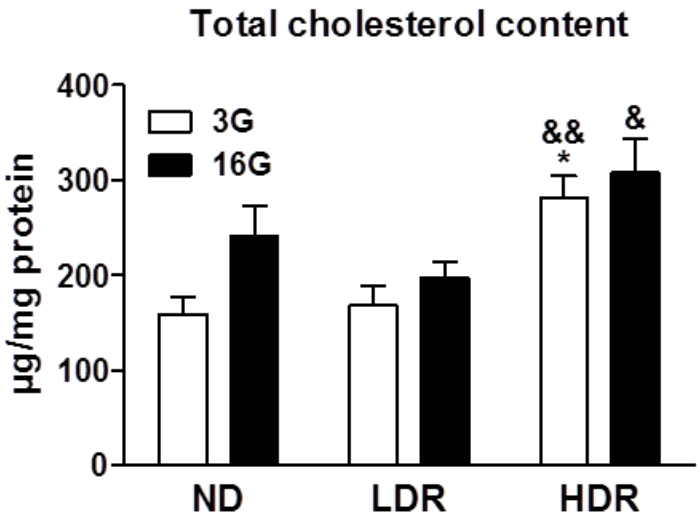

Figure 2.3. Increased total cholesterol content in HDR islets. Total cholesterol content of islets incubated at 3 mM (3G) or 16 mM (16G) glucose for 3h. Means ± SEM from 6 (ND and HDR) and 5 (LDR) mice. *$p<0.05$ vs ND, &$p<0.05$, &&$p<0.01$ for HDR vs LDR, for the same glucose concentration. One-way ANOVA, Tukey post-hoc test.

2.1.4.3 Increased PKCε expression in DIO islets.

PKCε is a negative regulator of insulin secretion and lipolysis (Cantley et al., 2009). As in the present work we noticed decreased GSIS in both LDR and HDR islets and in an earlier study that decreased GSIS in DIO islets correlated with lipolysis (Peyot et al., 2010), we examined the expression of PKCε in the DIO islets. As shown in Fig 4A and 4B, PKCε protein levels were increased more than two fold in LDR and HDR islets in comparison with ND islets. However, phospho-PKCε was only increased in HDR islets (Fig. 2.4A, 2.4C and 2.4D).

2.1.4.4 Altered gene expression in the HDR versus LDR and ND islets

We performed a microarray-based transcriptomic analysis on eight islet preparations from the ND, LDR and HDR groups. Body weight and blood parameters of the individual mice used for the microarray assay are shown in Fig. 2.5. Increased plasma levels of glucose, insulin and cholesterol were prominent in the HDR group whereas the same parameters, although slightly elevated in LDR, were close to the values of the control ND animals.

Among the 28853 genes detected on the gene-chip mouse gene 1.0 ST array, 1508 genes were differentially expressed (i.e. their expression changed by more than ±1.2-fold) between HDR and ND islets (S2 Table). Of these, 883 genes were upregulated and 625 were downregulated in HDR islets. LDR vs ND comparison showed the fewest expression differences (17 altogether) with only 14 genes upregulated and 3 genes downregulated in the LDR group (S3 Table). The surprising observation of extremely few expression changes despite the very different diet, is consistent with the 'compensation' phenotype of the LDR group and is reflected by the similar serum biochemistry results obtained from LDR and ND mice (Fig. 2.5). In the HDR vs LDR comparison, we found 1041 genes to be differentially expressed in HDR islets, of which 523 were upregulated and 518 were downregulated (S4 Table). Pathway enrichment analysis identified the top five enriched canonical pathways for each comparison (Fig. 2.6A). Major changes occurred in pathways related to cell-cycle and proliferation in the HDR vs ND comparison and in the HDR vs LDR comparison, which correlated with increased β-cell mass and proliferation index in HDR islets (Peyot et al., 2010).

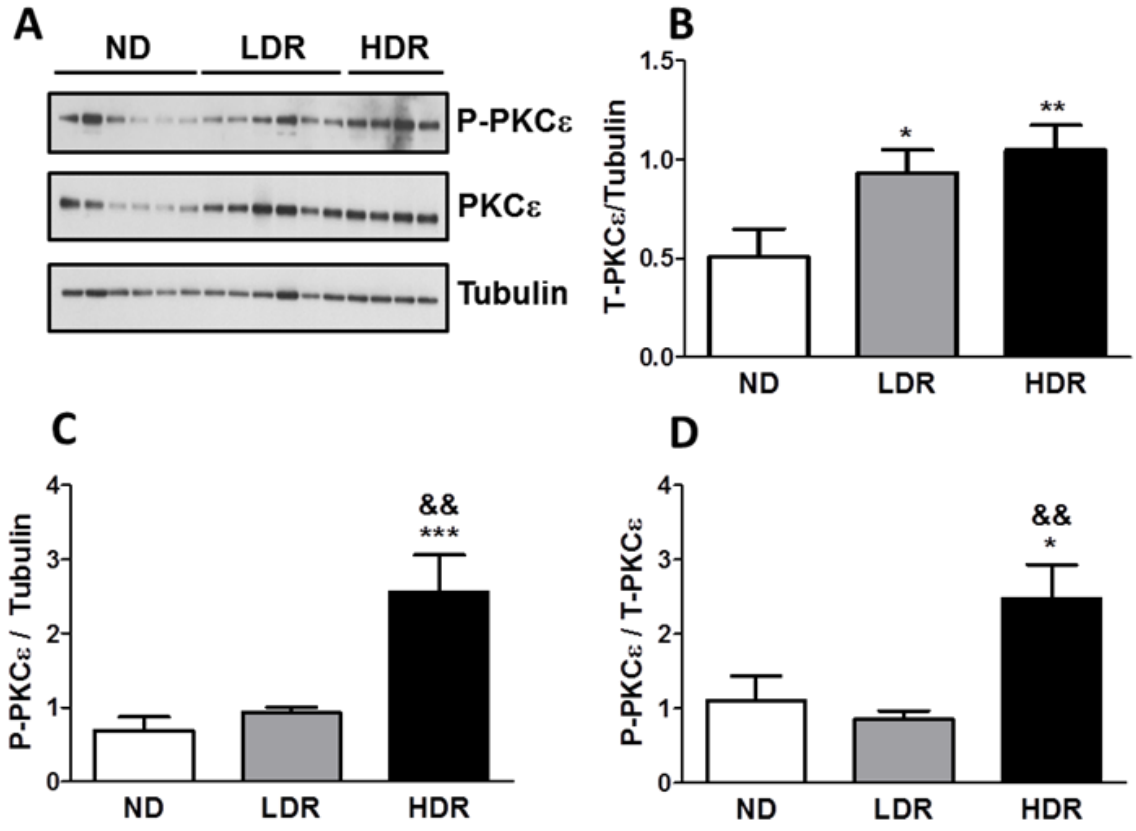

Figure 2.4. Increased total PKCε levels in DIO islets. Proteins from ND, LDR and HDR islets were probed with an antibody against total PKCε (T-PKCε) and phospho-Ser^{729} PKCε (P-PKCε). Tubulin or total PKCε were used for normalization. (A) Representative western blot of T-PKCε and P-PKCε, (B) expression level of T-PKCε normalized by tubulin, (C) P-PKCε level normalized by tubulin and (D) by total PKCε. Means ± SEM of 8 (ND), 13 (LDR) and 10 (HDR) mice. *p<0.05, **p<0.01 vs ND, One-way ANOVA, Tukey post-hoc test.

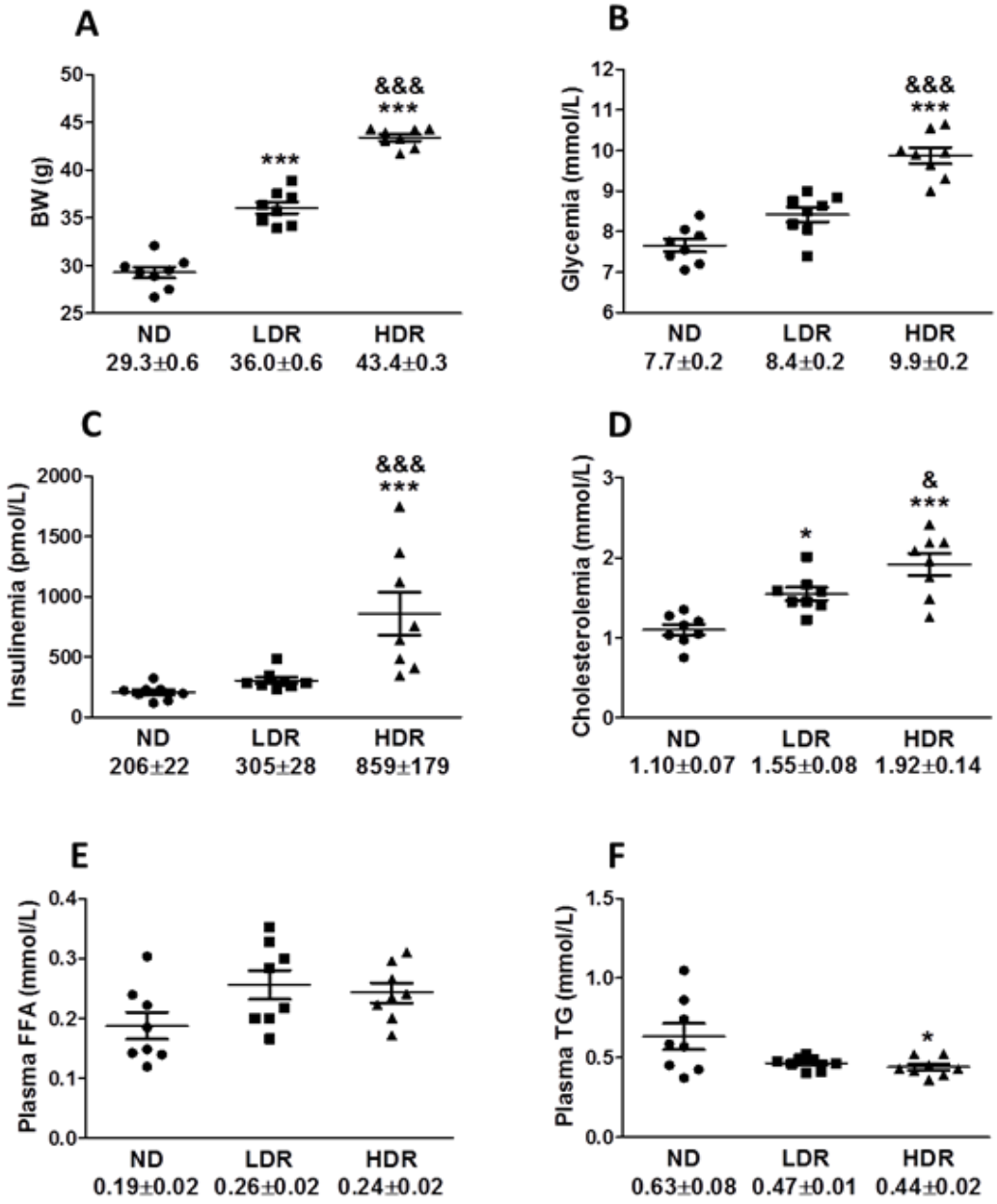

Figure 2.5. Individual metabolic parameters of C57BL/6N mice fed with a normal or HFD for 8 weeks used for islet gene expression analysis. (A) Body weight (BW), (B) glycemia, (C) insulinemia, (D) cholesterolemia, (E) plasma fatty acids and (F) plasma triglycerides. Means ± SEM of 8 animals per group are indicated below the X- axis for each graph. LDR or HDR versus ND: *P<0.05, ***P<0.001; HDR versus LDR: & P<0.05, && P<0.01, &&& P<0.001. One-way ANOVA-Bonferroni's multiple comparison post hoc test.

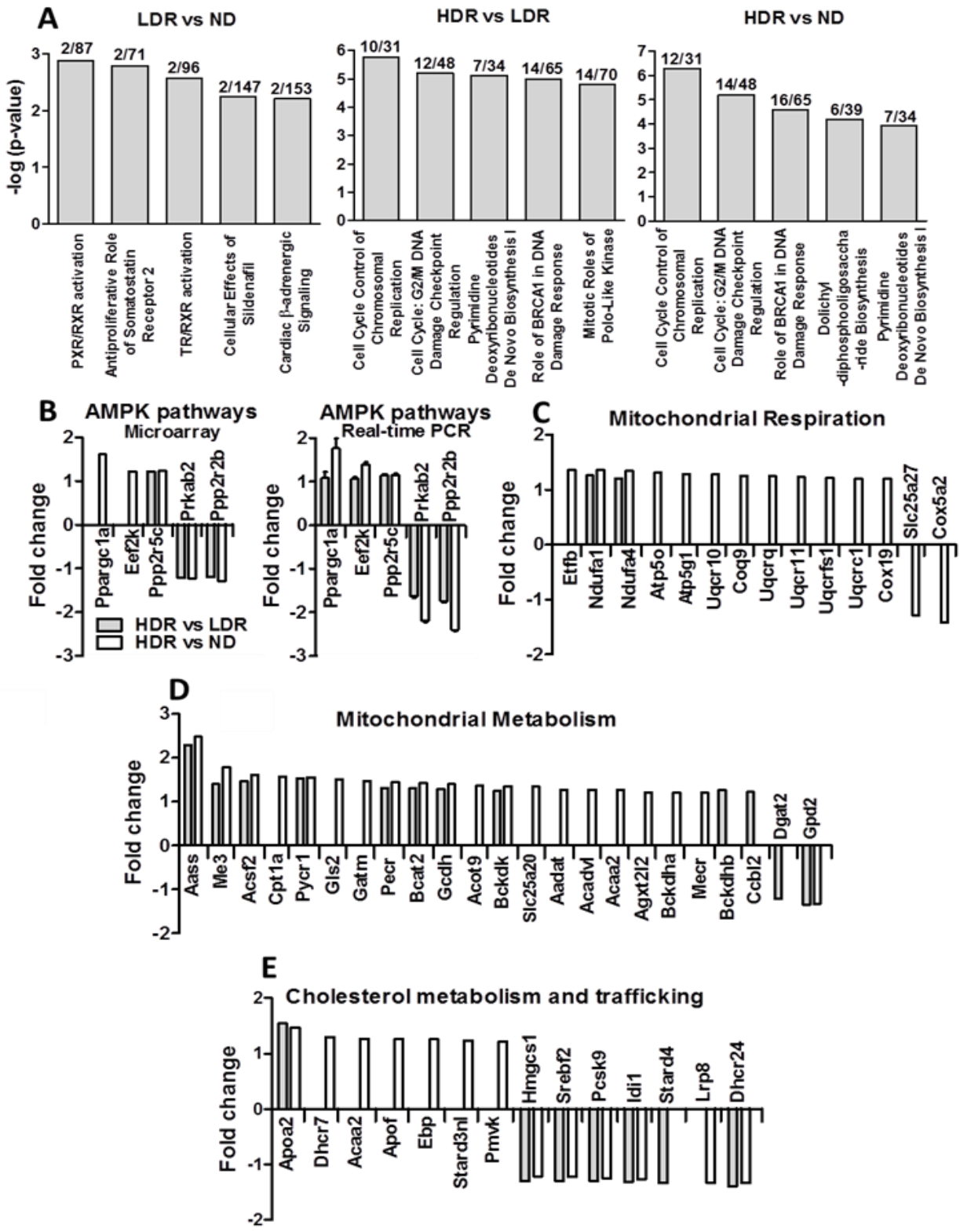
A
LDR vs ND
HDR vs LDR
HDR vs ND
-log (p-value)
2/87
2/71
2/96
2/147
2/153
10/31
12/48
7/34
14/65
14/70
12/31
14/48
16/65
6/39
7/34
PXR/RXR activation
Antiproliferative Role of Somatostatin Receptor 2
TR/RXR activation
Cellular Effects of Sildenafil
Cardiac β-adrenergic Signaling
Cell Cycle Control of Chromosomal Replication
Cell Cycle: G2/M DNA Damage Checkpoint Regulation
Pyrimidine Deoxyribonucleotides De Novo Biosynthesis I
Role of BRCA1 in DNA Damage Response
Mitotic Roles of Polo-Like Kinase
Cell Cycle Control of Chromosomal Replication
Cell Cycle: G2/M DNA Damage Checkpoint Regulation
Role of BRCA1 in DNA Damage Response
Dolichyl -diphosphooligosaccha -ride Biosynthesis
Pyrimidine Deoxyribonucleotides De Novo Biosynthesis I
B
AMPK pathways
Microarray
AMPK pathways
Real-time PCR
Fold change
Ppargc1a
Eef2k
Ppp2r5c
Prkab2
Ppp2r2b
HDR vs LDR
HDR vs ND
C
Mitochondrial Respiration
Etfb
Ndufa1
Ndufa4
Atp5o
Atp5g1
Uqcr10
Coq9
Uqcrq
Uqcr11
Uqcrfs1
Uqcrc1
Cox19
Slc25a27
Cox5a2
D
Mitochondrial Metabolism
Aass
Me3
Acsf2
Cpt1a
Pycr1
Gls2
Gatm
Pecr
Bcat2
Gcdh
Acot9
Bckdk
Slc25a20
Aadat
AcadM
Acaa2
Agxt2l2
Bckdha
Mecr
Bckdhb
Ccbl2
Dgat2
Gpd2
E
Cholesterol metabolism and trafficking
Apoa2
Dhcr7
Acaa2
Apof
Ebp
Stard3nl
Pmvk
Hmgcs1
Srebf2
Pcsk9
Idi1
Stard4
Lrp8
Dhcr24

Figure 2.6. mRNA profiling analysis of control and DIO mice. (A) Top five most significant enriched canonical pathways identified by Ingenuity Pathway Analysis (grey bars) using all the differentially expressed genes in LDR vs ND, HDR vs LDR and HDR vs ND islets comparisons that are listed according to their p-values expressed in –log (Y axis). The ratio of the number of differentially expressed genes over the total number of genes involved in each canonical pathway is reported on top of the bars. (B) AMPK pathways, (C) mitochondrial respiration, (D) mitochondrial metabolism and (E) cholesterol metabolism and trafficking gene expression by microarray analysis (B, C, D and E; +/- 1.2 fold change) and quantitative real time PCR (B; +/- 1.15 fold change) of HDR vs LDR (gray bar) and HDR vs ND (white bar).

As islets from DIO mice showed alterations in AMPK activity and signalling, we also examined gene expression changes in this pathway and found decreased AMPK-β subunit (*Prkab2*). Other genes that were altered in this pathway included the downstream direct targets, *Eef2k* and *Ppargc1a* and the upstream genes *Ppp2r2b* and *Ppp2r5c*, particularly in the HDR vs ND comparison (Fig. 2.6B). These expression changes in genes related to AMPK pathways were validated by real time PCR (Fig. 2.6B). Several genes related to mitochondrial respiration and metabolism were differentially expressed in the HDR islets (Fig. 2.6C and 2.6D), along with 17 genes coding for mitochondrial proteins (S2 and S4 Tables). Finally, we observed changes in the expression of various genes related to cholesterol metabolism and trafficking in HDR islets (Fig. 2.6E), in keeping with the elevated cholesterol synthesis and content in HDR islets. LDR islets in comparison to ND showed almost no change in the expression levels of the same pathways except for *Cpt1* and *Ppargc1a* that reflect enhanced fat oxidation, as expected in animals fed a high fat diet.

2.1.5 Discussion.

The present study reveals some of the underlying causes for islet β-cell dysfunction and defective GSIS in HFD fed mice (both LDR and HDR). The results implicate altered mitochondrial function, decreased AMPK activity and elevated expression of PKCε as key factors. However, unlike most DIO mouse studies, the animals were stratified with the goal of identifying specific differences that characterize a largely 'prediabetic' compensatory state (LDR group) from an 'early diabetic' state (HDR mice). This comparison revealed the following key

differences that will be discussed below: 1) a more pronounced mitochondrial dysfunction with marked mitochondrial membrane hyperpolarization; 2) a suppression of active AMPK relative to total AMPK; 3) reduced ACC activity, in association with enhanced fat oxidation (Peyot et al., 2010); 4) increased HMGCR activity in association with elevated islet cholesterol synthesis and plasma cholesterol; and finally 5) widespread changes in islet gene expression.

The $\Delta\psi_{mito}$ results indicating mitochondrial hyperpolarization at a high glucose concentration in HDR islets could be due to fewer protons reentering mitochondria via the ATP-synthase complex with a resultant decrease in ATP production (Michelakis, 2008). Interestingly, Wikstrom *et al.* (Wikstrom et al., 2007) observed an increased number of hyperpolarized mitochondria following a 24 h glucolipotoxic treatment of dispersed islet β-cells, suggesting that mitochondrial hyperpolarization can be associated with β-cell dysfunction under metabolic stress. Also, we previously observed that HDR islets show increased FFA oxidation compared to LDR and ND islets, without a change in glucose oxidation (Peyot et al., 2010), which could lead to an increase in the shuttling of protons into the mitochondrial inter-membrane space. This could explain the increase in $\Delta\psi_{mito}$ observed in HDR islets. Altered mitochondrial reactive oxygen species (ROS) production could contribute to β-cells dysfunction in HDR islets since hyperpolarization of $\Delta\psi_{mito}$ is associated with ROS production (Brand & Nicholls, 2011), and β-cells exposed to a glucolipotoxic insult show ROS accumulation both *in vitro* and *in vivo* (El-Assaad et al., 2010; C. Tang et al., 2007). However, the current ROS measurement tools are not very reliable and additional work is needed to test this possibility. Uncoupling did not appear to be a contributor to the lowered ATP production in DIO islets, like uncoupled respiration was unchanged in LDR and HDR islets. A recent study identified the accumulation of carnitine esters of hydroxylated FFA, in particular 3-hydroxy-tetradecanoyl-carnitine in isolated islets exposed to a glucolipotoxic insult (Doliba et al., 2015). Whether DIO islets also show this alteration that may cause dysfunction of mitochondrial energy metabolism (Stiles & Shirihai, 2012) is not known.

We further examined the possibility that the decreased ATP turnover and content in DIO mouse islets affects the activity of the energy sensor AMPK (N. B. Ruderman et al., 2013) which has been implicated in the control of insulin secretion, β-cell growth and apoptosis (da Silva Xavier et al., 2003; El-Assaad et al., 2010; Fu et al., 2013). AMPK phosphorylation of ACC and

HMGCR inactivates these enzymes to respectively promote β-oxidation of FFA (Fu et al., 2013) and to reduce cholesterol biosynthesis (Sato, Goldstein, & Brown, 1993). AMPK activation also reduces GSIS (da Silva Xavier et al., 2003; Leclerc et al., 2004) and β-cell proliferation (Fu et al., 2013; Fu et al., 2009). We found that despite an increase in total AMPK protein content in both LDR and HDR islets, phosphorylation status of AMPK under basal conditions was greatly decreased. Also net glucose-responsive AMPK activity in LDR and HDR islets was reduced, with changes in the HDR islets being more pronounced. Thus, the gradual decline in β-cell function from LDR to HDR islets correlates with corresponding decreases in AMPK activation.

Interestingly, despite the decreased AMPK activation in DIO islets, there was no corresponding effect on ACC phosphorylation: in fact, ACC phosphorylation was slightly elevated in HDR islets. The disassociation between AMPK phosphorylation and ACC phosphorylation appears to be unique to the HDR islets and resembles the dissociation observed in normal muscle during prolonged exercise, where is correlated with a shift in fuel utilization from glucose to FFA (Thomson et al., 2007; Wojtaszewski, Mourtzakis, Hillig, Saltin, & Pilegaard, 2002). The reason for this dissociation in islets is unclear. Inasmuch as total AMPK levels increase in HDR islets, the possibility that the dephosphorylated AMPK shows some activity towards ACC and thus causes elevated phospho-ACC needs to be considered. Nevertheless, the reduced activity of ACC due to its increased phosphorylation is expected to lower malonyl-CoA production in HDR islets so that mitochondrial β-oxidation is elevated, as observed previously (Peyot et al., 2010). This could be part of an adaptive protective mechanism important for nutrient detoxification at the expense of normal insulin secretion in HDR islets.

AMPK signaling is also regulated by protein phosphatase PP2a and a recent study showed that the regulatory subunit of protein phosphatase PP2a (PPP2R5C) plays an important role in the regulation of glucose and lipid metabolic homeostasis in hepatocytes, at least in part by regulating AMPK activation. In keeping with this possibility, PPP2R5C knockdown in rat hepatocytes has been shown to elevate AMPK phosphorylation (Cheng et al., 2015). In addition, we noticed that the *Ppp2r5c* gene was up-regulated in HDR islets and this might have diminished AMPK activation under the DIO conditions. Besides, it has been shown that glucose enhances PP2a activity, which activates ACC, probably by its dephosphorylation (Castermans et al., 2012; Kowluru, Chen, Modrick, & Stefanelli, 2001). In fact dissociation between phospho-AMPK and phospho-ACC levels has been noticed in renal tissue, in a recent study in high fat

diet fed mice (Kim et al., 2013). Thus an altered PP2a / PPP2R5C balance in DIO islets may be responsible for the dissociation between AMPK and ACC activity.

Even though glucose regulates AMPK activity, we did not notice a direct regulation of HMGCR phosphorylation / activity and cholesterol content by glucose in ND or DIO islets. However, the enhanced activity of HMGCR in HDR islets is possibly due to the inhibition of the AMPK pathway, contributing to the elevated cholesterol levels in these islets. Various studies have provided support for the view that cholesterol accumulation alters mitochondrial function and membrane fusion processes in various cell types (Garcia-Ruiz et al., 2009). In the β-cell, cholesterol accumulation has been implicated in the reduced exocytosis that occurs in T2D (Brunham et al., 2010; Kruit et al., 2011). Also, a recent study showed that isoprenoid intermediates of cholesterol biosynthesis are important for GSIS (Zuniga-Hertz et al., 2015). Thus, increased cholesterol levels, such as are observed in HDR but not LDR islets, could contribute to the markedly defective GSIS and β-cell failure in these mice.

The marked reduction in AMPK activity in HDR islets could contribute to the β-cell dysfunction of DIO islets by altering its cholesterol metabolism as well as the enhanced β-cell mass seen in our earlier study (Peyot et al., 2010). Thus, AMPK via its interaction with mTOR and other growth control pathways (N. B. Ruderman et al., 2013) is a major player in cell proliferation, and its activity is inversely correlated with β-cell growth (Fu et al., 2013). Interestingly, the major gene expression changes seen in HDR vs ND and in HDR vs LDR comparisons in the present study were related to cell cycle, cell proliferation and DNA replication and repair, all of which could relate to the much increased β-cell mass and proliferation seen in HDR mice (Peyot et al., 2010).

Lipid metabolism in the pancreatic β-cell, in particular the GL/FFA cycle, potentiates GSIS through the production of lipid-signaling molecules (e.g., diacylglycerol, 1-monoacylglycerol) (Prentki et al., 2013; Zhao et al., 2014; Zhao et al., 2015). Sn1,2-diacylglycerol, generated either by phospholipid hydrolysis or via the lipogenic arm of the GL/FFA cycle can activate certain members of protein kinase C family, including PKCε, which has been identified as a negative regulator of lipolysis and GSIS in pancreatic β-cells (Cantley et al., 2009). We noticed a two-fold increase in PKCε total protein levels in LDR and HDR islets, and observed an increase of PKCε phosphorylation, a potential indicator of PKCε activation

(Cenni et al., 2002) only in HDR islets. These changes may contribute to the secretory dysfunction and altered lipid partitioning observed in both LDR and HDR islets (Peyot et al., 2010).

A most surprising observation of this study was the similarity in gene expression profiles between LDR and ND islets (with only 17 genes being differentially expressed by more than ±1.2 fold) compared to the differences seen between HDR and ND islets (1508 differentially regulated genes) or HDR and LDR islets (1041 differentially regulated genes). Since HDR and LDR mice were fed the same high fat diet, it would be expected that a high fat diet shift would cause major changes in gene expression in all DIO mice, which in fact was not the case. The possibility should be considered that β-cell compensation in the prediabetic state (corresponding to the LDR group) is largely independent from transcriptional adaptive changes whereas the transition to early diabetes (HDR mice) results in part from major alterations in gene expression. The reason why some animals respond better to the obesogenic diet (HDR) than others (LDR) is not known. It could be related to subtle epigenetic differences that could impact in particular on appetite since HDR animals eat slightly more than LDR (Peyot et al., 2010). The compensation in the LDR group could be achieved via mechanisms independent of modifications in mRNA expression such as translational and posttranslational changes. For example the mRNA expression of AMPK subunits is unchanged in LDR islets, whereas the markedly reduced AMPK activity could drive compensatory effects such as β-cell growth.

2.1.6 Conclusion

This study provides insights into the biochemical basis of islet β-cell failure in HDR DIO mice (Fig. 7). The results favor the view that the pre-eminent β-cell dysfunction of HDR mice is due at least in part to chronically reduced AMPK activity, mitochondrial dysfunction with decreased ATP production, elevated cholesterol uptake, biosynthesis and deposition, and vast alterations in gene expression. The latter could be related to compensatory changes in β-cell growth that modify its phenotype as well as GSIS.

2.1.7 Acknowledgments.

The authors wish to thank Gilles Corbeil from the biochip and genotyping core of CRCHUM for microarray analysis.

2.1.8 Author Contributions.

Conceived and designed the experiments: EJ, EP, MLP, MP, NR. Performed the experiments: AA, CA, EP, JL, MLP, RL. Analyzed the data: AA, EJ, EP, MLP, MP, RS, SRMM, ZK. Contributed reagents/materials/analysis tools: RL. Wrote the paper: AA, EP, MLP, MP, SRMM.

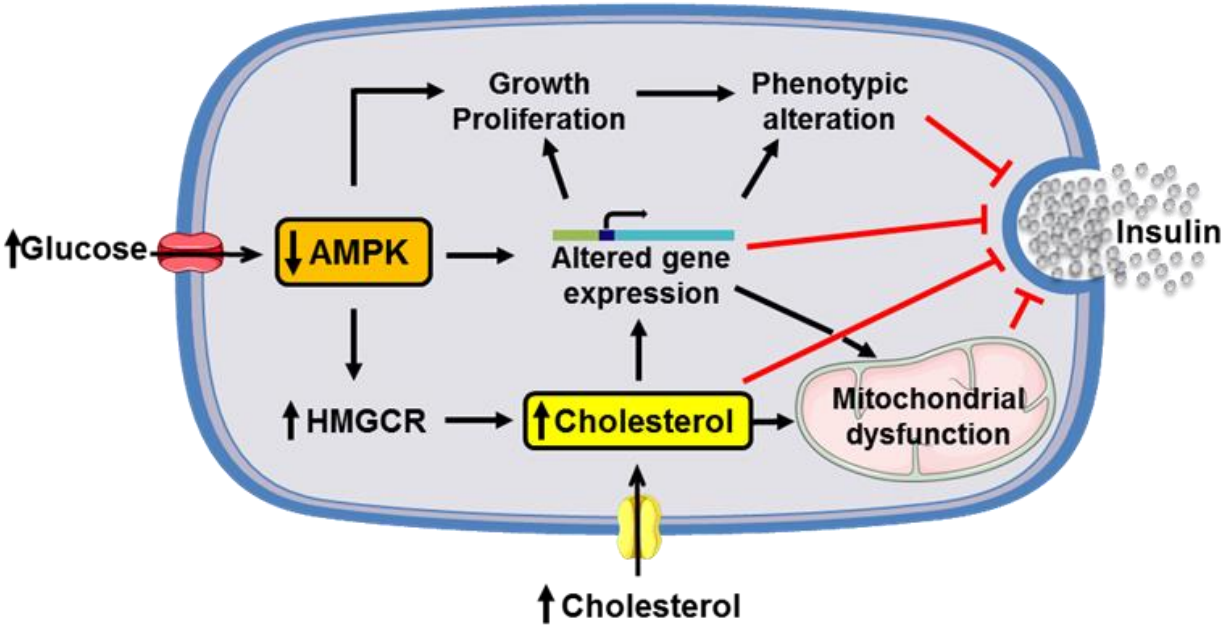

Figure 2.7. Model depicting the mechanisms contributing to β-cell dysfunction and failure in obese HDR mice. Hyperglycemic and hypercholesterolemic HDR mice are characterized by major changes in islet mRNA species expression, and suppression of AMPK activity that causes HMG-CoA reductase activation and increased cholesterol synthesis and deposition in islet β-cells. Cholesterol accumulation leads to mitochondrial dysfunction and reduced exocytotic release of insulin. Reduced AMPK activity may promote β-cell growth and proliferation as a compensatory mechanism, but can also lead to altered gene expression and modify various signaling pathways for insulin secretion, causing β-cell phenotypic alterations and defective insulin secretion.

2.2 Addendum.

2.2.1 ROS measurement.

Several studies have provided evidence for the role of ROS (in particular H_2O_2) in GSIS (P. Newsholme et al., 2009; Pi et al., 2007). Changes in ROS production from mitochondria could contribute to β-cells dysfunction in HDR islets since hyperpolarization of $\Delta\psi_{mito}$ is associated with ROS production (Brand & Nicholls, 2011; Suski et al., 2012) . We attempted to measure ROS production in the form of hydrogen peroxide (H_2O_2) (Fig. 2.8). Unfortunately,

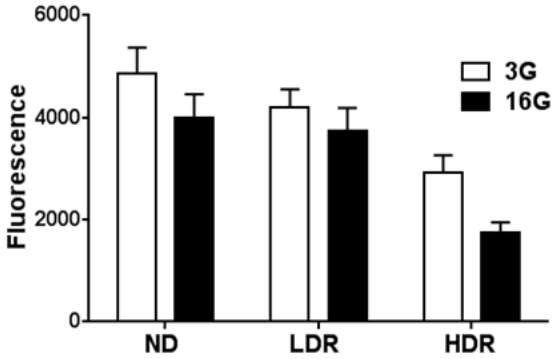

Figure 2.8. H_2O_2 production measurements in isolated mouse islets. H_2O_2 production measurements of islets incubated at 3 mM (3G) or 16 mM (16G) glucose for 20 min. Means ± SEM from 7 (ND and HDR) and 6 (LDR) mice. *p<0.05, **p<0.01 vs ND, &p<0.05, &&p<0.01 for HDR vs LDR, for the same glucose concentration. One-way ANOVA, Tukey post-hoc test.

we were not successful in optimizing the conditions for measuring H_2O_2 production in freshly isolated mouse islets under basal conditions, where we observed very high levels of H_2O_2 and no response to high glucose in our ND and LDR groups (we anticipated that a H_2O_2 would rise in response to high glucose). We optimized this assay in the lab and found that a richer medium for basal conditions with 4 mM glucose plus 2 mM glutamine and 50 µM carnitine to promote the β-oxydation of FFA can be used for better results. However, these are not the conditions of the other experimental work in the thesis and therefore the data were not included in the now published PLoS One paper. It should be noted, as discussed by Prentki et al. (Prentki et al.,

2013), that the vast majorities of islet *in vitro* studies used 2-3 mM glucose only as basal fuel. This results in fuel depletion, a condition of metabolic stress that may artefactually increase ROS production. This has been realized in recent targeted metabolomics studies. Thus, in the future studies should use richer media in nutrients for islet *in vitro* studies.

2.2.2 Method.

Hydrogen peroxide (H_2O_2) measurement was performed using Amplex-Red reagent (Thermo-Fisher Scientific A12222) which reacts with H_2O_2 in the present of horseradish peroxidase (HRP) (Sigma P8250). Intact freshly isolated islets from each DIO and control group were pre-incubated for 45 min in KRBH supplemented with 3 mM glucose and 0.5% BSA at 37°C after recovery for 2h in RPMI complete medium with 3 mM glucose. Then the islets were incubated in KRBH (0.5% BSA) in 3 or 16 mM glucose with 100 μM AmplexRed for 20 min. After the incubation, the islets were washed once with ice-cold PBS and then 0.1 M Tris-HCl + 0.1% BSA buffer was added and sonication was carried out for 5 sec. Then the lysates were transferred into black 96 well plates with clear bottom and HRP in 0.1 M Tris-HCl was added to a final concentration of 1 U/ml per well to start the reaction and incubated for 5min. The red-fluorescence oxidation product, resorufin, which has excitation and emission maxima of approximately 571 nm and 585 nm, respectively, was detected using a plate reader (FLUOstar Optima, BMG Labtech, Ortenberg, Germany). Non-specific fluorescence values, H_2O_2 (0.006%) and antioxidant (N-acetylcysteine 0.4 μM) controls were also included (This protocol was obtained from the Christopher J. Rhodes Lab, University of Chicago).

Chapter 3 – Summary and future direction of the project

3.1 Summary.

Diabetes is a global health problem whose increasing prevalence involves a complex mixture of genetic, lifestyle and environmental risk factors that vary among individuals. In 2012, diabetes was the direct cause of 1.5 million deaths world-wide and high blood glucose was the contributing factor for another 2.2 million deaths (WHO, 2016). T2D, which affects the majority of individuals with diabetes, is a metabolic disorder of fuel homoeostasis characterized by hyperglycemia and altered lipid metabolism caused by islet β-cell dysfunction and insulin resistance (Nolan et al., 2011). The complications of T2D, if not well controlled over time, can be severe and include damage to the heart, blood vessels, eyes, kidneys, nerves and eventually death. The best patient outcomes from existing diabetes treatments occur if the disease is diagnosed early and is well-controlled by medications, diet and physical activity. All drug treatments of diabetes focus on treating the symptoms and complications of diabetes but do not reverse the actual causes (Defronzo, 2009). Obesity is one of the major risk factors for T2D, especially when it is associated with dyslipidemia, hyperinsulinemia, and insulin resistance. In obese subjects, insulin resistance is a common feature and insulin secretion by the β-cell is increased to compensate for the reduction in insulin action and to maintain normoglycemia. When the β-cell fails to compensate for the increase in insulin resistance of peripheral tissues, obese individuals develop T2D. As a result, β-cell dysfunction plays a central role in the development of the obesity-associated T2D. Despite the progress in the knowledge of the mechanisms responsible for insulin secretion in the β-cell in response to glucose and fatty acids, the mechanisms causing β-cell dysfunction in disease situations are still poorly understood.

Animal models of T2D provide opportunities to study the complexity of T2D pathogenesis (Kaplan & Wagner, 2006); and the combined effects of obesity and T2D on the development of T2D and β-cell dysfunction can be studied in classical models, such as obese Zucker Diabetic Fatty rats, *ob/ob* and *db/db* mice (Delghingaro-Augusto et al., 2009; King, 2012; Nolan et al., 2006). However, these models are of an extreme nature with rapid development of severe T2D and due to genetic defects in leptin signaling that are rarely seen in human patients with T2D. The diet-induced obese (DIO) C57BL/6N mouse, which represents a polygenic model of mild T2D, may provide a closer model to human T2D. DIO mice gradually develop

hyperglycemia when fed a high fat diet and show insulin resistance and β-cell failure with defective GSIS (Pepin et al., 2016; Peyot et al., 2010; Winzell & Ahren, 2004). This model represents the interaction between environmental factors, diet and genetic background on the development of T2D.

Work done in the Prentki lab (Peyot et al., 2010) has shown that the DIO model can be used to uncover the differences between pre-diabetes and early diabetic states with the goal of identifying causal factors in β-cell failure. Work in my thesis has shown that DIO mice could be stratified into low (LDR) and high (HDR) diet responders based on their weight gain. The LDR have the characteristics of an obese pre-diabetes state in humans with overall β-cell compensation for insulin resistance and show only mild impairment in GSIS. The HDR are more obese, insulin resistant, hyperinsulinemic and hyperglycemic than the LDR group and show more prominent signs of β-cell dysfunction that altogether mimics the obese early diabetic state in humans. We have also shown that HDR mice display additional alterations in islet lipid metabolism, where free fatty acid oxidation and free cholesterol level are notably increased. Both LDR and HDR mice showed defective islet glycerolipid/free fatty acid (GL/FFA) cycling and lipolysis and decreased glucose-stimulated ATP content in DIO islets (Peyot et al., 2010). Based on these findings, we further investigated different metabolic parameters that may affect β-cell function to gain an insight into the molecular basis of β-cell adaptation and failure in this specific model (Pepin et al., 2016).

Our results revealed key metabolic differences between LDR, HDR and ND mice when freshly isolated islets from these groups were studied *ex-vivo* for mitochondrial metabolism, AMPK activity and signalling, the expression and activity of key enzymes of energy metabolism, cholesterol synthesis, and mRNA profiling. Severely compromised GSIS was seen in HDR islets, as compared to ND and LDR islets; and was associated with suppressed AMPK activity. HDR islets also showed reduced ACC activity and enhanced activity of HMGCR, which may contribute respectively to elevated fatty acid oxidation and increased cholesterol biosynthesis. HDR islets also displayed mitochondrial membrane hyperpolarization and reduced ATP turnover in the presence of elevated glucose. Expression of PKCε, which reduces both lipolysis and production of signals for insulin secretion (Schmitz-Peiffer et al., 2007), was elevated in DIO islets. Diet-induced changes in the islet transcriptome, consisting of genes whose expression

changed by more than 1.2-fold, were minor between LDR and ND islets (17 differentially expressed transcripts), but were prominent between HDR and ND islets (1508 differentially expressed transcripts). The minimal changes in gene expression in the LDR islets in comparison to the ND islets despite the difference in diet were surprising. The possibility should be considered that β-cell compensation in the pre-diabetic state (corresponding to the LDR group) is largely independent from transcriptional adaptive changes; whereas the transition to early diabetes (HDR mice) results in part from major alterations in gene expression. In HDR islets, the affected genes were related to cell cycle and proliferation, AMPK signaling, mitochondrial metabolism and cholesterol metabolism. Our findings favor the view that the pre-eminent β-cell dysfunction of HDR mice is due at least in part to chronically reduced AMPK activity and mitochondrial dysfunction with decreased ATP production, elevated cholesterol uptake, biosynthesis and deposition, and widespread alterations in gene expression. The latter could be related to compensatory changes in β-cell growth that modify its phenotype as well as GSIS (Pepin et al., 2016).

3.2 Future direction

These findings provide an insight into β-cell dysfunction in the DIO model; however, more studies should be done to further investigate this mechanism. Studies have shown that ROS can have a role in GSIS and may act as MCF (P. Newsholme et al., 2009; Pi et al., 2007). Furthermore, their production is linked to hyperpolarization of $\Delta\psi_{mito}$ that we found in the HDR islets (Brand & Nicholls, 2011; Suski et al., 2012). In addition, an increase in UCP2 mRNA was observed in HDR islets in our previous study (Peyot et al., 2010) and UCP2 upregulation is associated with reduced ROS production (Robson-Doucette, Sultan et al. 2011). Thus, measuring ROS production in these islets under appropriate experimental conditions as discussed in Section 2.1, may identify a further link between mitochondrial dysfunction and impaired GSIS in this model.

AMPK is directly activated by changes in ratios of AMP and ADP with ATP (Hardie & Hawley, 2001; N. Ruderman & Prentki, 2004). In our model AMPK activity is suppressed more strongly in the HDR islets in comparison to both ND and LDR islets (Pepin et al., 2016). Moreover, both LDR and HDR islets showed a decrease in the intracellular ATP content in response to high glucose in comparison to ND mice (Peyot et al., 2010). However, this assay

does not show the actual ratio between AMP, ADP and ATP; and measuring the concentrations of the three adenine nucleotides simultaneously could give more insight into the islet energy status and AMPK regulation in this model. Moreover, using targeted metabolomics in the islets of these three groups to measure glycolysis and TCA cycle intermediates, GL/FFA cycling metabolites, and redox components NAD(P)(H) and oxidized and reduced glutathione could give us more insight on the changes that happen related to metabolic signaling in the LDR and HDR islet group, especially in the MCF concentrations. These additional measurements should give us a more precise picture of the alterations of these islets and how GSIS is impaired in the different stages leading towards β- cell failure. In addition, while our study focused on the islets to study the causes and mechanism of β-cell dysfunction in this model; it would be also interesting to assess whether other organs in the body (including the brain, the liver and the adipose tissue) influence β- cell function in this model, for example by producing metabolic signals, neurotransmitters or hormones that may affect insulin secretion.

Our group is the first to show that C57BL/6N DIO mice can be stratified into two groups based on their body weight in response to HFD. Furthermore, the results show that their metabolic characteristics mimic the pre-diabetes state (LDR) and the obese early diabetic state in humans (HDR) as mentioned above. It would be interesting to know why this separation happens and also to gain more insight on the β- cell alterations in different states and degrees of insulin resistance. There are different possible explanations that could be considered like the effects of HFD on epigenetic modifications that could impact in particular on the appetite since HDR animals eat slightly more than LDR; and the composition of gut flora of the DIO mice. These possibilities are discussed below.

3.2.1 Epigenetic modifications and T2D.

Studies have shown that hereditary can influence the risk of T2D (Sladek et al., 2007; Voight et al., 2010). They revealed that the majority of T2D single nucleotide polymorphisms (SNPs) are associated with impaired insulin secretion rather than impaired insulin action (Rosengren et al., 2012; Ruchat et al., 2009; Travers & McCarthy, 2011). However, all these findings only explain a small proportion of the estimated heritability of T2D, suggesting that additional genetic factors remain to be identified (Travers & McCarthy, 2011). Environmental factors can have an influence on the genetic variants and modulate the risk of T2D through gene-environment

interactions (Franks, 2011). These interactions can occur through direct chemical modification of chromatin (called epigenetic modifications), including DNA methylation, post-translational histone modifications, and changes in the expression of microRNAs (miRNA) and long non-coding RNAs (lncRNAs) (Bernstein, Meissner, & Lander, 2007; Ling & Groop, 2009). Epigenetic modifications are changes that influence the chromatin structure and DNA accessibility and can thereby affect gene function and/or regulation without altering the primary genome sequence (Bird, 2007). In some cases, epigenetic modifications are stable and can be passed on to future generations, but in other cases they are dynamic and change in response to environmental stimuli, making them very important in complex multifactorial diseases such as obesity and T2D (Brookes & Shi, 2014; Jiang, Bressler, & Beaudet, 2004; Portela & Esteller, 2010).

In recent years, the role of epigenetic modifications in the development of T2D has become better defined (Villeneuve & Natarajan, 2010). One recent study has analyzed DNA methylation of 479,927 CpG sites and the transcriptome in pancreatic islets from T2D and non-diabetic donors. They identified 1,649 CpG sites and 853 genes, including TCF7L2, *THADA*, *KCNQ1*, *FTO*, and *IRSI*, with differential DNA methylation in T2D islets (Dayeh et al., 2014). They also reported increased expression and decreased methylation of the *CDKN1A* and *PDE7B* genes in T2D that could result in impaired GSIS. Furthermore, this identified candidate genes that may affect pancreatic β- and α-cells, as Exoc3l silencing reduced exocytosis and overexpression of *Cdkn1a*, *Pde7b* and *Sept9* perturbed insulin and glucagon secretion in clonal β- and α-cells, respectively. These observations provide evidence for a link between T2D associated epigenetic modifications and impaired insulin release (Dayeh et al., 2014).

The *PPARGC1A* gene in many tissues encodes a transcriptional coactivator that regulates mitochondrial oxidative metabolism and is a target of AMPK. Expression of this gene was positively correlated with GSIS from human β-cells (Ling et al., 2008). In β-cells from T2D islets, DNA methylation of the *PPARGC1A* promoter was reported to be doubled and the expression of *PPARGC1A* gene was significantly reduced in comparison to non-diabetic β-cells. This gene is downregulated in individuals that have an inactive lifestyle, which is one of the risk factors for T2D (Alibegovic et al., 2010). Our microarray analysis showed that expression of Ppargc1a is reduced in the HDR vs LDR and the HDR vs ND but not in the LDR vs ND. This change could be related to epigenetic modifications that would be interesting to investigate and

in particular there might be more epigenetic modifications in the HDR group, which shows more β- cell dysfunction than LDR islets.

miRNAs are involved in the regulation of GSIS. Overexpression of the islet-specific miR-375, reduces GSIS while its inhibition results in an increase in insulin secretion (Poy et al., 2004). Also it was reported that changes in miRNA-192 expression can affect insulin secretion (Oghbaei, Ahmadi Asl, Sheikhzadeh, Alipour, & Khamaneh, 2015). Thus, miRNAs may play a role in the etiology of T2D. In our study, microarray analysis showed that there are miRNA gene expression changes in the HDR vs LDR and the HDR vs ND but not in the LDR vs ND, which may indicate additonal mechanisms for the pathogenesis of β-cell dysfunction in the HDR group. Furthermore, the functional analysis of the microarray data showed that there are more genes involved in epigenetic regulation that change in the HDR group compared to the ND and LDR groups (Appendix 1). Altogether, these observations suggest that the HDR group could have more epigenetic modifications than the LDR, but this remains to be directly examined.

3.2.2 Gut flora and T2D.

Gut microbiota are increasingly being shown to play a key role in health maintenance and can be involved in the development of chronic inflammation, T2D, obesity, atherosclerosis, hypertension, and other conditions (Boulange, Neves, Chilloux, Nicholson, & Dumas, 2016; Gareau, Sherman, & Walker, 2010). Some microbiota form toxins that can enter the blood stream and cause inflammation, which may affect the liver and the adipose tissue to alter insulin sensitivity and metabolism activity (Cani & Delzenne, 2009). Gut microbiota can contribute to the pathophysiology of obesity through different mechanisms, including energy harvest from the diet, LPS-induced chronic inflammation, modulation of tissue fatty acid composition, bioconversion and gut-derived peptide secretion (Boulange et al., 2016; Gross et al., 2010; Musso, Gambino, & Cassader, 2010; Turnbaugh et al., 2006). Furthermore, some studies have shown that bile acids are metabolized by gut microbiota, which may affect lipid metabolism systemically (Conlon & Bird, 2015; Musso et al., 2010; Nie, Hu, & Yan, 2015; Ridlon, Kang, Hylemon, & Bajaj, 2014).

There are different kinds of gut microbiota. Bacteroidetes (important for protein and carbohydrate digestion in the gut), Firmicutes (involved in dietary fat processing), and Actinobacteria phyla represent 90% of the microbiota (Eckburg et al., 2005; Qin et al., 2010).

The microbiota composition can change qualitatively and quantitatively in response to physiological, dietary and climatogeographic factors (Zoetendal, Rajilic-Stojanovic, & de Vos, 2008). For example, it was shown that switching from a diet rich in fat and carbohydrates to a diet low in fat and rich in plant polysaccharides, or switching from a HFD to a diet with a low glycemic index, caused some substantial changes in the microbiota on the following day (Turnbaugh et al., 2009; Wu et al., 2011). A recent article showed that the effect of microbiota composition can change the outcome of an experiment that is done on identical batch of mice (i.e. the same strain, same vendor and same housing conditions) (Servick, 2016).

It is important to mention that despite all the studies that supported the hypothesis that changes in the microbiota could contribute to the obesity epidemic, direct support for this view has not yet been provided. A recent study has attempted to assess this hypothesis by performing a meta-analysis on 10 independent studies. They found that although there was some relationship between the microbial communities found in human feces and obesity, this association was weak and is confounded by large interpersonal variation and insufficient sample sizes (Sze & Schloss, 2016). Therefore, more studies are needed to assess how the gut microbiota is linked to obesity. This could provide new potential targets for reducing the risk of obesity associated T2D.

Evidence in clinical studies showed that insulin resistant obese and T2D individuals have altered gut microbiota composition compared with metabolically healthy individuals (Larsen et al., 2010; Tilg & Kaser, 2011; Tremaroli & Backhed, 2012). These alterations can modify the host energy metabolism and lead to the accumulation of gut derived bacterial inflammatory molecules (such as LPS, peptidoglycans and flagellin), which may accelerate the inflammation in T2D (Delzenne & Cani, 2011; Kootte et al., 2012).

A recent study has examined the effect of different glucose tolerance levels and dietary patterns on gut microbiota composition (the study subjects had normal glucose tolerance, pre-diabetes and T2D) (Egshatyan et al., 2016). The study demonstrated a link between different levels of glucose intolerance and the abundance of three genera of microbiota: Blautia, Serratia and Akkermansia bacteria. While all three genera are found in healthy individuals, their numbers greatly increased with increasing degrees of glucose intolerance and diabetes (Egshatyan et al., 2016). By comparing individuals with similar diets, they discovered that half of the patients with a high-calorie diet had a normal tolerance, the other half had T2D. This suggests an important

contribution of the microbiota on the progression of T2D and not of the diet itself. Also, certain microbiota can cause an immune response or form toxins that can cause inflammation to the liver and the adipose tissue and affect overall metabolism and insulin sensitivity (Cani, Amar, et al., 2007; Cani & Delzenne, 2009).

In our model where the mice were fed the same diet, the different responses in the LDR and the HDR groups might be explained by differences in gut microbiota composition (Cani, Neyrinck, et al., 2007; Hildebrandt et al., 2009). Investigating this could give us more insight on the effect of the gut microbiota on the development of T2D.

3.3 Conclusion.

The work that was done in this thesis was aimed to provide more insight into the molecular basis of β-cell adaptation and failure in obesity-associated T2D. We used a mouse model developed in our laboratory with a stratification of animals according to body weight gain in response to HFD, which could also be used in many future studies to uncover the role of the environment, genetic, epigenetic and gut flora changes in obesity and T2D predisposition. In research, working with different animal models has provided a huge array of genetic and phenotypic information that is useful in many fields, but it is important to mention that it is difficult to fully replicate the human genetic and environmental exposure in mouse models; as a result, many observations in mice do not translate directly to humans. In the diabetes field, most rodent models are of an extreme nature with rapid development of pronounced T2D and with genetic modifications that are rare in humans. Our stratified DIO model on the other hand, provides a polygenic model of mild T2D that more closely resembles human T2D. Saying that, it is important for anyone who plans to use animal models to evaluate their research rationale and hypothesis to see whether the questions they are asking could be applied or translated to humans.

Overall, this thesis provides insight into the biochemical basis of islet β-cell compensation and failure in a mouse model that mimics the pre-diabetic and early diabetic states in human subjects; and provides evidence that alerations in AMPK activity, cholesterol metabolism, mitochondrial dysfunction and β-cell gene expression may be involved in this process. Furthermore, our studies have lead to the surprising observation that the nutritional stress of a HFD leads to β-cell compensation in the pre-diabetic state (LDR mice) that does not

require significant adaptive changes in gene expression; whereas the transition to early diabetes (HDR mice) results in part from major alterations in gene expression.

References.

[1] Alappat, L., & Awad, A. B. (2010). Curcumin and obesity: evidence and mechanisms. *Nutr Rev, 68*(12), 729-738. doi:10.1111/j.1753-4887.2010.00341.x

[2] Alibegovic, A. C., Sonne, M. P., Hojbjerre, L., Bork-Jensen, J., Jacobsen, S., Nilsson, E., . . . Vaag, A. (2010). Insulin resistance induced by physical inactivity is associated with multiple transcriptional changes in skeletal muscle in young men. *Am J Physiol Endocrinol Metab, 299*(5), E752-763. doi:10.1152/ajpendo.00590.2009

[3] American Diabetes, A. (2014). Diagnosis and classification of diabetes mellitus. *Diabetes Care, 37 Suppl 1*, S81-90. doi:10.2337/dc14-S081

[4] Amos, A. F., McCarty, D. J., & Zimmet, P. (1997). The rising global burden of diabetes and its complications: estimates and projections to the year 2010. *Diabet Med, 14 Suppl 5*, S1-85.

[5] Andrikopoulos, S. (2010). Obesity and type 2 diabetes: slow down!--Can metabolic deceleration protect the islet beta cell from excess nutrient-induced damage? *Mol Cell Endocrinol, 316*(2), 140-146. doi:10.1016/j.mce.2009.09.031

[6] Andrikopoulos, S., Rosella, G., Gaskin, E., Thorburn, A., Kaczmarczyk, S., Zajac, J. D., & Proietto, J. (1993). Impaired regulation of hepatic fructose-1,6-bisphosphatase in the New Zealand obese mouse model of NIDDM. *Diabetes, 42*(12), 1731-1736.

[7] Anis, A. H., Zhang, W., Bansback, N., Guh, D. P., Amarsi, Z., & Birmingham, C. L. (2010). Obesity and overweight in Canada: an updated cost-of-illness study. *Obes Rev, 11*(1), 31-40. doi:10.1111/j.1467-789X.2009.00579.x

[8] Arner, P., & Langin, D. (2014). Lipolysis in lipid turnover, cancer cachexia, and obesity-induced insulin resistance. *Trends Endocrinol Metab, 25*(5), 255-262. doi:10.1016/j.tem.2014.03.002

[9] Ashcroft, F. M. (2005). ATP-sensitive potassium channelopathies: focus on insulin secretion. *J Clin Invest, 115*(8), 2047-2058. doi:10.1172/JCI25495

[10] Aston-Mourney, K., Wong, N., Kebede, M., Zraika, S., Balmer, L., McMahon, J. M., . . . Andrikopoulos, S. (2007). Increased nicotinamide nucleotide transhydrogenase levels predispose to insulin hypersecretion in a mouse strain susceptible to diabetes. *Diabetologia, 50*(12), 2476-2485. doi:10.1007/s00125-007-0814-x

[11] Attane, C., Peyot, M. L., Lussier, R., Zhang, D., Joly, E., Madiraju, S. R., & Prentki, M. (2016). Differential Insulin Secretion of High-Fat Diet-Fed C57BL/6NN and C57BL/6NJ Mice: Implications of Mixed Genetic Background in Metabolic Studies. *PLoS One, 11*(7), e0159165. doi:10.1371/journal.pone.0159165

[12] Baggio, L. L., & Drucker, D. J. (2006). Therapeutic approaches to preserve islet mass in type 2 diabetes. *Annu Rev Med, 57*, 265-281. doi:10.1146/annurev.med.57.110104.115624

[13] Bajaj, M., & Defronzo, R. A. (2003). Metabolic and molecular basis of insulin resistance. *J Nucl Cardiol, 10*(3), 311-323.

[14] Beall, C., Piipari, K., Al-Qassab, H., Smith, M. A., Parker, N., Carling, D., . . . Ashford, M. L. (2010). Loss of AMP-activated protein kinase alpha2 subunit in mouse beta-cells impairs

glucose-stimulated insulin secretion and inhibits their sensitivity to hypoglycaemia. *Biochem J, 429*(2), 323-333. doi:10.1042/BJ20100231

[15] Bergman, R. N., & Ader, M. (2000). Free fatty acids and pathogenesis of type 2 diabetes mellitus. *Trends Endocrinol Metab, 11*(9), 351-356.

[16] Bernstein, B. E., Meissner, A., & Lander, E. S. (2007). The mammalian epigenome. *Cell, 128*(4), 669-681. doi:10.1016/j.cell.2007.01.033

[17] Bird, A. (2007). Perceptions of epigenetics. *Nature, 447*(7143), 396-398. doi:10.1038/nature05913

[18] Bluher, M., Michael, M. D., Peroni, O. D., Ueki, K., Carter, N., Kahn, B. B., & Kahn, C. R. (2002). Adipose tissue selective insulin receptor knockout protects against obesity and obesity-related glucose intolerance. *Dev Cell, 3*(1), 25-38.

[19] Bonnefond, A., Froguel, P., & Vaxillaire, M. (2010). The emerging genetics of type 2 diabetes. *Trends Mol Med, 16*(9), 407-416. doi:10.1016/j.molmed.2010.06.004

[20] Boulange, C. L., Neves, A. L., Chilloux, J., Nicholson, J. K., & Dumas, M. E. (2016). Impact of the gut microbiota on inflammation, obesity, and metabolic disease. *Genome Med, 8*(1), 42. doi:10.1186/s13073-016-0303-2

[21] Bournat, J. C., & Brown, C. W. (2010). Mitochondrial dysfunction in obesity. *Curr Opin Endocrinol Diabetes Obes, 17*(5), 446-452. doi:10.1097/MED.0b013e32833c3026

[22] Boyd, A. E., 3rd, & Moss, L. G. (1993). When sugar is not so sweet: glucose toxicity. *J Clin Invest, 92*(1), 2. doi:10.1172/JCI116550

[23] Brand, M. D., & Nicholls, D. G. (2011). Assessing mitochondrial dysfunction in cells. *Biochem J, 435*(2), 297-312. doi:10.1042/BJ20110162

[24] Brookes, E., & Shi, Y. (2014). Diverse epigenetic mechanisms of human disease. *Annu Rev Genet, 48*, 237-268. doi:10.1146/annurev-genet-120213-092518

[25] Brunham, L. R., Kruit, J. K., Hayden, M. R., & Verchere, C. B. (2010). Cholesterol in beta-cell dysfunction: the emerging connection between HDL cholesterol and type 2 diabetes. *Curr Diab Rep, 10*(1), 55-60. doi:10.1007/s11892-009-0090-x

[26] Bruning, J. C., Michael, M. D., Winnay, J. N., Hayashi, T., Horsch, D., Accili, D., . . . Kahn, C. R. (1998). A muscle-specific insulin receptor knockout exhibits features of the metabolic syndrome of NIDDM without altering glucose tolerance. *Mol Cell, 2*(5), 559-569.

[27] Buck, D. W., 2nd, Jin da, P., Geringer, M., Hong, S. J., Galiano, R. D., & Mustoe, T. A. (2011). The TallyHo polygenic mouse model of diabetes: implications in wound healing. *Plast Reconstr Surg, 128*(5), 427e-437e. doi:10.1097/PRS.0b013e31822b7333

[28] Burant, C. F. (2013). Activation of GPR40 as a therapeutic target for the treatment of type 2 diabetes. *Diabetes Care, 36 Suppl 2*, S175-179. doi:10.2337/dcS13-2037

[29] Butler, A. E., Janson, J., Bonner-Weir, S., Ritzel, R., Rizza, R. A., & Butler, P. C. (2003). Beta-cell deficit and increased beta-cell apoptosis in humans with type 2 diabetes. *Diabetes, 52*(1), 102-110.

[30] Cani, P. D., Amar, J., Iglesias, M. A., Poggi, M., Knauf, C., Bastelica, D., . . . Burcelin, R. (2007). Metabolic endotoxemia initiates obesity and insulin resistance. *Diabetes, 56*(7), 1761-1772. doi:10.2337/db06-1491

[31] Cani, P. D., & Delzenne, N. M. (2009). The role of the gut microbiota in energy metabolism and metabolic disease. *Curr Pharm Des, 15*(13), 1546-1558.

[32] Cani, P. D., Neyrinck, A. M., Fava, F., Knauf, C., Burcelin, R. G., Tuohy, K. M., . . . Delzenne, N. M. (2007). Selective increases of bifidobacteria in gut microflora improve high-fat-diet-induced diabetes in mice through a mechanism associated with endotoxaemia. *Diabetologia, 50*(11), 2374-2383. doi:10.1007/s00125-007-0791-0

[33] Cantley, J., Burchfield, J. G., Pearson, G. L., Schmitz-Peiffer, C., Leitges, M., & Biden, T. J. (2009). Deletion of PKCepsilon selectively enhances the amplifying pathways of glucose-stimulated insulin secretion via increased lipolysis in mouse beta-cells. *Diabetes, 58*(8), 1826-1834. doi:10.2337/db09-0132

[34] Capurso, C., & Capurso, A. (2012). From excess adiposity to insulin resistance: the role of free fatty acids. *Vascul Pharmacol, 57*(2-4), 91-97. doi:10.1016/j.vph.2012.05.003

[35] Carling, D., Clarke, P. R., Zammit, V. A., & Hardie, D. G. (1989). Purification and characterization of the AMP-activated protein kinase. Copurification of acetyl-CoA carboxylase kinase and 3-hydroxy-3-methylglutaryl-CoA reductase kinase activities. *Eur J Biochem, 186*(1-2), 129-136.

[36] Carpentier, A., Mittelman, S. D., Lamarche, B., Bergman, R. N., Giacca, A., & Lewis, G. F. (1999). Acute enhancement of insulin secretion by FFA in humans is lost with prolonged FFA elevation. *Am J Physiol, 276*(6 Pt 1), E1055-1066.

[37] Castermans, D., Somers, I., Kriel, J., Louwet, W., Wera, S., Versele, M., . . . Thevelein, J. M. (2012). Glucose-induced posttranslational activation of protein phosphatases PP2A and PP1 in yeast. *Cell Res, 22*(6), 1058-1077. doi:10.1038/cr.2012.20

[38] Cenni, V., Doppler, H., Sonnenburg, E. D., Maraldi, N., Newton, A. C., & Toker, A. (2002). Regulation of novel protein kinase C epsilon by phosphorylation. *Biochem J, 363*(Pt 3), 537-545.

[39] Chatzigeorgiou, A., Halapas, A., Kalafatakis, K., & Kamper, E. (2009). The use of animal models in the study of diabetes mellitus. *In Vivo, 23*(2), 245-258.

[40] Chen, H., Charlat, O., Tartaglia, L. A., Woolf, E. A., Weng, X., Ellis, S. J., . . . Morgenstern, J. P. (1996). Evidence that the diabetes gene encodes the leptin receptor: identification of a mutation in the leptin receptor gene in db/db mice. *Cell, 84*(3), 491-495.

[41] Chen, Q., Vazquez, E. J., Moghaddas, S., Hoppel, C. L., & Lesnefsky, E. J. (2003). Production of reactive oxygen species by mitochondria: central role of complex III. *J Biol Chem, 278*(38), 36027-36031. doi:10.1074/jbc.M304854200

[42] Cheng, Y. S., Seibert, O., Kloting, N., Dietrich, A., Strassburger, K., Fernandez-Veledo, S., . . . Teleman, A. A. (2015). PPP2R5C Couples Hepatic Glucose and Lipid Homeostasis. *PLoS Genet, 11*(10), e1005561. doi:10.1371/journal.pgen.1005561

[43] Chimienti, F., Devergnas, S., Pattou, F., Schuit, F., Garcia-Cuenca, R., Vandewalle, B., . . . Seve, M. (2006). In vivo expression and functional characterization of the zinc transporter

ZnT8 in glucose-induced insulin secretion. *J Cell Sci, 119*(Pt 20), 4199-4206. doi:10.1242/jcs.03164

[44] Clee, S. M., & Attie, A. D. (2007). The genetic landscape of type 2 diabetes in mice. *Endocr Rev, 28*(1), 48-83. doi:10.1210/er.2006-0035

[45] Cnop, M., Hannaert, J. C., Hoorens, A., Eizirik, D. L., & Pipeleers, D. G. (2001). Inverse relationship between cytotoxicity of free fatty acids in pancreatic islet cells and cellular triglyceride accumulation. *Diabetes, 50*(8), 1771-1777.

[46] Collins, S. C., Hoppa, M. B., Walker, J. N., Amisten, S., Abdulkader, F., Bengtsson, M., . . . Rorsman, P. (2010). Progression of diet-induced diabetes in C57BL6J mice involves functional dissociation of Ca2(+) channels from secretory vesicles. *Diabetes, 59*(5), 1192-1201. doi:10.2337/db09-0791

[47] Conlon, M. A., & Bird, A. R. (2015). The impact of diet and lifestyle on gut microbiota and human health. *Nutrients, 7*(1), 17-44. doi:10.3390/nu7010017

[48] Corkey, B. E. (2012). Banting lecture 2011: hyperinsulinemia: cause or consequence? *Diabetes, 61*(1), 4-13. doi:10.2337/db11-1483

[49] Corton, J. M., Gillespie, J. G., & Hardie, D. G. (1994). Role of the AMP-activated protein kinase in the cellular stress response. *Curr Biol, 4*(4), 315-324.

[50] Corton, J. M., Gillespie, J. G., Hawley, S. A., & Hardie, D. G. (1995). 5-aminoimidazole-4-carboxamide ribonucleoside. A specific method for activating AMP-activated protein kinase in intact cells? *Eur J Biochem, 229*(2), 558-565.

[51] Cusi, K., Maezono, K., Osman, A., Pendergrass, M., Patti, M. E., Pratipanawatr, T., . . . Mandarino, L. J. (2000). Insulin resistance differentially affects the PI 3-kinase- and MAP kinase-mediated signaling in human muscle. *J Clin Invest, 105*(3), 311-320. doi:10.1172/JCI7535

[52] da Silva Xavier, G., Leclerc, I., Salt, I. P., Doiron, B., Hardie, D. G., Kahn, A., & Rutter, G. A. (2000). Role of AMP-activated protein kinase in the regulation by glucose of islet beta cell gene expression. *Proc Natl Acad Sci U S A, 97*(8), 4023-4028.

[53] da Silva Xavier, G., Leclerc, I., Varadi, A., Tsuboi, T., Moule, S. K., & Rutter, G. A. (2003). Role for AMP-activated protein kinase in glucose-stimulated insulin secretion and preproinsulin gene expression. *Biochem J, 371*(Pt 3), 761-774. doi:10.1042/BJ20021812

[54] da Silva Xavier, G., Mondragon, A., Sun, G., Chen, L., McGinty, J. A., French, P. M., & Rutter, G. A. (2012). Abnormal glucose tolerance and insulin secretion in pancreas-specific Tcf7l2-null mice. *Diabetologia, 55*(10), 2667-2676. doi:10.1007/s00125-012-2600-7

[55] Dayeh, T., Volkov, P., Salo, S., Hall, E., Nilsson, E., Olsson, A. H., . . . Ling, C. (2014). Genome-wide DNA methylation analysis of human pancreatic islets from type 2 diabetic and non-diabetic donors identifies candidate genes that influence insulin secretion. *PLoS Genet, 10*(3), e1004160. doi:10.1371/journal.pgen.1004160

[56] DeFronzo, R. A. (2004). Pathogenesis of type 2 diabetes mellitus. *Med Clin North Am, 88*(4), 787-835, ix. doi:10.1016/j.mcna.2004.04.013

[57] Defronzo, R. A. (2009). Banting Lecture. From the triumvirate to the ominous octet: a new paradigm for the treatment of type 2 diabetes mellitus. *Diabetes, 58*(4), 773-795. doi:10.2337/db09-9028

[58] DeFronzo, R. A., Bonadonna, R. C., & Ferrannini, E. (1992). Pathogenesis of NIDDM. A balanced overview. *Diabetes Care, 15*(3), 318-368.

[59] Delghingaro-Augusto, V., Nolan, C. J., Gupta, D., Jetton, T. L., Latour, M. G., Peshavaria, M., . . . Leahy, J. (2009). Islet beta cell failure in the 60% pancreatectomised obese hyperlipidaemic Zucker fatty rat: severe dysfunction with altered glycerolipid metabolism without steatosis or a falling beta cell mass. *Diabetologia, 52*(6), 1122-1132. doi:10.1007/s00125-009-1317-8

[60] Delzenne, N. M., & Cani, P. D. (2011). Gut microbiota and the pathogenesis of insulin resistance. *Curr Diab Rep, 11*(3), 154-159. doi:10.1007/s11892-011-0191-1

[61] Deng, Y., & Scherer, P. E. (2010). Adipokines as novel biomarkers and regulators of the metabolic syndrome. *Ann N Y Acad Sci, 1212*, E1-E19. doi:10.1111/j.1749-6632.2010.05875.x

[62] Diao, J., Allister, E. M., Koshkin, V., Lee, S. C., Bhattacharjee, A., Tang, C., . . . Wheeler, M. B. (2008). UCP2 is highly expressed in pancreatic alpha-cells and influences secretion and survival. *Proc Natl Acad Sci U S A, 105*(33), 12057-12062. doi:10.1073/pnas.0710434105

[63] Doliba, N. M., Liu, Q., Li, C., Chen, J., Chen, P., Liu, C., . . . Matschinsky, F. M. (2015). Accumulation of 3-hydroxytetradecenoic acid: Cause or corollary of glucolipotoxic impairment of pancreatic beta-cell bioenergetics? *Mol Metab, 4*(12), 926-939. doi:10.1016/j.molmet.2015.09.010

[64] Duchen, M. R. (2004). Mitochondria in health and disease: perspectives on a new mitochondrial biology. *Mol Aspects Med, 25*(4), 365-451. doi:10.1016/j.mam.2004.03.001

[65] Eckburg, P. B., Bik, E. M., Bernstein, C. N., Purdom, E., Dethlefsen, L., Sargent, M., . . . Relman, D. A. (2005). Diversity of the human intestinal microbial flora. *Science, 308*(5728), 1635-1638. doi:10.1126/science.1110591

[66] Egshatyan, L., Kashtanova, D., Popenko, A., Tkacheva, O., Tyakht, A., Alexeev, D., . . . Boytsov, S. (2016). Gut microbiota and diet in patients with different glucose tolerance. *Endocr Connect, 5*(1), 1-9. doi:10.1530/EC-15-0094

[67] El-Assaad, W., Buteau, J., Peyot, M. L., Nolan, C., Roduit, R., Hardy, S., . . . Prentki, M. (2003). Saturated fatty acids synergize with elevated glucose to cause pancreatic beta-cell death. *Endocrinology, 144*(9), 4154-4163. doi:10.1210/en.2003-0410

[68] El-Assaad, W., Joly, E., Barbeau, A., Sladek, R., Buteau, J., Maestre, I., . . . Prentki, M. (2010). Glucolipotoxicity alters lipid partitioning and causes mitochondrial dysfunction, cholesterol, and ceramide deposition and reactive oxygen species production in INS832/13 ss-cells. *Endocrinology, 151*(7), 3061-3073. doi:10.1210/en.2009-1238

[69] Elayat, A. A., el-Naggar, M. M., & Tahir, M. (1995). An immunocytochemical and morphometric study of the rat pancreatic islets. *J Anat, 186 (Pt 3)*, 629-637.

[70] Erion, D. M., & Shulman, G. I. (2010). Diacylglycerol-mediated insulin resistance. *Nat Med, 16*(4), 400-402. doi:10.1038/nm0410-400

[71] Fajans, S. S., Floyd, J. C., Jr., Knopf, R. F., & Conn, F. W. (1967). Effect of amino acids and proteins on insulin secretion in man. *Recent Prog Horm Res, 23*, 617-662.

[72] Farfari, S., Schulz, V., Corkey, B., & Prentki, M. (2000). Glucose-regulated anaplerosis and cataplerosis in pancreatic beta-cells: possible implication of a pyruvate/citrate shuttle in insulin secretion. *Diabetes, 49*(5), 718-726.

[73] Farooqi, S., & O'Rahilly, S. (2006). Genetics of obesity in humans. *Endocr Rev, 27*(7), 710-718. doi:10.1210/er.2006-0040

[74] Ferdaoussi, M., Bergeron, V., Zarrouki, B., Kolic, J., Cantley, J., Fielitz, J., . . . Poitout, V. (2012). G protein-coupled receptor (GPR)40-dependent potentiation of insulin secretion in mouse islets is mediated by protein kinase D1. *Diabetologia, 55*(10), 2682-2692. doi:10.1007/s00125-012-2650-x

[75] Fergusson, G., Ethier, M., Guevremont, M., Chretien, C., Attane, C., Joly, E., . . . Alquier, T. (2014). Defective insulin secretory response to intravenous glucose in C57Bl/6J compared to C57Bl/6N mice. *Mol Metab, 3*(9), 848-854. doi:10.1016/j.molmet.2014.09.006

[76] Fex, M., Haemmerle, G., Wierup, N., Dekker-Nitert, M., Rehn, M., Ristow, M., . . . Mulder, H. (2009). A beta cell-specific knockout of hormone-sensitive lipase in mice results in hyperglycaemia and disruption of exocytosis. *Diabetologia, 52*(2), 271-280. doi:10.1007/s00125-008-1191-9

[77] Franks, P. W. (2011). Gene x environment interactions in type 2 diabetes. *Curr Diab Rep, 11*(6), 552-561. doi:10.1007/s11892-011-0224-9

[78] Freeman, H. C., Hugill, A., Dear, N. T., Ashcroft, F. M., & Cox, R. D. (2006). Deletion of nicotinamide nucleotide transhydrogenase: a new quantitive trait locus accounting for glucose intolerance in C57BL/6J mice. *Diabetes, 55*(7), 2153-2156. doi:10.2337/db06-0358

[79] Fu, A., Eberhard, C. E., & Screaton, R. A. (2013). Role of AMPK in pancreatic beta cell function. *Mol Cell Endocrinol, 366*(2), 127-134. doi:10.1016/j.mce.2012.06.020

[80] Fu, A., Ng, A. C., Depatie, C., Wijesekara, N., He, Y., Wang, G. S., . . . Screaton, R. A. (2009). Loss of Lkb1 in adult beta cells increases beta cell mass and enhances glucose tolerance in mice. *Cell Metab, 10*(4), 285-295. doi:10.1016/j.cmet.2009.08.008

[81] Fuchsberger, C., Flannick, J., Teslovich, T. M., Mahajan, A., Agarwala, V., Gaulton, K. J., . . . McCarthy, M. I. (2016). The genetic architecture of type 2 diabetes. *Nature*. doi:10.1038/nature18642

[82] Garcia-Ruiz, C., Mari, M., Colell, A., Morales, A., Caballero, F., Montero, J., . . . Fernandez-Checa, J. C. (2009). Mitochondrial cholesterol in health and disease. *Histol Histopathol, 24*(1), 117-132.

[83] Gareau, M. G., Sherman, P. M., & Walker, W. A. (2010). Probiotics and the gut microbiota in intestinal health and disease. *Nat Rev Gastroenterol Hepatol, 7*(9), 503-514. doi:10.1038/nrgastro.2010.117

[84] Gauthier, M. S., Miyoshi, H., Souza, S. C., Cacicedo, J. M., Saha, A. K., Greenberg, A. S., & Ruderman, N. B. (2008). AMP-activated protein kinase is activated as a consequence of lipolysis in the adipocyte: potential mechanism and physiological relevance. *J Biol Chem, 283*(24), 16514-16524. doi:10.1074/jbc.M708177200

[85] Gerich, J. E. (1998). The genetic basis of type 2 diabetes mellitus: impaired insulin secretion versus impaired insulin sensitivity. *Endocr Rev, 19*(4), 491-503. doi:10.1210/edrv.19.4.0338

[86] Ghosh, A., Ronner, P., Cheong, E., Khalid, P., & Matschinsky, F. M. (1991). The role of ATP and free ADP in metabolic coupling during fuel-stimulated insulin release from islet beta-cells in the isolated perfused rat pancreas. *J Biol Chem, 266*(34), 22887-22892.

[87] Giacca, A., Xiao, C., Oprescu, A. I., Carpentier, A. C., & Lewis, G. F. (2011). Lipid-induced pancreatic beta-cell dysfunction: focus on in vivo studies. *Am J Physiol Endocrinol Metab, 300*(2), E255-262. doi:10.1152/ajpendo.00416.2010

[88] Goto, Y., Kakizaki, M., & Masaki, N. (1976). Production of spontaneous diabetic rats by repetition of selective breeding. *Tohoku J Exp Med, 119*(1), 85-90.

[89] Gray, J. P., Alavian, K. N., Jonas, E. A., & Heart, E. A. (2012). NAD kinase regulates the size of the NADPH pool and insulin secretion in pancreatic beta-cells. *Am J Physiol Endocrinol Metab, 303*(2), E191-199. doi:10.1152/ajpendo.00465.2011

[90] Gremlich, S., Bonny, C., Waeber, G., & Thorens, B. (1997). Fatty acids decrease IDX-1 expression in rat pancreatic islets and reduce GLUT2, glucokinase, insulin, and somatostatin levels. *J Biol Chem, 272*(48), 30261-30269.

[91] Gross, G., Jacobs, D. M., Peters, S., Possemiers, S., van Duynhoven, J., Vaughan, E. E., & van de Wiele, T. (2010). In vitro bioconversion of polyphenols from black tea and red wine/grape juice by human intestinal microbiota displays strong interindividual variability. *J Agric Food Chem, 58*(18), 10236-10246. doi:10.1021/jf101475m

[92] Guay, C., Madiraju, S. R., Aumais, A., Joly, E., & Prentki, M. (2007). A role for ATP-citrate lyase, malic enzyme, and pyruvate/citrate cycling in glucose-induced insulin secretion. *J Biol Chem, 282*(49), 35657-35665. doi:10.1074/jbc.M707294200

[93] Guilherme, A., Virbasius, J. V., Puri, V., & Czech, M. P. (2008). Adipocyte dysfunctions linking obesity to insulin resistance and type 2 diabetes. *Nat Rev Mol Cell Biol, 9*(5), 367-377. doi:10.1038/nrm2391

[94] Guo, S. (2014). Insulin signaling, resistance, and the metabolic syndrome: insights from mouse models into disease mechanisms. *J Endocrinol, 220*(2), T1-T23. doi:10.1530/JOE-13-0327

[95] Gurgul, E., Lortz, S., Tiedge, M., Jorns, A., & Lenzen, S. (2004). Mitochondrial catalase overexpression protects insulin-producing cells against toxicity of reactive oxygen species and proinflammatory cytokines. *Diabetes, 53*(9), 2271-2280.

[96] Hao, M., Head, W. S., Gunawardana, S. C., Hasty, A. H., & Piston, D. W. (2007). Direct effect of cholesterol on insulin secretion: a novel mechanism for pancreatic beta-cell dysfunction. *Diabetes, 56*(9), 2328-2338. doi:10.2337/db07-0056

[97] Hardie, D. G., & Hawley, S. A. (2001). AMP-activated protein kinase: the energy charge hypothesis revisited. *Bioessays, 23*(12), 1112-1119. doi:10.1002/bies.10009

[98] Hardie, D. G., Ross, F. A., & Hawley, S. A. (2012). AMPK: a nutrient and energy sensor that maintains energy homeostasis. *Nat Rev Mol Cell Biol, 13*(4), 251-262. doi:10.1038/nrm3311

[99] Hariri, N., & Thibault, L. (2010). High-fat diet-induced obesity in animal models. *Nutr Res Rev, 23*(2), 270-299. doi:10.1017/S0954422410000168

[100] Harmon, J. S., Gleason, C. E., Tanaka, Y., Oseid, E. A., Hunter-Berger, K. K., & Robertson, R. P. (1999). In vivo prevention of hyperglycemia also prevents glucotoxic effects on PDX-1 and insulin gene expression. *Diabetes, 48*(10), 1995-2000.

[101] Hawley, S. A., Davison, M., Woods, A., Davies, S. P., Beri, R. K., Carling, D., & Hardie, D. G. (1996). Characterization of the AMP-activated protein kinase kinase from rat liver and identification of threonine 172 as the major site at which it phosphorylates AMP-activated protein kinase. *J Biol Chem, 271*(44), 27879-27887.

[102] Heidrich, F., Schotola, H., Popov, A. F., Sohns, C., Schuenemann, J., Friedrich, M., . . . Schmitto, J. D. (2010). AMPK - Activated Protein Kinase and its Role in Energy Metabolism of the Heart. *Curr Cardiol Rev, 6*(4), 337-342. doi:10.2174/157340310793566073

[103] Henquin, J. C., Nenquin, M., Stiernet, P., & Ahren, B. (2006). In vivo and in vitro glucose-induced biphasic insulin secretion in the mouse: pattern and role of cytoplasmic Ca2+ and amplification signals in beta-cells. *Diabetes, 55*(2), 441-451.

[104] Herman, M. A., & Kahn, B. B. (2006). Glucose transport and sensing in the maintenance of glucose homeostasis and metabolic harmony. *J Clin Invest, 116*(7), 1767-1775. doi:10.1172/JCI29027

[105] Hildebrandt, M. A., Hoffmann, C., Sherrill-Mix, S. A., Keilbaugh, S. A., Hamady, M., Chen, Y. Y., . . . Wu, G. D. (2009). High-fat diet determines the composition of the murine gut microbiome independently of obesity. *Gastroenterology, 137*(5), 1716-1724 e1711-1712. doi:10.1053/j.gastro.2009.08.042

[106] Hiriart, M., & Aguilar-Bryan, L. (2008). Channel regulation of glucose sensing in the pancreatic beta-cell. *Am J Physiol Endocrinol Metab, 295*(6), E1298-1306. doi:10.1152/ajpendo.90493.2008

[107] Hohmeier, H. E., & Newgard, C. B. (2004). Cell lines derived from pancreatic islets. *Mol Cell Endocrinol, 228*(1-2), 121-128. doi:10.1016/j.mce.2004.04.017

[108] Hotamisligil, G. S., Arner, P., Caro, J. F., Atkinson, R. L., & Spiegelman, B. M. (1995). Increased adipose tissue expression of tumor necrosis factor-alpha in human obesity and insulin resistance. *J Clin Invest, 95*(5), 2409-2415. doi:10.1172/JCI117936

[109] Iancu, C. V., Mukund, S., Fromm, H. J., & Honzatko, R. B. (2005). R-state AMP complex reveals initial steps of the quaternary transition of fructose-1,6-bisphosphatase. *J Biol Chem, 280*(20), 19737-19745. doi:10.1074/jbc.M501011200

[110] Imbeault, P., Saint-Pierre, S., Almeras, N., & Tremblay, A. (1997). Acute effects of exercise on energy intake and feeding behaviour. *Br J Nutr, 77*(4), 511-521.

[111] Ivarsson, R., Quintens, R., Dejonghe, S., Tsukamoto, K., in 't Veld, P., Renstrom, E., & Schuit, F. C. (2005). Redox control of exocytosis: regulatory role of NADPH, thioredoxin, and glutaredoxin. *Diabetes, 54*(7), 2132-2142.

[112] Jacqueminet, S., Briaud, I., Rouault, C., Reach, G., & Poitout, V. (2000). Inhibition of insulin gene expression by long-term exposure of pancreatic beta cells to palmitate is dependent on the presence of a stimulatory glucose concentration. *Metabolism, 49*(4), 532-536.

[113] Jensen, M. V., Joseph, J. W., Ilkayeva, O., Burgess, S., Lu, D., Ronnebaum, S. M., . . . Newgard, C. B. (2006). Compensatory responses to pyruvate carboxylase suppression in islet beta-cells. Preservation of glucose-stimulated insulin secretion. *J Biol Chem, 281*(31), 22342-22351. doi:10.1074/jbc.M604350200

[114] Jetton, T. L., Lausier, J., LaRock, K., Trotman, W. E., Larmie, B., Habibovic, A., . . . Leahy, J. L. (2005). Mechanisms of compensatory beta-cell growth in insulin-resistant rats: roles of Akt kinase. *Diabetes, 54*(8), 2294-2304.

[115] Jiang, Y. H., Bressler, J., & Beaudet, A. L. (2004). Epigenetics and human disease. *Annu Rev Genomics Hum Genet, 5*, 479-510. doi:10.1146/annurev.genom.5.061903.180014

[116] Jin, T., & Liu, L. (2008). The Wnt signaling pathway effector TCF7L2 and type 2 diabetes mellitus. *Mol Endocrinol, 22*(11), 2383-2392. doi:10.1210/me.2008-0135

[117] Kahn, S. E., Hull, R. L., & Utzschneider, K. M. (2006). Mechanisms linking obesity to insulin resistance and type 2 diabetes. *Nature, 444*(7121), 840-846. doi:10.1038/nature05482

[118] Kaplan, J. R., & Wagner, J. D. (2006). Type 2 diabetes-an introduction to the development and use of animal models. *ILAR J, 47*(3), 181-185.

[119] Kawano, K., Hirashima, T., Mori, S., Saitoh, Y., Kurosumi, M., & Natori, T. (1992). Spontaneous long-term hyperglycemic rat with diabetic complications. Otsuka Long-Evans Tokushima Fatty (OLETF) strain. *Diabetes, 41*(11), 1422-1428.

[120] Kebede, M., Alquier, T., Latour, M. G., Semache, M., Tremblay, C., & Poitout, V. (2008). The fatty acid receptor GPR40 plays a role in insulin secretion in vivo after high-fat feeding. *Diabetes, 57*(9), 2432-2437. doi:10.2337/db08-0553

[121] Kershaw, E. E., & Flier, J. S. (2004). Adipose tissue as an endocrine organ. *J Clin Endocrinol Metab, 89*(6), 2548-2556. doi:10.1210/jc.2004-0395

[122] Kibbey, R. G., Pongratz, R. L., Romanelli, A. J., Wollheim, C. B., Cline, G. W., & Shulman, G. I. (2007). Mitochondrial GTP regulates glucose-stimulated insulin secretion. *Cell Metab, 5*(4), 253-264. doi:10.1016/j.cmet.2007.02.008

[123] Kilfoil, P. J., Tipparaju, S. M., Barski, O. A., & Bhatnagar, A. (2013). Regulation of ion channels by pyridine nucleotides. *Circ Res, 112*(4), 721-741. doi:10.1161/CIRCRESAHA.111.247940

[124] Kim, D., Lee, J. E., Jung, Y. J., Lee, A. S., Lee, S., Park, S. K., . . . Kang, K. P. (2013). Metformin decreases high-fat diet-induced renal injury by regulating the expression of adipokines and the renal AMP-activated protein kinase/acetyl-CoA carboxylase pathway in mice. *Int J Mol Med, 32*(6), 1293-1302. doi:10.3892/ijmm.2013.1508

[125] King, A. J. (2012). The use of animal models in diabetes research. *Br J Pharmacol, 166*(3), 877-894. doi:10.1111/j.1476-5381.2012.01911.x

[126] Klip, A., & Paquet, M. R. (1990). Glucose transport and glucose transporters in muscle and their metabolic regulation. *Diabetes Care, 13*(3), 228-243.

[127] Kluth, O., Mirhashemi, F., Scherneck, S., Kaiser, D., Kluge, R., Neschen, S., . . . Schurmann, A. (2011). Dissociation of lipotoxicity and glucotoxicity in a mouse model of obesity associated diabetes: role of forkhead box O1 (FOXO1) in glucose-induced beta cell failure. *Diabetologia, 54*(3), 605-616. doi:10.1007/s00125-010-1973-8

[128] Kootte, R. S., Vrieze, A., Holleman, F., Dallinga-Thie, G. M., Zoetendal, E. G., de Vos, W. M., . . . Nieuwdorp, M. (2012). The therapeutic potential of manipulating gut microbiota in obesity and type 2 diabetes mellitus. *Diabetes Obes Metab, 14*(2), 112-120. doi:10.1111/j.1463-1326.2011.01483.x

[129] Koshkin, V., Wang, X., Scherer, P. E., Chan, C. B., & Wheeler, M. B. (2003). Mitochondrial functional state in clonal pancreatic beta-cells exposed to free fatty acids. *J Biol Chem, 278*(22), 19709-19715. doi:10.1074/jbc.M209709200

[130] Kowluru, A. (2003). Regulatory roles for small G proteins in the pancreatic beta-cell: lessons from models of impaired insulin secretion. *Am J Physiol Endocrinol Metab, 285*(4), E669-684. doi:10.1152/ajpendo.00196.2003

[131] Kowluru, A., Chen, H. Q., Modrick, L. M., & Stefanelli, C. (2001). Activation of acetyl-CoA carboxylase by a glutamate- and magnesium-sensitive protein phosphatase in the islet beta-cell. *Diabetes, 50*(7), 1580-1587.

[132] Kruit, J. K., Wijesekara, N., Fox, J. E., Dai, X. Q., Brunham, L. R., Searle, G. J., . . . Hayden, M. R. (2011). Islet cholesterol accumulation due to loss of ABCA1 leads to impaired exocytosis of insulin granules. *Diabetes, 60*(12), 3186-3196. doi:10.2337/db11-0081

[133] Kurth-Kraczek, E. J., Hirshman, M. F., Goodyear, L. J., & Winder, W. W. (1999). 5' AMP-activated protein kinase activation causes GLUT4 translocation in skeletal muscle. *Diabetes, 48*(8), 1667-1671.

[134] Lamontagne, J., Pepin, E., Peyot, M. L., Joly, E., Ruderman, N. B., Poitout, V., . . . Prentki, M. (2009). Pioglitazone acutely reduces insulin secretion and causes metabolic deceleration of the pancreatic beta-cell at submaximal glucose concentrations. *Endocrinology, 150*(8), 3465-3474. doi:10.1210/en.2008-1557

[135] Larsen, N., Vogensen, F. K., van den Berg, F. W., Nielsen, D. S., Andreasen, A. S., Pedersen, B. K., . . . Jakobsen, M. (2010). Gut microbiota in human adults with type 2 diabetes differs from non-diabetic adults. *PLoS One, 5*(2), e9085. doi:10.1371/journal.pone.0009085

[136] Larson-Meyer, D. E., Newcomer, B. R., Ravussin, E., Volaufova, J., Bennett, B., Chalew, S., . . . Sothern, M. (2011). Intrahepatic and intramyocellular lipids are determinants of insulin resistance in prepubertal children. *Diabetologia, 54*(4), 869-875. doi:10.1007/s00125-010-2022-3

[137] Larsson, H., & Ahren, B. (1996). Islet dysfunction in obese women with impaired glucose tolerance. *Metabolism, 45*(4), 502-509.

[138] Latour, M. G., Alquier, T., Oseid, E., Tremblay, C., Jetton, T. L., Luo, J., . . . Poitout, V. (2007). GPR40 is necessary but not sufficient for fatty acid stimulation of insulin secretion in vivo. *Diabetes, 56*(4), 1087-1094. doi:10.2337/db06-1532

[139] Leahy, J. L. (2005). Pathogenesis of type 2 diabetes mellitus. *Arch Med Res, 36*(3), 197-209. doi:10.1016/j.arcmed.2005.01.003

[140] Leclerc, I., Woltersdorf, W. W., da Silva Xavier, G., Rowe, R. L., Cross, S. E., Korbutt, G. S., . . . Rutter, G. A. (2004). Metformin, but not leptin, regulates AMP-activated protein kinase in pancreatic islets: impact on glucose-stimulated insulin secretion. *Am J Physiol Endocrinol Metab, 286*(6), E1023-1031. doi:10.1152/ajpendo.00532.2003

[141] Leclercq, I. A., Da Silva Morais, A., Schroyen, B., Van Hul, N., & Geerts, A. (2007). Insulin resistance in hepatocytes and sinusoidal liver cells: mechanisms and consequences. *J Hepatol, 47*(1), 142-156. doi:10.1016/j.jhep.2007.04.002

[142] Lee, S. K., Opara, E. C., Surwit, R. S., Feinglos, M. N., & Akwari, O. E. (1995). Defective glucose-stimulated insulin release from perifused islets of C57BL/6J mice. *Pancreas, 11*(2), 206-211.

[143] Leloup, C., Tourrel-Cuzin, C., Magnan, C., Karaca, M., Castel, J., Carneiro, L., . . . Penicaud, L. (2009). Mitochondrial reactive oxygen species are obligatory signals for glucose-induced insulin secretion. *Diabetes, 58*(3), 673-681. doi:10.2337/db07-1056

[144] Li, N., Li, B., Brun, T., Deffert-Delbouille, C., Mahiout, Z., Daali, Y., . . . Maechler, P. (2012). NADPH oxidase NOX2 defines a new antagonistic role for reactive oxygen species and cAMP/PKA in the regulation of insulin secretion. *Diabetes, 61*(11), 2842-2850. doi:10.2337/db12-0009

[145] Lillioja, S., Mott, D. M., Howard, B. V., Bennett, P. H., Yki-Jarvinen, H., Freymond, D., . . . Bogardus, C. (1988). Impaired glucose tolerance as a disorder of insulin action. Longitudinal and cross-sectional studies in Pima Indians. *N Engl J Med, 318*(19), 1217-1225. doi:10.1056/NEJM198805123181901

[146] Lindstrom, P. (2007). The physiology of obese-hyperglycemic mice [ob/ob mice]. *ScientificWorldJournal, 7*, 666-685. doi:10.1100/tsw.2007.117

[147] Ling, C., Del Guerra, S., Lupi, R., Ronn, T., Granhall, C., Luthman, H., . . . Del Prato, S. (2008). Epigenetic regulation of PPARGC1A in human type 2 diabetic islets and effect on insulin secretion. *Diabetologia, 51*(4), 615-622. doi:10.1007/s00125-007-0916-5

[148] Ling, C., & Groop, L. (2009). Epigenetics: a molecular link between environmental factors and type 2 diabetes. *Diabetes, 58*(12), 2718-2725. doi:10.2337/db09-1003

[149] Loubatieres-Mariani, M. M., Chapal, J., Lignon, F., & Valette, G. (1979). Structural specificity of nucleotides for insulin secretory action from the isolated perfused rat pancreas. *Eur J Pharmacol, 59*(3-4), 277-286.

[150] MacDonald, M. J., Chaplen, F. W., Triplett, C. K., Gong, Q., & Drought, H. (2006). Stimulation of insulin release by glyceraldehyde may not be similar to glucose. *Arch Biochem Biophys, 447*(2), 118-126. doi:10.1016/j.abb.2006.01.019

[151] Maechler, P. (2013). Mitochondrial function and insulin secretion. *Mol Cell Endocrinol, 379*(1-2), 12-18. doi:10.1016/j.mce.2013.06.019

[152] Maechler, P., Li, N., Casimir, M., Vetterli, L., Frigerio, F., & Brun, T. (2010). Role of mitochondria in beta-cell function and dysfunction. *Adv Exp Med Biol, 654*, 193-216. doi:10.1007/978-90-481-3271-3_9

[153] Maechler, P., & Wollheim, C. B. (2001). Mitochondrial function in normal and diabetic beta-cells. *Nature, 414*(6865), 807-812. doi:10.1038/414807a

[154] Malaisse, W. J., Sener, A., Malaisse-Lagae, F., Welsh, M., Matthews, D. E., Bier, D. M., & Hellerstrom, C. (1982). The stimulus-secretion coupling of amino acid-induced insulin release. Metabolic response of pancreatic islets of L-glutamine and L-leucine. *J Biol Chem, 257*(15), 8731-8737.

[155] Mancini, A. D., & Poitout, V. (2013). The fatty acid receptor FFA1/GPR40 a decade later: how much do we know? *Trends Endocrinol Metab, 24*(8), 398-407. doi:10.1016/j.tem.2013.03.003

[156] Martin, B. C., Warram, J. H., Krolewski, A. S., Bergman, R. N., Soeldner, J. S., & Kahn, C. R. (1992). Role of glucose and insulin resistance in development of type 2 diabetes mellitus: results of a 25-year follow-up study. *Lancet, 340*(8825), 925-929.

[157] McCarthy, M. I., Rorsman, P., & Gloyn, A. L. (2013). TCF7L2 and diabetes: a tale of two tissues, and of two species. *Cell Metab, 17*(2), 157-159. doi:10.1016/j.cmet.2013.01.011

[158] Meijssen, S., Cabezas, M. C., Ballieux, C. G., Derksen, R. J., Bilecen, S., & Erkelens, D. W. (2001). Insulin mediated inhibition of hormone sensitive lipase activity in vivo in relation to endogenous catecholamines in healthy subjects. *J Clin Endocrinol Metab, 86*(9), 4193-4197. doi:10.1210/jcem.86.9.7794

[159] Mela, D. J. (2001). Determinants of food choice: relationships with obesity and weight control. *Obes Res, 9 Suppl 4*, 249S-255S. doi:10.1038/oby.2001.127

[160] Meshkani, R., & Adeli, K. (2009). Hepatic insulin resistance, metabolic syndrome and cardiovascular disease. *Clin Biochem, 42*(13-14), 1331-1346. doi:10.1016/j.clinbiochem.2009.05.018

[161] Michael, M. D., Kulkarni, R. N., Postic, C., Previs, S. F., Shulman, G. I., Magnuson, M. A., & Kahn, C. R. (2000). Loss of insulin signaling in hepatocytes leads to severe insulin resistance and progressive hepatic dysfunction. *Mol Cell, 6*(1), 87-97.

[162] Michelakis, E. D. (2008). Mitochondrial medicine: a new era in medicine opens new windows and brings new challenges. *Circulation, 117*(19), 2431-2434. doi:10.1161/CIRCULATIONAHA.108.775163

[163] Modi, H., Jacovetti, C., Tarussio, D., Metref, S., Madsen, O. D., Zhang, F. P., . . . Thorens, B. (2015). Autocrine Action of IGF2 Regulates Adult beta-Cell Mass and Function. *Diabetes, 64*(12), 4148-4157. doi:10.2337/db14-1735

[164] Morino, K., Petersen, K. F., & Shulman, G. I. (2006). Molecular mechanisms of insulin resistance in humans and their potential links with mitochondrial dysfunction. *Diabetes, 55 Suppl 2*, S9-S15. doi:10.2337/diabetes.

[165] Mulder, H., & Ling, C. (2009). Mitochondrial dysfunction in pancreatic beta-cells in Type 2 diabetes. *Mol Cell Endocrinol, 297*(1-2), 34-40. doi:10.1016/j.mce.2008.05.015

[166] Musso, G., Gambino, R., & Cassader, M. (2010). Obesity, diabetes, and gut microbiota: the hygiene hypothesis expanded? *Diabetes Care, 33*(10), 2277-2284. doi:10.2337/dc10-0556

[167] Nagasumi, K., Esaki, R., Iwachidow, K., Yasuhara, Y., Ogi, K., Tanaka, H., . . . Kaisho, Y. (2009). Overexpression of GPR40 in pancreatic beta-cells augments glucose-stimulated insulin secretion and improves glucose tolerance in normal and diabetic mice. *Diabetes, 58*(5), 1067-1076. doi:10.2337/db08-1233

[168] Newsholme, E. A., & Crabtree, B. (1976). Substrate cycles in metabolic regulation and in heat generation. *Biochem Soc Symp*(41), 61-109.

[169] Newsholme, P., Gaudel, C., & McClenaghan, N. H. (2010). Nutrient regulation of insulin secretion and beta-cell functional integrity. *Adv Exp Med Biol, 654*, 91-114. doi:10.1007/978-90-481-3271-3_6

[170] Newsholme, P., Morgan, D., Rebelato, E., Oliveira-Emilio, H. C., Procopio, J., Curi, R., & Carpinelli, A. (2009). Insights into the critical role of NADPH oxidase(s) in the normal and dysregulated pancreatic beta cell. *Diabetologia, 52*(12), 2489-2498. doi:10.1007/s00125-009-1536-z

[171] Nie, Y. F., Hu, J., & Yan, X. H. (2015). Cross-talk between bile acids and intestinal microbiota in host metabolism and health. *J Zhejiang Univ Sci B, 16*(6), 436-446. doi:10.1631/jzus.B1400327

[172] Nolan, C. J., Damm, P., & Prentki, M. (2011). Type 2 diabetes across generations: from pathophysiology to prevention and management. *Lancet, 378*(9786), 169-181. doi:10.1016/S0140-6736(11)60614-4

[173] Nolan, C. J., Madiraju, M. S., Delghingaro-Augusto, V., Peyot, M. L., & Prentki, M. (2006). Fatty acid signaling in the beta-cell and insulin secretion. *Diabetes, 55 Suppl 2*, S16-23. doi:10.2337/diabetes.

[174] Nolan, C. J., Ruderman, N. B., Kahn, S. E., Pedersen, O., & Prentki, M. (2015). Insulin resistance as a physiological defense against metabolic stress: implications for the management of subsets of type 2 diabetes. *Diabetes, 64*(3), 673-686. doi:10.2337/db14-0694

[175] Oakes, N. D., Thalen, P., Hultstrand, T., Jacinto, S., Camejo, G., Wallin, B., & Ljung, B. (2005). Tesaglitazar, a dual PPAR{alpha}/{gamma} agonist, ameliorates glucose and lipid intolerance in obese Zucker rats. *Am J Physiol Regul Integr Comp Physiol, 289*(4), R938-946. doi:10.1152/ajpregu.00252.2005

[176] Oghbaei, H., Ahmadi Asl, N., Sheikhzadeh, F., Alipour, M. R., & Khamaneh, A. M. (2015). The Effect of Regular Moderate Exercise on miRNA-192 Expression Changes in Kidney of Streptozotocin-Induced Diabetic Male Rats. *Adv Pharm Bull, 5*(1), 127-132. doi:10.5681/apb.2015.018

[177] Olson, L. K., Redmon, J. B., Towle, H. C., & Robertson, R. P. (1993). Chronic exposure of HIT cells to high glucose concentrations paradoxically decreases insulin gene transcription and alters binding of insulin gene regulatory protein. *J Clin Invest, 92*(1), 514-519. doi:10.1172/JCI116596

[178] Pepin, E., Al-Mass, A., Attane, C., Zhang, K., Lamontagne, J., Lussier, R., . . . Peyot, M. L. (2016). Pancreatic beta-Cell Dysfunction in Diet-Induced Obese Mice: Roles of AMP-Kinase, Protein Kinase Cepsilon, Mitochondrial and Cholesterol Metabolism, and Alterations in Gene Expression. *PLoS One, 11*(4), e0153017. doi:10.1371/journal.pone.0153017

[179] Perry, J. R., Voight, B. F., Yengo, L., Amin, N., Dupuis, J., Ganser, M., . . . Cauchi, S. (2012). Stratifying type 2 diabetes cases by BMI identifies genetic risk variants in LAMA1 and enrichment for risk variants in lean compared to obese cases. *PLoS Genet, 8*(5), e1002741. doi:10.1371/journal.pgen.1002741

[180] Peyot, M. L., Guay, C., Latour, M. G., Lamontagne, J., Lussier, R., Pineda, M., . . . Prentki, M. (2009). Adipose triglyceride lipase is implicated in fuel- and non-fuel-stimulated insulin secretion. *J Biol Chem, 284*(25), 16848-16859. doi:10.1074/jbc.M109.006650

[181] Peyot, M. L., Nolan, C. J., Soni, K., Joly, E., Lussier, R., Corkey, B. E., . . . Prentki, M. (2004). Hormone-sensitive lipase has a role in lipid signaling for insulin secretion but is nonessential for the incretin action of glucagon-like peptide 1. *Diabetes, 53*(7), 1733-1742.

[182] Peyot, M. L., Pepin, E., Lamontagne, J., Latour, M. G., Zarrouki, B., Lussier, R., . . . Prentki, M. (2010). Beta-cell failure in diet-induced obese mice stratified according to body weight gain: secretory dysfunction and altered islet lipid metabolism without steatosis or reduced beta-cell mass. *Diabetes, 59*(9), 2178-2187. doi:10.2337/db09-1452

[183] Phillips, M. S., Liu, Q., Hammond, H. A., Dugan, V., Hey, P. J., Caskey, C. J., & Hess, J. F. (1996). Leptin receptor missense mutation in the fatty Zucker rat. *Nat Genet, 13*(1), 18-19. doi:10.1038/ng0596-18

[184] Pi, J., Bai, Y., Zhang, Q., Wong, V., Floering, L. M., Daniel, K., . . . Collins, S. (2007). Reactive oxygen species as a signal in glucose-stimulated insulin secretion. *Diabetes, 56*(7), 1783-1791. doi:10.2337/db06-1601

[185] Poitout, V., Amyot, J., Semache, M., Zarrouki, B., Hagman, D., & Fontes, G. (2010). Glucolipotoxicity of the pancreatic beta cell. *Biochim Biophys Acta, 1801*(3), 289-298. doi:10.1016/j.bbalip.2009.08.006

[186] Poitout, V., & Lin, D. C. (2013). Modulating GPR40: therapeutic promise and potential in diabetes. *Drug Discov Today, 18*(23-24), 1301-1308. doi:10.1016/j.drudis.2013.09.003

[187] Poitout, V., & Robertson, R. P. (2002). Minireview: Secondary beta-cell failure in type 2 diabetes--a convergence of glucotoxicity and lipotoxicity. *Endocrinology, 143*(2), 339-342. doi:10.1210/endo.143.2.8623

[188] Poitout, V., & Robertson, R. P. (2008). Glucolipotoxicity: fuel excess and beta-cell dysfunction. *Endocr Rev, 29*(3), 351-366. doi:10.1210/er.2007-0023

[189] Polonsky, K. S., Sturis, J., & Bell, G. I. (1996). Seminars in Medicine of the Beth Israel Hospital, Boston. Non-insulin-dependent diabetes mellitus - a genetically programmed failure of the beta cell to compensate for insulin resistance. *N Engl J Med, 334*(12), 777-783. doi:10.1056/NEJM199603213341207

[190] Pongratz, R. L., Kibbey, R. G., Shulman, G. I., & Cline, G. W. (2007). Cytosolic and mitochondrial malic enzyme isoforms differentially control insulin secretion. *J Biol Chem, 282*(1), 200-207. doi:10.1074/jbc.M602954200

[191] Portela, A., & Esteller, M. (2010). Epigenetic modifications and human disease. *Nat Biotechnol, 28*(10), 1057-1068. doi:10.1038/nbt.1685

[192] Poy, M. N., Eliasson, L., Krutzfeldt, J., Kuwajima, S., Ma, X., Macdonald, P. E., . . . Stoffel, M. (2004). A pancreatic islet-specific microRNA regulates insulin secretion. *Nature, 432*(7014), 226-230. doi:10.1038/nature03076

[193] Prentki, M. (1996). New insights into pancreatic beta-cell metabolic signaling in insulin secretion. *Eur J Endocrinol, 134*(3), 272-286.

[194] Prentki, M., Joly, E., El-Assaad, W., & Roduit, R. (2002). Malonyl-CoA signaling, lipid partitioning, and glucolipotoxicity: role in beta-cell adaptation and failure in the etiology of diabetes. *Diabetes, 51 Suppl 3*, S405-413.

[195] Prentki, M., & Madiraju, S. R. (2008). Glycerolipid metabolism and signaling in health and disease. *Endocr Rev, 29*(6), 647-676. doi:10.1210/er.2008-0007

[196] Prentki, M., & Madiraju, S. R. (2012). Glycerolipid/free fatty acid cycle and islet beta-cell function in health, obesity and diabetes. *Mol Cell Endocrinol, 353*(1-2), 88-100. doi:10.1016/j.mce.2011.11.004

[197] Prentki, M., & Matschinsky, F. M. (1987). Ca2+, cAMP, and phospholipid-derived messengers in coupling mechanisms of insulin secretion. *Physiol Rev, 67*(4), 1185-1248.

[198] Prentki, M., Matschinsky, F. M., & Madiraju, S. R. (2013). Metabolic signaling in fuel-induced insulin secretion. *Cell Metab, 18*(2), 162-185. doi:10.1016/j.cmet.2013.05.018

[199] Prentki, M., & Nolan, C. J. (2006). Islet beta cell failure in type 2 diabetes. *J Clin Invest, 116*(7), 1802-1812. doi:10.1172/JCI29103

[200] Prentki, M., Tornheim, K., & Corkey, B. E. (1997). Signal transduction mechanisms in nutrient-induced insulin secretion. *Diabetologia, 40 Suppl 2*, S32-41.

[201] Qin, J., Li, R., Raes, J., Arumugam, M., Burgdorf, K. S., Manichanh, C., . . . Wang, J. (2010). A human gut microbial gene catalogue established by metagenomic sequencing. *Nature, 464*(7285), 59-65. doi:10.1038/nature08821

[202] Reaven, G. M. (1997). Banting Lecture 1988. Role of insulin resistance in human disease. 1988. *Nutrition, 13*(1), 65; discussion 64, 66.

[203] Reinbothe, T. M., Ivarsson, R., Li, D. Q., Niazi, O., Jing, X., Zhang, E., . . . Renstrom, E. (2009). Glutaredoxin-1 mediates NADPH-dependent stimulation of calcium-dependent insulin secretion. *Mol Endocrinol, 23*(6), 893-900. doi:10.1210/me.2008-0306

[204] Reznick, R. M., Zong, H., Li, J., Morino, K., Moore, I. K., Yu, H. J., . . . Shulman, G. I. (2007). Aging-associated reductions in AMP-activated protein kinase activity and mitochondrial biogenesis. *Cell Metab, 5*(2), 151-156. doi:10.1016/j.cmet.2007.01.008

[205] Ridlon, J. M., Kang, D. J., Hylemon, P. B., & Bajaj, J. S. (2014). Bile acids and the gut microbiome. *Curr Opin Gastroenterol, 30*(3), 332-338. doi:10.1097/MOG.0000000000000057

[206] Robertson, R. P., Harmon, J., Tran, P. O., Tanaka, Y., & Takahashi, H. (2003). Glucose toxicity in beta-cells: type 2 diabetes, good radicals gone bad, and the glutathione connection. *Diabetes, 52*(3), 581-587.

[207] Roduit, R., Nolan, C., Alarcon, C., Moore, P., Barbeau, A., Delghingaro-Augusto, V., . . . Prentki, M. (2004). A role for the malonyl-CoA/long-chain acyl-CoA pathway of lipid signaling in the regulation of insulin secretion in response to both fuel and nonfuel stimuli. *Diabetes, 53*(4), 1007-1019.

[208] Rosengren, A. H., Braun, M., Mahdi, T., Andersson, S. A., Travers, M. E., Shigeto, M., . . . Eliasson, L. (2012). Reduced insulin exocytosis in human pancreatic beta-cells with gene variants linked to type 2 diabetes. *Diabetes, 61*(7), 1726-1733. doi:10.2337/db11-1516

[209] Ruchat, S. M., Elks, C. E., Loos, R. J., Vohl, M. C., Weisnagel, S. J., Rankinen, T., . . . Perusse, L. (2009). Association between insulin secretion, insulin sensitivity and type 2 diabetes susceptibility variants identified in genome-wide association studies. *Acta Diabetol, 46*(3), 217-226. doi:10.1007/s00592-008-0080-5

[210] Ruderman, N., & Prentki, M. (2004). AMP kinase and malonyl-CoA: targets for therapy of the metabolic syndrome. *Nat Rev Drug Discov, 3*(4), 340-351. doi:10.1038/nrd1344

[211] Ruderman, N. B., Carling, D., Prentki, M., & Cacicedo, J. M. (2013). AMPK, insulin resistance, and the metabolic syndrome. *J Clin Invest, 123*(7), 2764-2772. doi:10.1172/JCI67227

[212] Rung, J., Cauchi, S., Albrechtsen, A., Shen, L., Rocheleau, G., Cavalcanti-Proenca, C., . . . Sladek, R. (2009). Genetic variant near IRS1 is associated with type 2 diabetes, insulin resistance and hyperinsulinemia. *Nat Genet, 41*(10), 1110-1115. doi:10.1038/ng.443

[213] Rutter, G. A., & Leclerc, I. (2009). The AMP-regulated kinase family: enigmatic targets for diabetes therapy. *Mol Cell Endocrinol, 297*(1-2), 41-49. doi:10.1016/j.mce.2008.05.020

[214] Sartipy, P., & Loskutoff, D. J. (2003). Monocyte chemoattractant protein 1 in obesity and insulin resistance. *Proc Natl Acad Sci U S A, 100*(12), 7265-7270. doi:10.1073/pnas.1133870100

[215] Sato, R., Goldstein, J. L., & Brown, M. S. (1993). Replacement of serine-871 of hamster 3-hydroxy-3-methylglutaryl-CoA reductase prevents phosphorylation by AMP-activated kinase and blocks inhibition of sterol synthesis induced by ATP depletion. *Proc Natl Acad Sci U S A, 90*(20), 9261-9265.

[216] Schmitz-Peiffer, C., Laybutt, D. R., Burchfield, J. G., Gurisik, E., Narasimhan, S., Mitchell, C. J., . . . Biden, T. J. (2007). Inhibition of PKCepsilon improves glucose-stimulated insulin secretion and reduces insulin clearance. *Cell Metab, 6*(4), 320-328. doi:10.1016/j.cmet.2007.08.012

[217] Schuit, F., De Vos, A., Farfari, S., Moens, K., Pipeleers, D., Brun, T., & Prentki, M. (1997). Metabolic fate of glucose in purified islet cells. Glucose-regulated anaplerosis in beta cells. *J Biol Chem, 272*(30), 18572-18579.

[218] Servick, K. (2016). Of mice and microbes. *Science, 353*(6301), 741-743. doi:10.1126/science.353.6301.741

[219] Shackelford, D. B., & Shaw, R. J. (2009). The LKB1-AMPK pathway: metabolism and growth control in tumour suppression. *Nat Rev Cancer, 9*(8), 563-575. doi:10.1038/nrc2676

[220] Sharma, A., Olson, L. K., Robertson, R. P., & Stein, R. (1995). The reduction of insulin gene transcription in HIT-T15 beta cells chronically exposed to high glucose concentration is associated with the loss of RIPE3b1 and STF-1 transcription factor expression. *Mol Endocrinol, 9*(9), 1127-1134. doi:10.1210/mend.9.9.7491105

[221] Simon, M. M., Greenaway, S., White, J. K., Fuchs, H., Gailus-Durner, V., Wells, S., . . . Brown, S. D. (2013). A comparative phenotypic and genomic analysis of C57BL/6J and C57BL/6N mouse strains. *Genome Biol, 14*(7), R82. doi:10.1186/gb-2013-14-7-r82

[222] Sladek, R., Rocheleau, G., Rung, J., Dina, C., Shen, L., Serre, D., . . . Froguel, P. (2007). A genome-wide association study identifies novel risk loci for type 2 diabetes. *Nature, 445*(7130), 881-885. doi:10.1038/nature05616

[223] Srinivasan, K., & Ramarao, P. (2007). Animal models in type 2 diabetes research: an overview. *Indian J Med Res, 125*(3), 451-472.

[224] Stanley, C. A., Lieu, Y. K., Hsu, B. Y., Burlina, A. B., Greenberg, C. R., Hopwood, N. J., . . . Poncz, M. (1998). Hyperinsulinism and hyperammonemia in infants with regulatory mutations of the glutamate dehydrogenase gene. *N Engl J Med, 338*(19), 1352-1357. doi:10.1056/NEJM199805073381904

[225] Stein, S. A., Maloney, K. L., & Pollin, T. I. (2014). Genetic Counseling for Diabetes Mellitus. *Curr Genet Med Rep, 2*(2), 56-67. doi:10.1007/s40142-014-0039-5

[226] Stiles, L., & Shirihai, O. S. (2012). Mitochondrial dynamics and morphology in beta-cells. *Best Pract Res Clin Endocrinol Metab, 26*(6), 725-738. doi:10.1016/j.beem.2012.05.004

[227] Straub, S. G., & Sharp, G. W. (2002). Glucose-stimulated signaling pathways in biphasic insulin secretion. *Diabetes Metab Res Rev, 18*(6), 451-463. doi:10.1002/dmrr.329

[228] Stumvoll, M., Goldstein, B. J., & van Haeften, T. W. (2005). Type 2 diabetes: principles of pathogenesis and therapy. *Lancet, 365*(9467), 1333-1346. doi:10.1016/S0140-6736(05)61032-X

[229] Sun, G., Tarasov, A. I., McGinty, J. A., French, P. M., McDonald, A., Leclerc, I., & Rutter, G. A. (2010). LKB1 deletion with the RIP2.Cre transgene modifies pancreatic beta-cell morphology and enhances insulin secretion in vivo. *Am J Physiol Endocrinol Metab, 298*(6), E1261-1273. doi:10.1152/ajpendo.00100.2010

[230] Surwit, R. S., Kuhn, C. M., Cochrane, C., McCubbin, J. A., & Feinglos, M. N. (1988). Diet-induced type II diabetes in C57BL/6J mice. *Diabetes, 37*(9), 1163-1167.

[231] Suski, J. M., Lebiedzinska, M., Bonora, M., Pinton, P., Duszynski, J., & Wieckowski, M. R. (2012). Relation between mitochondrial membrane potential and ROS formation. *Methods Mol Biol, 810*, 183-205. doi:10.1007/978-1-61779-382-0_12

[232] Sutherland, C., O'Brien, R. M., & Granner, D. K. (1996). New connections in the regulation of PEPCK gene expression by insulin. *Philos Trans R Soc Lond B Biol Sci, 351*(1336), 191-199. doi:10.1098/rstb.1996.0016

[233] Sze, M. A., & Schloss, P. D. (2016). Looking for a Signal in the Noise: Revisiting Obesity and the Microbiome. *MBio, 7*(4). doi:10.1128/mBio.01018-16

[234] Tang, C., Han, P., Oprescu, A. I., Lee, S. C., Gyulkhandanyan, A. V., Chan, G. N., . . . Giacca, A. (2007). Evidence for a role of superoxide generation in glucose-induced beta-cell dysfunction in vivo. *Diabetes, 56*(11), 2722-2731. doi:10.2337/db07-0279

[235] Tang, T., Abbott, M. J., Ahmadian, M., Lopes, A. B., Wang, Y., & Sul, H. S. (2013). Desnutrin/ATGL activates PPARdelta to promote mitochondrial function for insulin secretion in islet beta cells. *Cell Metab, 18*(6), 883-895. doi:10.1016/j.cmet.2013.10.012

[236] Tengholm, A., & Gylfe, E. (2009). Oscillatory control of insulin secretion. *Mol Cell Endocrinol, 297*(1-2), 58-72. doi:10.1016/j.mce.2008.07.009

[237] Thomson, D. M., Brown, J. D., Fillmore, N., Condon, B. M., Kim, H. J., Barrow, J. R., & Winder, W. W. (2007). LKB1 and the regulation of malonyl-CoA and fatty acid oxidation in muscle. *Am J Physiol Endocrinol Metab, 293*(6), E1572-1579. doi:10.1152/ajpendo.00371.2007

[238] Thorens, B. (2015). GLUT2, glucose sensing and glucose homeostasis. *Diabetologia, 58*(2), 221-232. doi:10.1007/s00125-014-3451-1

[239] Tilg, H., & Kaser, A. (2011). Gut microbiome, obesity, and metabolic dysfunction. *J Clin Invest, 121*(6), 2126-2132. doi:10.1172/JCI58109

[240] Toye, A. A., Lippiat, J. D., Proks, P., Shimomura, K., Bentley, L., Hugill, A., . . . Cox, R. D. (2005). A genetic and physiological study of impaired glucose homeostasis control in C57BL/6J mice. *Diabetologia, 48*(4), 675-686. doi:10.1007/s00125-005-1680-z

[241] Travers, M. E., & McCarthy, M. I. (2011). Type 2 diabetes and obesity: genomics and the clinic. *Hum Genet, 130*(1), 41-58. doi:10.1007/s00439-011-1023-8

[242] Tremaroli, V., & Backhed, F. (2012). Functional interactions between the gut microbiota and host metabolism. *Nature, 489*(7415), 242-249. doi:10.1038/nature11552

[243] Turnbaugh, P. J., Ley, R. E., Mahowald, M. A., Magrini, V., Mardis, E. R., & Gordon, J. I. (2006). An obesity-associated gut microbiome with increased capacity for energy harvest. *Nature, 444*(7122), 1027-1031. doi:10.1038/nature05414

[244] Turnbaugh, P. J., Ridaura, V. K., Faith, J. J., Rey, F. E., Knight, R., & Gordon, J. I. (2009). The effect of diet on the human gut microbiome: a metagenomic analysis in humanized gnotobiotic mice. *Sci Transl Med, 1*(6), 6ra14. doi:10.1126/scitranslmed.3000322

[245] Vetterli, L., Carobbio, S., Pournourmohammadi, S., Martin-Del-Rio, R., Skytt, D. M., Waagepetersen, H. S., . . . Maechler, P. (2012). Delineation of glutamate pathways and secretory responses in pancreatic islets with beta-cell-specific abrogation of the glutamate dehydrogenase. *Mol Biol Cell, 23*(19), 3851-3862. doi:10.1091/mbc.E11-08-0676

[246] Villeneuve, L. M., & Natarajan, R. (2010). The role of epigenetics in the pathology of diabetic complications. *Am J Physiol Renal Physiol, 299*(1), F14-25. doi:10.1152/ajprenal.00200.2010

[247] Viollet, B., Lantier, L., Devin-Leclerc, J., Hebrard, S., Amouyal, C., Mounier, R., . . . Andreelli, F. (2009). Targeting the AMPK pathway for the treatment of Type 2 diabetes. *Front Biosci (Landmark Ed), 14*, 3380-3400.

[248] Voight, B. F., Scott, L. J., Steinthorsdottir, V., Morris, A. P., Dina, C., Welch, R. P., . . . Consortium, G. (2010). Twelve type 2 diabetes susceptibility loci identified through large-scale association analysis. *Nat Genet, 42*(7), 579-589. doi:10.1038/ng.609

[249] Wang, Y. W., Sun, G. D., Sun, J., Liu, S. J., Wang, J., Xu, X. H., & Miao, L. N. (2013). Spontaneous type 2 diabetic rodent models. *J Diabetes Res, 2013*, 401723. doi:10.1155/2013/401723

[250] Wencel, H. E., Smothers, C., Opara, E. C., Kuhn, C. M., Feinglos, M. N., & Surwit, R. S. (1995). Impaired second phase insulin response of diabetes-prone C57BL/6J mouse islets. *Physiol Behav, 57*(6), 1215-1220.

[251] Wikstrom, J. D., Katzman, S. M., Mohamed, H., Twig, G., Graf, S. A., Heart, E., . . . Shirihai, O. S. (2007). beta-Cell mitochondria exhibit membrane potential heterogeneity that can be altered by stimulatory or toxic fuel levels. *Diabetes, 56*(10), 2569-2578. doi:10.2337/db06-0757

[252] Wikstrom, J. D., Sereda, S. B., Stiles, L., Elorza, A., Allister, E. M., Neilson, A., . . . Shirihai, O. S. (2012). A novel high-throughput assay for islet respiration reveals uncoupling of rodent and human islets. *PLoS One, 7*(5), e33023. doi:10.1371/journal.pone.0033023

[253] Winzell, M. S., & Ahren, B. (2004). The high-fat diet-fed mouse: a model for studying mechanisms and treatment of impaired glucose tolerance and type 2 diabetes. *Diabetes, 53 Suppl 3*, S215-219.

[254] Wojtaszewski, J. F., Mourtzakis, M., Hillig, T., Saltin, B., & Pilegaard, H. (2002). Dissociation of AMPK activity and ACCbeta phosphorylation in human muscle during prolonged exercise. *Biochem Biophys Res Commun, 298*(3), 309-316.

[255] Woods, S. C., Seeley, R. J., Porte, D., Jr., & Schwartz, M. W. (1998). Signals that regulate food intake and energy homeostasis. *Science, 280*(5368), 1378-1383.

[256] Wu, G. D., Chen, J., Hoffmann, C., Bittinger, K., Chen, Y. Y., Keilbaugh, S. A., . . . Lewis, J. D. (2011). Linking long-term dietary patterns with gut microbial enterotypes. *Science, 334*(6052), 105-108. doi:10.1126/science.1208344

[257] Yajima, H., Komatsu, M., Schermerhorn, T., Aizawa, T., Kaneko, T., Nagai, M., . . . Hashizume, K. (1999). cAMP enhances insulin secretion by an action on the ATP-sensitive K+ channel-independent pathway of glucose signaling in rat pancreatic islets. *Diabetes, 48*(5), 1006-1012.

[258] Yang, Y., & Santamaria, P. (2006). Lessons on autoimmune diabetes from animal models. *Clin Sci (Lond), 110*(6), 627-639. doi:10.1042/CS20050330

[259] Ye, D. Z., Tai, M. H., Linning, K. D., Szabo, C., & Olson, L. K. (2006). MafA expression and insulin promoter activity are induced by nicotinamide and related compounds in INS-1 pancreatic beta-cells. *Diabetes, 55*(3), 742-750.

[260] Yoshinari, O., & Igarashi, K. (2011). Anti-diabetic effect of pyroglutamic acid in type 2 diabetic Goto-Kakizaki rats and KK-Ay mice. *Br J Nutr, 106*(7), 995-1004. doi:10.1017/S0007114511001279

[261] Zawalich, W. S., Bonnet-Eymard, M., & Zawalich, K. C. (1997). Signal transduction in pancreatic beta-cells: regulation of insulin secretion by information flow in the phospholipase C/protein kinase C pathway. *Front Biosci, 2*, d160-172.

[262] Zhang, J., McKenna, L. B., Bogue, C. W., & Kaestner, K. H. (2014). The diabetes gene Hhex maintains delta-cell differentiation and islet function. *Genes Dev, 28*(8), 829-834. doi:10.1101/gad.235499.113

[263] Zhao, S., Mugabo, Y., Iglesias, J., Xie, L., Delghingaro-Augusto, V., Lussier, R., . . . Prentki, M. (2014). alpha/beta-Hydrolase domain-6-accessible monoacylglycerol controls glucose-stimulated insulin secretion. *Cell Metab, 19*(6), 993-1007. doi:10.1016/j.cmet.2014.04.003

[264] Zhao, S., Poursharifi, P., Mugabo, Y., Levens, E. J., Vivot, K., Attane, C., . . . Prentki, M. (2015). alpha/beta-Hydrolase domain-6 and saturated long chain monoacylglycerol regulate insulin secretion promoted by both fuel and non-fuel stimuli. *Mol Metab, 4*(12), 940-950. doi:10.1016/j.molmet.2015.09.012

[265] Zisman, A., Peroni, O. D., Abel, E. D., Michael, M. D., Mauvais-Jarvis, F., Lowell, B. B., . . . Kahn, B. B. (2000). Targeted disruption of the glucose transporter 4 selectively in muscle causes insulin resistance and glucose intolerance. *Nat Med, 6*(8), 924-928. doi:10.1038/78693

[266] Zoetendal, E. G., Rajilic-Stojanovic, M., & de Vos, W. M. (2008). High-throughput diversity and functionality analysis of the gastrointestinal tract microbiota. *Gut, 57*(11), 1605-1615. doi:10.1136/gut.2007.133603

[267] Zuniga-Hertz, J. P., Rebelato, E., Kassan, A., Khalifa, A. M., Ali, S. S., Patel, H. H., & Abdulkader, F. (2015). Distinct pathways of cholesterol biosynthesis impact on insulin secretion. *J Endocrinol, 224*(1), 75-84. doi:10.1530/JOE-14-0348

Appendix 1 – Supporting information (Chapter 2)

The following tables have been published in: Pepin, E., **A. Al-Mass**, C. Attane, K. Zhang, J. Lamontagne, R. Lussier, S. R. Madiraju, E. Joly, N. B. Ruderman, **R. Sladek, M. Prentki** and M. L. Peyot (2016). "Pancreatic beta-Cell Dysfunction in Diet-Induced Obese Mice: Roles of AMP-Kinase, Protein Kinase Cepsilon, Mitochondrial and Cholesterol Metabolism, and Alterations in Gene Expression." PLoS One 11(4): e0153017.

Table S1. PCR primer sequences used for Quantitative Real Time PCR.

GENE	GenBank accession no	Primer sequences (5'-3')
Eef2k	NM_007908.4	S: GTGAATCAGAGCACCAGGCT AS: ATCCCCGGAGTTCTCTGACA
Ppargc1a	NM_008904.2	S: TAGAGTGTGCTGCTCTGGTTG AS: GATTGGTCGCTACACCACTTC
Ppp2r2b	NM_028392.3	S: AATTCAACCACACGGGAGAG AS: GGTTCATGGCTCTGGAATGT
Ppp2r5c	NM_012023.3	S: TATATCACCCACAACCGGAAC AS: ACGTTGGTTCATCCTCTTCTG
Prkab2	NM_182997.2	S: CATCTCTGGGTCCTTCAACAA AS: TACTGATGCTCTCCCTCTGGA
Beta-Actin	NM_007393.5	S: CATGGATGACGATATCGCTGC AS:GTACGACCAGAGGCATACAGG

Primers: S, sense; AS, antisense.

Table S2. Functional classification of differentially expressed genes in HDR vs ND islets.

Gene Symbol	Gene description	FDR step up ($p < 0.05$ n = 1508)	Fold-Change Increase: 883 Decrease: 625
Carbohydrate metabolism			
Me3	malic enzyme 3, NADP(+)-dependent, mitochondrial	2,68E-06	1,786
Gmds	GDP-mannose 4, 6-dehydratase	8,13E-05	1,529
Bpgm	2,3-bisphosphoglycerate mutase	2,25E-04	1,349
Gla	galactosidase, alpha	2,45E-04	1,316
Mpdu1	mannose-P-dolichol utilization defect 1	3,58E-04	1,307
Pgk1	phosphoglycerate kinase 1	3,29E-04	1,272
Pgls	6-phosphogluconolactonase	4,94E-04	1,245
Galns	galactosamine (N-acetyl)-6-sulfate sulfatase	4,04E-03	1,217
Mdh1	malate dehydrogenase 1, NAD (soluble)	3,38E-04	1,212
Gale	galactose-4-epimerase, UDP	3,10E-02	1,209
Tsta3	tissue specific transplantation antigen P35B	1,32E-03	1,209
Pgm5	phosphoglucomutase 5	2,38E-02	-1,215
Ppp1r1a	protein phosphatase 1, regulatory (inhibitor) subunit 1A	5,67E-04	-1,227
Rbp4	retinol binding protein 4, plasma	1,16E-02	-1,235
Slc2a2	solute carrier family 2 (facilitated glucose transporter), member 2	1,20E-02	-1,241
Rpia	ribose 5-phosphate isomerase A	4,31E-03	-1,390
Cryl1	crystallin, lambda 1	6,60E-04	-1,411
Khk	ketohexokinase	1,97E-03	-1,461
Aldoc	aldolase C, fructose-bisphosphate	7,33E-04	-1,511
Hpse	heparanase	1,06E-03	-1,779
Glycan metabolism			
Alg8	asparagine-linked glycosylation 8 homolog (yeast, Alpha-1,3-Glucosyltransferase)	1,92E-03	1,417
Dpm3	dolichyl-phosphate mannosyltransferase polypeptide 3	7,03E-04	1,381
Alg3	asparagine-linked glycosylation 3 homolog (yeast, Alpha-1,3-Mannosyltransferase)	3,07E-03	1,357
Pomgnt1	protein O-linked mannose beta1,2-N-acetylglucosaminyltransferase	9,03E-06	1,354
Alg12	asparagine-linked glycosylation 12 homolog (yeast, Alpha-1,6-Mannosyltransferase)	1,18E-04	1,344
Alg14	asparagine-linked glycosylation 14 homolog (yeast)	7,77E-03	1,342
Glb1	galactosidase, beta 1	9,30E-06	1,340
Pomt1	protein-O-mannosyltransferase 1	2,65E-04	1,316
Alg5	asparagine-linked glycosylation 5 homolog (yeast, Dolichyl-Phosphate Beta-Glucosyltransferase)	4,23E-04	1,299
Alg6	asparagine-linked glycosylation 6 homolog (yeast, Alpha-1,3-Glucosyltransferase)	3,06E-03	1,263
Man2b1	mannosidase 2, alpha B1	6,56E-06	1,247

St3gal1	ST3 beta-galactoside alpha-2,3-sialyltransferase	1,39E-03	1,239
Hs3st1	heparan sulfate (glucosamine) 3-O-sulfotransferase 1	6,39E-05	-1,250
Amino acid metabolism			
Aass	aminoadipate-semialdehyde synthase	2,35E-04	2,476
Pycr1	pyrroline-5-carboxylate reductase 1	1,37E-05	1,556
Gls2	glutaminase 2 (liver, mitochondrial)	3,99E-03	1,511
Psat1	phosphoserine aminotransferase 1	7,99E-04	1,503
Gatm	glycine amidinotransferase (L-arginine:glycine amidinotransferase)	8,03E-04	1,472
Bcat2	branched chain aminotransferase 2, mitochondrial	4,84E-04	1,429
Gcdh	glutaryl-Coenzyme A dehydrogenase	9,39E-05	1,398
Odc1	ornithine decarboxylase, structural 1	4,08E-03	1,358
Bckdk	branched chain ketoacid dehydrogenase kinase	6,08E-05	1,355
Grhpr	glyoxylate reductase/hydroxypyruvate reductase	2,92E-04	1,325
Phgdh	3-phosphoglycerate dehydrogenase	1,69E-02	1,305
Gamt	guanidinoacetate methyltransferase	3,93E-02	1,303
Pycr2	pyrroline-5-carboxylate reductase family, member 2	6,27E-05	1,300
Aadat	aminoadipate aminotransferase	5,33E-03	1,277
Got1	glutamate oxaloacetate transaminase 1, soluble	2,94E-04	1,267
Ckb	creatine kinase, brain	4,39E-03	1,266
Cad	carbamoyl-phosphate synthetase 2, aspartate transcarbamylase	1,26E-02	1,251
Vars	valyl-tRNA synthetase	7,44E-04	1,230
Aoc3	amine oxidase, copper containing 3	5,58E-03	1,224
Aldh9a1	aldehyde dehydrogenase 9, subfamily A1	2,34E-05	1,219
Srm	spermidine synthase	3,85E-02	1,213
Agxt2l2	alanine-glyoxylate aminotransferase 2-like 2	8,76E-03	1,210
Bckdha	branched chain ketoacid dehydrogenase E1, alpha polypeptide	1,24E-02	1,204
Pycrl	pyrroline-5-carboxylate reductase-like	1,56E-03	1,201
Kynu	kynureninase (L-kynurenine hydrolase)	4,99E-02	-1,226
Mat2a	methionine adenosyltransferase II, alpha	1,46E-03	-1,371
Gad1	glutamic acid decarboxylase 1	1,44E-02	-1,487
Ass1	argininosuccinate synthetase 1	1,39E-03	-1,530
Nucleotide/pyrophosphate metabolism			
Gucy2c	guanylate cyclase 2c	8,62E-07	3,598
Rrm2	ribonucleotide reductase M2	9,34E-05	2,071
Tyms	thymidylate synthase	3,32E-03	1,437
Rasl10b	RAS-like, family 10, member B	6,67E-04	1,415
Ppa1	pyrophosphatase (inorganic) 1	5,99E-04	1,387
Dhfr	dihydrofolate reductase	3,19E-03	1,354
Impdh2	inosine 5'-phosphate dehydrogenase 2	2,53E-03	1,302
Adcy4	adenylate cyclase 4	3,68E-03	1,291

Nme2	Nucleoside Diphosphate Kinase 2	1,38E-04	1,284
Ctps	cytidine 5'-triphosphate synthase	1,52E-02	1,274
Guk1	guanylate kinase 1	1,22E-04	1,230
Gda	guanine deaminase	2,75E-02	1,212
Sult3a1	sulfotransferase family 3A, member 1	3,74E-03	1,209
Impdh1	inosine 5'-phosphate dehydrogenase 1	1,66E-03	1,202
Nme1	Nucleoside Diphosphate Kinase 1	3,50E-03	1,202
Nme5	Nucleoside Diphosphate Kinase 5	4,50E-03	-1,260
Nme4	Nucleoside Diphosphate Kinase 4	6,39E-05	-1,278
Lipid metabolism			
Pnliprp2	pancreatic lipase-related protein 2	3,25E-02	2,417
Acsf2	acyl-CoA synthetase family member 2	2,52E-04	1,614
Cel	carboxyl ester lipase	4,56E-02	1,613
Cpt1a	carnitine palmitoyltransferase 1a, liver	5,29E-06	1,576
Lmf1	lipase maturation factor 1	7,13E-06	1,552
Cd36	CD36 antigen	2,90E-02	1,505
Pecr	peroxisomal trans-2-enoyl-CoA reductase	2,43E-05	1,448
Fabp4	fatty acid binding protein 4, adipocyte	4,16E-04	1,436
Acer2	alkaline ceramidase 2	1,28E-02	1,423
Ces2g	carboxylesterase 2G	9,26E-04	1,417
Acot9	acyl-CoA thioesterase 9	2,81E-03	1,371
Slc25a20	solute carrier family 25 (mitochondrial carnitine/acylcarnitine translocase) member 20	3,05E-04	1,345
Ppapdc1b	phosphatidic acid phosphatase type 2 domain containing 1B	2,89E-05	1,344
Mgll	monoglyceride lipase	5,52E-03	1,287
Hsd3b7	hydroxy-delta-5-steroid dehydrogenase, 3 beta- and steroid Delta isomerase-7	1,37E-03	1,284
Acadvl	acyl-Coenzyme A dehydrogenase, very long chain	7,35E-05	1,276
Elovl7	ELOVL family member 7, elongation of long chain fatty acid	4,32E-04	1,270
Cds1	CDP-diacylglycerol synthase 1	7,17E-03	1,266
Pemt	phosphatidylethanolamine N-methyltransferase	6,01E-03	1,249
Cyp2j6	cytochrome P450, family 2, subfamily j, polypeptide 6	6,90E-04	1,248
Pla2g12a	phospholipase A2, group XIIA	8,63E-05	1,234
Mboat1	membrane bound O-acyltransferase domain containing 1	2,29E-02	1,232
Hsd17b12	hydroxysteroid (17-beta) dehydrogenase 12	2,36E-03	1,221
Anxa3	annexin A3	3,28E-03	1,221
Gde1	glycerophosphodiester phosphodiesterase 1	8,15E-05	1,216
Lipa	lysosomal acid lipase A	6,97E-03	1,210
Acot11	acyl-CoA thioesterase 11	3,88E-03	1,206
Mecr	mitochondrial trans-2-enoyl-CoA reductase	2,93E-03	1,200
Scd3	stearoyl-coenzyme A desaturase 3	1,77E-03	-1,207

Arv1	ARV1 homolog (yeast)	1,20E-03	-1,207
Asah1	N-acylsphingosine amidohydrolase 1	1,14E-04	-1,223
Osbpl6	oxysterol binding protein-like 6	5,12E-03	-1,226
Cyp2s1	cytochrome P450, family 2, subfamily s, polypeptide 1	3,35E-03	-1,270
Apod	apolipoprotein D	3,14E-02	-1,272
Ugt8a	UDP galactosyltransferase 8A	1,96E-02	-1,276
Gpd2	glycerol phosphate dehydrogenase 2, mitochondrial	1,49E-02	-1,326
Scd2	stearoyl-Coenzyme A desaturase 2	3,73E-06	-1,390
Gpr120	G protein-coupled receptor 120	6,67E-04	-1,408
Lpl	lipoprotein lipase	1,02E-04	-1,675
Scd1	stearoyl-Coenzyme A desaturase 1	2,05E-04	-2,115
Cholesterol metabolism and transport			
Apoa2	apolipoprotein A-II	1,49E-03	1,469
Dhcr7	7-dehydrocholesterol reductase	7,44E-04	1,302
Acaa2	acetyl-Coenzyme A acyltransferase 2	8,93E-04	1,271
Apof	apolipoprotein F	9,32E-03	1,265
Ebp	phenylalkylamine Ca2+ antagonist (emopamil) binding protein	6,25E-04	1,260
Stard3nl	STARD3 N-terminal like	3,66E-05	1,239
Pmvk	phosphomevalonate kinase	7,22E-04	1,210
Hmgcs1	3-hydroxy-3-methylglutaryl-Coenzyme A synthase 1	4,55E-02	-1,211
Klb	klotho beta	2,21E-02	-1,218
Srebf2	sterol regulatory element binding factor 2	2,51E-03	-1,223
Pcsk9	proprotein convertase subtilisin/kexin type 9	5,32E-03	-1,247
Idi1	isopentenyl-diphosphate delta isomerase	2,82E-02	-1,264
Osbp2	oxysterol binding protein 2	2,59E-04	-1,297
Lrp8	low density lipoprotein receptor-related protein 8, apolipoprotein	1,67E-04	-1,332
Dhcr24	24-dehydrocholesterol reductase	1,20E-03	-1,336
Metabolism-miscellaneous			
Aldh1a3	aldehyde dehydrogenase family 1, subfamily A3	2,25E-04	3,241
Gc	group specific component	8,62E-07	1,893
Hsd17b13	hydroxysteroid (17-beta) dehydrogenase 13	4,09E-02	1,711
Gsto2	glutathione S-transferase omega 2	1,83E-03	1,605
Mosc2	MOCO sulphurase C-terminal domain containing 2	2,68E-05	1,493
Bcmo1	beta-carotene 15,15'-monooxygenase	9,04E-05	1,480
Nans	N-acetylneuraminic acid synthase (sialic acid synthase)	8,52E-05	1,471
Gsto1	glutathione S-transferase omega 1	2,08E-04	1,418
Iyd	iodotyrosine deiodinase	8,51E-04	1,414
Cmas	cytidine monophospho-N-acetylneuraminic acid synthetase	2,89E-05	1,411
Dio1	deiodinase, iodothyronine, type I	8,28E-06	1,400
Dhrs3	dehydrogenase/reductase (SDR family) member 3	4,80E-03	1,345

Fpgs	folylpolyglutamyl synthetase	7,53E-03	1,310
Ephx3	epoxide hydrolase 3	1,77E-02	1,272
Tmem14c	transmembrane protein 14C	2,56E-03	1,258
Art3	ADP-ribosyltransferase 3	2,09E-03	1,257
Retsat	retinol saturase (all trans retinol 13,14 reductase)	1,94E-02	1,253
Ggh	gamma-glutamyl hydrolase	1,98E-02	1,228
Coasy	Coenzyme A synthase	8,93E-04	1,216
Chpf2	chondroitin polymerizing factor 2	3,41E-02	1,214
Vkorc1	vitamin K epoxide reductase complex, subunit 1	6,25E-03	1,211
Pnpo	pyridoxine 5'-phosphate oxidase	8,37E-04	1,206
Gstm7	glutathione S-transferase, mu 7	9,37E-03	-1,225
Gstt1	glutathione S-transferase, theta 1	3,30E-03	-1,226
Nos1	nitric oxide synthase 1, neuronal	4,42E-02	-1,238
Fmo5	flavin containing monooxygenase 5	1,79E-03	-1,414
Gstm3	glutathione S-transferase, mu 3	3,91E-05	-1,453
Inmt	indolethylamine N-methyltransferase	1,70E-02	-1,459
Gstm1	glutathione S-transferase, mu 1	1,32E-04	-1,615
Ndst4	N-deacetylase/N-sulfotransferase (heparin glucosaminyl) 4	8,71E-04	-1,832
Mitochondrial respiration			
Etfb	electron transferring flavoprotein, beta polypeptide	3,34E-05	1,360
Ndufa1	NADH dehydrogenase (ubiquinone) 1 alpha subcomplex, 1	3,81E-04	1,360
Ndufa4	NADH dehydrogenase (ubiquinone) 1 alpha subcomplex, 4	1,19E-03	1,350
Atp5o	ATP synthase, H+ transporting, mitochondrial F1 complex, O subunit	8,13E-05	1,312
Atp5g1	ATP synthase, H+ transporting, mitochondrial F0 complex, subunitC1 (subunit 9)	3,35E-03	1,286
Uqcr10	ubiquinol-cytochrome c reductase, complex III subunit X	1,60E-03	1,283
Coq9	coenzyme Q9 homolog (yeast)	1,54E-06	1,260
Uqcrq	ubiquinol-cytochrome c reductase, complex III subunit VII	5,73E-05	1,251
Uqcr11	ubiquinol-cytochrome c reductase, complex III subunit XI	1,74E-03	1,231
Uqcrfs1	ubiquinol-cytochrome c reductase, Rieske iron-sulfur polypeptide 1	5,75E-04	1,217
Uqcrc1	ubiquinol-cytochrome c reductase core protein 1	4,23E-03	1,208
Cox19	COX19 cytochrome c oxidase assembly homolog (S. cerevisiae)	1,55E-03	1,201
Slc25a27	solute carrier family 25, member 27 (UCP4)	5,46E-03	-1,286
Cox6a2	cytochrome c oxidase, subunit VI a, polypeptide 2	6,59E-03	-1,422
Oxidation-reduction process			
Dhrs7	dehydrogenase/reductase (SDR family) member 7	1,02E-04	1,360
Dhrs7b	dehydrogenase/reductase (SDR family) member 7B	9,04E-05	1,287

BC003331	cDNA sequence BC003331	2,82E-04	1,250
Dhrs1	dehydrogenase/reductase (SDR family) member 1	9,80E-05	1,213
Tmx3	thioredoxin-related transmembrane protein 3	5,64E-04	-1,231
Akr1c12	aldo-keto reductase family 1, member C12	8,53E-04	-1,279
Akr1c19	aldo-keto reductase family 1, member C19	1,26E-04	-1,503
Cell cycle			
Ccnb1	cyclin B1	3,73E-04	3,189
Top2a	topoisomerase (DNA) II alpha	4,65E-04	2,927
Mki67	antigen identified by monoclonal antibody Ki 67	1,90E-04	2,871
Reg2	regenerating islet-derived 2	1,10E-02	2,767
Ccnb2	cyclin B2	2,04E-04	2,736
Anln	anillin, actin binding protein	3,95E-04	2,683
Kif11	kinesin family member 11	2,08E-04	2,595
Plk1	polo-like kinase 1 (Drosophila)	8,51E-04	2,585
Bub1	budding uninhibited by benzimidazoles 1 homolog (S. cerevisiae)	9,80E-04	2,568
Ect2	ect2 oncogene	2,95E-04	2,511
Nek2	NIMA (never in mitosis gene a)-related expressed kinase 2	4,09E-04	2,377
Tpx2	TPX2, microtubule-associated protein homolog (Xenopus laevis)	5,81E-04	2,375
Prc1	protein regulator of cytokinesis 1	2,68E-04	2,372
Ccna2	cyclin A2	6,91E-04	2,343
D2Ertd750e	DNA segment, Chr 2, ERATO Doi 750, expressed	2,27E-04	2,331
Casc5	cancer susceptibility candidate 5	6,48E-04	2,272
Stmn1	stathmin 1	8,78E-04	2,228
Cdk1	cyclin-dependent kinase 1	2,66E-04	2,220
Cdc20	cell division cycle 20 homolog (S. cerevisiae)	1,74E-04	2,207
Dtl	denticleless homolog (Drosophila)	2,48E-04	2,169
Cks2	CDC28 protein kinase regulatory subunit 2	6,82E-04	2,147
Nusap1	nucleolar and spindle associated protein 1	9,07E-04	2,086
Dlgap5	discs, large (Drosophila) homolog-associated protein 5	6,03E-04	2,034
Sgol2	shugoshin-like 2 (S. pombe)	1,18E-04	2,011
Ncaph	non-SMC condensin I complex, subunit H	7,53E-04	2,000
Cenpe	centromere protein E	1,21E-03	1,981
Cenpf	centromere protein F	1,08E-03	1,949
C79407	expressed sequence C79407	7,80E-04	1,945
Ckap2l	cytoskeleton associated protein 2-like	8,31E-04	1,927
Ckap2	cytoskeleton associated protein 2	2,92E-04	1,915
Nuf2	NUF2, NDC80 kinetochore complex component, homolog (S. cerevisiae)	2,96E-04	1,903
Aurkb	aurora kinase B	2,56E-03	1,900
Kif23	kinesin family member 23	7,16E-04	1,867

Kntc1	kinetochore associated 1	3,86E-04	1,855
Rad51	RAD51 homolog (S. cerevisiae)	2,72E-03	1,846
Kif20a	kinesin family member 20A	1,62E-03	1,837
Cenpm	centromere protein M	1,35E-04	1,827
Aspm	asp (abnormal spindle)-like, microcephaly associated (Drosophila)	1,55E-03	1,823
Mastl	microtubule associated serine/threonine kinase-like	8,70E-04	1,815
Reg3b	regenerating islet-derived 3 beta	1,38E-02	1,811
Cdkn3	cyclin-dependent kinase inhibitor 3	4,37E-04	1,810
Mcm5	minichromosome maintenance deficient 5, cell division cycle	7,22E-04	1,801
Aurka	aurora kinase A	1,17E-03	1,791
Ncapg	non-SMC condensin I complex, subunit G	7,13E-04	1,761
Mcm2	minichromosome maintenance deficient 2 mitotin (S. cerevisiae)	4,52E-04	1,748
Cenpn	centromere protein N	3,38E-04	1,740
Bub1b	BUB1 mitotic checkpoint serine/threonine kinase B	5,69E-04	1,739
Ncapg2	non-SMC condensin II complex, subunit G2	1,12E-03	1,731
Foxm1	forkhead box M1	1,26E-03	1,708
Zwilch	Zwilch, kinetochore associated, homolog (Drosophila)	6,90E-04	1,694
Cgref1	cell growth regulator with EF hand domain 1	2,07E-04	1,693
Cenpa	centromere protein A	2,71E-03	1,693
Cdca3	cell division cycle associated 3	2,09E-03	1,682
Cenpk	centromere protein K	2,08E-04	1,677
Spag5	sperm associated antigen 5	3,03E-03	1,648
E2f1	E2F transcription factor 1	1,06E-05	1,637
Smc2	structural maintenance of chromosomes 2	1,07E-03	1,627
Fam111a	family with sequence similarity 111, member A	3,90E-03	1,622
Cdca8	cell division cycle associated 8	5,09E-03	1,616
E2f8	E2F transcription factor 8	2,40E-03	1,604
Kif20b	kinesin family member 20B	7,72E-04	1,604
Spc24	SPC24, NDC80 kinetochore complex component, homolog (S. cerevisiae)	2,10E-04	1,598
Mad2l1	MAD2 mitotic arrest deficient-like 1 (yeast)	3,03E-03	1,582
Kif4	kinesin family member 4	6,56E-03	1,578
Oip5	Opa interacting protein 5	3,01E-03	1,578
Cenpi	centromere protein I	1,92E-03	1,562
Racgap1	Rac GTPase-activating protein 1	6,67E-04	1,559
Mcm6	minichromosome maintenance deficient 6 (MIS5 homolog, S. pombe)	3,93E-03	1,557
Cdca2	cell division cycle associated 2	1,52E-03	1,553
Hells	helicase, lymphoid specific	2,46E-03	1,549
Cks1b	CDC28 protein kinase 1b	7,85E-04	1,545
Ccnf	cyclin F	4,36E-03	1,533

Kif2c	kinesin family member 2C	3,82E-03	1,519
Ttk	Ttk protein kinase	1,38E-03	1,517
Cdc25c	cell division cycle 25 homolog C (S. pombe)	2,23E-03	1,512
Ncapd2	non-SMC condensin I complex, subunit D2	3,54E-03	1,498
Mcm7	minichromosome maintenance deficient 7 (S. cerevisiae)	1,29E-03	1,483
Melk	maternal embryonic leucine zipper kinase	2,43E-03	1,482
Kif18a	kinesin family member 18A	4,97E-03	1,477
Cdt1	chromatin licensing and DNA replication factor 1	3,54E-03	1,475
Kif22	kinesin family member 22	3,07E-03	1,461
Ndc80	NDC80 homolog, kinetochore complex component (S. cerevisiae)	1,08E-02	1,448
Sgol1	shugoshin-like 1 (S. pombe)	3,37E-03	1,445
Mcm3	minichromosome maintenance deficient 3 (S. cerevisiae)	1,61E-02	1,444
Clspn	claspin homolog (Xenopus laevis)	1,14E-03	1,435
Mcm8	minichromosome maintenance deficient 8 (S. cerevisiae)	1,30E-03	1,433
Dbf4	DBF4 homolog (S. cerevisiae)	2,40E-03	1,432
Chaf1b	chromatin assembly factor 1, subunit B (p60)	7,67E-03	1,424
Cdca5	cell division cycle associated 5	5,22E-03	1,416
Cdc6	cell division cycle 6 homolog (S. cerevisiae)	3,58E-04	1,413
Uhrf1	ubiquitin-like, containing PHD and RING finger domains, 1	5,58E-03	1,404
Aaas	achalasia, adrenocortical insufficiency, alacrimia	2,29E-03	1,401
Reg3g	regenerating islet-derived 3 gamma	9,00E-04	1,397
Kif15	kinesin family member 15	1,39E-03	1,380
Cdkn2c	cyclin-dependent kinase inhibitor 2C (p18, inhibits CDK4)	1,34E-03	1,372
Cenph	centromere protein H	1,73E-02	1,371
Tacc2	transforming, acidic coiled-coil containing protein 2	4,75E-05	1,371
Plk4	polo-like kinase 4 (Drosophila)	2,50E-03	1,364
Fam64a	family with sequence similarity 64, member A	1,35E-02	1,363
Dsn1	DSN1, MIND kinetochore complex component, homolog (S. cerevisiae)	1,15E-02	1,338
E2f7	E2F transcription factor 7	2,60E-03	1,336
Gins1	GINS complex subunit 1 (Psf1 homolog)	2,87E-03	1,332
Mcm10	minichromosome maintenance deficient 10 (S. cerevisiae)	1,07E-02	1,327
Mlf1ip	myeloid leukemia factor 1 interacting protein	6,18E-03	1,314
Fam83d	family with sequence similarity 83, member D	3,64E-03	1,305
Arhgef10	Rho guanine nucleotide exchange factor (GEF) 10	8,18E-04	1,305
Cdc45	cell division cycle 45 homolog (S. cerevisiae)	1,72E-03	1,305
Leprel4	leprecan-like 4	1,05E-04	1,301
Pkmyt1	protein kinase, membrane associated tyrosine/threonine 1	1,12E-03	1,298

Mcm4	minichromosome maintenance deficient 4 homolog (S. cerevisiae)	2,35E-02	1,295
Cep76	centrosomal protein 76	1,37E-03	1,292
Cdk5rap3	CDK5 regulatory subunit associated protein 3	5,05E-05	1,284
Espl1	extra spindle poles-like 1 (S. cerevisiae)	9,53E-03	1,268
Haus1	HAUS augmin-like complex, subunit 1	4,14E-02	1,264
Cenpp	centromere protein P	2,28E-02	1,261
Gps1	G protein pathway suppressor 1	3,58E-04	1,259
Haus4	HAUS augmin-like complex, subunit 4	9,29E-03	1,250
Rbl1	retinoblastoma-like 1 (p107)	9,66E-03	1,246
Cep55	centrosomal protein 55	1,31E-02	1,242
Rint1	RAD50 interactor 1	3,69E-03	1,237
Incenp	inner centromere protein	2,70E-02	1,235
Usp2	ubiquitin specific peptidase 2	3,02E-04	1,234
Nsl1	NSL1, MIND kinetochore complex component, homolog (S. cerevisiae)	5,69E-03	1,233
Jtb	jumping translocation breakpoint	6,52E-05	1,233
E2f2	E2F transcription factor 2	3,18E-03	1,228
Pmf1	polyamine-modulated factor 1	4,32E-03	1,226
Sept11	septin 11	8,07E-05	1,226
Cdc25a	cell division cycle 25 homolog A (S. pombe)	6,49E-03	1,219
Smc4	structural maintenance of chromosomes 4	4,04E-02	1,217
Nudcd2	NudC domain containing 2	5,56E-03	1,213
Poc1a	POC1 centriolar protein homolog A (Chlamydomonas)	3,76E-03	1,206
Chaf1a	chromatin assembly factor 1, subunit A (p150)	2,94E-02	1,205
Btrc	beta-transducin repeat containing protein	3,73E-06	-1,203
Syce2	synaptonemal complex central element protein 2	1,26E-03	-1,205
Cspp1	centrosome and spindle pole associated protein 1	6,02E-03	-1,208
Ep300	E1A binding protein p300	1,77E-03	-1,209
Foxn3	forkhead box N3	9,61E-04	-1,219
Scaper	S phase cyclin A-associated protein in the ER	3,77E-03	-1,219
Ccnt2	cyclin T2	4,53E-02	-1,225
Cdk19	cyclin-dependent kinase 19	1,39E-02	-1,280
Chd7	chromodomain helicase DNA binding protein 7	2,84E-03	-1,301
Ttc28	tetratricopeptide repeat domain 28	1,85E-03	-1,354
Phf16	PHD finger protein 16	4,22E-04	-1,366
Klhl13	kelch-like 13 (Drosophila)	5,42E-04	-1,402
DNA repair/DNA recombination/DNA replication			
Asf1b	ASF1 anti-silencing function 1 homolog B (S. cerevisiae)	2,65E-04	2,496
Pole	polymerase (DNA directed), epsilon	5,42E-04	1,896
Fignl1	fidgetin-like 1	9,37E-05	1,846
Fen1	flap structure specific endonuclease 1	6,81E-04	1,680

Neil3	nei like 3 (E. coli)	3,80E-03	1,627
Rrm1	ribonucleotide reductase M1	2,16E-03	1,465
Gen1	Gen homolog 1, endonuclease (Drosophila)	1,08E-03	1,463
Pole2	polymerase (DNA directed), epsilon 2 (p59 subunit)	7,74E-04	1,448
Fancd2	Fanconi anemia, complementation group D2	5,10E-03	1,442
Fancb	Fanconi anemia, complementation group B	2,60E-03	1,440
Brca1	breast cancer 1	2,57E-03	1,437
Rad18	RAD18 homolog (S. cerevisiae)	6,90E-04	1,437
Rpa2	replication protein A2	3,57E-04	1,385
Pola2	polymerase (DNA directed), alpha 2	2,00E-03	1,384
Rfc4	replication factor C (activator 1) 4	3,85E-03	1,370
Gins2	GINS complex subunit 2 (Psf2 homolog)	5,51E-03	1,361
Brip1	BRCA1 interacting protein C-terminal helicase 1	1,33E-03	1,351
Exo1	exonuclease 1	4,88E-03	1,340
Rad51ap1	RAD51 associated protein 1	8,53E-04	1,332
Pold2	polymerase (DNA directed), delta 2, regulatory subunit	7,41E-03	1,315
Fanci	Fanconi anemia, complementation group I	8,17E-03	1,314
Hmgb2	high mobility group box 2	3,13E-02	1,299
Rexo2	REX2, RNA exonuclease 2 homolog (S. cerevisiae)	6,67E-04	1,282
Rfc5	replication factor C (activator 1) 5	3,47E-03	1,281
Rad54b	RAD54 homolog B (S. cerevisiae)	6,81E-03	1,280
Fanca	Fanconi anemia, complementation group A	1,53E-02	1,272
Topbp1	topoisomerase (DNA) II binding protein 1	3,91E-03	1,271
Dna2	DNA replication helicase 2 homolog (yeast)	1,20E-02	1,236
Lig1	ligase I, DNA, ATP-dependent	2,74E-02	1,230
Brca2	breast cancer 2	7,71E-03	1,222
Poll	polymerase (DNA directed), lambda	1,34E-02	1,207
Nfkbil2	nuclear factor of kappa light polypeptide gene enhancer In B-Cells Inhibitor-Like 2	7,75E-03	1,207
Ung	uracil DNA glycosylase	4,30E-03	1,207
Rad9b	RAD9 homolog B (S. cerevisiae)	1,30E-03	-1,215
Mns1	meiosis-specific nuclear structural protein 1	9,08E-04	-1,239
Rdm1	RAD52 motif 1	9,41E-03	-1,243
Dclre1c	DNA cross-link repair 1C, PSO2 homolog (S. cerevisiae)	3,25E-03	-1,246
Rev1	REV1 homolog (S. cerevisiae)	9,45E-04	-1,249
Cdc14b	CDC14 cell division cycle 14 homolog B (S. cerevisiae)	1,51E-04	-1,276
Nucleosome assembly			
Hist1h2bb	histone cluster 1, H2bb	3,03E-02	1,430
Hist1h1b	histone cluster 1, H1b	1,15E-02	1,409
Hirip3	HIRA interacting protein 3	3,70E-03	1,338
Hist2h3b	histone cluster 2, H3b	3,78E-04	1,332

Hist1h3c	histone cluster 1, H3c	1,81E-04	1,328
Hist1h3b	histone cluster 1, H3b	1,57E-04	1,323
Hist1h3i	histone cluster 1, H3i	3,21E-04	1,323
Hist1h3e	histone cluster 1, H3e	2,05E-04	1,321
Hist1h3g	histone cluster 1, H3g	2,21E-04	1,320
Hist1h3d	histone cluster 1, H3d	2,45E-04	1,314
Hist1h3h	histone cluster 1, H3h	2,00E-04	1,311
Hist2h2bb	histone cluster 2, H2bb	7,66E-03	1,272
Hist1h1a	histone cluster 1, H1a	2,98E-02	1,271
Hist1h2an	histone cluster 1, H2an	5,12E-03	1,224
Hist1h2ao	histone cluster 1, H2ao	2,72E-03	1,223
Hist1h2af	histone cluster 1, H2af	3,49E-03	1,220
Hist1h2ai	histone cluster 1, H2ai	2,57E-03	1,215
Hist1h2ah	histone cluster 1, H2ah	3,35E-03	1,214
Hist1h2ae	histone cluster 1, H2ae	8,91E-03	1,208
Hist1h4j	histone cluster 1, H4j	1,60E-02	-1,200
Hist2h2be	histone cluster 2, H2be	3,00E-04	-1,250
Epigenic regulation			
Esco2	establishment of cohesion 1 homolog 2 (S. cerevisiae)	2,05E-03	1,908
Smyd2	SET and MYND domain containing 2	9,34E-05	1,208
Mll5	myeloid/lymphoid or mixed-lineage leukemia 5	8,79E-04	-1,205
Phc3	polyhomeotic-like 3 (Drosophila)	8,08E-03	-1,211
Tet3	tet oncogene family member 3	2,24E-02	-1,218
Kdm6b	KDM1 lysine (K)-specific demethylase 6B	9,64E-04	-1,218
Dnmt3a	DNA methyltransferase 3A	5,35E-03	-1,224
Mll3	myeloid/lymphoid or mixed-lineage leukemia 3	2,56E-02	-1,248
Apobec3	apolipoprotein B mRNA editing enzyme, catalytic polypeptide like-3	6,72E-04	-1,259
Cbx7	chromobox homolog 7	3,58E-03	-1,302
A1cf	APOBEC1 complementation factor	2,46E-03	-1,315
Tet2	tet oncogene family member 2	4,75E-03	-1,340
Phf15	PHD finger protein 15	2,67E-03	-1,376
Tet1	tet oncogene 1	6,11E-03	-1,465
Apoptosis			
Dapl1	death associated protein-like 1	2,88E-06	2,186
Myc	myelocytomatosis oncogene	6,25E-03	1,973
Nupr1	nuclear protein 1	1,25E-03	1,709
Fam167a	family with sequence similarity 167, member A	1,86E-03	1,551
Stk17b	serine/threonine kinase 17b (apoptosis-inducing)	3,59E-04	1,418
Birc5	baculoviral IAP repeat-containing 5	2,86E-03	1,404
Clptm1l	CLPTM1-like	1,51E-04	1,396
Tpd52l1	tumor protein D52-like 1	4,64E-04	1,352

Plekhf1	pleckstrin homology domain containing, family F (with FYVE domain) member 1	5,26E-04	1,298
Perp	PERP, TP53 apoptosis effector	5,65E-03	1,281
Lgals12	lectin, galactose binding, soluble 12	4,20E-03	1,273
Atp6v1g2	ATPase, H+ transporting, lysosomal V1 subunit G2	1,79E-04	1,271
Cd38	CD38 antigen	6,77E-03	1,265
Krt18	keratin 18	9,37E-05	1,256
Tmbim4	transmembrane BAX inhibitor motif containing 4	1,13E-04	1,253
Clu	clusterin	1,49E-03	1,253
Ptrh2	peptidyl-tRNA hydrolase 2	4,00E-03	1,237
Irak3	interleukin-1 receptor-associated kinase 3	8,51E-03	1,235
Chek2	CHK2 checkpoint homolog (S. pombe)	5,30E-04	1,233
Fam82a2	family with sequence similarity 82, member A2	4,82E-05	1,218
Aven	apoptosis, caspase activation inhibitor	8,67E-04	1,216
Hyou1	hypoxia up-regulated 1	2,09E-05	1,215
Unc13b	unc-13 homolog B (C. elegans)	2,53E-04	1,214
Parl	presenilin associated, rhomboid-like	1,70E-03	1,203
Faim2	Fas apoptotic inhibitory molecule 2	4,41E-02	-1,202
Pdcd7	programmed cell death 7	2,28E-02	-1,210
Plagl2	pleiomorphic adenoma gene-like 2	1,08E-03	-1,218
Robo1	roundabout homolog 1 (Drosophila)	2,46E-03	-1,232
Ank2	ankyrin 2, brain	7,87E-03	-1,236
Rnf122	ring finger protein 122	1,69E-02	-1,245
Syngap1	synaptic Ras GTPase activating protein 1 homolog (rat)	1,32E-03	-1,252
Olfm4	olfactomedin 4	1,09E-02	-1,269
Robo2	roundabout homolog 2 (Drosophila)	4,73E-03	-1,291
Bcl2l11	BCL2-like 11 (apoptosis facilitator)	9,71E-04	-1,321
Amigo2	adhesion molecule with Ig like domain 2	5,71E-03	-1,322
Serpinb9	serine (or cysteine) peptidase inhibitor, clade B, member 9	9,39E-03	-1,332
Aatk	apoptosis-associated tyrosine kinase	6,82E-04	-1,333
Pycard	PYD and CARD domain containing	3,13E-04	-1,336
Eef1a2	eukaryotic translation elongation factor 1 alpha 2	7,31E-03	-1,341
Higd1a	HIG1 domain family, member 1A	2,24E-02	-1,344
Trim35	tripartite motif-containing 35	1,92E-05	-1,349
Unc5c	unc-5 homolog C (C. elegans)	9,24E-03	-1,402
Kcnip3	Kv channel interacting protein 3, calsenilin	1,01E-02	-1,419
Peg10	paternally expressed 10	5,84E-03	-1,674
Vip	vasoactive intestinal polypeptide	2,05E-02	-1,828
Oxidative stress/DNA damage response			
Gpx2	glutathione peroxidase 2	1,79E-05	2,070
Osgin1	oxidative stress induced growth inhibitor 1	5,21E-04	1,501

Chek1	checkpoint kinase 1 homolog (S. pombe)	6,72E-04	1,475
Prdx4	peroxiredoxin 4	1,34E-03	1,469
Tacc3	transforming, acidic coiled-coil containing protein 3	1,57E-03	1,407
Gtse1	G two S phase expressed protein 1	8,59E-03	1,319
Pon2	paraoxonase 2	5,80E-05	1,284
Tiparp	TCDD-inducible poly(ADP-ribose) polymerase	8,02E-04	1,269
Ehd2	EH-domain containing 2	1,47E-02	1,256
Atox1	ATX1 (antioxidant protein 1) homolog 1 (yeast)	5,42E-04	1,253
Sp100	nuclear antigen Sp100	1,97E-02	1,234
Gpx1	glutathione peroxidase 1	3,97E-03	1,230
Ppp2r5c	protein phosphatase 2, regulatory subunit B (B56), gamma	1,73E-06	1,230
Phlda3	pleckstrin homology-like domain, family A, member 3	1,45E-02	1,203
Gpx8	glutathione peroxidase 8 (putative)	2,55E-02	1,201
Txndc11	thioredoxin domain containing 11	1,26E-03	1,200
Pxdn	peroxidasin homolog (Drosophila)	2,06E-02	-1,235
Pot1b	protection of telomeres 1B	5,95E-03	-1,239
Nfe2l2	nuclear factor, erythroid derived 2, like 2	8,84E-05	-1,250
Transcription factors			
Tcf19	transcription factor 19	1,75E-04	1,956
Mybl1	myeloblastosis oncogene-like 1	3,96E-03	1,472
Etv5	ets variant gene 5	1,24E-02	1,335
Tcf7l1	transcription factor 7-like 1 (T-cell specific, HMG box)	8,87E-03	1,264
Bach2	BTB and CNC homology 2	1,58E-03	1,250
Stat5b	signal transducer and activator of transcription 5B	4,74E-03	-1,204
Smad2	MAD homolog 2 (Drosophila)	1,75E-05	-1,209
Hsf4	heat shock transcription factor 4	4,36E-03	-1,216
Nfat5	nuclear factor of activated T-cells 5	7,93E-03	-1,233
Erf	Ets2 repressor factor	1,41E-03	-1,238
Cux2	cut-like homeobox 2	4,76E-03	-1,242
Arid3b	AT rich interactive domain 3B (BRIGHT-like)	3,40E-03	-1,243
Prdm5	PR domain containing 5	3,35E-03	-1,245
Prdm2	PR domain containing 2, with ZNF domain	1,86E-03	-1,268
Dach1	dachshund 1 (Drosophila)	9,45E-04	-1,269
Mnx1	motor neuron and pancreas homeobox 1	1,79E-02	-1,274
Egr1	early growth response 1	4,36E-02	-1,287
Arnt2	aryl hydrocarbon receptor nuclear translocator 2	1,40E-03	-1,308
Elf4	E74-like factor 4 (ets domain transcription factor)	3,92E-03	-1,314
Hivep3	human immunodeficiency virus type I enhancer binding protein 3	5,66E-04	-1,335
Per3	period homolog 3 (Drosophila)	9,22E-03	-1,403
Arx	aristaless related homeobox	9,34E-05	-1,405

Neurog3	neurogenin 3	6,24E-03	-1,411
Gtf3c2	general transcription factor IIIC, polypeptide 2, beta 110 kDa	3,57E-02	-1,417
Hhex	hematopoietically expressed homeobox	1,48E-03	-1,450
Fos	FBJ osteosarcoma oncogene	4,68E-02	-1,481
Plag1	pleiomorphic adenoma gene 1	1,97E-03	-1,498
Pou3f4	POU domain, class 3, transcription factor 4	5,30E-04	-1,537
Mafb	v-maf musculoaponeurotic fibrosarcoma oncogene homolog B	4,58E-03	-1,607
Fosb	FBJ osteosarcoma oncogene B	2,94E-02	-1,789
Nuclear receptor and related proteins			
Nr4a2	nuclear receptor subfamily 4, group A, member 2	3,57E-04	1,450
Ncoa1	nuclear receptor coactivator 1	1,33E-03	-1,202
Nr6a1	nuclear receptor subfamily 6, group A, member 1	3,58E-03	-1,252
Nr3c2	nuclear receptor subfamily 3, group C, member 2	5,60E-03	-1,268
Thra	thyroid hormone receptor alpha	4,52E-04	-1,365
Ccdc62	coiled-coil domain containing 62	1,31E-03	-1,385
Transcription regulation/alternative splicing			
Rnase1	ribonuclease, RNase A family, 1 (pancreatic)	4,05E-02	1,725
Atad2	ATPase family, AAA domain containing 2	9,39E-05	1,543
Lmo1	LIM domain only 1	8,49E-05	1,536
Zcchc12	zinc finger, CCHC domain containing 12	3,52E-04	1,534
Zfp367	zinc finger protein 367	1,09E-03	1,507
Ldb2	LIM domain binding 2	1,40E-03	1,374
Carhsp1	calcium regulated heat stable protein 1	1,27E-03	1,360
Ezh2	enhancer of zeste homolog 2 (Drosophila)	7,11E-04	1,354
Bhlha15	basic helix-loop-helix family, member a15	1,35E-02	1,325
Wdhd1	WD repeat and HMG-box DNA binding protein 1	1,33E-02	1,310
Parn	poly(A)-specific ribonuclease (deadenylation nuclease)	2,69E-04	1,309
Dom3z	DOM-3 homolog Z (C. elegans)	3,35E-03	1,303
Gemin6	gem (nuclear organelle) associated protein 6	1,20E-03	1,301
Mbnl3	muscleblind-like 3 (Drosophila)	3,87E-03	1,296
Srp9	signal recognition particle 9	5,77E-05	1,282
Rnaseh2c	ribonuclease H2, subunit C	2,12E-03	1,280
Lmcd1	LIM and cysteine-rich domains 1	3,33E-03	1,264
Armcx3	armadillo repeat containing, X-linked 3	2,01E-03	1,217
Polr1d	polymerase (RNA) I polypeptide D	1,32E-02	1,201
Taf1a	TATA box binding protein (Tbp)-associated factor, RNA polymerase I, A, 48kDa	9,83E-04	-1,202
Ppargc1b	peroxisome proliferative activated receptor, gamma, coactivator 1 beta	2,84E-03	-1,203
Zfml	zinc finger, matrin-like	2,40E-03	-1,203
Zfp192	zinc finger protein 192	1,62E-02	-1,203

Cnot6	CCR4-NOT transcription complex, subunit 6	2,05E-04	-1,204
Zbtb3	zinc finger and BTB domain containing 3	3,57E-03	-1,204
Ssbp2	single-stranded DNA binding protein 2	1,65E-03	-1,204
Zfp160	zinc finger protein 160	1,61E-03	-1,207
Ebf4	early B-cell factor 4	5,75E-04	-1,207
Zfp873	zinc finger protein 873	8,10E-03	-1,208
Zfp553	zinc finger protein 553	6,09E-04	-1,212
Elp4	elongation protein 4 homolog (S. cerevisiae)	2,60E-03	-1,212
Zfp28	zinc finger protein 28	5,80E-03	-1,212
Mov10	Moloney leukemia virus 10	1,79E-03	-1,214
Luc7l3	LUC7-like 3 (S. cerevisiae)	8,93E-03	-1,217
Fryl	furry homolog-like (Drosophila)	1,07E-03	-1,218
Ewsr1	Ewing sarcoma breakpoint region 1	4,29E-03	-1,219
Chd3	chromodomain helicase DNA binding protein 3	1,18E-03	-1,221
Zfp420	zinc finger protein 420	7,40E-03	-1,222
Zfp454	zinc finger protein 454	1,13E-03	-1,222
Zfp287	zinc finger protein 287	8,03E-03	-1,225
Zfp26	zinc finger protein 26	4,23E-03	-1,225
Basp1	brain abundant, membrane attached signal protein 1	3,89E-02	-1,227
Patz1	POZ (BTB) and AT hook containing zinc finger 1	2,25E-04	-1,228
Mcts2	malignant T cell amplified sequence 2	4,26E-02	-1,231
Rbm27	RNA binding motif protein 27	8,28E-06	-1,236
Gcfc1	GC-rich sequence DNA-binding factor 1	3,69E-04	-1,237
Tef	thyrotroph embryonic factor	1,57E-02	-1,240
Zfp264	zinc finger protein 264	4,34E-04	-1,240
Zfp300	zinc finger protein 300	6,05E-03	-1,243
Gm14420	predicted gene 14420	4,71E-02	-1,245
Zfp709	zinc finger protein 709	1,21E-02	-1,248
Zfp2	zinc finger protein 2	5,70E-04	-1,252
Gm4979	predicted gene 4979	6,18E-04	-1,252
Zfp788	zinc finger protein 788	1,45E-03	-1,254
Smarca1	SWI/SNF related, matrix associated, actin dependent regulator of chromatin, subfamily a, member 1	1,36E-02	-1,257
Ankrd12	ankyrin repeat domain 12	2,72E-03	-1,261
Chd6	chromodomain helicase DNA binding protein 6	3,68E-03	-1,262
Zfp595	zinc finger protein 595	4,50E-03	-1,267
Zfp467	zinc finger protein 467	2,83E-03	-1,272
Gm13051	predicted gene 13051	8,23E-04	-1,272
Zfp618	zinc fingerprotein 618	1,71E-03	-1,277
Zfp455	zinc finger protein 455	8,80E-04	-1,277
Ikzf4	IKAROS family zinc finger 4	7,82E-03	-1,281
Prpf39	PRP39 pre-mRNA processing factor 39 homolog (yeast)	6,03E-03	-1,282

Zfp72	zinc finger protein 72	5,92E-03	-1,284
Pou6f2	POU domain, class 6, transcription factor 2	3,51E-02	-1,287
Sp4	trans-acting transcription factor 4	2,75E-03	-1,294
Srsf7	serine/arginine-rich splicing factor 7	4,15E-05	-1,296
Zfp317	zinc finger protein 317	1,45E-03	-1,301
Clk1	CDC-like kinase 1	2,82E-02	-1,314
Zkscan16	zinc finger with KRAB and SCAN domains 16	1,43E-02	-1,324
Irx1	Iroquois related homeobox 1 (Drosophila)	1,56E-02	-1,330
Mll1	myeloid/lymphoid or mixed-lineage leukemia 1	5,64E-03	-1,342
Zbtb20	zinc finger and BTB domain containing 20	1,01E-03	-1,342
Camta1	calmodulin binding transcription activator 1	1,04E-05	-1,343
Klhl3	kelch-like 3 (Drosophila)	1,13E-03	-1,345
Etohi1	ethanol induced 1	2,19E-02	-1,361
Tra2a	transformer 2 alpha homolog (Drosophila)	4,98E-03	-1,362
Zfp583	zinc finger protein 583	5,82E-05	-1,389
Zfp398	zinc finger protein 398	2,48E-04	-1,394
Bhlhe41	basic helix-loop-helix family, member e41	1,61E-04	-1,395
Rcor2	REST corepressor 2	1,39E-03	-1,448
Gas5	growth arrest specific 5	9,65E-03	-1,460
Mamld1	mastermind-like domain containing 1	3,90E-04	-1,529
Dbp	D site albumin promoter binding protein	9,03E-03	-1,547
Zim1	zinc finger, imprinted 1	3,09E-04	-1,603
Msi1	Musashi homolog 1(Drosophila)	4,34E-04	-1,628
Protein synthesis/translation regulation/protein folding/endoplasmic reticulum stress			
Derl3	Der1-like domain family, member 3	1,00E-05	2,508
Kdelr3	KDEL (Lys-Asp-Glu-Leu) endoplasmic reticulum protein retention receptor 3	5,93E-05	2,387
Erp27	endoplasmic reticulum protein 27	4,94E-02	1,939
Fkbp11	FK506 binding protein 11	1,37E-05	1,549
Sec11c	SEC11 homolog C (S. cerevisiae)	6,27E-05	1,464
Dnajb11	DnaJ (Hsp40) homolog, subfamily B, member 11	4,64E-04	1,455
Spcs1	signal peptidase complex subunit 1 homolog	7,08E-04	1,436
Prkcsh	protein kinase C substrate 80K-H	5,53E-05	1,414
Qsox1	quiescin Q6 sulfhydryl oxidase 1	1,04E-04	1,410
Pdrg1	p53 and DNA damage regulated 1	1,03E-04	1,382
Mrps12	mitochondrial ribosomal protein S12	4,52E-04	1,350
Sel1l	sel-1 suppressor of lin-12-like (C. elegans)	1,61E-04	1,344
Edem2	ER degradation enhancer, mannosidase alpha-like 2	1,13E-04	1,341
Golm1	golgi membrane protein 1	2,27E-04	1,328
Ppib	peptidylprolyl isomerase B	3,02E-04	1,325
Pacrg	PARK2 co-regulated	1,24E-03	1,324
Syvn1	synovial apoptosis inhibitor 1, synoviolin	1,66E-03	1,318

Hars	histidyl-tRNA synthetase	5,41E-04	1,315
Edem1	ER degradation enhancer, mannosidase alpha-like 1	5,72E-05	1,314
Paip2b	poly(A) binding protein interacting protein 2B	9,30E-06	1,311
Tmem48	transmembrane protein 48	9,92E-03	1,307
Ppic	peptidylprolyl isomerase C	3,30E-02	1,303
Tor2a	torsin family 2, member A	1,93E-04	1,299
Hspb6	heat shock protein, alpha-crystallin-related, B6	1,18E-02	1,299
Nucb1	nucleobindin 1	2,11E-05	1,297
Pdia6	protein disulfide isomerase associated 6	1,81E-04	1,296
Dnajc3	DnaJ (Hsp40) homolog, subfamily C, member 3	3,54E-05	1,286
Os9	amplified in osteosarcoma	1,75E-05	1,280
Pdia4	protein disulfide isomerase associated 4	6,11E-03	1,264
Fkbp2	FK506 binding protein 2	3,99E-05	1,261
Ptrh1	peptidyl-tRNA hydrolase 1 homolog (S. cerevisiae)	4,25E-03	1,259
Yif1a	Yip1 interacting factor homolog A (S. cerevisiae)	4,18E-03	1,256
Eif3i	eukaryotic translation initiation factor 3, subunit I	1,57E-04	1,256
Selm	selenoprotein M	4,66E-04	1,255
Pdia5	protein disulfide isomerase associated 5	6,27E-05	1,253
Kars	lysyl-tRNA synthetase	1,74E-04	1,250
Prorsd1	prolyl-tRNA synthetase domain containing 1	7,90E-04	1,240
Ier3ip1	immediate early response 3 interacting protein 1	1,49E-04	1,240
Rps8	ribosomal protein S8	1,23E-03	1,236
Eef1g	eukaryotic translation elongation factor 1 gamma	3,36E-02	1,229
Qtrt1	queuine tRNA-ribosyltransferase 1	1,70E-04	1,228
Rps14	ribosomal protein S14	2,10E-03	1,227
H47	histocompatibility 47	1,62E-04	1,226
Arfgap3	ADP-ribosylation factor GTPase activating protein 3	1,18E-04	1,225
Eef2k	eukaryotic elongation factor-2 kinase	3,70E-03	1,225
Manf	mesencephalic astrocyte-derived neurotrophic factor	1,40E-03	1,223
Hbs1l	Hbs1-like (S. cerevisiae)	1,22E-04	1,223
Tyw1	tRNA-yW synthesizing protein 1 homolog (S. cerevisiae)	2,09E-05	1,219
Rps29	ribosomal protein S29	4,48E-04	1,219
Rplp1	ribosomal protein, large, P1	1,98E-03	1,219
Dnajc10	DnaJ (Hsp40) homolog, subfamily C, member 10	8,10E-04	1,217
BB287469	expressed sequence BB287469	2,73E-02	1,216
Rnf5	ring finger protein 5	6,20E-03	1,215
Ftsj1	FtsJ homolog 1 (E. coli)	2,86E-03	1,212
Sil1	endoplasmic reticulum chaperone SIL1 homolog (S. cerevisiae)	3,41E-04	1,212
Dars2	aspartyl-tRNA synthetase 2 (mitochondrial)	5,65E-04	1,209
Uba52	ubiquitin A-52 residue ribosomal protein fusion product 1	1,26E-04	1,207

Ssr3	signal sequence receptor, gamma	8,77E-05	1,207
Zc3h3	zinc finger CCCH type containing 3	1,14E-02	-1,219
Rpp25	ribonuclease P 25 subunit (human)	2,60E-02	-1,243
C1ql2	complement component 1, q subcomponent-like 2	1,51E-02	-1,304
Hspa12a	heat shock protein 12A	2,90E-03	-1,313
Rpl23a	ribosomal protein L23a	7,30E-04	-1,335
Macrod2	MACRO domain containing 2	7,77E-03	-1,363
Igf2bp2	insulin-like growth factor 2 mRNA binding protein 2	4,08E-05	-1,510
Ppil6	peptidylprolyl isomerase (cyclophilin)-like 6	3,34E-05	-1,779
Vesicle transport/Protein trafficking			
Rab18	RAB18, member RAS oncogene family	3,82E-03	1,511
Copz2	coatomer protein complex, subunit zeta 2	8,28E-06	1,491
Tmed3	transmembrane emp24 domain containing 3	1,02E-05	1,453
Sytl1	synaptotagmin-like 1	6,74E-04	1,408
Slc18a1	solute carrier family 18 (vesicular monoamine), member 1	4,75E-05	1,349
Mcfd2	multiple coagulation factor deficiency 2	2,74E-04	1,335
Sec16b	SEC16 homolog B (S. cerevisiae)	2,15E-04	1,319
Ssr4	signal sequence receptor, delta	1,71E-05	1,314
Srprb	signal recognition particle receptor, B subunit	1,22E-04	1,293
Rab26	RAB26, member RAS oncogene family	2,60E-04	1,292
Timm17b	translocase of inner mitochondrial membrane 17b	1,45E-03	1,285
Cpne4	copine IV	1,16E-02	1,272
Gorasp1	golgi reassembly stacking protein 1	3,02E-04	1,269
Bloc1s1	biogenesis of lysosome-related organelles complex-1, subunit 1	2,92E-04	1,255
Erp29	endoplasmic reticulum protein 29	2,43E-03	1,255
Nbas	neuroblastoma amplified sequence	9,86E-04	1,243
Scfd2	Sec1 family domain containing 2	7,89E-04	1,233
Rab39b	RAB39B, member RAS oncogene family	8,17E-03	1,232
Ubl4	ubiquitin-like 4	6,29E-05	1,229
Dnajc19	DnaJ (Hsp40) homolog, subfamily C, member 19	7,13E-03	1,218
Rrbp1	ribosome binding protein 1	7,05E-05	1,211
Tmed9	transmembrane emp24 protein transport domain containing 9	5,42E-04	1,206
Cog6	component of oligomeric golgi complex 6	1,67E-04	1,204
Bet1	blocked early in transport 1 homolog (S. cerevisiae)	9,45E-03	1,204
Kdelc1	KDEL (Lys-Asp-Glu-Leu) containing 1	7,11E-03	-1,205
Syt14	synaptotagmin XIV	5,16E-04	-1,210
Cabp7	calcium binding protein 7	8,05E-03	-1,223
Pclo	piccolo (presynaptic cytomatrix protein)	2,57E-02	-1,230
Stx11	syntaxin 11	2,96E-02	-1,264
Rab3b	RAB3B, member RAS oncogene family	1,42E-03	-1,331

Kalrn	kalirin, RhoGEF kinase	2,01E-04	-1,515
Posttranslational modification/ubiquination/glycosylation			
Ube2c	ubiquitin-conjugating enzyme E2C	1,76E-04	2,247
Zdhhc22	zinc finger, DHHC-type containing 22	7,74E-03	1,873
Otud7a	OTU domain containing 7A	4,17E-05	1,588
Trim59	tripartite motif-containing 59	1,45E-02	1,565
Man1a	mannosidase 1, alpha	2,80E-06	1,456
Mogs	mannosyl-oligosaccharide glucosidase	6,51E-04	1,432
Qpctl	glutaminyl-peptide cyclotransferase-like	8,28E-06	1,428
Gyltl1b	glycosyltransferase-like 1B	1,21E-03	1,372
Rnf215	ring finger protein 215	2,69E-05	1,363
Bard1	BRCA1 associated RING domain 1	2,15E-03	1,346
Gmppb	GDP-mannose pyrophosphorylase B	5,39E-03	1,336
Ube2t	ubiquitin-conjugating enzyme E2T (putative)	9,96E-04	1,302
Uba5	ubiquitin-like modifier activating enzyme 5	2,69E-04	1,301
Krtcap2	keratinocyte associated protein 2	1,01E-03	1,260
Rpn2	ribophorin II	8,28E-06	1,256
Trim68	tripartite motif-containing 68	4,42E-03	1,252
Asb9	ankyrin repeat and SOCS box-containing 9	1,55E-02	1,248
Dhdds	dehydrodolichyl diphosphate synthase	9,37E-04	1,236
Dpagt1	dolichyl-phosphate (UDP-N-acetylglucosamine) N-acetylglucosaminephosphotransferase 1 (GlcNAc-1-P transferase)	6,54E-03	1,221
Wdyhv1	WDYHV motif containing 1	2,02E-06	1,220
Dolk	dolichol kinase	5,01E-05	1,219
Neurl1B	neuralized homolog 1B (Drosophila)	2,06E-02	1,213
Aga	aspartylglucosaminidase	6,27E-05	1,209
Gpaa1	GPI anchor attachment protein 1	3,99E-03	1,208
Mpi	mannose phosphate isomerase	1,20E-03	1,208
Ube2s	ubiquitin-conjugating enzyme E2S	7,00E-04	1,205
Zdhhc23	zinc finger, DHHC domain containing 23	2,75E-02	-1,203
B3gnt8	UDP-GlcNAc:betaGal beta-1,3-N-acetylglucosaminyltransferase 8	8,77E-04	-1,204
Ttll3	tubulin tyrosine ligase-like family, member 3	3,35E-03	-1,205
March4	membrane-associated ring finger (C3HC4) 4	7,66E-04	-1,216
Ttll13	tubulin tyrosine ligase-like family, member 13	4,24E-03	-1,217
Setd2	SET domain containing 2	2,96E-03	-1,219
Rnf34	ring finger protein 34	2,04E-03	-1,224
Pdzrn4	PDZ domain containing RING finger 4	1,03E-02	-1,230
Unkl	unkempt-like (Drosophila)	6,25E-03	-1,230
Uba7	ubiquitin-like modifier activating enzyme 7	2,49E-04	-1,268
Rimklb	ribosomal modification protein rimK-like family member B	2,93E-03	-1,277

Rnf208	ring finger protein 208	1,44E-02	-1,292
Ube2ql1	ubiquitin-conjugating enzyme E2Q family-like 1	9,50E-04	-1,316
Mdm4	transformed mouse 3T3 cell double minute 4	2,82E-04	-1,323
Galnt13	UDP-N-acetyl-alpha-D-galactosamine: Polypeptide N-Acetylgalactosaminyltransferase 13	2,75E-03	-1,331
Galntl4	UDP-N-acetyl-alpha-D-galactosamine: Polypeptide N-Acetylgalactosaminyltransferase-Like 4	5,71E-03	-1,333
Galnt14	UDP-N-acetyl-alpha-D-galactosamine: Polypeptide N-Acetylgalactosaminyltransferase 14	1,92E-04	-1,361
Rbbp6	retinoblastoma binding protein 6	2,80E-06	-1,423
Proteosome/lysosome/autophagy/phagocytosis			
Wipi1	WD repeat domain, phosphoinositide interacting 1	4,17E-05	1,364
Tmem49	transmembrane protein 49	3,85E-04	1,334
Atg4a	autophagy-related 4A (yeast)	3,04E-05	1,286
Snca	synuclein, alpha	2,65E-03	1,276
Ctsh	cathepsin H	3,45E-03	1,254
Mfge8	milk fat globule-EGF factor 8 protein	2,96E-03	1,251
Elmo1	engulfment and cell motility 1, ced-12 homolog (C. elegans)	1,13E-04	1,244
Tmem9	transmembrane protein 9	1,06E-03	1,244
Sh3kbp1	SH3-domain kinase binding protein 1	3,80E-04	1,223
Ift88	intraflagellar transport 88 homolog (Chlamydomonas)	2,67E-03	-1,203
Mcoln3	mucolipin 3	4,30E-03	-1,498
Dnajc13	DnaJ (Hsp40) homolog, subfamily C, member 13	2,72E-03	-1,260
Peptidase/protease and related inhibitors			
Spink3	serine peptidase inhibitor, Kazal type 3	2,47E-02	2,874
Serpina7	serine (or cysteine) peptidase inhibitor, Clade A (Alpha-1 Antiproteinase, Antitrypsin), Member 7	1,54E-04	2,635
Prss1	protease, serine, 1 (trypsin 1)	3,46E-02	1,764
Cela3b	chymotrypsin-like elastase family, member 3B	2,36E-02	1,718
Serpinb1a	serine (or cysteine) peptidase inhibitor, clade B, member 1a	4,30E-02	1,557
Prss2	protease, serine, 2	4,05E-02	1,532
Pappa2	pappalysin 2	1,97E-03	1,460
Prss23	protease, serine, 23	3,73E-04	1,429
Serpini1	serine (or cysteine) peptidase inhibitor, clade I, member 1	1,54E-06	1,405
Pamr1	peptidase domain containing associated with muscle regeneration 1	1,73E-06	1,386
Ctrb1	chymotrypsinogen B1	1,90E-02	1,358
Tmprss4	transmembrane protease, serine 4	1,04E-03	1,344
Dpp3	dipeptidylpeptidase 3	8,03E-04	1,279
Serpinb8	serine (or cysteine) peptidase inhibitor, clade B, member 8	2,37E-03	1,267
Adamts9	a disintegrin-like and metallopeptidase (reprolysin type)	5,16E-03	1,264
Tmprss2	transmembrane protease, serine 2	3,96E-02	1,263

Prss8	protease, serine, 8 (prostasin)	4,47E-03	1,251
Spg7	spastic paraplegia 7 homolog (human)	2,05E-04	1,239
Cpa1	carboxypeptidase A1	4,49E-02	1,237
C1rl	complement component 1, r subcomponent-like	1,42E-02	1,231
Lxn	latexin	3,01E-02	1,224
Npepl1	aminopeptidase-like 1	2,51E-03	1,221
Timp3	tissue inhibitor of metalloproteinase 3	2,51E-02	1,215
Hgfac	hepatocyte growth factor activator	3,19E-03	1,213
Tasp1	taspase, threonine aspartase 1	1,57E-03	1,210
Tysnd1	trypsin domain containing 1	4,66E-03	1,207
Afg3l1	AFG3(ATPase family gene 3)-like 1 (yeast)	3,32E-03	1,202
Capn9	calpain 9	4,11E-02	-1,201
Serpind1	serine (or cysteine) peptidase inhibitor, clade D, (heparin cofactor), member 1	1,73E-02	-1,206
Uspl1	ubiquitin specific peptidase like 1	2,10E-02	-1,209
Adamts18	a disintegrin-like and metallopeptidase (reprolysin type 1, motif 18	1,85E-02	-1,220
Agbl4	ATP/GTP binding protein-like 4	1,94E-02	-1,222
Usp29	ubiquitin specific peptidase 29	1,08E-02	-1,228
Dpp6	dipeptidylpeptidase 6	7,50E-03	-1,246
Lonrf1	LON peptidase N-terminal domain and ring finger 1	9,53E-03	-1,269
Pcsk6	proprotein convertase subtilisin/kexin type 6	5,64E-03	-1,293
Cpm	carboxypeptidase M	4,79E-02	-1,363
Usp11	ubiquitin specific peptidase 11	1,64E-03	-1,418
Thsd4	thrombospondin, type I, domain containing 4	7,53E-04	-1,432
Reln	reelin	1,38E-03	-1,918
Cytoskeleton and related proteins			
Gas2l3	growth arrest-specific 2 like 3	1,68E-03	1,910
Frmd5	FERM domain containing 5	1,35E-04	1,636
Kif18b	kinesin family member 18B	3,96E-03	1,599
Diap3	diaphanous homolog 3 (Drosophila)	9,38E-04	1,428
Acta2	actin, alpha 2, smooth muscle, aorta	2,14E-02	1,375
Dnahc9	dynein, axonemal, heavy chain 9	5,50E-04	1,367
Kif14	kinesin family member 14	5,33E-03	1,352
Cd93	CD93 antigen	9,32E-04	1,326
AI428936	expressed sequence AI428936	4,00E-03	1,305
Pak3	p21 protein (Cdc42/Rac)-activated kinase 3	1,48E-04	1,294
Sepx1	selenoprotein X 1	1,38E-03	1,274
Pdlim1	PDZ and LIM domain 1 (elfin)	9,24E-03	1,254
Msn	moesin	3,69E-03	1,245
Smtn	smoothelin	1,45E-03	1,242
Trdn	triadin	5,50E-04	1,234

Iqsec2	IQ motif and Sec7 domain 2	1,54E-04	1,233
Osbpl3	oxysterol binding protein-like 3	5,07E-03	1,228
Csrp1	cysteine and glycine-rich protein 1	6,17E-03	1,216
Ckap4	cytoskeleton-associated protein 4	4,32E-03	1,209
Coro7	coronin 7	5,84E-03	1,208
Tmsb10	thymosin, beta 10	3,10E-02	1,200
Atxn7	ataxin 7	1,05E-03	-1,221
Ccdc141	coiled-coil domain containing 141	4,47E-02	-1,202
Cep350	centrosomal protein 350	1,88E-02	-1,205
Cnn3	calponin 3, acidic // 3 G1|3	1,81E-02	-1,248
Cobl	cordon-bleu	1,81E-03	-1,274
Dnahc2	dynein, axonemal, heavy chain 2	1,87E-04	-1,237
Dnalc1	Dnalc1	4,52E-04	-1,232
Dpysl2	dihydropyrimidinase-like 2	1,71E-03	-1,223
Edn3	endothelin 3	4,30E-03	-1,570
Eml5	echinoderm microtubule associated protein like 5	3,05E-02	-1,231
Epb4.1	erythrocyte protein band 4.1	1,70E-03	-1,207
Epb4.1l3	erythrocyte protein band 4.1-like 3	8,12E-04	-1,247
Epb4.1l4a	erythrocyte protein band 4.1-like 4a	1,02E-03	-1,571
Epb4.9	erythrocyte protein band 4.9	2,72E-03	-1,207
Ezr	ezrin	4,03E-04	-1,227
Fmn2	formin 2	4,19E-04	-1,253
Kif5a	kinesin family member 5A	3,87E-03	-1,239
Kifc3	kinesin family member C3	1,93E-04	-1,243
Mtap2	microtubule-associated protein 2	5,33E-04	-1,208
Mtss1	metastasis suppressor 1	1,77E-04	-1,275
Myo3a	myosin IIIA	8,05E-05	-1,646
Myo9a	myosin Ixa	2,02E-03	-1,501
Ppp1r12b	protein phosphatase 1, regulatory (inhibitor) subunit 12B	1,29E-02	-1,216
Scin	scinderin	1,43E-03	-1,224
Sgce	sarcoglycan, epsilon	4,38E-03	-1,386
Sntg1	syntrophin, gamma 1	1,68E-02	-1,213
Syne2	synaptic nuclear envelope 2	4,18E-02	-1,325
Tenc1	tensin like C1 domain-containing phosphatase	3,72E-03	-1,211
Thsd7a	thrombospondin, type I, domain containing 7A	8,71E-03	-1,246
Tmsb15l	thymosin beta 15b like	1,62E-03	-1,415
Tnik	TRAF2 and NCK interacting kinase	1,12E-03	-1,352
Tppp3	tubulin polymerization-promoting protein family member 3	2,47E-03	-1,530
Tubb3	tubulin, beta 3	2,21E-02	-1,234
Wipf2	WAS/WASL interacting protein family, member 2	8,12E-04	-1,209

Channels and transporters			
Ttyh1	tweety homolog 1 (Drosophila)	4,03E-04	2,143
Slc2a6	solute carrier family 2 (facilitated glucose transporter), member 6	3,50E-05	2,142
Slc17a9	solute carrier family 17, member 9	6,14E-05	1,929
Cngb3	cyclic nucleotide gated channel beta 3	3,92E-05	1,833
Slc38a10	solute carrier family 38, member 10	5,75E-05	1,728
Rhd	Rh blood group, D antigen	8,15E-05	1,703
Car4	carbonic anhydrase 4	1,02E-04	1,694
Slco1a5	solute carrier organic anion transporter family, member 5	1,01E-02	1,660
Abcb6	ATP-binding cassette, sub-family B (MDR/TAP), member 6	1,37E-05	1,624
Trpc4	transient receptor potential cation channel, subfamily C, member 4	1,37E-04	1,624
Rbp7	retinol binding protein 7, cellular	1,36E-04	1,561
Slc39a11	solute carrier family 39 (metal ion transporter), member 11	4,37E-04	1,521
Kcnab3	potassium voltage-gated channel, shaker-related subfamily	2,17E-04	1,472
Kcnk10	potassium channel, subfamily K, member 10	4,18E-04	1,448
Slc4a10	solute carrier family 4, sodium bicarbonate cotransporter, member 10	7,30E-06	1,420
Slc26a2	solute carrier family 26 (sulfate transporter), member 2	1,43E-04	1,411
Kcnh1	potassium voltage-gated channel, subfamily H (eag-related)	6,35E-04	1,396
Slc46a1	solute carrier family 46, member 1	1,45E-04	1,392
Kcnip2	Kv channel-interacting protein 2	3,99E-03	1,390
Cacng3	calcium channel, voltage-dependent, gamma subunit 3	2,49E-03	1,383
Slc1a5	solute carrier family 1 (neutral amino acid transporter), member 5	1,06E-02	1,378
Pex5l	peroxisomal biogenesis factor 5-like	6,39E-05	1,371
Abcc9	ATP-binding cassette, sub-family C (CFTR/MRP), member 9	1,70E-03	1,346
Slc35c2	solute carrier family 35, member C2	2,43E-05	1,336
Tomm40l	translocase of outer mitochondrial membrane 40 homolog (yeast)-like	2,24E-05	1,321
Kcnk1	potassium channel, subfamily K, member 1	9,14E-05	1,313
Slc35f4	solute carrier family 35, member F4	3,69E-03	1,311
Slc35b1	solute carrier family 35, member B1	6,27E-05	1,301
Slco1a6	solute carrier organic anion transporter family, member 6	4,82E-02	1,294
Atp13a2	ATPase type 13A2	4,75E-05	1,288
Slc39a10	solute carrier family 39 (zinc transporter), member 10	7,10E-05	1,288
Slc12a2	solute carrier family 12, member 2	4,18E-04	1,278
Slc39a13	solute carrier family 39 (metal ion transporter), member 13	6,29E-04	1,276
Slc6a9	solute carrier family 6 (neurotransmitter transporter,	2,94E-02	1,274

	glycine), member 9		
Abca4	ATP-binding cassette, sub-family A (ABC1), member 4	1,38E-03	1,272
Slc31a1	solute carrier family 31, member 1	2,84E-04	1,264
Tmc6	transmembrane channel-like gene family 6	1,31E-03	1,263
Kcnk6	potassium inwardly-rectifying channel, subfamily K, member 6	9,04E-03	1,262
Slc25a10	solute carrier family 25 (mitochondrial carrier; dicarboxylate transporter), member 10	7,72E-04	1,259
Atp6v0e2	ATPase, H+ transporting, lysosomal V0 subunit E2	1,84E-04	1,257
Slc12a4	solute carrier family 12, member 4	7,83E-05	1,248
Slc22a2	solute carrier family 22 (organic cation transporter), member 2	1,03E-03	1,246
Ano1	anoctamin 1, calcium activated chloride channel	2,20E-02	1,245
Slc35f1	solute carrier family 35, member F1	4,79E-04	1,243
Slc39a7	solute carrier family 39 (zinc transporter), member 7	1,24E-03	1,233
Slc30a7	solute carrier family 30 (zinc transporter), member 7	4,52E-04	1,231
Slc7a4	solute carrier family 7 (cationic amino acid transporter), member 4	6,96E-03	1,226
Slc29a3	solute carrier family 29 (nucleoside transporters), member 3	9,56E-04	1,224
Slc41a2	solute carrier family 41, member 2	5,30E-03	1,223
Kcnk13	potassium channel, subfamily K, member 13	2,80E-02	1,219
Slc27a4	solute carrier family 27 (fatty acid transporter), member 4	1,35E-04	1,211
Ipo4	importin 4	7,08E-04	1,210
Slc2a13	solute carrier family 2 (facilitated glucose transporter), member 13	7,26E-03	1,209
Rag1ap1	recombination activating gene 1 activating protein 1	1,32E-03	1,204
Slc7a1	solute carrier family 7 (cationic amino acid transporter), member 1	1,81E-02	1,202
Slc6a17	solute carrier family 6 (neurotransmitter transporter), member 17	3,58E-04	1,200
Slc41a1	solute carrier family 41, member 1	1,64E-03	1,200
Sfxn4	sideroflexin 4	7,85E-03	-1,209
Unc80	unc-80 homolog (C. elegans)	7,44E-03	-1,210
Atp1b2	ATPase, Na+/K+ transporting, beta 2 polypeptide	3,03E-03	-1,212
Cacna2d2	calcium channel, voltage-dependent, alpha 2/delta subunit	4,40E-03	-1,216
Kcna1	potassium voltage-gated channel, shaker-related subfamily, member 1	4,36E-02	-1,216
Tmed8	transmembrane emp24 domain containing 8	3,54E-03	-1,218
Slc44a1	solute carrier family 44, member 1	7,52E-04	-1,220
Tmem30b	transmembrane protein 30B	9,38E-04	-1,221
Cacna1c	calcium channel, voltage-dependent, L type, alpha 1C	1,01E-02	-1,222
Rangrf	RAN guanine nucleotide release factor	1,20E-02	-1,222
Atp8a2	ATPase, aminophospholipid transporter-like, class I, type 8A, member 2	1,81E-02	-1,224

Aqp4	aquaporin 4	5,35E-03	-1,225
Slc12a6	solute carrier family 12, member 6	2,15E-02	-1,226
Kpna3	karyopherin (importin) alpha 3	9,03E-06	-1,226
Cacna1a	calcium channel, voltage-dependent, P/Q type, alpha 1A subunit	3,34E-03	-1,228
Slc16a7	solute carrier family 16 (monocarboxylic acid transporters), member 7	2,35E-02	-1,242
Kcnk3	potassium channel, subfamily K, member 3	4,94E-04	-1,246
Abca8b	ATP-binding cassette, sub-family A (ABC1), member 8b	2,21E-02	-1,247
Scnn1a	sodium channel, nonvoltage-gated 1 alpha	3,34E-02	-1,250
Gpm6a	glycoprotein m6a	3,56E-02	-1,260
Syngr3	synaptogyrin 3	3,22E-03	-1,264
Atp7a	ATPase, Cu++ transporting, alpha polypeptide	8,86E-04	-1,279
Cacng4	calcium channel, voltage-dependent, gamma subunit 4	4,38E-02	-1,287
Ap1s2	adaptor-related protein complex 1, sigma 2 subunit	9,44E-03	-1,314
Psd	pleckstrin and Sec7 domain containing	1,35E-03	-1,314
Trpm5	transient receptor potential cation channel, subfamily M, member 5	2,06E-03	-1,338
Slc7a2	solute carrier family 7 (cationic amino acid transporter, Y+ System),Member 2	9,34E-04	-1,351
Kcnj3	potassium inwardly-rectifying channel, subfamily J, member 3	1,26E-02	-1,371
Sv2b	synaptic vesicle glycoprotein 2 b	1,39E-03	-1,395
Nlgn2	neuroligin 2	5,80E-05	-1,396
Jph3	junctophilin 3	2,05E-04	-1,406
Kcnj12	potassium inwardly-rectifying channel, subfamily J, member 12	5,51E-03	-1,409
Kcng3	potassium voltage-gated channel, subfamily G, member 3	2,67E-03	-1,415
Slc29a4	solute carrier family 29 (nucleoside transporters), member 4	4,75E-05	-1,450
Hhatl	hedgehog acyltransferase-like	4,24E-04	-1,456
Slc30a1	solute carrier family 30 (zinc transporter), member 1	5,35E-04	-1,464
Tmem106a	transmembrane protein 106A	6,52E-05	-1,485
Mt1	metallothionein 1	1,70E-04	-1,689
Aqp7	aquaporin 7	1,12E-04	-1,775
Hormones/growth factors/receptors/neuropeptides and exocytosis			
Mc5r	melanocortin 5 receptor	1,49E-03	2,629
Gabra4	gamma-aminobutyric acid (GABA) A receptor, subunit alpha	1,52E-04	2,479
Tnfrsf23	tumor necrosis factor receptor superfamily, member 23	3,52E-04	1,937
Sycn	syncollin	1,32E-02	1,781
Inhba	inhibin beta-A	6,49E-06	1,709
Tgfb3	transforming growth factor, beta 3	2,55E-05	1,553
Egf	epidermal growth factor	7,13E-06	1,533

Nucb2	nucleobindin 2	6,08E-06	1,525
Rab3d	RAB3D, member RAS oncogene family	2,47E-06	1,469
Oxtr	oxytocin receptor	8,43E-03	1,435
Ldlrad3	low density lipoprotein receptor class A domain containing 3	5,01E-03	1,382
Stc1	stanniocalcin 1	4,62E-03	1,381
Gabbr2	gamma-aminobutyric acid (GABA) B receptor, 2	2,68E-06	1,340
Ffar2	free fatty acid receptor 2	1,31E-02	1,333
Cadps2	Ca2+-dependent activator protein for secretion 2	6,52E-05	1,319
Olfr558	olfactory receptor 558	1,29E-02	1,319
Sidt2	SID1 transmembrane family, member 2	7,46E-06	1,318
Ednrb	endothelin receptor type B	6,12E-03	1,316
Vgf	VGF nerve growth factor inducible	6,67E-04	1,296
Gprc5b	G protein-coupled receptor, family C, group 5, member B	9,43E-03	1,293
Olfr115	olfactory receptor 115	4,33E-03	1,276
Gabrq	gamma-aminobutyric acid (GABA) A receptor, subunit theta	3,36E-03	1,269
Gpr180	G protein-coupled receptor 180	7,45E-06	1,265
Olfr1015	olfactory receptor 1015	3,85E-02	1,255
Olfr857	olfactory receptor 857	2,11E-02	1,245
Ror1	receptor tyrosine kinase-like orphan receptor 1	3,61E-02	1,236
Olfr203	olfactory receptor 203	1,29E-02	1,236
Ros1	Ros1 proto-oncogene	1,51E-02	1,234
Olfr804	olfactory receptor 804	5,44E-04	1,234
Ednra	endothelin receptor type A	4,94E-02	1,233
Olfr1295	olfactory receptor 1295	5,94E-03	1,229
Olfr174	olfactory receptor 174	4,64E-04	1,219
Olfr361	olfactory receptor 361	1,12E-03	1,219
Lin7a	lin-7 homolog A (C. elegans)	2,61E-02	1,215
Pdgfrb	platelet derived growth factor receptor, beta polypeptide	1,63E-02	1,212
Vegfc	vascular endothelial growth factor C	8,40E-04	1,210
Shank1	SH3/ankyrin domain gene 1	1,64E-04	-1,209
Trpm2	transient receptor potential cation channel, subfamily M, member 2	2,23E-02	-1,210
Fgfr4	fibroblast growth factor receptor 4	1,88E-03	-1,210
Rara	retinoic acid receptor, alpha	7,30E-03	-1,213
Stxbp3a	syntaxin binding protein 3A	3,48E-03	-1,219
Maob	monoamine oxidase B	1,07E-03	-1,226
Ephb2	Eph receptor B2	2,38E-03	-1,226
Olfr814	olfactory receptor 814	6,51E-04	-1,237
Avpr1b	arginine vasopressin receptor 1B	6,32E-03	-1,239
Tmem123	transmembrane protein 123	6,08E-06	-1,245

Fgf14	fibroblast growth factor 14	2,60E-03	-1,250
Tfrc	transferrin receptor	1,00E-02	-1,250
Sorcs2	sortilin-related VPS10 domain containing receptor 2	4,10E-03	-1,251
Hgf	hepatocyte growth factor	1,74E-02	-1,252
Grik5	glutamate receptor, ionotropic, kainate 5 (gamma 2)	1,76E-04	-1,256
Grin2c	glutamate receptor, ionotropic, NMDA2C (epsilon 3)	3,47E-02	-1,258
Cacna1b	calcium channel, voltage-dependent, N type, alpha 1B	9,19E-03	-1,271
S1pr2	sphingosine-1-phosphate receptor 2	6,68E-03	-1,276
Cd79a	CD79A antigen (immunoglobulin-associated alpha)	4,68E-03	-1,285
Rnf213	ring finger protein 213	1,69E-02	-1,290
Sorcs1	VPS10 domain receptor protein SORCS 1	9,54E-04	-1,304
Mrap2	melanocortin 2 receptor accessory protein 2	1,25E-02	-1,326
Gpr137b	G protein-coupled receptor 137B	1,31E-03	-1,361
Rab3c	RAB3C, member RAS oncogene family	9,19E-05	-1,372
Gria2	glutamate receptor, ionotropic, AMPA2 (alpha 2)	5,35E-03	-1,375
Tac1	tachykinin 1	4,59E-02	-1,376
Olfm2	olfactomedin 2	6,08E-06	-1,417
Gipr	gastric inhibitory polypeptide receptor	4,04E-03	-1,437
Gria3	glutamate receptor, ionotropic, AMPA3 (alpha 3)	8,85E-04	-1,459
Ghrl	ghrelin	2,85E-02	-1,469
Sult1c2	sulfotransferase family, cytosolic, 1C, member 2	6,65E-03	-1,477
Cntfr	ciliary neurotrophic factor receptor	2,41E-04	-1,541
Glra1	glycine receptor, alpha 1 subunit	2,71E-03	-1,557
Itpr1	inositol 1,4,5-triphosphate receptor 1	9,01E-04	-1,621
Agt	angiotensinogen (serpin peptidase inhibitor, clade A, member 8)	1,01E-03	-1,661
Chrna4	cholinergic receptor, nicotinic, alpha polypeptide 4	1,06E-05	-1,766
Olfr1322	olfactory receptor 1322	2,51E-02	-2,026
Stxbp5l	syntaxin binding protein 5-like	8,28E-06	-2,098
Signal transduction			
C1qtnf1	C1q and tumor necrosis factor related protein 1	2,16E-03	1,751
Cthrc1	collagen triple helix repeat containing 1	9,39E-05	1,746
Apcdd1	adenomatosis polyposis coli down-regulated 1	2,42E-04	1,485
Shcbp1	Shc SH2-domain binding protein 1	6,54E-03	1,422
Tspan6	tetraspanin 6	8,04E-04	1,409
Clps	colipase, pancreatic	3,23E-02	1,409
Cdk18	cyclin-dependent kinase 18	1,54E-04	1,367
Mctp1	multiple C2 domains, transmembrane 1	2,79E-02	1,352
Cyb561	cytochrome b-561	2,05E-04	1,350
Ell2	elongation factor RNA polymerase II 2	1,02E-05	1,290
Steap4	STEAP family member 4	8,24E-03	1,279
Taar1	trace amine-associated receptor 1	4,52E-04	1,273

Tspan15	tetraspanin 15	5,58E-03	1,257
Taar4	trace amine-associated receptor 4	2,30E-02	1,256
Rgs5	regulator of G-protein signaling 5	1,79E-03	1,254
Gpr135	G protein-coupled receptor 135	2,50E-02	1,230
Gna14	guanine nucleotide binding protein, alpha 14	2,51E-03	1,228
Igfbp3	insulin-like growth factor binding protein 3	1,33E-02	1,228
Dusp6	dual specificity phosphatase 6	4,91E-02	1,218
Pcp4	Purkinje cell protein 4	4,54E-03	1,212
Rasa3	RAS p21 protein activator 3	3,39E-02	1,209
Crb1	crumbs homolog 1 (Drosophila)	1,85E-03	1,208
Ms4a7	membrane-spanning 4-domains, subfamily A, member 7	1,95E-02	1,203
Tbl3	transducin (beta)-like 3	2,20E-02	1,200
Axin2	axin2	2,93E-02	-1,200
Dos	downstream of Stk11	2,89E-03	-1,203
Strn	striatin, calmodulin binding protein	1,55E-02	-1,205
Cdon	cell adhesion molecule-related/down-regulated by oncogenes	5,13E-03	-1,205
Bid	BH3 interacting domain death agonist	1,05E-02	-1,207
Il6st	interleukin 6 signal transducer	2,79E-03	-1,207
Gabbr1	gamma-aminobutyric acid (GABA) B receptor, 1	1,04E-02	-1,208
Cntnap1	contactin associated protein-like 1	9,37E-05	-1,209
Notch1	Notch gene homolog 1 (Drosophila)	1,92E-03	-1,211
Dnaja1	DnaJ (Hsp40) homolog, subfamily A, member 1	2,05E-02	-1,220
Arhgef9	CDC42 guanine nucleotide exchange factor (GEF) 9	2,22E-02	-1,223
Dusp10	dual specificity phosphatase 10	4,76E-03	-1,227
Adrbk2	adrenergic receptor kinase, beta 2	8,72E-03	-1,233
Inpp5e	inositol polyphosphate-5-phosphatase E	7,10E-03	-1,236
Sema3e	sema domain, immunoglobulin domain (Ig), short basic Domain, Secreted,(Semaphorin) 3E	6,78E-03	-1,239
Gpr21	G protein-coupled receptor 21	3,58E-02	-1,242
Magi2	membrane associated guanylate kinase, WW and PDZ domain	2,00E-02	-1,249
Gpr179	G protein-coupled receptor 179	2,31E-03	-1,255
Fam126a	family with sequence similarity 126, member A	3,00E-04	-1,265
Odz2	odd Oz/ten-m homolog 2 (Drosophila)	4,08E-03	-1,284
Lrp1	low density lipoprotein receptor-related protein 1	2,85E-02	-1,293
Dact1	dapper homolog 1, antagonist of beta-catenin (xenopus)	2,10E-02	-1,306
Crhr1	corticotropin releasing hormone receptor 1	9,42E-03	-1,307
Pik3c2g	phosphatidylinositol 3-kinase, C2 domain containing, gamma	2,96E-02	-1,308
Arhgap5	Rho GTPase activating protein 5	1,25E-03	-1,311
Lpp	LIM domain containing preferred translocation partner in lipoma	1,07E-03	-1,314
Mapk15	mitogen-activated protein kinase 15	3,37E-03	-1,321

Gprc5c	G protein-coupled receptor, family C, group 5, member C	7,00E-03	-1,335
Baiap3	BAI1-associated protein 3	7,78E-03	-1,358
Gpr98	G protein-coupled receptor 98	3,09E-03	-1,373
Psd4	pleckstrin and Sec7 domain containing 4	3,37E-03	-1,417
Gpr75	G protein-coupled receptor 75	1,01E-03	-1,422
Nrcam	neuron-glia-CAM-related cell adhesion molecule	1,36E-02	-1,425
Sfrp5	secreted frizzled-related sequence protein 5	9,32E-04	-1,455
Dpp10	dipeptidylpeptidase 10	7,62E-04	-1,629
Npy	neuropeptide Y	6,97E-05	-2,110
AMPK and mTOR pathways			
Ppargc1a	peroxisome proliferative activated receptor, gamma, coactivator 1 alpha	1,09E-03	1,612
Akt1s1	AKT1 substrate 1 (proline-rich)	2,17E-04	1,316
Akt3	thymoma viral proto-oncogene 3	4,09E-04	-1,208
Prkab2	protein kinase, AMP-activated, beta 2 non-catalytic subunit	4,66E-03	-1,226
Rps6ka5	ribosomal protein S6 kinase, polypeptide 5	2,93E-02	-1,237
Rictor	RPTOR independent companion of MTOR, complex 2	1,09E-03	-1,266
Pten	phosphatase and tensin homolog	3,81E-02	-1,411
Nptx1	neuronal pentraxin 1	1,38E-03	-1,430
Insulin signaling pathway			
Shc4	SHC (Src homology 2 domain containing) family, member 4	2,68E-04	1,514
Dok5	docking protein 5	1,91E-03	1,306
Doc2b	double C2, beta	1,40E-02	-1,245
Grb10	growth factor receptor bound protein 10	6,83E-03	-1,250
Shc2	SHC (Src homology 2 domain containing) transforming prot	1,90E-03	-1,284
Srsf3	arginine-rich splicing factor 3	1,07E-03	-1,421
Nnat	neuronatin	9,36E-04	-1,530
Igfbp5	insulin-like growth factor binding protein 5	2,08E-04	-1,608
GTPase activity and regulation			
Depdc1a	DEP domain containing 1a	1,38E-03	1,874
Arhgap11a	Rho GTPase activating protein 11A	1,09E-03	1,831
Arhgdig	Rho GDP dissociation inhibitor (GDI) gamma	5,34E-05	1,622
Rasd2	RASD family, member 2	2,59E-03	1,477
Rasgrf2	RAS protein-specific guanine nucleotide-releasing factor	3,00E-04	1,472
Arhgef19	Rho guanine nucleotide exchange factor (GEF) 19	5,44E-03	1,468
Ralgapa2	Ral GTPase activating protein, alpha subunit 2 (catalytic)	3,73E-06	1,447
Arhgap19	Rho GTPase activating protein 19	1,27E-02	1,439
Rapgef5	Rap guanine nucleotide exchange factor (GEF) 5	3,60E-03	1,377
Iqgap3	IQ motif containing GTPase activating protein 3	3,27E-02	1,343

Dennd2d	DENN/MADD domain containing 2D	7,97E-05	1,285
Arhgef37	Rho guanine nucleotide exchange factor (GEF) 37	3,74E-03	1,269
Limk1	LIM-domain containing, protein kinase	1,63E-03	1,264
Vav3	vav 3 oncogene	4,89E-04	1,239
Arhgap18	Rho GTPase activating protein 18	7,02E-04	1,227
Rhoc	ras homolog gene family, member C	6,76E-03	1,211
Gng12	guanine nucleotide binding protein (G protein), gamma 1	1,22E-02	1,202
Rasgrf1	RAS protein-specific guanine nucleotide-releasing factor	4,91E-02	-1,200
Rreb1	ras responsive element binding protein 1	8,01E-04	-1,200
Dab2ip	disabled homolog 2 (Drosophila) interacting protein	1,82E-04	-1,209
Dennd4c	DENN/MADD domain containing 4C	7,51E-03	-1,217
Gmip	Gem-interacting protein	2,05E-04	-1,219
Radil	Ras association and DIL domains	2,81E-03	-1,220
Srgap3	SLIT-ROBO Rho GTPase activating protein 3	9,03E-04	-1,223
Sept3	septin 3	4,05E-03	-1,225
Tbc1d2b	TBC1 domain family, member 2B	2,27E-03	-1,225
Rem2	rad and gem related GTP binding protein 2	3,56E-02	-1,239
Rragb	Ras-related GTP binding B	7,44E-04	-1,241
Spata13	spermatogenesis associated 13	2,83E-02	-1,242
Agap2	ArfGAP with GTPase domain, ankyrin repeat and PH domain	1,72E-02	-1,245
Psd3	pleckstrin and Sec7 domain containing 3	1,16E-02	-1,253
Rasgef1a	RasGEF domain family, member 1A	5,61E-03	-1,289
Rab12	RAB12, member RAS oncogene family	7,66E-04	-1,321
Dock6	dedicator of cytokinesis 6	2,44E-03	-1,329
Rit2	Ras-like without CAAX 2	6,25E-03	-1,368
Srgap1	SLIT-ROBO Rho GTPase activating protein 1	2,03E-03	-1,405
Mlph	melanophilin	1,10E-03	-1,488
Kinases/phosphatases and related proteins			
Pbk	PDZ binding kinase	8,40E-04	2,426
Akap6	A kinase (PRKA) anchor protein 6	2,02E-06	1,993
Dusp23	dual specificity phosphatase 23	6,67E-05	1,436
Ckmt1	creatine kinase, mitochondrial 1, ubiquitous	8,00E-06	1,373
Mapkapk3	mitogen-activated protein kinase-activated protein kinase	7,22E-04	1,347
Pi4k2b	phosphatidylinositol 4-kinase type 2 beta	4,36E-04	1,287
Dak	dihydroxyacetone kinase 2 homolog (yeast)	5,69E-05	1,284
Ppapdc3	phosphatidic acid phosphatase type 2 domain containing 3	2,38E-03	1,260
Ak3	adenylate kinase 3	8,28E-06	1,259
Stk32b	serine/threonine kinase 32B	2,31E-02	1,246
Met	met proto-oncogene	8,36E-03	1,243

Mtmr11	myotubularin related protein 11	1,01E-03	1,238
Ppp2r3c	protein phosphatase 2, regulatory subunit B", gamma	8,29E-04	1,227
Lrrc67	leucine rich repeat containing 67	1,61E-02	1,223
Tek	endothelial-specific receptor tyrosine kinase	2,27E-02	1,216
Ibtk	inhibitor of Bruton agammaglobulinemia tyrosine kinase	2,05E-03	1,209
Camk1d	calcium/calmodulin-dependent protein kinase ID	3,06E-02	1,208
Prkce	protein kinase C, epsilon	5,35E-04	-1,202
Agphd1	aminoglycoside phosphotransferase domain containing 1	2,08E-02	-1,203
Pank1	pantothenate kinase 1	1,54E-02	-1,209
Ulk4	unc-51-like kinase 4 (C. elegans)	1,55E-03	-1,218
Inpp4a	inositol polyphosphate-4-phosphatase, type I	5,94E-03	-1,235
Phlpp2	PH domain and leucine rich repeat protein phosphatase	2,17E-04	-1,238
Dusp18	dual specificity phosphatase 18	2,86E-03	-1,240
Camk4	calcium/calmodulin-dependent protein kinase IV	2,80E-03	-1,241
Rad54l2	RAD54 like 2 (S. cerevisiae)	5,26E-03	-1,244
Cdkl1	cyclin-dependent kinase-like 1 (CDC2-related kinase)	5,64E-03	-1,257
Itpkb	inositol 1,4,5-trisphosphate 3-kinase B	3,67E-04	-1,269
Ccnl1	cyclin L1	1,40E-04	-1,275
Dmpk	dystrophia myotonica-protein kinase	9,84E-04	-1,277
Dbn1	drebrin 1	7,62E-04	-1,286
Ppp2r2b	protein phosphatase 2 (formerly 2A), regulatory subunit	1,21E-04	-1,288
Ptprd	protein tyrosine phosphatase, receptor type, D	2,83E-02	-1,291
Wnk1	WNK lysine deficient protein kinase 1	2,82E-02	-1,421
Nudt11	nudix (nucleoside diphosphate linked moiety X)-type motif 11	4,30E-03	-1,423
Ncs1	neuronal calcium sensor 1	4,23E-04	-1,465
Upp1	uridine phosphorylase 1	4,36E-05	-1,517
Mast1	microtubule associated serine/threonine kinase 1	2,65E-04	-1,587
Cell-cell signaling			
Hmmr	hyaluronan mediated motility receptor (RHAMM)	2,84E-04	2,501
Vipr2	vasoactive intestinal peptide receptor 2	2,04E-03	1,215
Dll1	delta-like 1 (Drosophila)	6,45E-04	-1,343
Extracellular matrix/collagen formation			
Leprel1	leprecan-like 1	2,22E-04	2,021
F13a1	coagulation factor XIII, A1 subunit	2,88E-06	1,861
Sgcd	sarcoglycan, delta (dystrophin-associated glycoprotein)	1,12E-04	1,608
Smoc1	SPARC related modular calcium binding 1	1,57E-04	1,566
Hapln4	hyaluronan and proteoglycan link protein 4	4,48E-05	1,519
Spon2	spondin 2, extracellular matrix protein	1,41E-03	1,497
Frem2	Fras1 related extracellular matrix protein 2	2,89E-05	1,493
Lepre1	leprecan 1	8,77E-04	1,339

Naglu	alpha-N-acetylglucosaminidase (Sanfilippo disease IIIB)	2,27E-04	1,327
Lama5	laminin, alpha 5	4,06E-03	1,269
Plod3	procollagen-lysine, 2-oxoglutarate 5-dioxygenase 3	2,55E-04	1,244
P4ha2	Prolyl 4-Hydroxylase, Alpha Polypeptide II	1,69E-02	1,210
Col6a6	collagen, type VI, alpha 6	3,57E-02	-1,232
Ltbp1	latent transforming growth factor beta binding protein 1	1,99E-03	-1,271
Mfap1a	microfibrillar-associated protein 1A	1,35E-04	-1,290
Egflam	EGF-like, fibronectin type III and laminin G domains	5,58E-04	-1,472
Chemokines/cytokines/adhesion molecules/innate immunity and related proteins			
Cd44	CD44 antigen	8,28E-06	1,729
Susd2	sushi domain containing 2	8,77E-05	1,638
Tubb6	tubulin, beta 6	8,08E-03	1,547
Emilin1	elastin microfibril interfacer 1	8,13E-05	1,533
Troap	trophinin associated protein	8,25E-04	1,495
Thbs1	thrombospondin 1	1,44E-02	1,466
Il1r2	interleukin 1 receptor, type II	3,81E-03	1,450
Cldn1	claudin 1	2,72E-04	1,421
Pcdh18	protocadherin 18	4,19E-03	1,419
Nid2	nidogen 2	8,99E-05	1,407
Otoa	otoancorin	1,64E-03	1,390
Clec14a	C-type lectin domain family 14, member a	6,48E-04	1,382
Vstm2a	V-set and transmembrane domain containing 2A	5,39E-04	1,365
Fam19a1	family with sequence similarity 19, member A1	4,25E-03	1,335
Cd34	CD34 antigen	1,68E-03	1,335
Igsf5	immunoglobulin superfamily, member 5	1,05E-03	1,335
Gja1	gap junction protein, alpha 1	2,77E-02	1,329
Jam2	junction adhesion molecule 2	1,81E-04	1,325
Muc4	mucin 4	4,89E-04	1,324
Cldn3	claudin 3	9,94E-04	1,290
Eng	endoglin	7,52E-04	1,280
Gucy1b3	guanylate cyclase 1, soluble, beta 3	2,12E-03	1,275
Mif	macrophage migration inhibitory factor	4,68E-03	1,272
Lama4	laminin, alpha 4	1,11E-02	1,266
Amigo3	adhesion molecule with Ig like domain 3	6,81E-03	1,263
Lgals9	lectin, galactose binding, soluble 9	2,96E-02	1,259
Rpsa	ribosomal protein SA	3,94E-05	1,257
Cd200	CD200 antigen	3,02E-04	1,251
Gp5	glycoprotein 5 (platelet)	3,37E-03	1,249
Clec1a	C-type lectin domain family 1, member a	4,00E-02	1,246
Lpar1	lysophosphatidic acid receptor 1	3,03E-03	1,245
Dsc2	desmocollin 2	3,97E-03	1,233

Crlf1	cytokine receptor-like factor 1	4,03E-03	1,226
Crisp2	cysteine-rich secretory protein 2	6,64E-03	1,222
Dock4	dedicator of cytokinesis 4	2,77E-02	1,218
Crlf2	cytokine receptor-like factor 2	5,30E-03	1,217
Actr1b	ARP1 actin-related protein 1 homolog B, centractin beta (Yeast)	8,12E-04	1,210
Igsf11	immunoglobulin superfamily, member 11	8,04E-03	1,206
Ccrl2	chemokine (C-C motif) receptor-like 2	1,85E-02	1,205
Tjp2	tight junction protein 2	1,57E-03	-1,204
Zfr2	zinc finger RNA binding protein 2	2,12E-03	-1,209
Sned1	sushi, nidogen and EGF-like domains 1	4,30E-04	-1,215
Iglon5	IgLON family member 5	1,09E-02	-1,215
Pcdh9	protocadherin 9	3,51E-02	-1,218
Cd24a	CD24a antigen	2,88E-02	-1,219
Igsf9b	immunoglobulin superfamily, member 9B	4,31E-03	-1,232
Il18	interleukin 18	1,10E-02	-1,234
Cxcl13	chemokine (C-X-C motif) ligand 13	2,81E-02	-1,235
Ier2	immediate early response 2	6,72E-03	-1,239
Cldn11	claudin 11	1,21E-03	-1,247
Pkhd1	polycystic kidney and hepatic disease 1	1,38E-02	-1,263
Csf1	colony stimulating factor 1 (macrophage)	2,68E-03	-1,273
Cntn3	contactin 3	2,08E-04	-1,290
Ppfia2	protein tyrosine phosphatase, receptor type, f polypeptide (PTPRF), interacting protein (liprin), alpha 2	5,12E-03	-1,293
Dscam	Down syndrome cell adhesion molecule	5,09E-03	-1,298
Tnr	tenascin R	1,43E-02	-1,300
Ppl	periplakin	2,97E-02	-1,313
Cer1	cerberus 1 homolog (Xenopus laevis)	2,77E-03	-1,324
Hmgb1	high mobility group box 1	1,80E-02	-1,340
Ntm	neurotrimin	8,79E-03	-1,346
C8b	complement component 8, beta polypeptide	2,41E-04	-1,363
Syt1	synaptotagmin I	1,24E-02	-1,369
Ncam2	neural cell adhesion molecule 2	1,41E-03	-1,388
L1cam	L1 cell adhesion molecule	2,12E-03	-1,389
Cdh22	cadherin 22	6,71E-04	-1,397
Cdh7	cadherin 7, type 2	1,06E-03	-1,482
Dnm1	dynamin 1	9,79E-06	-1,577
Igsf21	immunoglobin superfamily, member 21	8,81E-04	-1,587
Flrt1	fibronectin leucine rich transmembrane protein 1	1,37E-03	-1,616
Pcdh15	protocadherin 15	1,39E-04	-1,682
HLA-related			
H2-T22	histocompatibility 2, T region locus 22	6,14E-05	1,314

Tapbpl	TAP binding protein-like	1,48E-04	1,259
H13	histocompatibility 13	2,17E-04	1,243
Other functions			
Cuzd1	CUB and zona pellucida-like domains 1	2,06E-02	2,735
Pdyn	prodynorphin	3,63E-04	2,585
Sema3c	sema domain, immunoglobulin domain (Ig), short basic domain	7,05E-05	2,474
Necab2	N-terminal EF-hand calcium binding protein 2	6,50E-07	2,060
Mfi2	antigen p97 (melanoma associated) identified by monoclonal antibodies 133.2 and 96.5	1,48E-04	1,962
S100z	S100 calcium binding protein, zeta	2,70E-03	1,818
Creld2	cysteine-rich with EGF-like domains 2	4,82E-05	1,631
Stil	Scl/Tal1 interrupting locus	1,79E-03	1,628
Tmem160	transmembrane protein 160	1,79E-05	1,524
Gnat2	guanine nucleotide binding protein, alpha transducing 2	7,69E-04	1,515
Nrm	nurim (nuclear envelope membrane protein)	1,74E-03	1,485
Car5b	carbonic anhydrase 5b, mitochondrial	1,12E-03	1,483
Yif1b	Yip1 interacting factor homolog B (S. cerevisiae)	9,19E-05	1,475
Mum1l1	melanoma associated antigen (mutated) 1-like 1	4,49E-02	1,440
St7	suppression of tumorigenicity 7	4,71E-04	1,381
Csn3	casein kappa	4,05E-03	1,377
Pon3	paraoxonase 3	2,49E-04	1,376
Rassf4	Ras association (RalGDS/AF-6) domain family member 4	1,51E-04	1,371
Tmem150a	transmembrane protein 150A	1,51E-04	1,366
Nomo1	nodal modulator 1	1,75E-05	1,358
Fez1	fasciculation and elongation protein zeta 1 (zygin I)	2,89E-05	1,358
Morc1	microrchidia 1	5,50E-04	1,342
Lrrtm2	leucine rich repeat transmembrane neuronal 2	2,68E-03	1,334
Tmem66	transmembrane protein 66	7,45E-06	1,332
Atp13a1	ATPase type 13A1	1,87E-04	1,309
Gmfg	glia maturation factor, gamma	9,64E-03	1,297
Prom1	prominin 1	1,64E-02	1,290
Zdhhc24	zinc finger, DHHC domain containing 24	8,88E-05	1,284
Arfip2	ADP-ribosylation factor interacting protein 2	5,95E-04	1,276
Dcx	doublecortin	2,06E-02	1,270
Pxmp4	peroxisomal membrane protein 4	6,39E-05	1,270
Sprr1a	small proline-rich protein 1A	4,73E-02	1,242
Tal2	T-cell acute lymphocytic leukemia 2	2,56E-03	1,241
Cc2d2a	coiled-coil and C2 domain containing 2A	5,93E-05	1,239
Sez6l2	seizure related 6 homolog like 2	1,73E-04	1,238
Shisa2	shisa homolog 2 (Xenopus laevis)	7,27E-03	1,223
Chid1	chitinase domain containing 1	6,03E-04	1,220

Pex11c	peroxisomal biogenesis factor 11 gamma	2,97E-03	1,215
Wdr62	WD repeat domain 62	9,26E-03	1,213
Ogfod2	2-oxoglutarate and iron-dependent oxygenase domain containing 2	5,71E-04	1,212
Mgp	matrix Gla protein	2,86E-02	1,209
Timm50	translocase of inner mitochondrial membrane 50 homolog (yeast)	7,59E-04	1,206
Pdzd11	PDZ domain containing 11	1,19E-02	1,205
Tmem43	transmembrane protein 43	2,24E-04	1,204
Fam114a1	family with sequence similarity 114, member A1	2,81E-04	1,204
Dpysl5	dihydropyrimidinase-like 5	9,50E-03	-1,208
Evpl	envoplakin	3,15E-04	-1,210
Zcchc11	zinc finger, CCHC domain containing 11	6,66E-04	-1,215
Sp140	Sp140 nuclear body protein	2,62E-02	-1,217
D5Ertd579e	DNA segment, Chr 5, ERATO Doi 579, expressed	2,72E-02	-1,220
Olfml3	olfactomedin-like 3	3,16E-02	-1,230
Hpca	hippocalcin	4,84E-04	-1,233
Tnrc6c	trinucleotide repeat containing 6C	2,32E-04	-1,234
Plp1	proteolipid protein (myelin) 1	3,63E-02	-1,234
Fam113b	family with sequence similarity 113, member B	5,79E-03	-1,234
Sobp	sine oculis-binding protein homolog (Drosophila)	5,93E-05	-1,236
Sftpa1	surfactant associated protein A1	3,65E-02	-1,242
Zswim6	zinc finger, SWIM domain containing 6	4,13E-03	-1,242
Fcho1	FCH domain only 1	6,35E-05	-1,250
Cryba2	crystallin, beta A2	1,64E-02	-1,252
Iqcb1	IQ calmodulin-binding motif containing 1	1,39E-04	-1,256
Phldb2	pleckstrin homology-like domain, family B, member 2	4,88E-03	-1,258
Acrbp	proacrosin binding protein	1,16E-02	-1,260
Nsg1	neuron specific gene family member 1	5,33E-04	-1,268
Mrfap1	Morf4 family associated protein 1	6,60E-03	-1,280
Dlgap1	discs, large (Drosophila) homolog-associated protein 1	4,75E-03	-1,285
Mreg	melanoregulin	1,59E-02	-1,292
Tcp11	t-complex protein 11	7,92E-03	-1,301
Edaradd	EDAR (ectodysplasin-A receptor)-associated death domain	2,60E-03	-1,306
Dab1	disabled homolog 1 (Drosophila)	2,54E-04	-1,314
Gap43	growth associated protein 43	1,62E-03	-1,325
AW551984	expressed sequence AW551984	1,49E-03	-1,329
Olfm3	olfactomedin 3	6,87E-03	-1,330
Dzip1	DAZ interacting protein 1	1,06E-03	-1,335
Astn2	astrotactin 2	1,34E-03	-1,335
Zbtb7c	zinc finger and BTB domain containing 7C	7,22E-04	-1,350
Tekt2	tektin 2	2,55E-04	-1,357

Nav3	neuron navigator 3	9,88E-04	-1,368
Zfp62	zinc finger protein 62	1,95E-04	-1,374
Car15	carbonic anhydrase 15	8,16E-04	-1,403
F3	coagulation factor III	7,45E-06	-1,505
Edil3	EGF-like repeats and discoidin I-like domains 3	1,00E-03	-1,524
Mfap2	microfibrillar-associated protein 2	1,04E-04	-1,561
Gfra3	glial cell line derived neurotrophic factor family recepto	2,07E-03	-1,690
Mt2	metallothionein 2	3,85E-05	-1,877
Unknown functions			
Try5	trypsin 5	8,45E-03	2,093
Tmem179	transmembrane protein 179	2,75E-04	1,876
Svopl	SV2 related protein homolog (rat)-like	6,85E-05	1,865
Myo15b	myosin XVB	1,89E-05	1,864
Try10	trypsin 10	2,41E-02	1,837
Prr11	proline rich 11	1,79E-03	1,800
Gm5409	predicted pseudogene 5409	1,67E-02	1,677
Slfn9	schlafen 9	2,23E-03	1,676
Tmed6	transmembrane emp24 protein transport domain containing 6	2,84E-03	1,645
Sdf2l1	stromal cell-derived factor 2-like 1	6,39E-05	1,530
Fam70a	family with sequence similarity 70, member A	6,27E-05	1,518
Ankrd34b	ankyrin repeat domain 34B	2,21E-02	1,496
Gpr165	G protein-coupled receptor 165	2,18E-02	1,492
Ccdc85a	coiled-coil domain containing 85A	2,82E-04	1,481
Btnl9	butyrophilin-like 9	1,47E-05	1,440
Sel1l3	sel-1 suppressor of lin-12-like 3 (C. elegans)	9,23E-05	1,428
Ttc13	tetratricopeptide repeat domain 13 /	1,45E-05	1,412
Wdr90	WD repeat domain 90	5,29E-04	1,405
Fam46a	family with sequence similarity 46, member A	1,26E-03	1,388
Rell1	RELT-like 1	1,02E-05	1,356
Tmem125	transmembrane protein 125	8,57E-03	1,350
Maged2	melanoma antigen, family D, 2	1,15E-03	1,348
Spt1	salivary protein 1	2,62E-02	1,347
Tmem212	transmembrane protein 212	7,13E-04	1,330
Ccdc107	coiled-coil domain containing 107	9,19E-05	1,313
Heatr5b	HEAT repeat containing 5B	3,58E-04	1,312
Gm2897	predicted gene 2897	1,68E-03	1,304
Fam194a	family with sequence similarity 194, member A	3,09E-03	1,299
Sval2	seminal vesicle antigen-like 2	8,63E-05	1,299
Ttc39c	tetratricopeptide repeat domain 39C	5,95E-04	1,298
Gpr108	G protein-coupled receptor 108	2,06E-04	1,295
Pter	phosphotriesterase related	7,97E-03	1,295

Gm5465	predicted gene 5465	1,42E-02	1,290
Tmem238	transmembrane protein 238	3,43E-04	1,290
D17Wsu104e	DNA segment, Chr 17, Wayne State University 104, expression	5,93E-05	1,287
Reep5	receptor accessory protein 5	7,96E-05	1,279
Tmem176a	transmembrane protein 176A	1,05E-03	1,278
Trabd	TraB domain containing	6,55E-05	1,276
Cyyr1	cysteine and tyrosine-rich protein 1	3,24E-04	1,276
Lrrc39	leucine rich repeat containing 39	2,89E-03	1,274
Ddrgk1	DDRGK domain containing 1	1,76E-04	1,273
Vmn1r103	vomeronasal 1 receptor 103	6,51E-03	1,268
Fam173a	family with sequence similarity 173, member A	1,19E-03	1,268
Mfap3l	microfibrillar-associated protein 3-like	1,38E-03	1,267
Gm3696	predicted gene 3696	6,87E-04	1,265
Tmem223	transmembrane protein 223	9,30E-04	1,260
Yipf2	Yip1 domain family, member 2	8,49E-04	1,260
Tmem117	transmembrane protein 117	4,84E-04	1,255
Tc2n	tandem C2 domains, nuclear	1,80E-02	1,253
Tmem218	transmembrane protein 218	9,06E-04	1,252
Ccdc18	coiled-coil domain containing 18	8,12E-04	1,251
Vmn1r4	vomeronasal 1 receptor 4	1,10E-03	1,249
Ifrd2	interferon-related developmental regulator 2	4,52E-04	1,246
Tmem205	transmembrane protein 205	9,03E-04	1,245
Gm447	predicted gene 447	1,23E-03	1,244
Fbxo48	F-box protein 48	1,26E-02	1,243
Tmem214	transmembrane protein 214	2,66E-04	1,240
Npdc1	neural proliferation, differentiation and control gene 1	1,45E-04	1,231
Nlrp4f	NLR family, pyrin domain containing 4F	9,04E-03	1,230
R3hcc1	R3H domain and coiled-coil containing 1	1,51E-03	1,228
Gm561	predicted gene 561	6,56E-03	1,228
Tmem120b	transmembrane protein 120B	3,60E-03	1,224
Tmem144	transmembrane protein 144	3,85E-04	1,223
Dnajc28	DnaJ (Hsp40) homolog, subfamily C, member 28	5,37E-03	1,220
D10Jhu81e	DNA segment, Chr 10, Johns Hopkins University 81 expression	2,41E-04	1,219
Serf2	small EDRK-rich factor 2	1,74E-03	1,217
Gm10406	predicted gene 10406	8,18E-03	1,211
Gm5105	predicted gene 5105	1,70E-02	1,211
Armcx6	armadillo repeat containing, X-linked 6	2,67E-03	1,210
Ccdc134	coiled-coil domain containing 134	3,75E-02	1,209
Gm6590	predicted gene 6590	5,36E-03	1,207
Smyd5	SET and MYND domain containing 5	9,19E-03	1,207

Cxx1a	CAAX box 1 homolog A (human)	4,74E-04	1,204
Gm996	predicted gene 996	3,47E-02	1,204
Gm10267	predicted gene 10267	4,15E-03	1,203
Ifi27l1	interferon, alpha-inducible protein 27 like 1	5,73E-03	1,202
Nol4	nucleolar protein 4	4,27E-03	-1,201
Zcchc7	zinc finger, CCHC domain containing 7	7,68E-03	-1,202
Zc3h13	zinc finger CCCH type containing 13	4,57E-03	-1,203
Phxr1	per-hexamer repeat gene 1	4,75E-03	-1,204
Gm7241	predicted pseudogene 7241	1,37E-02	-1,205
Zfp125	zinc finger protein 125	1,49E-02	-1,206
Fnbp4	formin binding protein 4	1,09E-03	-1,206
Vwa5b2	von Willebrand factor A domain containing 5B2	1,51E-02	-1,208
H2-K2	histocompatibility 2, K region locus 2	3,45E-02	-1,209
Zfp760	zinc finger protein 760	1,14E-02	-1,210
Gm10033	predicted gene 10033	1,84E-02	-1,210
Mxra7	matrix-remodelling associated 7	6,13E-03	-1,212
Zfp619	zinc finger protein 619	3,03E-03	-1,212
Fam172a	family with sequence similarity 172, member A	8,18E-04	-1,214
Emid1	EMI domain containing 1	4,30E-03	-1,214
Ahdc1	AT hook, DNA binding motif, containing 1	5,71E-04	-1,216
Gm10786	predicted gene 10786	2,82E-02	-1,216
Gm10589	predicted gene 10589	1,82E-02	-1,217
Rnf157	ring finger protein 157	5,42E-03	-1,218
Zfp871	zinc finger protein 871	1,25E-02	-1,218
Sfrs18	serine/arginine-rich splicing factor 18	1,70E-02	-1,220
Bod1l	biorientation of chromosomes in cell division 1-like	1,41E-02	-1,220
Wdr47	WD repeat domain 47	4,65E-04	-1,225
Aard	alanine and arginine rich domain containing protein	3,43E-02	-1,230
Fam36a	family with sequence similarity 36, member A	2,28E-02	-1,233
Nbeal1	neurobeachin like 1	4,80E-02	-1,236
Gm10838	predicted gene 10838	9,13E-03	-1,238
Zfp781	zinc finger protein 781	1,22E-03	-1,240
AU019823	expressed sequence AU019823	8,28E-06	-1,240
Klhl32	kelch-like 32 (Drosophila)	2,62E-03	-1,240
Plekha5	pleckstrin homology domain containing, family A member 5	2,72E-03	-1,241
Fam82b	family with sequence similarity 82, member B	3,60E-03	-1,242
Trp53i11	transformation related protein 53 inducible protein	6,90E-04	-1,247
Gm13139	predicted gene 13139	1,92E-02	-1,250
Zfp758	zinc finger protein 758	2,81E-04	-1,250
Nynrin	NYN domain and retroviral integrase containing	1,78E-02	-1,251
Gm1043	predicted gene 1043	4,13E-04	-1,251

Fam78b	family with sequence similarity 78, member B	1,82E-04	-1,253
Zfp229	zinc finger protein	1,85E-02	-1,253
Ceacam10	carcinoembryonic antigen-related cell adhesion molecule 10	4,26E-02	-1,255
Phf20l1	PHD finger protein 20-like 1	6,14E-04	-1,255
Gm1027	predicted gene 1027	8,14E-04	-1,260
Bend7	BEN domain containing 7	9,38E-04	-1,261
Gm13251	predicted gene 13251	9,03E-03	-1,266
Gm6999	predicted gene 6999	1,93E-02	-1,267
Anp32-ps	acidic (leucine-rich) nuclear phosphoprotein 32 family, pseudogene	8,30E-03	-1,269
DXBay18	DNA segment, Chr X, Baylor 18	5,47E-03	-1,272
Zcchc2	zinc finger, CCHC domain containing 2	1,31E-03	-1,273
Ankrd33b	ankyrin repeat domain 33B	2,61E-02	-1,274
Fhdc1	FH2 domain containing 1	6,08E-06	-1,280
Zfp568	zinc finger protein 568	9,22E-03	-1,287
Gm6712	predicted gene 6712	3,77E-03	-1,288
BC068157	cDNA sequence BC068157	1,38E-03	-1,290
Gm13235	predicted gene 13235	1,49E-02	-1,290
Gpr137b-ps	G protein-coupled receptor 137B, pseudogene	2,74E-03	-1,290
Ociad2	OCIA domain containing 2	1,16E-02	-1,292
Csmd2	CUB and Sushi multiple domains 2	1,19E-02	-1,293
3110048L19Rik	zinc finger pseudogene	2,80E-04	-1,296
Tmem229b	transmembrane protein 229B	2,17E-04	-1,300
Zmym5	zinc finger, MYM-type 5	5,82E-04	-1,313
Gm3365	predicted gene 3365	2,36E-03	-1,314
Pisd-ps2	phosphatidylserine decarboxylase, pseudogene 2	7,00E-04	-1,315
Lancl3	LanC lantibiotic synthetase component C-like 3 (bacterial)	1,53E-02	-1,317
Xkr6	X Kell blood group precursor related family member 6	2,74E-04	-1,318
Wdr78	WD repeat domain 78	1,17E-04	-1,321
Rbm33	RNA binding motif protein 33	3,45E-02	-1,327
Gm9958	predicted gene 9958	1,22E-04	-1,327
Ccdc48	coiled-coil domain containing 48	2,04E-05	-1,330
Gm5595	predicted gene 5595	5,68E-03	-1,330
Gm7125	high mobility group nucleosomal binding domain 2	1,61E-03	-1,333
Zfp872	zinc finger protein 872	3,77E-02	-1,334
Ctxn2	cortexin 2	4,40E-02	-1,334
Dbpht2	DNA binding protein with his-thr domain	8,30E-04	-1,335
Ankrd45	ankyrin repeat domain 45	2,24E-04	-1,344
Fam159b	family with sequence similarity 159, member B	1,22E-04	-1,354
Gipc2	GIPC PDZ domain containing family, member 2	1,06E-03	-1,360
Auts2	autism susceptibility candidate 2	9,08E-04	-1,368

Mctp2	multiple C2 domains, transmembrane 2	7,30E-03	-1,368
Tmem215	transmembrane protein 215	3,16E-04	-1,389
Fam196a	family with sequence similarity 196, member A	8,40E-04	-1,454
Lrrc36	leucine rich repeat containing 36	2,01E-04	-1,455
Samd14	sterile alpha motif domain containing 14	4,84E-04	-1,460
T2	brachyury 2	5,44E-04	-1,475
Clip4	CAP-GLY domain containing linker protein family, member 4	2,69E-02	-1,477
Fam166a	family with sequence similarity 166, member A	4,25E-03	-1,485
Pisd-ps1	phosphatidylserine decarboxylase, pseudogene 1	2,41E-04	-1,487
Mest	mesoderm specific transcript	1,46E-02	-1,516
Gm10796	predicted gene 10796	2,32E-02	-1,518
Vwa5b1	von Willebrand factor A domain containing 5B1	5,52E-04	-1,519
Lrrc16b	leucine rich repeat containing 16B	1,11E-03	-1,524
Pnet-ps	prenatal ethanol induced mRNA, pseudogene	1,79E-02	-1,524
Wdr49	WD repeat domain 49	2,09E-03	-1,534
Gm609	predicted gene 609	6,82E-04	-1,544
Fam46d	family with sequence similarity 46, member D	1,03E-02	-1,546
Gm11992	predicted gene 11992	1,11E-03	-1,607
Gm10632	predicted gene 10632	8,18E-04	-1,651
Gm281	predicted gene 281	1,25E-04	-1,946

Table S3. Functional classification of differentially expressed genes in LDR vs ND islets.

Gene Symbol	Gene description	FDR step up (p < 0.05 n = 17)	Fold-Change Increase: 14 Decrease: 3
Carbohydrate metabolism			
Pfkp	phosphofructokinase, platelet	2,89E-02	1,275
Nucleotide/pyrophosphate metabolism			
Gucy2c	guanylate cyclase 2c	2,89E-02	1,812
Lipid metabolism			
Cpt1a	carnitine palmitoyltransferase 1a, liver	5,29E-04	1,521
Posttranslational modification/ubiquitination/glycosylation			
Man1a	mannosidase 1, alpha	4,61E-02	1,200
Channels and transporters			
Kcnh8	potassium voltage-gated channel, subfamily H (eag-related)	3,75E-02	1,389
Slc4a10	solute carrier family 4, sodium bicarbonate cotransporter	1,50E-02	1,269
Slc35f1	solute carrier family 35, member F1	3,76E-02	1,217
Hormones/growth factor/Receptors/neuropeptides and exocytosis			
Plxna3	plexin A3	1,50E-02	1,322
Apln	apelin	3,00E-02	-1,211
Npy	neuropeptide Y	1,50E-02	-1,972
AMPK and mTOR pathways			
Ppargc1a	peroxisome proliferative activated receptor, gamma, coa	1,50E-02	1,706
GTPase activity and regulation			
Gng4	guanine nucleotide binding protein (G protein),gamma 4	1,50E-02	1,212
Kinases/Phosphatatase and related proteins			
Akap6	A kinase (PRKA) anchor protein 6	4,16E-02	1,377
Chemokines/cytokines/adhesion molecules/innate immunity and related proteins			
C8b	complement component 8, beta polypeptide	4,16E-02	-1,286
Other functions			
Necab2	N-terminal EF-hand calcium binding protein 2	1,90E-02	1,397
Unknown functions			
Myo15b	myosin XVB	3,75E-02	1,487
Btnl9	butyrophilin-like 9	3,32E-02	1,261

Table S4. Functional classification of differentially expressed genes in HDR vs LDR islets.

Gene symbol	Gene description	FDR step up (p< 0.05 n =1041)	Fold-Change Increase: 523 Decrease: 518
Carbohydrate metabolism			
Gmds	GDP-mannose 4, 6-dehydratase	1,35E-03	1,417

Me3	malic enzyme 3, NADP(+)-dependent, mitochondrial	1,27E-03	1,397
Mpdu1	mannose-P-dolichol utilization defect 1	3,48E-03	1,245
Gla	galactosidase, alpha	4,54E-03	1,229
Bpgm	2,3-bisphosphoglycerate mutase	8,97E-03	1,221
Pgk1	phosphoglycerate kinase 1	3,51E-03	1,215
Galnt9	UDP-N-acetyl-alpha-D-galactosamine:polypeptide N-Acetylgalactosaminyltransferase 9	2,26E-02	-1,211
Pklr	pyruvate kinase liver and red blood cell	1,75E-03	-1,214
Slc2a2	solute carrier family 2 (facilitated glucose transporter), member 2	2,52E-02	-1,227
Slc2a3	solute carrier family 2 (facilitated glucose transporter), member 3	2,91E-02	-1,238
Ppp1r1a	protein phosphatase 1, regulatory (inhibitor) subunit 1A	1,13E-03	-1,247
Rbp4	retinol binding protein 4, plasma	1,24E-02	-1,253
Eno2	enolase 2, gamma neuronal	1,16E-02	-1,258
Gcnt4	glucosaminyl (N-acetyl) transferase 4, core 2 (beta-1,6 Acetylglucosaminyltransferase)	4,45E-03	-1,274
Khk	ketohexokinase	4,77E-02	-1,274
Rpia	ribose 5-phosphate isomerase A	2,01E-02	-1,320
Cryl1	crystallin, lambda 1	3,48E-03	-1,354
Aldoc	aldolase C, fructose-bisphosphate	2,63E-03	-1,471
Hpse	heparanase	2,03E-03	-1,809
Glycan metabolism			
Alg8	asparagine-linked glycosylation 8 homolog (yeast, Alpha-1,3-Glucosyltransferase)	1,05E-02	1,342
Dpm3	dolichyl-phosphate mannosyltransferase polypeptide 3	3,78E-03	1,328
Alg3	asparagine-linked glycosylation 3 homolog (yeast, Alpha-1,3-Mannosyltransferase)	1,14E-02	1,310
Glb1	galactosidase, beta 1	2,26E-04	1,278
Alg5	asparagine-linked glycosylation 5 homolog (yeast, Dolichyl-Phosphate Beta-Glucosyltransferase)	1,84E-03	1,277
Alg12	asparagine-linked glycosylation 12 homolog (yeast, Alpha-1,6-Mannosyltransferase)	3,08E-03	1,241
Pomt1	protein-O-mannosyltransferase 1	4,58E-03	1,231
Pomgnt1	protein O-linked mannose beta1,2-N-acetylglucosaminyltransferase	1,29E-03	1,223
Amino acid metabolism			
Aass	aminoadipate-semialdehyde synthase	1,46E-03	2,296
Pycr1	pyrroline-5-carboxylate reductase 1	1,15E-04	1,533
Bcat2	branched chain aminotransferase 2, mitochondrial	6,94E-03	1,312
Gcdh	glutaryl-Coenzyme A dehydrogenase	2,11E-03	1,292
Bckdhb	branched chain ketoacid dehydrogenase E1, beta polypeptide	1,15E-04	1,263
Ckb	creatine kinase, brain	1,12E-02	1,247
Bckdk	branched chain ketoacid dehydrogenase kinase	2,18E-03	1,242
Ccbl2	cysteine conjugate-beta lyase 2	3,73E-02	1,221
Th	tyrosine hydroxylase	2,38E-02	-1,347

Gad1	glutamic acid decarboxylase 1	6,05E-03	-1,641
Nucleotide/pyrophosphate metabolism			
Gucy2c	guanylate cyclase 2c	5,96E-04	1,986
Rrm2	ribonucleotide reductase M2	1,39E-03	1,831
Rasl10b	RAS-like, family 10, member B	1,34E-03	1,447
Tyms	thymidylate synthase	6,07E-03	1,434
Dhfr	dihydrofolate reductase	1,18E-02	1,307
Ppa1	pyrophosphatase (inorganic) 1	5,44E-03	1,305
Adcy4	adenylate cyclase 4	1,26E-02	1,256
Nme2	Nucleoside Diphosphate Kinase 2	1,73E-03	1,230
Nme1	Nucleoside Diphosphate Kinase 1	5,02E-03	1,209
Dck	deoxycytidine kinase	3,38E-02	1,205
Nme4	Nucleoside Diphosphate Kinase 4	6,53E-04	-1,242
Nme5	Nucleoside Diphosphate Kinase 5	8,14E-03	-1,257
Lipid metabolism			
Acsf2	acyl-CoA synthetase family member 2	3,42E-03	1,460
Lmf1	lipase maturation factor 1	2,23E-04	1,432
Pecr	peroxisomal trans-2-enoyl-CoA reductase	1,35E-03	1,306
Elovl7	ELOVL family member 7, elongation of long chain fatty acid	1,35E-03	1,271
Thrsp	thyroid hormone responsive SPOT14 homolog (Rattus)	9,60E-03	1,265
Ppapdc1b	phosphatidic acid phosphatase type 2 domain containing 1B	1,13E-03	1,252
Mboat1	membrane bound O-acyltransferase domain containing 1	2,55E-02	1,248
Pla2g12a	phospholipase A2, group XIIA	6,53E-04	1,213
Plcd1	phospholipase C, delta 1	7,80E-03	1,205
Cyp2j6	cytochrome P450, family 2, subfamily j, polypeptide 6	5,02E-03	1,204
Pla2g6	phospholipase A2, group VI	1,15E-04	1,201
Hsd3b7	hydroxy-delta-5-steroid dehydrogenase, 3 beta- and steroid Delta isomerase-7	1,91E-02	1,201
Pikfyve	phosphoinositide kinase, FYVE finger containing	1,73E-02	-1,212
Dgat2	diacylglycerol O-acyltransferase 2	3,41E-03	-1,213
Arv1	ARV1 homolog (yeast)	2,25E-03	-1,214
Pid1	phosphotyrosine interaction domain containing 1	1,05E-02	-1,217
Aloxe3	arachidonate lipoxygenase 3	2,39E-02	-1,219
Tmem86b	transmembrane protein 86B	1,72E-02	-1,220
Scd2	stearoyl-Coenzyme A desaturase 2	1,02E-03	-1,227
Acsl3	acyl-CoA synthetase long-chain family member 3	2,96E-03	-1,243
Acot11	acyl-CoA thioesterase 11	6,11E-03	-1,258
Vldlr	very low density lipoprotein receptor	3,30E-03	-1,268
Sc4mol	sterol-C4-methyl oxidase-like	4,54E-03	-1,287
Gpr120	G protein-coupled receptor 120	8,70E-03	-1,298
Gpd2	glycerol phosphate dehydrogenase 2, mitochondrial	1,65E-02	-1,350

Lpl	lipoprotein lipase	3,07E-03	-1,451
Scd1	stearoyl-Coenzyme A desaturase 1	1,54E-02	-1,569
Cholesterol metabolism and transport			
Apoa2	apolipoprotein A-II	1,609E-03	1,543
Klb	klotho beta	2,232E-02	-1,238
Pcsk9	proprotein convertase subtilisin/kexin type 9	3,319E-03	-1,295
Srebf2	sterol regulatory element binding factor 2	1,241E-03	-1,296
Hmgcs1	3-hydroxy-3-methylglutaryl-Coenzyme A synthase 1	1,19E-02	-1,305
Idi1	isopentenyl-diphosphate delta isomerase	2,042E-02	-1,310
Stard4	StAR-related lipid transfer (START) domain containing 4	6,261E-04	-1,330
Dhcr24	24-dehydrocholesterol reductase	1,412E-03	-1,386
Metabolism-miscellaneous			
Aldh1a3	aldehyde dehydrogenase family 1, subfamily A3	5,49E-04	3,493
Gc	group specific component	5,92E-05	1,636
Gsto2	glutathione S-transferase omega 2	4,49E-03	1,579
Iyd	iodotyrosine deiodinase	3,46E-03	1,372
Nans	N-acetylneuraminic acid synthase (sialic acid synthase)	2,09E-03	1,338
Bcmo1	beta-carotene 15,15'-monooxygenase	3,08E-03	1,321
Cmas	cytidine monophospho-N-acetylneuraminic acid synthetase	1,33E-03	1,290
Mosc2	MOCO sulphurase C-terminal domain containing 2	2,62E-03	1,289
Dio1	deiodinase, iodothyronine, type I	1,13E-03	1,254
Gsto1	glutathione S-transferase omega 1	1,28E-02	1,243
Nampt	nicotinamide phosphoribosyltransferase	2,31E-03	-1,205
Gstm3	glutathione S-transferase, mu 3	1,33E-03	-1,327
Gstm1	glutathione S-transferase, mu 1	3,05E-03	-1,427
Ndst4	N-deacetylase/N-sulfotransferase (heparin glucosaminyl) 4	3,30E-03	-1,747
Mitochondrial respiration			
Ndufa1	NADH dehydrogenase (ubiquinone) 1 alpha subcomplex, 1	5,89E-03	1,263
Ndufa4	NADH dehydrogenase (ubiquinone) 1 alpha subcomplex, 4	3,62E-02	1,210
Oxidation-reduction process			
Dhrs7	dehydrogenase/reductase (SDR family) member 7	1,84E-03	1,275
Dhrs7b	dehydrogenase/reductase (SDR family) member 7B	7,42E-04	1,258
Hsd17b7	hydroxysteroid (17-beta) dehydrogenase 7	8,24E-03	-1,220
Akr1c19	aldo-keto reductase family 1, member C19	1,35E-02	-1,267
Cell cycle			
Ccnb1	cyclin B1	1,39E-03	3,109
Ccnb2	cyclin B2	5,88E-04	2,848
Top2a	topoisomerase (DNA) II alpha	1,62E-03	2,826
Mki67	antigen identified by monoclonal antibody Ki 67	1,13E-03	2,727
Plk1	polo-like kinase 1 (Drosophila)	2,20E-03	2,551
Anln	anillin, actin binding protein	1,62E-03	2,551

Bub1	budding uninhibited by benzimidazoles 1 homolog (S. cerevisiae)	2,75E-03	2,485
Kif11	kinesin family member 11	1,33E-03	2,445
Cks2	CDC28 protein kinase regulatory subunit 2	2,03E-03	2,416
Ect2	ect2 oncogene	1,45E-03	2,383
Ccna2	cyclin A2	1,68E-03	2,363
Nek2	NIMA (never in mitosis gene a)-related expressed kinase 2	1,39E-03	2,349
Tpx2	TPX2, microtubule-associated protein homolog (Xenopus laevis)	1,74E-03	2,337
Cdk1	cyclin-dependent kinase 1	6,26E-04	2,336
Casc5	cancer susceptibility candidate 5	1,48E-03	2,328
D2Ertd750e	DNA segment, Chr 2, ERATO Doi 750, expressed	9,01E-04	2,324
Stmn1	stathmin 1	1,80E-03	2,277
Cdc20	cell division cycle 20 homolog (S. cerevisiae)	5,96E-04	2,234
Nusap1	nucleolar and spindle associated protein 1	1,39E-03	2,227
Dtl	denticleless homolog (Drosophila)	8,88E-04	2,181
Prc1	protein regulator of cytokinesis 1	1,93E-03	2,138
Dlgap5	discs, large (Drosophila) homolog-associated protein 5	1,44E-03	2,073
Cenpf	centromere protein F	2,20E-03	1,970
Aurkb	aurora kinase B	3,77E-03	1,941
Cenpe	centromere protein E	3,44E-03	1,922
C79407	expressed sequence C79407	2,26E-03	1,907
Ckap2l	cytoskeleton associated protein 2-like	2,26E-03	1,899
Ckap2	cytoskeleton associated protein 2	1,29E-03	1,894
Ncaph	non-SMC condensin I complex, subunit H	3,10E-03	1,883
Nuf2	NUF2, NDC80 kinetochore complex component, homolog (S. cerevisiae)	1,33E-03	1,869
Rad51	RAD51 homolog (S. cerevisiae)	5,65E-03	1,824
Sgol2	shugoshin-like 2 (S. pombe)	1,35E-03	1,821
Kntc1	kinetochore associated 1	1,53E-03	1,813
Kif20a	kinesin family member 20A	4,14E-03	1,794
Ncapg	non-SMC condensin I complex, subunit G	1,61E-03	1,785
Aspm	asp (abnormal spindle)-like, microcephaly associated (Drosophila)	4,49E-03	1,764
Cenpm	centromere protein M	8,86E-04	1,756
Kif23	kinesin family member 23	3,51E-03	1,742
Aurka	aurora kinase A	3,51E-03	1,735
Cdca3	cell division cycle associated 3	3,19E-03	1,713
Cdkn3	cyclin-dependent kinase inhibitor 3	2,26E-03	1,708
Spag5	sperm associated antigen 5	3,51E-03	1,707
Mcm5	minichromosome maintenance deficient 5, cell division cycle	3,19E-03	1,702
Zwilch	Zwilch, kinetochore associated, homolog (Drosophila)	6,90E-04	1,694
Foxm1	forkhead box M1	3,09E-03	1,686

Bub1b	BUB1 mitotic checkpoint serine/threonine kinase B	2,27E-03	1,674
Cenpa	centromere protein A	5,69E-03	1,673
Mastl	microtubule associated serine/threonine kinase-like	5,01E-03	1,672
Cenpn	centromere protein N	1,92E-03	1,649
Oip5	Opa interacting protein 5	3,02E-03	1,648
Fam111a	family with sequence similarity 111, member A	6,09E-03	1,635
Cgref1	cell growth regulator with EF hand domain 1	1,33E-03	1,631
Cdca8	cell division cycle associated 8	7,82E-03	1,628
Kif4	kinesin family member 4	7,96E-03	1,616
E2f8	E2F transcription factor 8	4,47E-03	1,603
Cenpk	centromere protein K	1,41E-03	1,600
Spc24	SPC24, NDC80 kinetochore complex component, homolog (S. cerevisiae)	1,24E-03	1,561
Cdca2	cell division cycle associated 2	3,04E-03	1,555
Kif20b	kinesin family member 20B	2,80E-03	1,554
Cdc25c	cell division cycle 25 homolog C (S. pombe)	2,98E-03	1,547
Racgap1	Rac GTPase-activating protein 1	1,90E-03	1,546
Ncapg2	non-SMC condensin II complex, subunit G2	1,03E-02	1,544
Melk	maternal embryonic leucine zipper kinase	2,73E-03	1,531
Hells	helicase, lymphoid specific	5,74E-03	1,525
Ccnf	cyclin F	8,17E-03	1,523
Mcm2	minichromosome maintenance deficient 2 mitotin (S. cerevisiae)	7,09E-03	1,522
Kif2c	kinesin family member 2C	7,19E-03	1,511
Ttk	Ttk protein kinase	3,13E-03	1,507
Cenpi	centromere protein I	7,19E-03	1,494
Cks1b	CDC28 protein kinase 1b	3,08E-03	1,491
E2f1	E2F transcription factor 1	3,69E-04	1,481
Smc2	structural maintenance of chromosomes 2	1,03E-02	1,467
Mcm6	minichromosome maintenance deficient 6 (MIS5 homolog, S. pombe)	1,71E-02	1,462
Cdca5	cell division cycle associated 5	5,19E-03	1,460
Mcm3	minichromosome maintenance deficient 3 (S. cerevisiae)	2,14E-02	1,459
Ndc80	NDC80 homolog, kinetochore complex component	1,59E-02	1,455
Kif22	kinesin family member 22	5,95E-03	1,454
Fam64a	family with sequence similarity 64, member A	7,53E-03	1,446
Ncapd2	non-SMC condensin I complex, subunit D2	1,11E-02	1,444
Cdt1	chromatin licensing and DNA replication factor 1	1,01E-02	1,431
Clspn	claspin homolog (Xenopus laevis)	3,24E-03	1,413
Cdkn2c	cyclin-dependent kinase inhibitor 2C (p18, inhibits CDK4)	1,79E-03	1,410
Kif15	kinesin family member 15	2,06E-03	1,408
Mad2l1	MAD2 mitotic arrest deficient-like 1 (yeast)	3,02E-02	1,407
Sgol1	shugoshin-like 1 (S. pombe)	9,54E-03	1,406

Cdc6	cell division cycle 6 homolog (S. cerevisiae)	1,58E-03	1,389
Cenph	centromere protein H	2,40E-02	1,380
Chaf1b	chromatin assembly factor 1, subunit B (p60)	2,34E-02	1,372
Dbf4	DBF4 homolog (S. cerevisiae)	9,77E-03	1,371
Uhrf1	ubiquitin-like, containing PHD and RING finger domains, 1	1,46E-02	1,370
Fam83d	family with sequence similarity 83, member D	2,45E-03	1,364
Mcm10	minichromosome maintenance deficient 10 (S. cerevisiae)	9,86E-03	1,362
Dsn1	DSN1, MIND kinetochore complex component, homolog (S. cerevisiae)	1,50E-02	1,351
Kif18a	kinesin family member 18A	3,79E-02	1,346
Mcm8	minichromosome maintenance deficient 8 (S. cerevisiae)	9,97E-03	1,338
Mcm7	minichromosome maintenance deficient 7 (S. cerevisiae)	2,32E-02	1,318
E2f7	E2F transcription factor 7	7,37E-03	1,310
Cep55	centrosomal protein 55	5,99E-03	1,305
Pkmyt1	protein kinase, membrane associated tyrosine/threonine 1	2,77E-03	1,292
Arhgef10	Rho guanine nucleotide exchange factor (GEF) 10	2,49E-03	1,290
Gins1	GINS complex subunit 1 (Psf1 homolog)	1,30E-02	1,279
Smc4	structural maintenance of chromosomes 4	2,15E-02	1,272
Cdc45	cell division cycle 45 homolog (S. cerevisiae)	6,47E-03	1,272
Espl1	extra spindle poles-like 1 (S. cerevisiae)	1,71E-02	1,262
Reg3g	regenerating islet-derived 3 gamma	2,38E-02	1,250
Cenpp	centromere protein P	4,77E-02	1,242
Plk4	polo-like kinase 4 (Drosophila)	3,94E-02	1,237
Nsl1	NSL1, MIND kinetochore complex component, homolog (S. cerevisiae)	8,70E-03	1,237
Haus4	HAUS augmin-like complex, subunit 4	2,30E-02	1,229
Pmf1	polyamine-modulated factor 1	7,23E-03	1,227
Chaf1a	chromatin assembly factor 1, subunit A (p150)	3,30E-02	1,218
Jtb	jumping translocation breakpoint	6,26E-04	1,206
S100a4	S100 calcium binding protein A4	2,98E-03	1,200
Eapp	E2F-associated phosphoprotein	5,37E-03	-1,214
Fam190a	family with sequence similarity 190, member A	2,47E-03	-1,228
Dcaf12l1	DDB1 and CUL4 associated factor 12-like 1	3,28E-03	-1,231
Klhl13	kelch-like 13 (Drosophila)	2,10E-02	-1,241
Chd7	chromodomain helicase DNA binding protein 7	1,50E-02	-1,301
Ttc28	tetratricopeptide repeat domain 28	3,83E-03	-1,350
Phf16	PHD finger protein 16	1,33E-03	-1,370
DNA repair/DNA recombination/DNA replication			
Asf1b	ASF1 anti-silencing function 1 homolog B (S. cerevisiae)	1,33E-03	2,400
Pole	polymerase (DNA directed), epsilon	2,20E-03	1,814
Neil3	nei like 3 (E. coli)	3,90E-03	1,698
Fignl1	fidgetin-like 1	1,33E-03	1,686

Fen1	flap structure specific endonuclease 1	5,69E-03	1,531
Fancd2	Fanconi anemia, complementation group D2	8,04E-03	1,448
Brip1	BRCA1 interacting protein C-terminal helicase 1	1,61E-03	1,396
Pole2	polymerase (DNA directed), epsilon 2 (p59 subunit)	4,07E-03	1,384
Fancb	Fanconi anemia, complementation group B	9,91E-03	1,381
Brca1	breast cancer 1	1,08E-02	1,371
Rad51ap1	RAD51 associated protein 1	1,34E-03	1,370
Fanca	Fanconi anemia, complementation group A	5,28E-03	1,364
Exo1	exonuclease 1	6,20E-03	1,359
Fanci	Fanconi anemia, complementation group I	7,29E-03	1,352
Gins2	GINS complex subunit 2 (Psf2 homolog)	1,10E-02	1,349
Rrm1	ribonucleotide reductase M1	2,28E-02	1,332
Rfc4	replication factor C (activator 1) 4	1,39E-02	1,322
Rpa2	replication protein A2	3,72E-03	1,302
Hmgb2	high mobility group box 2	4,68E-02	1,298
Rad18	RAD18 homolog (S. cerevisiae)	1,29E-02	1,297
Rad54b	RAD54 homolog B (S. cerevisiae)	1,86E-02	1,254
Rexo2	REX2, RNA exonuclease 2 homolog (S. cerevisiae)	5,28E-03	1,228
Dna2	DNA replication helicase 2 homolog (yeast)	2,56E-02	1,222
Ogg1	8-oxoguanine DNA-glycosylase 1	3,07E-03	1,218
Topbp1	topoisomerase (DNA) II binding protein 1	2,50E-02	1,211
Rad54l	RAD54 like (S. cerevisiae)	1,16E-02	1,208
Rfc5	replication factor C (activator 1) 5	2,98E-02	1,207
Ercc6l	excision repair cross-complementing rodent repair Deficiency,Complementation Group 6-Like	2,23E-02	1,207
Poll	polymerase (DNA directed), lambda	2,18E-02	1,206
Dclre1c	DNA cross-link repair 1C, PSO2 homolog (S. cerevisiae)	1,59E-02	-1,204
Msh2	mutS homolog 2 (E. coli)	1,13E-02	-1,207
Rev1	REV1 homolog (S. cerevisiae)	2,73E-03	-1,239
Cdc14b	CDC14 cell division cycle 14 homolog B (S. cerevisiae)	1,34E-03	-1,243
Rad9b	RAD9 homolog B (S. cerevisiae)	1,55E-03	-1,243
Rdm1	RAD52 motif 1	3,86E-03	-1,312
Nucleosome assembly			
Cenpw	centromere protein W	3,04E-02	1,249
Hist1h1a	histone cluster 1, H1a	3,63E-02	1,284
Hist1h1b	histone cluster 1, H1b	1,25E-02	1,440
Hist1h2ab	histone cluster 1, H2ab	2,31E-02	1,481
Hist1h2af	histone cluster 1, H2af	8,82E-03	1,205
Hist1h2ag	histone cluster 1, H2ag	2,78E-02	1,205
Hist1h2ah	histone cluster 1, H2ah	7,61E-03	1,205
Hist1h2ak	histone cluster 1, H2ak	3,70E-02	1,265
Hist1h2an	histone cluster 1, H2an	8,25E-03	1,225

Hist1h2ao	histone cluster 1, H2ao	6,78E-03	1,211
Hist1h2bb	histone cluster 1, H2bb	1,70E-02	1,541
Hist1h2bh	histone cluster 1, H2bh	2,21E-02	1,535
Hist1h3b	histone cluster 1, H3b	1,55E-03	1,273
Hist1h3c	histone cluster 1, H3c	1,61E-03	1,280
Hist1h3d	histone cluster 1, H3d	1,90E-03	1,269
Hist1h3e	histone cluster 1, H3e	1,81E-03	1,271
Hist1h3g	histone cluster 1, H3g	1,73E-03	1,276
Hist1h3h	histone cluster 1, H3h	1,62E-03	1,267
Hist1h3i	histone cluster 1, H3i	1,93E-03	1,285
Hist2h2bb	histone cluster 2, H2bb	5,84E-03	1,314
Hist2h3b	histone cluster 2, H3b	2,40E-03	1,286
Epigenic regulation			
Esco2	establishment of cohesion 1 homolog 2 (S. cerevisiae)	5,95E-03	1,831
Rbm15b	RNA binding motif protein 15B	7,26E-03	1,205
Prdm11	PR domain containing 11	7,08E-03	-1,202
Mll2	myeloid/lymphoid or mixed-lineage leukemia 2	2,30E-02	-1,208
Eif2c1	eukaryotic translation initiation factor 2C, 1	1,73E-03	-1,209
Phc3	polyhomeotic-like 3 (Drosophila)	2,83E-02	-1,217
Tet3	tet oncogene family member 3	1,84E-02	-1,248
Mll3	myeloid/lymphoid or mixed-lineage leukemia 3	2,71E-02	-1,268
A1cf	APOBEC1 complementation factor	8,73E-03	-1,278
Dnmt3a	DNA methyltransferase 3A	2,65E-03	-1,280
Cbx7	chromobox homolog 7	4,51E-03	-1,321
Kdm6b	KDM1 lysine (K)-specific demethylase 6B	2,26E-04	-1,321
Tet2	tet oncogene family member 2	7,19E-03	-1,348
Phf15	PHD finger protein 15	2,49E-03	-1,427
Tet1	tet oncogene 1	1,39E-02	-1,436
Apoptosis			
Dapl1	death associated protein-like 1	2,26E-04	1,778
Stk17b	serine/threonine kinase 17b (apoptosis-inducing)	1,69E-03	1,385
Birc5	baculoviral IAP repeat-containing 5	8,21E-03	1,370
Clptm1l	CLPTM1-like	1,33E-03	1,347
Atp6v1g2	ATPase, H+ transporting, lysosomal V1 subunit G2	2,26E-04	1,319
Tpd52l1	tumor protein D52-like 1	3,74E-03	1,286
Plekhf1	pleckstrin homology domain containing, family F (with FYVE domain) member 1	5,74E-03	1,229
Lgals12	lectin, galactose binding, soluble 12	1,91E-02	1,227
Clu	clusterin	7,92E-03	1,214
Trim35	tripartite motif-containing 35	1,79E-03	-1,217
Rnf122	ring finger protein 122	4,46E-02	-1,217
Syngap1	synaptic Ras GTPase activating protein 1 homolog (rat)	6,04E-03	-1,220

Tnfaip8	tumor necrosis factor, alpha-induced protein 8	2,10E-02	-1,232
Pycard	PYD and CARD domain containing	4,06E-03	-1,257
Aatk	apoptosis-associated tyrosine kinase	6,83E-03	-1,257
Robo2	roundabout homolog 2 (Drosophila)	8,21E-03	-1,289
Robo1	roundabout homolog 1 (Drosophila)	1,39E-03	-1,295
Ank2	ankyrin 2, brain	1,81E-03	-1,341
Bcl2l11	BCL2-like 11 (apoptosis facilitator)	1,58E-03	-1,348
Serpinb9	serine (or cysteine) peptidase inhibitor, clade B, member 9	1,11E-02	-1,351
Unc5c	unc-5 homolog C (C. elegans)	7,90E-03	-1,455
Amigo2	adhesion molecule with Ig like domain 2	1,35E-03	-1,484
Oxidative stress/DNA damage response			
Gpx2	glutathione peroxidase 2	4,64E-03	1,496
Chek1	checkpoint kinase 1 homolog (S. pombe)	1,98E-03	1,461
Prdx4	peroxiredoxin 4	8,59E-03	1,378
Gtse1	G two S phase expressed protein 1	7,98E-03	1,355
Osgin1	oxidative stress induced growth inhibitor 1	9,17E-03	1,345
Tacc3	transforming, acidic coiled-coil containing protein 3	1,03E-02	1,325
Phlda3	pleckstrin homology-like domain, family A, member 3	1,31E-02	1,225
Ppp2r5c	protein phosphatase 2, regulatory subunit B (B56), gamma	1,77E-05	1,222
Txnrd3	thioredoxin reductase 3	4,81E-02	-1,232
Atm	ataxia telangiectasia mutated homolog (human)	3,91E-02	-1,243
Transcription Factors			
Tcf19	transcription factor 19	1,37E-03	1,823
Mybl1	myeloblastosis oncogene-like 1	2,67E-02	1,358
Etv5	ets variant gene 5	3,83E-02	1,288
Bach2	BTB and CNC homology 2	4,51E-03	1,235
Carf	calcium response factor	4,96E-02	-1,201
Prdm2	PR domain containing 2, with ZNF domain	1,16E-02	-1,217
Elf4	E74-like factor 4 (ets domain transcription factor)	4,19E-02	-1,218
Dach1	dachshund 1 (Drosophila)	6,31E-03	-1,222
Arid3b	AT rich interactive domain 3B (BRIGHT-like)	6,59E-03	-1,238
Hivep3	human immunodeficiency virus type I enhancer binding protein 3	7,05E-03	-1,251
Nfat5	nuclear factor of activated T-cells 5	8,55E-03	-1,251
Mlxipl	MLX interacting protein-like	1,85E-02	-1,265
Arx	aristaless related homeobox	3,05E-03	-1,275
Hlf	hepatic leukemia factor	6,27E-03	-1,275
Myt1	myelin transcription factor 1	1,65E-02	-1,278
Hhex	hematopoietically expressed homeobox	3,20E-02	-1,283
Pou3f4	POU domain, class 3, transcription factor 4	8,67E-03	-1,374
Mnx1	motor neuron and pancreas homeobox 1	3,56E-03	-1,406
Mafb	v-maf musculoaponeurotic fibrosarcoma oncogene homolog	4,18E-02	-1,418

	B		
Per3	period homolog 3 (Drosophila)	2,15E-03	-1,592
Plag1	pleiomorphic adenoma gene 1	1,49E-03	-1,613
Nr1d1	nuclear receptor subfamily 1, group D, member 1	1,85E-02	-1,636
Nuclear receptor and related proteins			
Nr4a2	nuclear receptor subfamily 4, group A, member 2	4,36E-03	1,342
Ncoa1	nuclear receptor coactivator 1	1,86E-03	-1,219
Thra	thyroid hormone receptor alpha	4,04E-03	-1,291
Nr3c2	nuclear receptor subfamily 3, group C, member 2	1,53E-03	-1,383
Transcription regulation/alternative splicing			
Zfp367	zinc finger protein 367	4,71E-03	1,445
Atad2	ATPase family, AAA domain containing 2	2,61E-03	1,376
Ezh2	enhancer of zeste homolog 2 (Drosophila)	2,06E-03	1,343
Carhsp1	calcium regulated heat stable protein 1	5,42E-03	1,317
Ldb2	LIM domain binding 2	1,30E-02	1,283
Wdhd1	WD repeat and HMG-box DNA binding protein 1	3,27E-02	1,281
Gemin6	gem (nuclear organelle) associated protein 6	3,83E-03	1,280
Hey1	hairy/enhancer-of-split related with YRPW motif 1	4,08E-02	1,257
Zcchc12	zinc finger, CCHC domain containing 12	4,52E-02	1,250
Zfp57	zinc finger protein 57	5,74E-03	1,227
Mbnl3	muscleblind-like 3 (Drosophila)	3,53E-02	1,213
Parn	poly(A)-specific ribonuclease (deadenylation nuclease)	7,66E-03	1,208
Armcx3	armadillo repeat containing, X-linked 3	5,25E-03	1,206
Srp9	signal recognition particle 9	1,60E-03	1,206
Rnaseh2c	ribonuclease H2, subunit C	2,25E-02	1,204
Srsf7	serine/arginine-rich splicing factor 7	1,78E-03	-1,202
Tnrc6a	trinucleotide repeat containing 6a	2,02E-02	-1,203
Ppargc1b	peroxisome proliferative activated receptor, gamma, coactivator 1 beta	4,78E-03	-1,205
Tle3	transducin-like enhancer of split 3, homolog Of Drosophila E(Sp1)	2,94E-03	-1,206
Bmi1	Bmi1 polycomb ring finger oncogene	3,51E-03	-1,210
Srfbp1	serum response factor binding protein 1	9,17E-03	-1,210
Rbm27	RNA binding motif protein 27	1,18E-04	-1,210
Ssbp2	single-stranded DNA binding protein 2	2,65E-03	-1,213
Sin3a	transcriptional regulator, SIN3A (yeast)	3,99E-03	-1,213
Prpf39	PRP39 pre-mRNA processing factor 39 homolog (yeast)	3,87E-02	-1,214
Zfp455	zinc finger protein 455	7,96E-03	-1,217
Rcor3	REST corepressor 3	1,43E-02	-1,217
Polr3g	polymerase (RNA) III (DNA directed) polypeptide G	2,67E-02	-1,219
Chd6	chromodomain helicase DNA binding protein 6	1,61E-02	-1,221
Bat2l	HLA-B associated transcript 2-like	2,30E-03	-1,221

Zfp583	zinc finger protein 583	4,85E-03	-1,226
Prox1	prospero-related homeobox 1	1,61E-03	-1,227
Bcorl1	BCL6 co-repressor-like 1	1,39E-03	-1,231
Ankrd12	ankyrin repeat domain 12	8,26E-03	-1,238
Zfp654	zinc finger protein 654	1,23E-02	-1,240
Bcor	BCL6 interacting corepressor	5,49E-03	-1,243
Zbtb10	zinc finger and BTB domain containing 10	3,00E-02	-1,246
Zfp28	zinc finger protein 28	3,64E-03	-1,252
Cstf3	cleavage stimulation factor, 3' pre-RNA, subunit 3	3,79E-02	-1,253
Elp4	elongation protein 4 homolog (S. cerevisiae)	1,81E-03	-1,254
Zfp317	zinc finger protein 317	7,53E-03	-1,255
Zfp2	zinc finger protein 2	1,44E-03	-1,257
Tra2a	transformer 2 alpha homolog (Drosophila)	4,29E-02	-1,258
Klf7	Kruppel-like factor 7 (ubiquitous)	9,29E-03	-1,260
Zfp618	zinc fingerprotein 618	4,36E-03	-1,265
Ikzf4	IKAROS family zinc finger 4	1,42E-02	-1,275
Mov10	Moloney leukemia virus 10	1,13E-03	-1,275
Irx2	Iroquois related homeobox 2 (Drosophila)	4,32E-02	-1,278
Cdx4	caudal type homeobox 4	4,15E-02	-1,279
Irx1	Iroquois related homeobox 1 (Drosophila)	4,57E-02	-1,285
Chd3	chromodomain helicase DNA binding protein 3	6,26E-04	-1,289
Zfp398	zinc finger protein 398	4,01E-03	-1,291
Mll1	myeloid/lymphoid or mixed-lineage leukemia 1	2,11E-02	-1,292
Pou6f2	POU domain, class 6, transcription factor 2	4,30E-02	-1,300
Sp4	trans-acting transcription factor 4	3,45E-03	-1,314
Tef	thyrotroph embryonic factor	4,95E-03	-1,325
Rcor2	REST corepressor 2	1,23E-02	-1,340
Prdm1	PR domain containing 1, with ZNF domain	2,51E-02	-1,351
Klhl3	kelch-like 3 (Drosophila)	1,97E-03	-1,363
Zbtb20	zinc finger and BTB domain containing 20	5,00E-03	-1,364
Mamld1	mastermind-like domain containing 1	6,70E-03	-1,372
Chd5	chromodomain helicase DNA binding protein 5	1,39E-03	-1,385
Zkscan16	zinc finger with KRAB and SCAN domains 16	7,61E-03	-1,401
Bhlhe41	basic helix-loop-helix family, member e41	5,29E-04	-1,407
Msi1	Musashi homolog 1(Drosophila)	6,51E-03	-1,448
Zim1	zinc finger, imprinted 1	1,52E-03	-1,559
Dbp	D site albumin promoter binding protein	2,95E-03	-1,760
Protein synthesis/translation regulation/protein folding/endoplasmic reticulum stress			
Derl3	Der1-like domain family, member 3	1,28E-04	2,300
Kdelr3	KDEL (Lys-Asp-Glu-Leu) endoplasmic reticulum protein retention receptor 3	5,01E-04	2,208
Fkbp11	FK506 binding protein 11	1,15E-04	1,528

Fam129a	family with sequence similarity 129, member A	2,06E-02	1,423
Dnajb11	DnaJ (Hsp40) homolog, subfamily B, member 11	2,32E-03	1,403
Sec11c	SEC11 homolog C (S. cerevisiae)	9,62E-04	1,379
Spcs1	signal peptidase complex subunit 1 homolog	5,55E-03	1,350
Prkcsh	protein kinase C substrate 80K-H	6,67E-04	1,346
Qsox1	quiescin Q6 sulfhydryl oxidase 1	1,63E-03	1,321
Pdrg1	p53 and DNA damage regulated 1	1,43E-03	1,310
Ppib	peptidylprolyl isomerase B	2,07E-03	1,281
Paip2b	poly(A) binding protein interacting protein 2B	1,28E-04	1,276
Pdia4	protein disulfide isomerase associated 4	8,85E-03	1,271
Pdia6	protein disulfide isomerase associated 6	1,32E-03	1,270
Golm1	golgi membrane protein 1	2,40E-03	1,265
Edem2	ER degradation enhancer, mannosidase alpha-like 2	1,97E-03	1,261
Nucb1	nucleobindin 1	3,69E-04	1,247
Pacrg	PARK2 co-regulated	1,22E-02	1,245
Hspb6	heat shock protein, alpha-crystallin-related, B6	4,64E-02	1,244
Os9	amplified in osteosarcoma	2,26E-04	1,242
Rps8	ribosomal protein S8	2,47E-03	1,239
Edem1	ER degradation enhancer, mannosidase alpha-like 1	1,62E-03	1,227
Dnajc3	DnaJ (Hsp40) homolog, subfamily C, member 3	1,18E-03	1,214
H47	histocompatibility 47	1,18E-03	1,207
Manf	mesencephalic astrocyte-derived neurotrophic factor	4,48E-03	1,207
Ssr3	signal sequence receptor, gamma	3,69E-04	1,205
Mrps12	mitochondrial ribosomal protein S12	2,44E-02	1,200
Utp15	UTP15, U3 small nucleolar ribonucleoprotein, homolog (yeast)	8,04E-03	-1,204
Zc3h3	zinc finger CCCH type containing 3	2,43E-02	-1,206
Sez6l	seizure related 6 homolog like	5,02E-03	-1,210
Rpl23a	ribosomal protein L23a	4,01E-03	-1,287
Igf2bp2	insulin-like growth factor 2 mRNA binding protein 2	1,62E-03	-1,348
Macrod2	MACRO domain containing 2	1,39E-02	-1,356
Hspa12a	heat shock protein 12A	2,38E-03	-1,362
Ppil6	peptidylprolyl isomerase (cyclophilin)-like 6	1,72E-03	-1,497
Vesicle transport/Protein trafficking			
Rab18	RAB18, member RAS oncogene family	9,32E-03	1,477
Copz2	coatomer protein complex, subunit zeta 2	1,15E-04	1,452
Sytl1	synaptotagmin-like 1	5,07E-03	1,330
Tmed3	transmembrane emp24 domain containing 3	6,53E-04	1,314
Ssr4	signal sequence receptor, delta	1,57E-04	1,290
Sec16b	SEC16 homolog B (S. cerevisiae)	3,45E-03	1,239
Srprb	signal recognition particle receptor, B subunit	1,64E-03	1,236
Mall	mal, T-cell differentiation protein-like	3,69E-02	1,234

Slc18a1	solute carrier family 18 (vesicular monoamine), member 1	2,20E-03	1,230
Plvap	plasmalemma vesicle associated protein	1,23E-02	1,202
Erp29	endoplasmic reticulum protein 29	1,67E-02	1,200
Syt14	synaptotagmin XIV	1,61E-03	-1,206
Vps13c	vacuolar protein sorting 13C (yeast)	1,56E-02	-1,223
Vps13d	vacuolar protein sorting 13 D (yeast)	1,22E-02	-1,231
Pclo	piccolo (presynaptic cytomatrix protein)	1,49E-02	-1,281
Cabp7	calcium binding protein 7	3,48E-03	-1,284
Rab3b	RAB3B, member RAS oncogene family	6,73E-03	-1,285
Kalrn	kalirin, RhoGEF kinase	1,96E-03	-1,421
Postranslational modification/ubiquination/glycosylation			
Ube2c	ubiquitin-conjugating enzyme E2C	4,32E-04	2,357
Trim59	tripartite motif-containing 59	1,84E-02	1,592
Mogs	mannosyl-oligosaccharide glucosidase	5,37E-03	1,343
Otud7a	OTU domain containing 7A	3,40E-03	1,341
Asb9	ankyrin repeat and SOCS box-containing 9	5,28E-03	1,332
Gyltl1b	glycosyltransferase-like 1B	9,23E-03	1,294
Bard1	BRCA1 associated RING domain 1	1,05E-02	1,290
Qpctl	glutaminyl-peptide cyclotransferase-like	7,05E-04	1,286
Rnf215	ring finger protein 215	1,39E-03	1,249
Man1a	mannosidase 1, alpha	2,15E-03	1,214
Ube2s	ubiquitin-conjugating enzyme E2S	1,62E-03	1,209
Krtcap2	keratinocyte associated protein 2	7,96E-03	1,208
Uba5	ubiquitin-like modifier activating enzyme 5	7,50E-03	1,204
Dpagt1	dolichyl-phosphate (UDP-N-acetylglucosamine) N-acetylglucosaminephosphotransferase 1	1,71E-02	1,203
Rpn2	ribophorin II	2,34E-04	1,202
Parp9	poly (ADP-ribose) polymerase family, member 9	6,21E-03	-1,205
Setd2	SET domain containing 2	7,60E-03	-1,205
Rnf43	ring finger protein 43	1,91E-03	-1,211
Herc3	hect domain and RLD 3	6,90E-03	-1,211
Dtx3l	deltex 3-like (Drosophila)	3,69E-04	-1,221
Rimklb	ribosomal modification protein rimK-like family member B	1,70E-02	-1,223
March4	membrane-associated ring finger (C3HC4) 4	1,62E-03	-1,223
Mdm4	transformed mouse 3T3 cell double minute 4	5,84E-03	-1,229
Fbxl12	F-box and leucine-rich repeat protein 12	5,92E-03	-1,233
Rbbp6	retinoblastoma binding protein 6	1,02E-03	-1,236
Rnf208	ring finger protein 208	4,67E-02	-1,248
Zdhhc23	zinc finger, DHHC domain containing 23	1,42E-02	-1,252
Uba7	ubiquitin-like modifier activating enzyme 7	5,49E-04	-1,292
Galnt14	UDP-N-acetyl-alpha-D-galactosamine: Polypeptide N-Acetylgalactosaminyltransferase 14	1,33E-03	-1,331

Parp14	poly (ADP-ribose) polymerase family, member 14	6,57E-03	-1,339
Herc6	hect domain and RLD 6	1,84E-03	-1,341
Galntl4	UDP-N-acetyl-alpha-D-galactosamine: Polypeptide N-Acetylgalactosaminyltransferase-Like 4	2,81E-03	-1,420
Galnt13	UDP-N-acetyl-alpha-D-galactosamine: Polypeptide N-Acetylgalactosaminyltransferase 13	1,42E-03	-1,429
Proteosome/lysosome/autophagy/phagocytosis			
Wipi1	WD repeat domain, phosphoinositide interacting 1	1,57E-03	1,256
Ift88	intraflagellar transport 88 homolog (Chlamydomonas)	2,34E-03	-1,231
Wdfy3	WD repeat and FYVE domain containing 3	7,59E-03	-1,232
Vps13a	vacuolar protein sorting 13A (yeast)	8,49E-03	-1,239
Dnajc13	DnaJ (Hsp40) homolog, subfamily C, member 13	9,48E-03	-1,240
Mcoln3	mucolipin 3	1,11E-03	-1,770
Peptidase/protease and related inhibitors			
Serpina7	serine (or cysteine) peptidase inhibitor, Clade A (Alpha-1 Antiproteinase, Antitrypsin), Member 7	8,64E-04	2,515
Pappa2	pappalysin 2	1,35E-03	1,584
Prss23	protease, serine, 23	5,63E-03	1,419
C1rl	complement component 1, r subcomponent-like	1,03E-02	1,267
Serpinb8	serine (or cysteine) peptidase inhibitor, clade B, member 8	4,71E-03	1,263
Plat	plasminogen activator, tissue	1,68E-02	1,257
Serpini1	serine (or cysteine) peptidase inhibitor, clade I, member 1	2,26E-04	1,251
Prss16	protease, serine, 16 (thymus)	1,88E-02	1,220
Erap1	endoplasmic reticulum aminopeptidase 1	1,61E-03	-1,201
Zufsp	zinc finger with UFM1-specific peptidase domain	2,49E-02	-1,221
Lmln	leishmanolysin-like (metallopeptidase M8 family)	9,01E-03	-1,221
Agbl4	ATP/GTP binding protein-like 4	2,23E-02	-1,236
Usp11	ubiquitin specific peptidase 11	2,52E-02	-1,282
Usp29	ubiquitin specific peptidase 29	4,59E-03	-1,290
Lonrf1	LON peptidase N-terminal domain and ring finger 1	2,40E-03	-1,380
Cpm	carboxypeptidase M	3,59E-02	-1,429
Pcsk6	proprotein convertase subtilisin/kexin type 6	1,18E-03	-1,454
Thsd4	thrombospondin, type I, domain containing 4	1,30E-03	-1,484
Reln	reelin	9,36E-03	-1,711
Cytoskeleton and related proteins			
Gas2l3	growth arrest-specific 2 like 3	3,47E-03	1,902
Kif18b	kinesin family member 18B	5,65E-03	1,624
Frmd5	FERM domain containing 5	4,62E-03	1,409
Kif14	kinesin family member 14	7,09E-03	1,368
Diap3	diaphanous homolog 3 (Drosophila)	4,97E-03	1,365
Cd93	CD93 antigen	2,92E-03	1,307
Synpo2	synaptopodin 2	5,90E-03	1,244
Csrp1	cysteine and glycine-rich protein 1	7,65E-03	1,228

Pak3	p21 protein (Cdc42/Rac)-activated kinase 3	2,25E-03	1,227
Psrc1	proline/serine-rich coiled-coil 1	2,07E-03	1,226
Spc25	SPC25, NDC80 kinetochore complex component, homolog (S. cerevisiae)	1,40E-02	1,225
Smtn	smoothelin	4,74E-03	1,223
Dynll1	dynein light chain LC8-type 1	4,00E-03	1,216
Cep72	centrosomal protein 72	1,77E-02	1,206
Tmsb10	thymosin, beta 10	4,53E-02	1,201
Cldn4	claudin 4	1,39E-02	-1,200
Pcm1	pericentriolar material 1	1,68E-03	-1,202
Baiap2	Brain-Specific Angiogenesis Inhibitor 1-Associated Protein 2	1,30E-02	-1,206
Kifc3	kinesin family member C3	1,41E-03	-1,216
Trio	triple functional domain (PTPRF interacting)	1,54E-02	-1,219
Armc4	armadillo repeat containing 4	1,52E-03	-1,224
Scin	scinderin	2,78E-03	-1,226
Tubb3	tubulin, beta 3	3,36E-02	-1,233
Tpm3	tropomyosin 3, gamma	6,10E-03	-1,237
Kif3c	kinesin family member 3C	1,11E-02	-1,238
Kif5a	kinesin family member 5A	3,51E-03	-1,267
Tnik	TRAF2 and NCK interacting kinase	1,03E-02	-1,269
Nebl	nebulette	9,08E-03	-1,296
Epb4.1l3	erythrocyte protein band 4.1-like 3	6,96E-04	-1,301
Tmsb15l	thymosin beta 15b like	1,49E-02	-1,311
Sntg1	syntrophin, gamma 1	2,40E-03	-1,333
Syne1	synaptic nuclear envelope 1	3,34E-02	-1,346
Myo3a	myosin IIIA	6,78E-03	-1,359
Syne2	synaptic nuclear envelope 2	2,87E-02	-1,389
Myo9a	myosin Ixa	2,98E-03	-1,527
Edn3	endothelin 3	9,81E-03	-1,536
Epb4.1l4a	erythrocyte protein band 4.1-like 4a	1,37E-03	-1,653
Channels and transporters			
Slc2a6	solute carrier family 2 (facilitated glucose transporter), member 6	2,92E-04	2,014
Ttyh1	tweety homolog 1 (Drosophila)	2,80E-03	1,927
Slc17a9	solute carrier family 17, member 9	3,69E-04	1,868
Slco1a5	solute carrier organic anion transporter family, member 5	7,96E-03	1,768
Cngb3	cyclic nucleotide gated channel beta 3	6,53E-04	1,658
Car4	carbonic anhydrase 4	7,97E-04	1,622
Rhd	Rh blood group, D antigen	9,19E-04	1,594
Kcnh1	potassium voltage-gated channel, subfamily H (eag-related)	3,69E-04	1,529
Kcnip2	Kv channel-interacting protein 2	2,47E-03	1,473
Slc39a11	solute carrier family 39 (metal ion transporter), member 11	2,30E-03	1,458

Tmem38b	transmembrane protein 38B	3,89E-02	1,457
Slco1a6	solute carrier organic anion transporter family, member 6	1,12E-02	1,444
Kcnk10	potassium channel, subfamily K, member 10	1,64E-03	1,423
Slc38a10	solute carrier family 38, member 10	4,46E-03	1,409
Abcb6	ATP-binding cassette, sub-family B (MDR/TAP), member 6	1,33E-03	1,391
Slc1a5	solute carrier family 1 (neutral amino acid transporter), member 5	1,45E-02	1,389
Slc35f4	solute carrier family 35, member F4	2,98E-03	1,358
Abcc9	ATP-binding cassette, sub-family C (CFTR/MRP), member 9	5,82E-03	1,313
Rbp7	retinol binding protein 7, cellular	1,22E-02	1,303
Slc46a1	solute carrier family 46, member 1	2,56E-03	1,291
Abca4	ATP-binding cassette, sub-family A (ABC1), member 4	2,15E-03	1,288
Synpr	synaptoporin	1,33E-03	1,274
Trpc4	transient receptor potential cation channel, subfamily C,	4,44E-02	1,255
Kcnk1	potassium channel, subfamily K, member 1	1,47E-03	1,249
Atp13a2	ATPase type 13A2	5,49E-04	1,248
Tomm40l	translocase of outer mitochondrial membrane 40 homolog (yeast)-like	7,38E-04	1,242
Slc39a13	solute carrier family 39 (metal ion transporter), member 13	3,45E-03	1,239
Slc35b1	solute carrier family 35, member B1	1,33E-03	1,236
Slc26a2	solute carrier family 26 (sulfate transporter), member 2	1,29E-02	1,227
Slc31a1	solute carrier family 31, member 1	2,34E-03	1,221
Slc35c2	solute carrier family 35, member C2	1,66E-03	1,219
Slc35a2	solute carrier family 35 (UDP-galactose transporter), member 35	5,96E-04	1,218
Tmc6	transmembrane channel-like gene family 6	9,22E-03	1,212
Lhfp	lipoma HMGIC fusion partner	2,22E-02	1,209
Accn1	amiloride-sensitive cation channel 1, neuronal	3,74E-02	-1,203
Cacna2d1	calcium channel, voltage-dependent, alpha2/delta subunit	1,57E-03	-1,206
Tmem30b	transmembrane protein 30B	3,12E-03	-1,206
Tmem151b	transmembrane protein 151B	4,19E-03	-1,227
Tmed8	transmembrane emp24 domain containing 8	4,93E-03	-1,227
Tmem87b	transmembrane protein 87B	1,33E-03	-1,228
Sfxn4	sideroflexin 4	6,47E-03	-1,236
Unc80	unc-80 homolog (C. elegans)	5,93E-03	-1,239
Cacna1c	calcium channel, voltage-dependent, L type, alpha 1C subunit	9,90E-03	-1,243
Cacna1a	calcium channel, voltage-dependent, P/Q type, alpha 1A subunit	3,44E-03	-1,251
Prrt1	proline-rich transmembrane protein 1	3,60E-02	-1,255
Slc7a2	solute carrier family 7 (cationic amino acid transporter, Y+ System),Member 2	1,14E-02	-1,257
Slc16a9	solute carrier family 16 (monocarboxylic acid transporters), member 9	4,62E-02	-1,258

Aqp4	aquaporin 4	4,19E-03	-1,258
Dync2h1	dynein cytoplasmic 2 heavy chain 1	3,83E-02	-1,283
Slc12a7	solute carrier family 12, member 7	1,18E-02	-1,286
Tmem146	transmembrane protein 146	5,73E-03	-1,289
Atp1b2	ATPase, Na+/K+ transporting, beta 2 polypeptide	1,13E-03	-1,294
Trpm5	transient receptor potential cation channel, subfamily M, member 5	6,38E-03	-1,310
Psd	pleckstrin and Sec7 domain containing	2,58E-03	-1,320
Nlgn2	neuroligin 2	5,96E-04	-1,343
Atp8a2	ATPase, aminophospholipid transporter-like, class I, type 8A, member 2	2,92E-03	-1,344
Sv2b	synaptic vesicle glycoprotein 2 b	6,05E-03	-1,345
Ap1s2	adaptor-related protein complex 1, sigma 2 subunit	8,84E-03	-1,347
Hhatl	hedgehog acyltransferase-like	3,37E-03	-1,372
Slc30a1	solute carrier family 30 (zinc transporter), member 1	3,24E-03	-1,392
Lgi1	leucine-rich repeat LGI family, member 1	2,49E-03	-1,394
Jph3	junctophilin 3	6,68E-04	-1,413
Tmem106a	transmembrane protein 106A	6,26E-04	-1,425
Tmem132b	transmembrane protein 132B	5,19E-03	-1,427
Kcnj12	potassium inwardly-rectifying channel, subfamily J, member 12	6,83E-03	-1,434
Kcnh8	potassium voltage-gated channel, subfamily H (eag-related), member 8	1,33E-03	-1,442
Slc29a4	solute carrier family 29 (nucleoside transporters), member 4	1,18E-04	-1,496
Lyve1	lymphatic vessel endothelial hyaluronan receptor 1	2,56E-02	-1,541
Kcng3	potassium voltage-gated channel, subfamily G, member 3	1,33E-03	-1,558
Mt1	metallothionein 1	1,35E-03	-1,599
Aqp7	aquaporin 7	1,24E-03	-1,656
Hormones/growth factors/receptors/neuropeptides and exocytosis			
Mc5r	melanocortin 5 receptor	5,54E-03	2,412
Tnfrsf23	tumor necrosis factor receptor superfamily, member 23	2,06E-03	1,808
Gabra4	gamma-aminobutyric acid (GABA) A receptor, subunit alpha	8,83E-03	1,781
Inhba	inhibin beta-A	1,20E-04	1,594
Tgfb3	transforming growth factor, beta 3	3,10E-04	1,477
Nucb2	nucleobindin 2	1,23E-04	1,433
Aplnr	apelin receptor	4,81E-02	1,410
Egf	epidermal growth factor	2,65E-04	1,395
Gprc5b	G protein-coupled receptor, family C, group 5, member B	3,80E-03	1,379
Oxtr	oxytocin receptor	2,72E-02	1,376
Ffar2	free fatty acid receptor 2	1,22E-02	1,369
Rab3d	RAB3D, member RAS oncogene family	1,15E-04	1,355
Olfr558	olfactory receptor 558	1,43E-02	1,341
Ldlrad3	low density lipoprotein receptor class A domain containing 3	1,61E-02	1,337

Vgf	VGF nerve growth factor inducible	1,20E-03	1,328
Ros1	Ros1 proto-oncogene	8,24E-03	1,286
Ccbp2	chemokine binding protein 2	1,05E-02	1,274
Ednra	endothelin receptor type A	4,53E-02	1,261
Gabrq	gamma-aminobutyric acid (GABA) A receptor, subunit theta	7,09E-03	1,260
Gast	gastrin	3,22E-03	1,229
Fgf1	fibroblast growth factor 1	1,58E-02	1,207
Olfr765	olfactory receptor 765	3,20E-02	1,203
Fzd7	frizzled homolog 7 (Drosophila)	7,66E-03	-1,205
Spry2	sprouty homolog 2 (Drosophila)	4,41E-02	-1,205
Adora1	adenosine A1 receptor	1,34E-03	-1,208
Glul	glutamate-ammonia ligase (glutamine synthetase)	1,60E-03	-1,209
Jmjd1c	jumonji domain containing 1C	1,36E-02	-1,210
Stxbp3a	syntaxin binding protein 3A	1,69E-02	-1,212
Cnr1	cannabinoid receptor 1 (brain)	2,38E-03	-1,218
Sorcs2	sortilin-related VPS10 domain containing receptor 2	1,35E-02	-1,223
Avpr1b	arginine vasopressin receptor 1B	1,37E-02	-1,227
Itpr3	inositol 1,4,5-triphosphate receptor 3	3,84E-03	-1,228
Maob	monoamine oxidase B	2,06E-03	-1,233
Ephb2	Eph receptor B2	3,47E-03	-1,236
Olfm2	olfactomedin 2	1,33E-03	-1,241
Grik5	glutamate receptor, ionotropic, kainate 5 (gamma 2)	8,59E-04	-1,247
Plxna3	plexin A3	2,99E-03	-1,248
Itpr2	inositol 1,4,5-triphosphate receptor 2	2,28E-02	-1,259
Hgf	hepatocyte growth factor	1,95E-02	-1,270
Rims3	regulating synaptic membrane exocytosis 3	1,57E-02	-1,278
Fgf14	fibroblast growth factor 14	2,30E-03	-1,285
Tnfrsf14	tumor necrosis factor receptor superfamily, member 14	9,77E-03	-1,287
Rara	retinoic acid receptor, alpha	2,10E-03	-1,294
Igf1r	insulin-like growth factor I receptor	5,74E-03	-1,303
Trpm2	transient receptor potential cation channel, subfamily M, member 2	4,39E-03	-1,311
Epha7	Eph receptor A7	2,69E-02	-1,317
Itgb8	integrin beta 8	3,29E-03	-1,317
Cntfr	ciliary neurotrophic factor receptor	1,23E-02	-1,318
Rab3c	RAB3C, member RAS oncogene family	8,59E-04	-1,328
Tfrc	transferrin receptor	2,95E-03	-1,342
Cd79a	CD79A antigen (immunoglobulin-associated alpha)	2,80E-03	-1,345
Cacna1b	calcium channel, voltage-dependent, N type, alpha 1B	3,90E-03	-1,347
Gpr137b	G protein-coupled receptor 137B	2,73E-03	-1,362
Rnf213	ring finger protein 213	5,65E-03	-1,393
Gria3	glutamate receptor, ionotropic, AMPA3 (alpha 3)	3,99E-03	-1,404

Gipr	gastric inhibitory polypeptide receptor	1,03E-02	-1,404
Chrna4	cholinergic receptor, nicotinic, alpha polypeptide 4	2,17E-03	-1,407
Grin2c	glutamate receptor, ionotropic, NMDA2C (epsilon 3)	5,02E-03	-1,417
Tgfbr3	transforming growth factor, beta receptor III	2,49E-02	-1,430
Itpr1	inositol 1,4,5-triphosphate receptor 1	2,80E-03	-1,583
Sult1c2	sulfotransferase family, cytosolic, 1C, member 2	2,54E-03	-1,639
Glra1	glycine receptor, alpha 1 subunit	2,40E-03	-1,644
Stxbp5l	syntaxin binding protein 5-like	2,26E-04	-1,844
Signal transduction			
C1qtnf1	C1q and tumor necrosis factor related protein 1	4,65E-03	1,731
Cthrc1	collagen triple helix repeat containing 1	1,33E-03	1,605
Mctp1	multiple C2 domains, transmembrane 1	2,34E-02	1,401
Apcdd1	adenomatosis polyposis coli down-regulated 1	3,00E-03	1,373
Shcbp1	Shc SH2-domain binding protein 1	2,36E-02	1,360
Cyb561	cytochrome b-561	8,30E-04	1,347
Taar4	trace amine-associated receptor 4	1,32E-02	1,312
Cdk18	cyclin-dependent kinase 18	1,58E-03	1,307
Tspan6	tetraspanin 6	9,06E-03	1,304
Ell2	elongation factor RNA polymerase II 2	5,92E-05	1,304
Ctnnal1	catenin (cadherin associated protein), alpha-like 1	4,39E-02	1,292
Gna14	guanine nucleotide binding protein, alpha 14	1,61E-03	1,280
Igfbp3	insulin-like growth factor binding protein 3	9,17E-03	1,265
Steap4	STEAP family member 4	2,27E-02	1,252
Anxa2	annexin A2	2,39E-02	1,238
Diap2	diaphanous homolog 2 (Drosophila)	4,03E-03	-1,200
Gprasp2	G protein-coupled receptor associated sorting protein 2	2,14E-02	-1,201
Strn	striatin, calmodulin binding protein	2,44E-02	-1,205
Slc20a1	solute carrier family 20, member 1	1,63E-02	-1,205
Bcl9	B-cell CLL/lymphoma 9	2,17E-03	-1,206
Arhgef9	CDC42 guanine nucleotide exchange factor (GEF) 9	4,57E-02	-1,208
Sufu	suppressor of fused homolog (Drosophila)	1,97E-03	-1,210
Arhgap5	Rho GTPase activating protein 5	2,21E-02	-1,211
Atxn1	ataxin 1	8,37E-03	-1,211
Hfe	hemochromatosis	2,25E-03	-1,212
Adrbk2	adrenergic receptor kinase, beta 2	2,09E-02	-1,216
Cbl	Casitas B-lineage lymphoma	2,36E-03	-1,216
Appl2	adaptor protein, phosphotyrosine interaction, PH domain and leucine zipper containing 2	1,66E-03	-1,217
Akt2	thymoma viral proto-oncogene 2	4,04E-03	-1,219
Dok7	docking protein 7	2,16E-04	-1,219
Cdon	cell adhesion molecule-related/down-regulated by oncogenes	5,76E-03	-1,221
Gabbr1	gamma-aminobutyric acid (GABA) B receptor, 1	1,03E-02	-1,226

Tspan12	tetraspanin 12	1,62E-02	-1,238
Axin2	axin2	1,87E-02	-1,240
Rasa2	RAS p21 protein activator 2	2,06E-03	-1,240
Gpr179	G protein-coupled receptor 179	4,04E-03	-1,257
Odz2	odd Oz/ten-m homolog 2 (Drosophila)	9,93E-03	-1,266
Grk5	G protein-coupled receptor kinase 5	2,87E-02	-1,271
Inpp5e	inositol polyphosphate-5-phosphatase E	4,98E-03	-1,276
Lpp	LIM domain containing preferred translocation partner in lipoma	5,42E-03	-1,278
Bid	BH3 interacting domain death agonist	3,24E-03	-1,278
Sema3e	sema domain, immunoglobulin domain (Ig), short basic domain, secreted, (semaphorin)	3,94E-03	-1,288
Atrnl1	attractin like 1	4,57E-03	-1,290
Mapk15	mitogen-activated protein kinase 15	8,45E-03	-1,301
Magi2	membrane associated guanylate kinase, WW and PDZ domain	1,00E-02	-1,310
Dpp10	dipeptidylpeptidase 10	1,86E-02	-1,395
Gpr75	G protein-coupled receptor 75	3,07E-03	-1,397
Gprc5c	G protein-coupled receptor, family C, group 5, member	4,09E-03	-1,407
Gpr98	G protein-coupled receptor 98	2,30E-03	-1,441
Psd4	pleckstrin and Sec7 domain containing 4	4,47E-03	-1,441
Baiap3	BAI1-associated protein 3	3,86E-03	-1,449
AMPK and mTOR pathways			
Akt1s1	AKT1 substrate 1 (proline-rich)	3,64E-03	1,235
Prkab2	protein kinase, AMP-activated, beta 2 non-catalytic subunit	9,86E-03	-1,216
Rps6ka5	ribosomal protein S6 kinase, polypeptide 5	1,58E-02	-1,295
Rictor	RPTOR independent companion of MTOR, complex 2	1,39E-03	-1,302
Nptx1	neuronal pentraxin 1	7,52E-03	-1,359
Insulin signaling pathway			
Shc4	SHC (Src homology 2 domain containing) family, member 4	1,84E-03	1,445
Insrr	insulin receptor-related receptor	2,16E-02	-1,203
Grb10	growth factor receptor bound protein 10	2,54E-02	-1,213
Shc2	SHC (Src homology 2 domain containing) transforming protein 2	2,85E-03	-1,298
Igfbp5	insulin-like growth factor binding protein 5	7,96E-03	-1,378
Nnat	neuronatin	6,35E-04	-1,690
GTPase activity and regulation			
Depdc1a	DEP domain containing 1a	2,61E-03	1,894
Arhgap11a	Rho GTPase activating protein 11A	5,00E-03	1,713
Rasgrf2	RAS protein-specific guanine nucleotide-releasing factor	6,53E-04	1,511
Arhgap19	Rho GTPase activating protein 19	2,92E-02	1,403
Iqgap3	IQ motif containing GTPase activating protein 3	2,80E-02	1,391
Arhgef37	Rho guanine nucleotide exchange factor (GEF) 37	1,74E-03	1,346

Arhgdig	Rho GDP dissociation inhibitor (GDI) gamma	1,03E-02	1,300
Rapgef5	Rap guanine nucleotide exchange factor (GEF) 5	3,88E-02	1,261
Ralgapa2	Ral GTPase activating protein, alpha subunit 2 (catalytic)	2,30E-03	1,214
Vav3	vav 3 oncogene	2,82E-03	1,208
Sept3	septin 3	7,70E-03	-1,221
Rab12	RAB12, member RAS oncogene family	8,59E-03	-1,241
Dennd4c	DENN/MADD domain containing 4C	6,85E-03	-1,242
Tbc1d2b	TBC1 domain family, member 2B	2,31E-03	-1,252
Rasgef1a	RasGEF domain family, member 1A	1,84E-02	-1,254
Gbp6	guanylate binding protein 6	2,58E-02	-1,267
Rab19	RAB19, member RAS oncogene family	1,62E-03	-1,276
Dock5	dedicator of cytokinesis 5	1,39E-02	-1,291
Rragb	Ras-related GTP binding B	4,76E-04	-1,310
Rit2	Ras-like without CAAX 2	1,81E-02	-1,330
Dock6	dedicator of cytokinesis 6	4,13E-03	-1,334
Spata13	spermatogenesis associated 13	3,48E-03	-1,397
Srgap1	SLIT-ROBO Rho GTPase activating protein 1	3,99E-03	-1,403
Trib1	tribbles homolog 1 (Drosophila)	2,99E-02	-1,455
Dock10	dedicator of cytokinesis 10	5,42E-03	-1,461
Rem2	rad and gem related GTP binding protein 2	2,03E-03	-1,463
Mlph	melanophilin	1,33E-03	-1,572
Kinases/Phosphatases and related proteins			
Pbk	PDZ binding kinase	2,03E-03	2,427
Akap6	A kinase (PRKA) anchor protein 6	1,35E-03	1,448
Dusp23	dual specificity phosphatase 23	1,22E-03	1,350
Ckmt1	creatine kinase, mitochondrial 1, ubiquitous	1,41E-03	1,220
Stk32a	serine/threonine kinase 32A	7,36E-03	1,213
Dak	dihydroxyacetone kinase 2 homolog (yeast)	1,39E-03	1,213
Ppapdc3	phosphatidic acid phosphatase type 2 domain containing 3	1,83E-02	1,200
Prkx	protein kinase, X-linked	1,62E-03	-1,201
Ppp2r2b	protein phosphatase 2 (formerly 2A), regulatory subunit	3,43E-03	-1,201
Pip5k1c	phosphatidylinositol-4-phosphate 5-kinase, type 1 gamma	2,26E-04	-1,202
Akap8	A kinase (PRKA) anchor protein 8	3,09E-03	-1,203
Prkcb	protein kinase C, beta	1,39E-03	-1,207
Prkce	protein kinase C, epsilon	1,35E-03	-1,209
Mpp3	membrane protein, palmitoylated 3 (MAGUK p55 subfamily member 3	7,23E-03	-1,209
Ccnl1	cyclin L1	2,23E-03	-1,211
Ptpru	protein tyrosine phosphatase, receptor type, U	4,38E-03	-1,219
Ankrd44	ankyrin repeat domain 44	2,03E-02	-1,223
Ulk4	unc-51-like kinase 4 (C. elegans)	2,62E-03	-1,226
Tec	tec protein tyrosine kinase	8,50E-03	-1,228

Camk1g	calcium/calmodulin-dependent protein kinase I gamma	7,53E-03	-1,229
Map3k2	mitogen-activated protein kinase kinase kinase 2	5,87E-03	-1,230
Agphd1	aminoglycoside phosphotransferase domain containing 1	1,74E-02	-1,230
Camk2n1	calcium/calmodulin-dependent protein kinase II inhibitor	1,38E-03	-1,237
Spata5	spermatogenesis associated 5	1,05E-02	-1,241
Phlpp2	PH domain and leucine rich repeat protein phosphatase	6,67E-04	-1,244
Itpkb	inositol 1,4,5-trisphosphate 3-kinase B	1,61E-03	-1,252
Dusp18	dual specificity phosphatase 18	3,36E-03	-1,259
Inpp4a	inositol polyphosphate-4-phosphatase, type I	3,83E-03	-1,279
Rad54l2	RAD54 like 2 (S. cerevisiae)	3,42E-03	-1,290
Cdkl1	cyclin-dependent kinase-like 1 (CDC2-related kinase)	3,99E-03	-1,301
Ppp2r2c	protein phosphatase 2 (formerly 2A), regulatory subunit B, gamma	2,45E-02	-1,383
Upp1	uridine phosphorylase 1	1,08E-03	-1,395
Nek5	NIMA (never in mitosis gene a)-related expressed kinase 5	4,64E-03	-1,430
Ncs1	neuronal calcium sensor 1	1,61E-03	-1,443
Mast1	microtubule associated serine/threonine kinase 1	4,75E-04	-1,667
Cell-cell signaling			
Hmmr	hyaluronan mediated motility receptor (RHAMM)	2,84E-04	2,501
Dll1	delta-like 1 (Drosophila)	1,62E-03	-1,345
Extracellular matrix/collagen formation			
F13a1	coagulation factor XIII, A1 subunit	5,92E-05	1,765
Sgcd	sarcoglycan, delta (dystrophin-associated glycoprotein)	6,53E-04	1,570
Postn	periostin, osteoblast specific factor	2,84E-02	1,567
Leprel1	leprecan-like 1	1,96E-02	1,508
Hapln4	hyaluronan and proteoglycan link protein 4	6,53E-04	1,425
Frem2	Fras1 related extracellular matrix protein 2	3,69E-04	1,420
Spon2	spondin 2, extracellular matrix protein	7,25E-03	1,418
Lama5	laminin, alpha 5	2,75E-03	1,319
Smoc1	SPARC related modular calcium binding 1	1,84E-02	1,288
Lepre1	leprecan 1	5,74E-03	1,280
Naglu	alpha-N-acetylglucosaminidase (Sanfilippo disease IIIB)	3,44E-03	1,247
Sparc	secreted acidic cysteine rich glycoprotein	1,30E-02	1,247
Hapln1	hyaluronan and proteoglycan link protein 1	5,95E-03	1,223
Plod3	procollagen-lysine, 2-oxoglutarate 5-dioxygenase 3	2,25E-03	1,204
Mfap1a	microfibrillar-associated protein 1A	3,57E-03	-1,202
Mmp16	matrix metallopeptidase 16	4,19E-03	-1,205
Vcan	versican	3,06E-02	-1,233
Egflam	EGF-like, fibronectin type III and laminin G domains	5,93E-03	-1,359
Col6a6	collagen, type VI, alpha 6	5,75E-03	-1,367
Chemokines/cytokines/adhesion molecules/innate immunity and related proteins			
Il1r2	interleukin 1 receptor, type II	1,84E-03	1,584

Susd2	sushi domain containing 2	6,26E-04	1,582
Troap	trophinin associated protein	1,74E-03	1,511
Tubb6	tubulin, beta 6	1,86E-02	1,509
Ccl3	chemokine (C-C motif) ligand 3	2,82E-02	1,368
Pcdh18	protocadherin 18	1,85E-02	1,348
Cd44	CD44 antigen	3,10E-03	1,346
Otoa	otoancorin	6,87E-03	1,340
Emilin1	elastin microfibril interfacer 1	4,04E-03	1,331
Clec14a	C-type lectin domain family 14, member a	3,51E-03	1,328
Nid2	nidogen 2	2,11E-03	1,295
Cd34	CD34 antigen	7,25E-03	1,291
Fam19a1	family with sequence similarity 19, member A1	1,91E-02	1,279
Lama4	laminin, alpha 4	1,89E-02	1,262
Igsf5	immunoglobulin superfamily, member 5	1,05E-02	1,253
Cntn1	contactin 1	1,66E-03	1,245
Sema3f	sema domain, immunoglobulin domain (Ig), short basic domain	8,73E-03	1,218
Rpsa	ribosomal protein SA	6,71E-04	1,209
Vstm2a	V-set and transmembrane domain containing 2A	2,78E-02	1,207
Jam2	junction adhesion molecule 2	7,95E-03	1,205
Nrxn1	neurexin I	3,99E-03	-1,202
Il18bp	interleukin 18 binding protein	4,48E-02	-1,203
Pcdhb8	protocadherin beta 8	8,23E-03	-1,203
Sema4f	sema domain, immunoglobulin domain (Ig), TM domain, and s	1,03E-02	-1,208
AK129341	cDNA sequence AK129341	1,94E-02	-1,210
Ppfia2	protein tyrosine phosphatase, receptor type, f polypeptide (PTPRF), interacting protein (liprin), alpha 2	4,37E-02	-1,211
Plekha2	pleckstrin homology domain-containing, family A (phosphoinositide binding specific) member 2	2,73E-02	-1,214
Dscam	Down syndrome cell adhesion molecule	4,06E-02	-1,218
Igsf9b	immunoglobulin superfamily, member 9B	9,17E-03	-1,223
Csf1	colony stimulating factor 1 (macrophage)	1,41E-02	-1,224
Pvrl1	poliovirus receptor-related 1	8,17E-03	-1,232
Tjp2	tight junction protein 2	1,37E-03	-1,243
Il18	interleukin 18	1,03E-02	-1,258
Oas1g	2'-5' oligoadenylate synthetase 1G	7,96E-03	-1,258
Mslnl	mesothelin-like	2,25E-03	-1,268
Ddx58	DEAD (Asp-Glu-Ala-Asp) box polypeptide 58	1,35E-03	-1,268
Pcdh9	protocadherin 9	2,02E-02	-1,268
Pard3	par-3 (partitioning defective 3) homolog (C. elegans)	3,36E-03	-1,271
Dnm1	dynamin 1	3,44E-03	-1,283
Tnr	tenascin R	2,85E-02	-1,285

Cx3cl1	chemokine (C-X3-C motif) ligand 1	1,57E-03	-1,287
L1cam	L1 cell adhesion molecule	1,81E-02	-1,293
Hpgds	hematopoietic prostaglandin D synthase	4,52E-02	-1,295
Ppl	periplakin	4,68E-02	-1,308
Dhx58	DEXH (Asp-Glu-X-His) box polypeptide 58	1,42E-02	-1,311
Ncam2	neural cell adhesion molecule 2	9,29E-03	-1,312
Pkhd1	polycystic kidney and hepatic disease 1	8,73E-03	-1,313
Syt1	synaptotagmin I	3,64E-02	-1,321
Cd274	CD274 antigen	7,78E-03	-1,327
Cer1	cerberus 1 homolog (Xenopus laevis)	2,47E-03	-1,369
Igsf21	immunoglobin superfamily, member 21	4,64E-03	-1,498
Cdh7	cadherin 7, type 2	2,03E-03	-1,500
Cdh22	cadherin 22	3,69E-04	-1,531
Pcdh15	protocadherin 15	8,30E-04	-1,634
Flrt1	fibronectin leucine rich transmembrane protein 1	1,97E-03	-1,671
HLA-related			
H2-T22	histocompatibility 2, T region locus 22	1,13E-03	1,252
Other functions			
Pdyn	prodynorphin	2,83E-03	2,241
Sema3c	sema domain, immunoglobulin domain (Ig), short basic domain	1,72E-03	2,001
S100z	S100 calcium binding protein, zeta	1,23E-02	1,671
Stil	Scl/Tal1 interrupting locus	4,85E-03	1,589
Mfi2	antigen p97 (melanoma associated) identified by monoclonal antibodies 133.2 and 96.5	5,65E-03	1,585
Creld2	cysteine-rich with EGF-like domains 2	3,84E-04	1,564
Necab2	N-terminal EF-hand calcium binding protein 2	3,69E-04	1,474
Car5b	carbonic anhydrase 5b, mitochondrial	4,74E-03	1,425
Csn3	casein kappa	4,18E-03	1,415
Tmem160	transmembrane protein 160	4,32E-04	1,411
Gnat2	guanine nucleotide binding protein, alpha transducing 2	7,97E-03	1,387
Nrm	nurim (nuclear envelope membrane protein)	1,41E-02	1,369
Yif1b	Yip1 interacting factor homolog B (S. cerevisiae)	1,62E-03	1,365
Dcx	doublecortin	7,66E-03	1,358
Morc1	microrchidia 1	1,34E-03	1,358
Gmfg	glia maturation factor, gamma	6,57E-03	1,349
Entpd1	ectonucleoside triphosphate diphosphohydrolase 1	1,45E-02	1,339
St7	suppression of tumorigenicity 7	4,62E-03	1,298
Pon3	paraoxonase 3	3,42E-03	1,287
Krtap17-1	keratin associated protein 17-1	1,90E-02	1,285
Aspn	asporin	3,32E-02	1,282
Nomo1	nodal modulator 1	5,06E-04	1,278

Tmem150a	transmembrane protein 150A	3,84E-03	1,254
Prom1	prominin 1	4,57E-02	1,254
Lrrtm2	leucine rich repeat transmembrane neuronal 2	2,66E-02	1,241
Crygb	crystallin, gamma B	8,64E-03	1,241
Fez1	fasciculation and elongation protein zeta 1 (zygin I)	1,72E-03	1,235
Atp13a1	ATPase type 13A1	2,92E-03	1,234
Nbl1	neuroblastoma, suppression of tumorigenicity 1	4,73E-03	1,229
Arfip2	ADP-ribosylation factor interacting protein 2	5,28E-03	1,220
Tmem66	transmembrane protein 66	7,42E-04	1,218
Sez6l2	seizure related 6 homolog like 2	1,35E-03	1,211
Spaca1	sperm acrosome associated 1	3,10E-02	1,210
Gap43	growth associated protein 43	3,54E-02	-1,205
Iqcb1	IQ calmodulin-binding motif containing 1	1,74E-03	-1,207
Nbeal2	neurobeachin-like 2	2,09E-03	-1,207
Fam113b	family with sequence similarity 113, member B	1,66E-02	-1,211
Zfp62	zinc finger protein 62	1,28E-02	-1,217
Zcchc11	zinc finger, CCHC domain containing 11	1,62E-03	-1,218
Phldb2	pleckstrin homology-like domain, family B, member 2	2,02E-02	-1,218
Vwa5a	von Willebrand factor A domain containing 5A	2,10E-03	-1,225
Zswim6	zinc finger, SWIM domain containing 6	1,05E-02	-1,225
Dzip1	DAZ interacting protein 1	1,71E-02	-1,232
Tuft1	tuftelin 1	7,92E-03	-1,238
Edaradd	EDAR (ectodysplasin-A receptor)-associated death domain	1,70E-02	-1,241
Tcp11	t-complex protein 11	2,20E-02	-1,271
Erc2	ELKS/RAB6-interacting/CAST family member 2	4,74E-03	-1,277
Car15	carbonic anhydrase 15	1,37E-02	-1,278
AW551984	expressed sequence AW551984	7,23E-03	-1,281
Mfap2	microfibrillar-associated protein 2	1,53E-02	-1,281
Nav3	neuron navigator 3	4,36E-03	-1,325
Zbtb7c	zinc finger and BTB domain containing 7C	1,61E-03	-1,362
Mreg	melanoregulin	6,66E-03	-1,378
Tekt2	tektin 2	6,26E-04	-1,381
Dlgap1	discs, large (Drosophila) homolog-associated protein 1	1,62E-03	-1,390
F3	coagulation factor III	1,15E-04	-1,448
Ifit1	interferon-induced protein with tetratricopeptide repeats	1,49E-02	-1,542
Mt2	metallothionein 2	2,26E-04	-1,823
Unknown functions			
Tmem179	transmembrane protein 179	1,69E-03	1,767
Prr11	proline rich 11	5,59E-03	1,728
Svopl	SV2 related protein homolog (rat)-like	1,62E-03	1,617
Slfn9	schlafen 9	1,12E-02	1,552

Sdf2l1	stromal cell-derived factor 2-like 1	5,15E-04	1,479
Heatr5b	HEAT repeat containing 5B	2,65E-04	1,395
Ccdc85a	coiled-coil domain containing 85A	3,33E-03	1,372
Maged2	melanoma antigen, family D, 2	3,51E-03	1,326
Ttc13	tetratricopeptide repeat domain 13	4,98E-04	1,312
Wdr90	WD repeat domain 90	8,43E-03	1,287
Fam46a	family with sequence similarity 46, member A	1,39E-02	1,285
Gm996	predicted gene 996	1,15E-02	1,278
Tmem212	transmembrane protein 212	4,56E-03	1,275
Fam55d	family with sequence similarity 55, member D	2,35E-02	1,271
Pter	phosphotriesterase related	2,32E-02	1,262
Gm5465	predicted gene 5465	3,76E-02	1,257
Gm5105	predicted gene 5105	1,12E-02	1,249
Tmem176a	transmembrane protein 176A	4,67E-03	1,245
Ccdc18	coiled-coil domain containing 18	2,98E-03	1,231
Yipf2	Yip1 domain family, member 2	5,28E-03	1,218
Tmem218	transmembrane protein 218	4,93E-03	1,216
Fam70a	family with sequence similarity 70, member A	2,81E-02	1,215
D17Wsu104e	DNA segment, Chr 17, Wayne State University 104, expression	1,49E-03	1,214
Armcx6	armadillo repeat containing, X-linked 6	4,46E-03	1,214
Sval2	seminal vesicle antigen-like 2	2,31E-03	1,213
Reep5	receptor accessory protein 5	2,06E-03	1,203
Samd9l	sterile alpha motif domain containing 9-like	2,84E-03	-1,201
Wdr78	WD repeat domain 78	5,85E-03	-1,202
Bend7	BEN domain containing 7	8,02E-03	-1,206
Plekha5	pleckstrin homology domain containing, family A member 5	1,06E-02	-1,209
Nol4	nucleolar protein 4	5,26E-03	-1,213
Fhdc1	FH2 domain containing 1	2,26E-04	-1,213
Gm9958	predicted gene 9958	4,36E-03	-1,218
Fam159b	family with sequence similarity 159, member B	6,51E-03	-1,219
Xkr6	X Kell blood group precursor related family member 6	6,51E-03	-1,220
Gm10336	predicted gene 10336	3,51E-03	-1,220
Wdr47	WD repeat domain 47	1,54E-03	-1,221
Mllt6	myeloid/lymphoid or mixed-lineage leukemia (Trithorax Homolog,Drosophila); Translocated To, 6	1,73E-03	-1,221
Rnf157	ring finger protein 157	8,17E-03	-1,222
Zfp229	zinc finger protein	4,91E-02	-1,224
Klhl18	kelch-like 18 (Drosophila)	8,11E-03	-1,225
Zfp568	zinc finger protein 568	4,59E-02	-1,225
Gm10786	predicted gene 10786	2,64E-02	-1,239
Vwa5b2	von Willebrand factor A domain containing 5B2	1,11E-02	-1,240

Dbpht2	DNA binding protein with his-thr domain	1,16E-02	-1,241
Fnbp4	formin binding protein 4	1,30E-03	-1,241
Ahdc1	AT hook, DNA binding motif, containing 1	7,97E-04	-1,245
Zcchc2	zinc finger, CCHC domain containing 2	4,92E-03	-1,246
Kbtbd4	kelch repeat and BTB (POZ) domain containing 4	2,45E-03	-1,247
Zcwpw2	zinc finger, CW type with PWWP domain 2	3,44E-02	-1,251
Bod1l	biorientation of chromosomes in cell division 1-like	1,07E-02	-1,252
Gm5595	predicted gene 5595	3,39E-02	-1,255
Nynrin	NYN domain and retroviral integrase containing	2,39E-02	-1,258
Ociad2	OCIA domain containing 2	3,29E-02	-1,259
Gpr137b-ps	G protein-coupled receptor 137B, pseudogene	9,13E-03	-1,259
Zfp619	zinc finger protein 619	1,84E-03	-1,260
Zmym5	zinc finger, MYM-type 5	4,02E-03	-1,261
Aard	alanine and arginine rich domain containing protein	2,72E-02	-1,265
Fam169a	family with sequence similarity 169, member A	6,54E-03	-1,270
Klhl32	kelch-like 32 (Drosophila)	1,92E-03	-1,285
Lrrc36	leucine rich repeat containing 36	7,66E-03	-1,288
BC068157	cDNA sequence BC068157	2,78E-03	-1,292
Mctp2	multiple C2 domains, transmembrane 2	3,50E-02	-1,294
Nbeal1	neurobeachin like 1	2,64E-02	-1,296
Heatr5b	HEAT repeat containing 5B	1,73E-03	-1,303
Auts2	autism susceptibility candidate 2	4,99E-03	-1,313
T2	brachyury 2	1,13E-02	-1,318
Gm609	predicted gene 609	2,25E-02	-1,326
Samd14	sterile alpha motif domain containing 14	5,15E-03	-1,352
Trim12a	tripartite motif-containing 12A	2,36E-02	-1,358
Pisd-ps1	phosphatidylserine decarboxylase, pseudogene 1	3,68E-03	-1,361
Tmem215	transmembrane protein 215	1,35E-03	-1,374
Gipc2	GIPC PDZ domain containing family, member 2	1,77E-03	-1,383
Vwa5b1	von Willebrand factor A domain containing 5B1	4,02E-03	-1,423
Wdr49	WD repeat domain 49	7,24E-03	-1,476
Lancl3	LanC lantibiotic synthetase component C-like 3 (bacterial)	2,46E-03	-1,495
Lrrc16b	leucine rich repeat containing 16B	1,44E-03	-1,596
Fam196a	family with sequence similarity 196, member A	2,26E-04	-1,678
Gm11992	predicted gene 11992	1,20E-03	-1,740